1-1-2017

Evaluating Sediment Accumulation Behind Dams In The Great Lakes Watershed From Past To Present

Fatemeh Alighalehbabakhani Alighalehbabakhani
Wayne State University,

EVALUATING SEDIMENT ACCUMULATION BEHIND DAMS IN THE GREAT LAKES WATERSHED FROM PAST TO PRESENT

FATEMEH ALIGHALEHBABAKHANI

DISSERTATION

Submitted to the Graduate School

of Wayne State University,

Detroit, Michigan

in partial fulfillment of the requirements

for the degree of

DOCTOR OF PHILOSOPHY

2017

MAJOR: CIVIL ENGINEERING

Approved By:

Carol J. Miller 12-14-2016

Adviser Date

DEDICATION

This thesis work is dedicated to my parents, who have always loved me unconditionally and taught me to work hard for achievements. This work also dedicated to my husband, Mohsen, who has encouraged and supported me during the challenges of school and life. I am truly thankful for having you in my life.

ACKNOWLEDGMENTS

Firstly, I would like to express my gratitude to my advisor Prof. Carol Miller for the support of my study and research, for her kindness, motivation, and knowledeg. I was so lucky to have her as my advisor, teacher, and mentor. I could not have pictured having a better advisor for my Ph.D research and study.

Besides my advisor, I would like to thank the rest of my thesis committee members and instructors, Dr. Jeffery Howard, and Dr. Shawn McElmurry, Dr. James Selegean.

I am grateful to Dr. James E. Almendinger, senior scientist at St. Croix Watershed Research Station, for enlightening me at some aspects of SWAT software.

TABLE OF CONTENTS

LIST OF TABLES

LIST OF FIGURES

CHAPTER 1 INTRODUCTION

1.1. Background

Sedimentation is the most important factor in the longevity of dams. Reservoir sedimentation and the consequence long term loss of storage capacity have been a serious threat. As the sediment loads accumulate within the reservoir, the dam gradually loses its capacity to serve multiple functions including water supply, electrical generation, irrigation, flood control, and recreation purpose. Although, more than six decades researches have been done on the dam sedimentation, sedimentation is still serious technical threat for dam industry (Mc Cully, 1996). There is only limited information, and few measurements regarding the sediment accumulation rate within the reservoir. For evaluating the dams function, and the economic feasibility of water resource, calculating the life expectancy of dams is essentially required. More than 75,000 dams, over 3 ft height, exist in the United States, impounding approximately 17% of rivers in the nation (Natural Resources Defense Council, 2014). More than 7,000 dams (Kelly, 2013) were built in the Great Lake Basin, which many of them were built between 100, and 120 years ago, so they are very old, unsafe, and no longer serve their purposes (American Rivers, 2014).

In the United State, the recent trends promote the removal of some dams in hopes to restore healthy rivers and riverside community. Before any dam removal, extensive research is required to be completed, in order to evaluate the quantity and quality of sediments trapped within the reservoir. Dam removal may significantly release sediment to the downstream of dams that may results in decreasing water quality (or increasing water turbidity) and increasing sediment deposition on the landscape and channels

(Warrick et al., 2015). The U.S. Army Corps of Engineers typically spend between $20-40 million annually to remove 1.5- 3 million m^3 of sediment from navigation channels and harbors that they maintain.

As most dams are reaching their capacity for sediment storage, this research investigated the historical rate of sediment trapping, as well as the remaining storage capacity. The hydrology and sediment yield models were developed in order to evaluate how the storage capacity has altered over time and forecast the remaining storage capacity.

Twelve reservoirs throughout the Great Lakes Watershed were selected and analyzed for their greater applicability to the entire watershed. Both historic and new data were collected on these dams to determine how the storage capacity has changed over time and to forecast the remaining life-span of the impoundments. The estimated sediment accumulation rates through this dissertation were compared with the measured sediment trapping rate by radionuclide dating, and bathymetric subtraction approaches which have done in some of the study reservoirs.

This study also serves to improve understanding of the natural sediment yield in the Great Lake Watershed. In this research the effect of human interferes including; the land use change, and dam construction on sediment yield, have been evaluated. It should be noted that any impact associated with the climate change is not considered in this work, so the current study does not directly determine the pre- European settlement era sediment.

1.2. Hypothesis

The hypothesis of this research is:

"*Development of several sediment yield models in the Great Lakes Watershed can assist at estimating sediment accumulation rate within the man- made reservoirs, and evaluating human interfere impacts on the sediment yield since pre- European settlement. Finally propagating the results of this study to the other reservoirs in the Great Lakes Region.*"

Several reservoirs in the Great Lakes Watershed have been selected as a case study to approve this hypothesis. Each of the study watersheds are dominated by specific land use. For instance; Ballville, Independence, Webber, Riley, Upper Green Lake, Goshen are in agricultural dominated watersheds. Potter's Falls, Brown Bridge, Mio and Alcona watersheds are mostly covered by forest. The watersheds that contain Lake Rockwell, and Ford Lake dams are urban- forest- farmland basins.

CHAPTER 2 LITERATURE REVIEW

2.1. Sediment

Sediment is fragment material that is broken down by the process of weathering and erosion. Eroded soil is gradually mobilized in the watershed by hillslope erosion processes such as sheet or rill erosion. The typical soil erosion unit adopted is t/yr. The mount of sediment passing a specific watershed location is called *sediment yield*. Sediment yield can also be defined as total sediment volume delivered to a specified location in the watershed, divided by the drainage area of that specified location for a specific time period. The sediment yield unit is $t/km^2/yr$ or $m^3/km^2/yr$. The amount of sediment load reaching the watershed outlet for a specific time period is called *sediment delivery* and its unit is m^3/yr or t/yr. Sediment yield can be substantially less than soil erosion in the basin. Because just only a part or probably a small part of the sediment eroded within a basin will reach to the basin outlet and be represented in the sediment yield (Wallings, 1983). A part of sediment eroded traps in the temporary or permanent storage (Wallings, 1983). The ratio of sediment delivery at the basin outlet to net erosion within the basin is called a *sediment delivery ratio*. This ratio typically is less than 1. The magnitude of the sediment delivery ratio for a specific basin depends on land use, vegetation cover, soil structure, relief, slope characteristics, and channel condition.

Sediment transport is the movement of sediment particle by water. River sediment can be transported in two different forms – as sediment in *suspension* and sediment in the *bed load*. The size fraction associated with suspended sediment is clay-silt size (between 0.002 and 0.063 mm), and they usually are carried along by the water flow. When the sediment particles are floating within the water column they are considered

suspended. For quantifying concentration of sediment in suspension phase in surface waters, two laboratory analytical methods, suspended sediment concentration (SSC) and total suspended solid (TSS) are applied. Despite the similarity in the meaning, SSC and TSS can be examined differently and they cannot be used interchangeably. SSC can be calculated by measuring the dry weight of entire water sample, while TSS are obtained by measuring the dry weight of subsample of the original. In natural water, the method for measuring SSC, results in relatively reliable results (Gray et al., 2000). However, TSS measurement method, are designed for analyses of wastewater samples.

Some sediment particle may also come from the upstream reaches, and flow along the river to the downstream in the form of *wash load*. Wash load is mostly clays and some fine silts size, so their velocity is small, and they are usually suspended in water columns. Concentration of wash load is pretty uniform, in the water column, and it is mostly composition of a grains that are found slightly in the bed.

Bed load is a part of sediment transport (total load) which moves by rolling, sliding, and bouncing along the bed (Figure 1). When the power of flow is strong enough to overcome the weight and cohesion of the sediment, bedload occurs. Total sediment load in a stream is the composition of both bed load and suspended load.

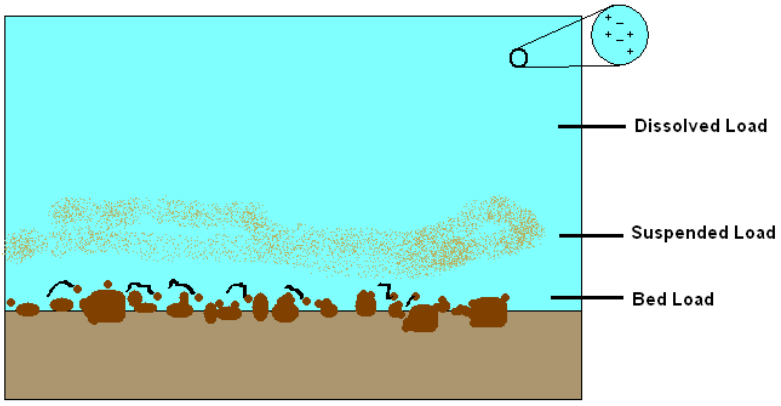

Figure 1-Different Types of Sediment Load, Photo Credit by Wikipedia

Typically, 5- 20% of the total load represents the bedload carried by a river (Czuba et al., 2011). In Sandusky River, the bedload transport is less than 5 percent of total sediment load (Hindall, 1991). Two important factors in sediment transport are the settling velocity (the velocity which sediment falls through a water column.) and the boundary layer shear stress. The settling velocity is a function of the particle size, density, and fluid viscosity. Shear stress represents the required force of water flow to move sediment, and is influenced by river depth, water viscosity, and roughness of sediment. Sediment transport is influenced by the particle (sediment) availability and stream transport capacity (Ramos, et al., 2015).

For better understanding the sources, and sinks of sediment within a specific basin, the sediment budget can be helpful. The main erosion sources of sediment are river bank and bed erosion, rill and gully erosion, and overland runoff. Wetlands, floodplains, reservoirs, channels, landscape can trap sediment and act as the sinks of sediment (Figure 2).

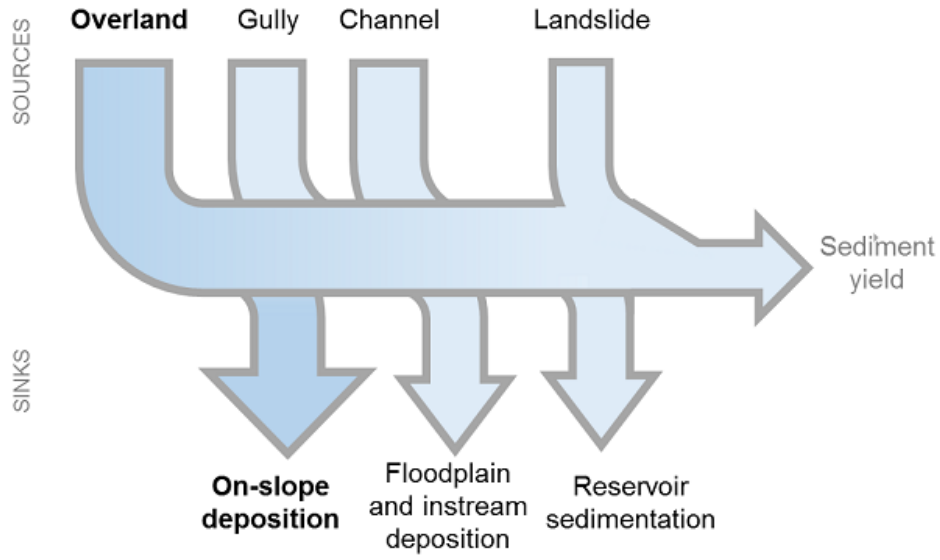

Figure 2- The General Catchment Sediment Budget. Photo Credit InVEST (Integrated Valuation of Ecosystem Services and Tradeoffs) 3.1.3 User's Guide,

Natural processes such as river bank erosion, bed river erosion, overland flow, sheet, rill and gully erosion contribute at elevating suspended sediment and bed load. Climate factors such as wind speed, rainfall intensity, also geography factors like topography, land cover, vegetation and finally soil structure and composition are the primary factors controlling the rate and magnitude of soil erosion (Terrence et al., 2002). The major cause of soil erosion is human interaction. Human activities such as urbanization, deforestation, and using various farm practice result in elevated erosion rate (Jordan et al., 2014; Terrence et al., 2002). In the United States different landscapes have been affected intensively by human activities since European settling, one of these impacts is changing land use. Immediately after the arrival of European colonists, a considerable portion of forests disappeared, while farmlands, corn, and wheat spread across the country. Land cover changes alter the function of a watershed by changing the runoff pattern (hydrograph) and water quality (Randhir and Hawes, 2009).

Urbanization that associated with increasing impervious surface, results in altering drainage pattern and increasing runoff. Also, runoff from urban area carries the major water pollutant absorbed by suspended sediment. The land cover change affects the sediment load (TSS loading) to the river. Expanding forest results in decreasing TSS loading into the river, while agriculture and pasture area are positively related to the TSS loading. Regarding to the urban area describing a linear relationship between urban expansion and TSS loading is challenging (Jordan et al., 2014).

Some agricultural practices such as agricultural tillage, removal of tree, erode soil and allowe runoff to deliver a considerable amount of TSS into the waterbody (Imeson, 2012). Recently new agricultural practices such as no- till operations, tile drainage

operation and reduced fertilizer used over the last decade increased to reduce soil erosion and sediment- assisted nutrient into the water bodies.

Different studies have been done to evaluate the effect of European Settlement on the amount of sediment yield. For instance, the sediment yields into the Lake Pepin, a large natural impoundment, in the Mississippi Basin has increased by an order of magnitude since European Settlement (Engstrom et al., 2009). About 17% of the Lake Pepin volume has been filled by sediment, and with current sediment accumulation rate the lake will be full in another 340 years (Engstrom et al., 2009). In the Sao Francison River watershed, in the eastern Brazil since pre- European Settlement the sediment yield has been increased from approximately 7 Mt/a to 27 Mt/a (Creech et al., 2015). Sediment delivery from the Le Sueur River in the Minnesota River watershed is about 0.90 in current landuse with assuming no till management, and 0.84 in the current land use under till management, and 0.73 in pre- European land use (Maalim et al., 2013).

Runoff pass over land or through the ground, and carry pollutants and deposit them into the water body such as rivers, reservoirs, and then introduce them into the ground water. Non- point source (NPS) pollution is the main reason that approximately 40% of surveyed rivers, reservoirs and estuaries are not clean enough to meet water quality standards. The latest National Water Quality Inventory indicates that agricultural area has the leading role to water quality impairments- responsible for up to 60% of the impaired river miles (Environmental Protection Agency, 2012). Since the 1970s, Lake Erie has had episodic algal bloom problems associated with elevated nutrient loads. More recently, in the summer of 2011 and 2014, significant algae bloom which have been derived from the desorption of sediment-bound phosphorus, impacted the western basin of Lake Erie and

the Toledo water intake (Molder et al., 2015), that resulted in drinking water restriction to about half a million people in the State of Ohio.

There are various agricultural practices that can positively impact sediment loading and nutrient transport. These include no-till operation, till drainage operations, and decreased fertilizer usage (Macrae et al., 2007). An additional factor that impacts the nutrient transport to the water body is rainfall intensity as it impacts nutrient transport through local erosion (Adamowski et al., 2010). In addition to algae growth problems, excessive sediment transport reduces downstream water quality, (Mukundan et al., 2013) and eventually deteriorates the natural habitat for some creatures because of increasing turbidity. The amount of nutrient yield to the water body in agricultural watershed strongly depends on quantity and quality of suspended sediment yields (Molder et al., 2015). Because nutrient can be adsorbed on the sediments sourced from agricultural watersheds (Bosch et al., 2013). Among sediment particles, clay- sized particles are the most important contributor of nutrient into the water body, because of the small particle size (and hence, large surface area), high exchange capacity, and charged surfaces (Stone and English, 1993; Leote and Epping, 2015).

A relatively small portion of the sediment passes the watershed outlet, and the reminders are trapped in temporary storage and in the next rainfall events they might leave the watershed. Typically, sediment with the first flood event after dry seasons have considerable influence on water bodies, and reservoirs (Ramos et al., 2015). These flood events can result in pollution spikes that last from a few minutes to several days, and cause algae growth expansion and contaminated water (Yevenes and Mannaerts, 2011). During flood events, the sediment delivered into a reservoir is at its highest value

(McCully, 1996; Ramos et al., 2015). In the US about half of the river's annual sediment load may be carried during 5 to 10 days of flood (McCully, 1996). Finding a relationship between flood events and water quality is not simple, because this relationship depends on the basin topography, land use, topography, remobilization of sediments and pollutants (Oeurng et al., 2010; Klein and Koelmans, 2011) recorded in a basin in the south of France 85 to 95% of the annual sediment load was transported during flood events. (Rovira, and Batalla, 2006) Estimated more than 90% of the annual sediment load in a catchment in Cataluña, Spain was delivered during storm events. The amount of suspended sediment transported in the single storm depends on storm's duration, time, and storm's magnitude (Rovira and Batalla, 2006)

2.2. Sediment Trap Efficiency within the Impoundments

Many dams have been constructed since many years ago for multiple purposes, including the provision of water supply for residential and agricultural uses, flood control, and power generation. Similar to any structure, dam construction is governed by engineering design guidance and rules. In addition, proper function and life cycle of the structure requires appropriate maintenance. One of the main factors that affecting dam life span is the amount of sediment trapped behind the dam. Dam construction can reduce water velocity so sediment that comes along the inflow, deposits within the reservoir. Such deposition shortens the useful life of water structure.

The environmental impacts of constructing dams are different, it influences the biological, chemical and physical aspect of rivers environments. Dams separate fish species. The average population of salmon and trout enters the Columbia River is estimated to be between 10 and 16 million, before constructing dams in the 19th century.

However currently only some 1.5 million salmons and trout enter the Columbia River (Rivers, 2016). In some cases, dams have degraded river ecosystems, and reduced fisheries (Stanley and Doyle, 2003). The water running off from different landscapes, and carry different pollutant and debris, and eventually dump them into the reservoir.

The chemical composition of water at the upstream of the dam (within the reservoir) is different from free- flowing the river. Water temperature increase and oxygen decreases at the reservoir upstream of the dam, so the water quality decrease, and eventually deteriorate natural habitat for some fish populations. At the downstream of the dam, because of reduced velocity, water is more saline that makes the environment less suitable for some fishes.

Evaluating the life expectancy of dams is necessary for the evaluation of dam's function and the economic feasibility of a water resource for long time. The capacity of reservoirs can be significantly affected by sediment trapping within the reservoirs. There are many different variables that affect life expectancy of a reservoir, between these variables, water discharge and sediment load in the rivers are two main contributing factors at estimating sediment trap behind dams, reservoir age, geometry and size of particles are other important factors (Gill, 1979).

Sediment Trap efficiency is the ratio of annual total weight sediment accumulation within a reservior to the annual sediment inflow to the reservoir. Several researches have been done to correlate sediment trap efficiency with one of more of influential factors, including; reservoir geometry and age, inflow, drainage area of reservoir, size of sediment particle. In 1941 Brune and Allen developed a curve to correlate the percentage of soil erosion in the impoundment with drainage area (Brune, 1953). The sediment trap

efficiency based on this curve is less than the reality, because this method is based on the erosion rate (which was measured by surveys) rather than sediment accumulation rate within the reservoir (Brune, 1953). In 1944, Brown developed a curve to relate sediment trap efficiency to storage capacity- drainage area (C/A) ratio (Gill, 1979). Capacity -Area ratio is reservoir capacity (ac-ft) divided by drainage area (mi^2). The Brown Curve is replicated in Figure 3, and its formula is listed in Equation 1.

$$E = 100[1 - 1/(1 + k\,C/A)]$$

Equation 1

Where:

E= Sediment trap efficiency (%)

C= Capacity of reservoir (ac- ft)

A= Drainage area of the reservoir (mi^2),

K= Coefficient which varies from 0.046 to 1, (k= 0.1 is recommended for average conditions, and values k= 1.0, 0.1 and 0.046 may be used for coarse, medium, and fine sediments, respectively.)

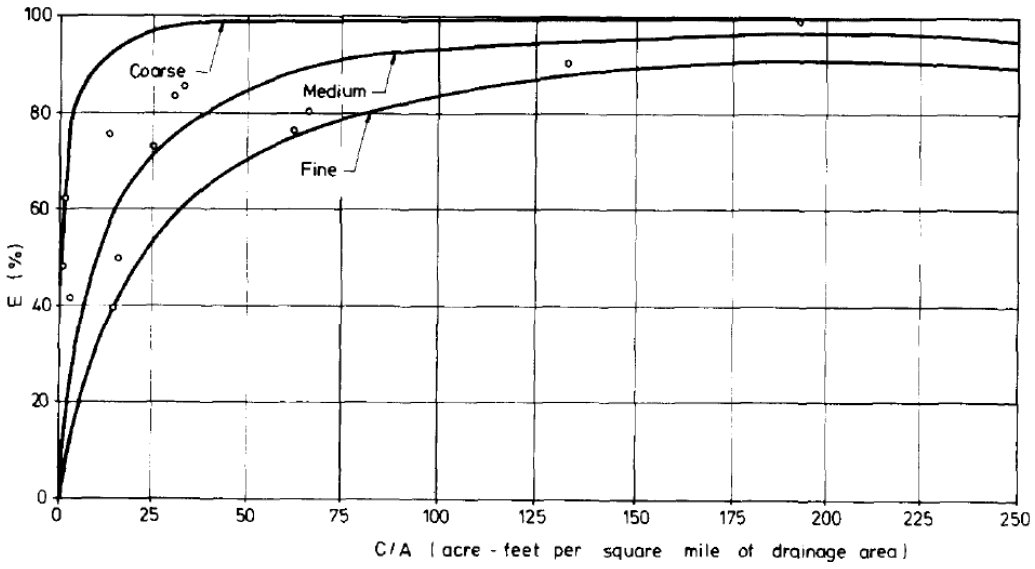

Figure 3- Sediment Trap Efficiency Curve from Brown (1944)

In 1948 Churchill added both detention time, and velocity of inflow into the trap efficiency curve. He divided the period of retention by the mean velocity, and defined this ratio as *sedimentation index*. Figure 4 displays Churchill Curve which relates the trapping efficiency to sedimentation index. Tennessee Valley Authority Reservoir data were used for developing the Curve in Figure 4. If measuring detention time and mean velocity cannot be measured in the field, with dividing the reservoir capacity by the average daily inflow rate, detention time can be calculated. Also with dividing the average daily inflow by the reservoir cross section, mean velocity can be estimated.

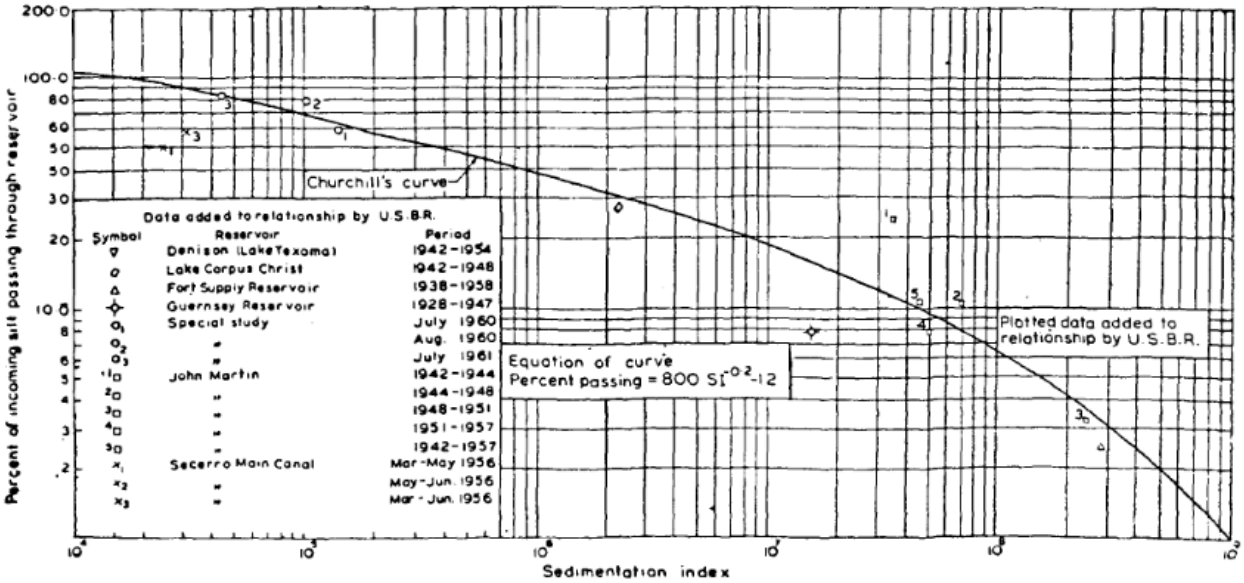

Figure 4- Sediment Trap Efficiency Curve from Churchill (1948)

The Brown's equation is a simplified format and just drainage area and capacity of reservoirs have been included at estimating sediment trap efficiency, while there are many other variables that are attributed into the sediment trap efficiency equation. One of these variables is characteristic of annual inflow to the reservoir (C/I) which was investigated its effect on trap efficiency by Brune in 1953 (Brune, 1953). Brune examined the trapping efficiency of 44 reservoirs, 40 of these reservoirs were normally ponded

reservoir, two of them were desilting basins, and the reminders were semi- dry reservoirs. Brune correlated the trapping efficiency of the reservoir (E) with the ratio of reservoir capacity to mean annual inflow (C/ I) (Brune, 1953). Like the Brown's equation, Brune Curves have been differentiated based on sediment size. Three curves for fine, medium, and coarse sediment size are displayed in Figure 5. Equation 2, Equation 3, and Equation 4 provide pretty close fit to the three curve proposed by Brune (Brune, 1953).

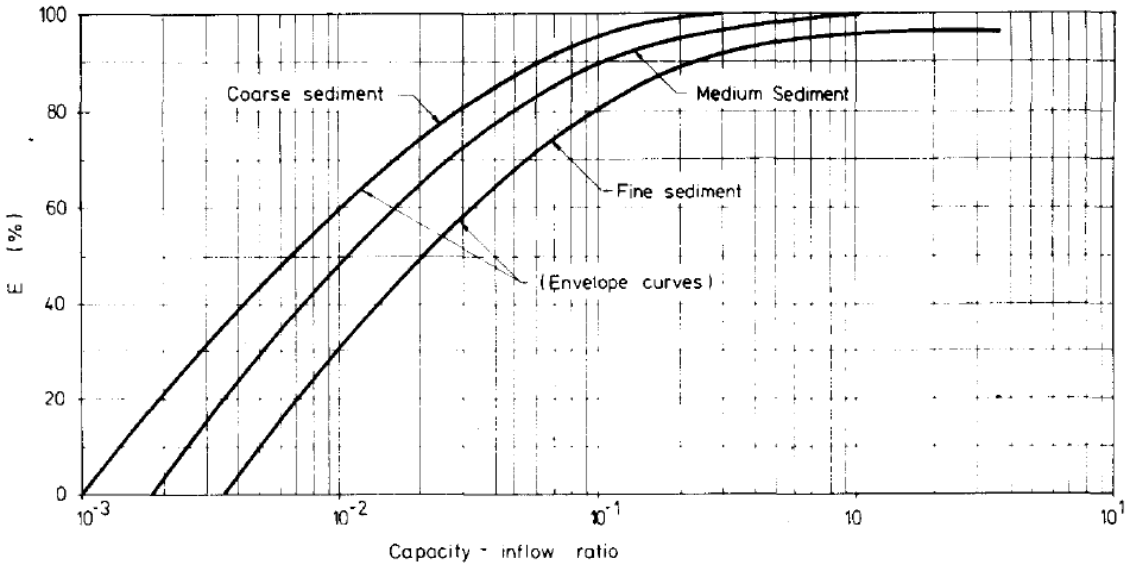

Figure 5- Sediment Trap Efficiency Curve from Brune (1953)

$$E = (C/I)^2/[0.994701(C/I)^2 + 0.006297(C/I) + 0.3 \times 10^{-5}]$$

Equation 2- Coarse Sediments

$$E = (C/I)/(0.012 + 1.02C/I)$$

Equation 3- Medium Sediments

$$E = (C/I)^3/[1.02655(C/I)^3 + 0.02621(C/I)^2 - 0.133 \times 10^{-3}(C/I) + 0.1 \times 10^{-5}]$$

Equation 4- Fine Sediments

Brown's method just requires the reservoir capacity, and watershed area, so this method is simple in comparison to the other methods. If the annual inflow rate of reservoir

is known the Brune curve can provide more accurate sediment trap efficiency in comparison to Brown method. Churchill method requires some additional data regarding to the reservoir surface area. It should be mentioned that none of these methods consider the sediment inflow characteristic.

2.3. Watershed Modeling System

Due to the lack of historical sediment data, in many cases a fully quantitative sediment budget is impossible. Several numerical modeling tools can be used for predicting hydrologic runoff, landscape and stream erosion, sediment yield, sediment transportation and deposition in a watershed. Some of these tools include ANSWERS (Areal Nonpoint Source Watershed Environment Response Simulation) (Beasley et al., 1980), PRMS (Precipitation- Runoff Modeling System) (Leavesley et al., 1983), AGNPS (Agricultural Non- Point Source Pollution Model) (Young et al., 1987), SWAT (Soil and Water Assessment Tools) (Neitsch et al., 2011), HSPF (Hydrological Simulation Program-Fortran) (Bicknell et al., 1993), HEC_HMS (Hydrologic Model System) (USACE, 2010), GSSHA (Gridded Surface Subsurface Hydrologic Analysis) (Downer and Ogden, 2006), etc. In this research, SWAT has been used to develop the sediment dynamics in the modeling framework. SWAT stands for Soil Water Assessment Tool, which was developed in 1998 for the USDA Agricultural Research Service (ARS). SWAT is a physically-based continuous (daily time step) model intended for the prediction of long-term water and sediment yields from a watershed. SWAT simulates flow, nutrient, pesticide, soil erosion and sediment yield from the watershed. This tool can be used to estimate the impact of watershed changes (including climate change, land use change, reservoir management, agricultural practices, groundwater withdrawals, and water

transfer) on the transfer of water, sediment and nutrients in the watershed. SWAT requires input data from GIS layers such as soil data, digital elevation model (DEM), land use data, climate data (precipitation, temperature, wind speed, solar radiation) to evaluate watershed hydrology, sediment yield, and nutrient dynamics. For modeling purposes, SWAT divides the watershed into subbasins, and each subbasin is further divided to smaller units termed Hydrologic Response Units (HRUs). Each HRU is assumed to be represented by a single soil characteristic, slope, and land use. The use of HRUs provides computational efficiency, allowing for large watersheds to be simulated over long periods of time.

2.3.1. **Hydrology in SWAT**

Water balance is an effective factor in all types of problems that happen in the watershed studied with SWAT. Hydrology simulation of SWAT is divided in two different phases, the land phase of the hydrologic cycle and the movement of water in the channels. The land phase can control the movement of overland sediment and nutrient into the channel, and the second division controls water, sediment and nutrient movement in the channel network of the watershed to the outlet. Figure 6 illustrates land phase division of hydrologic cycle.

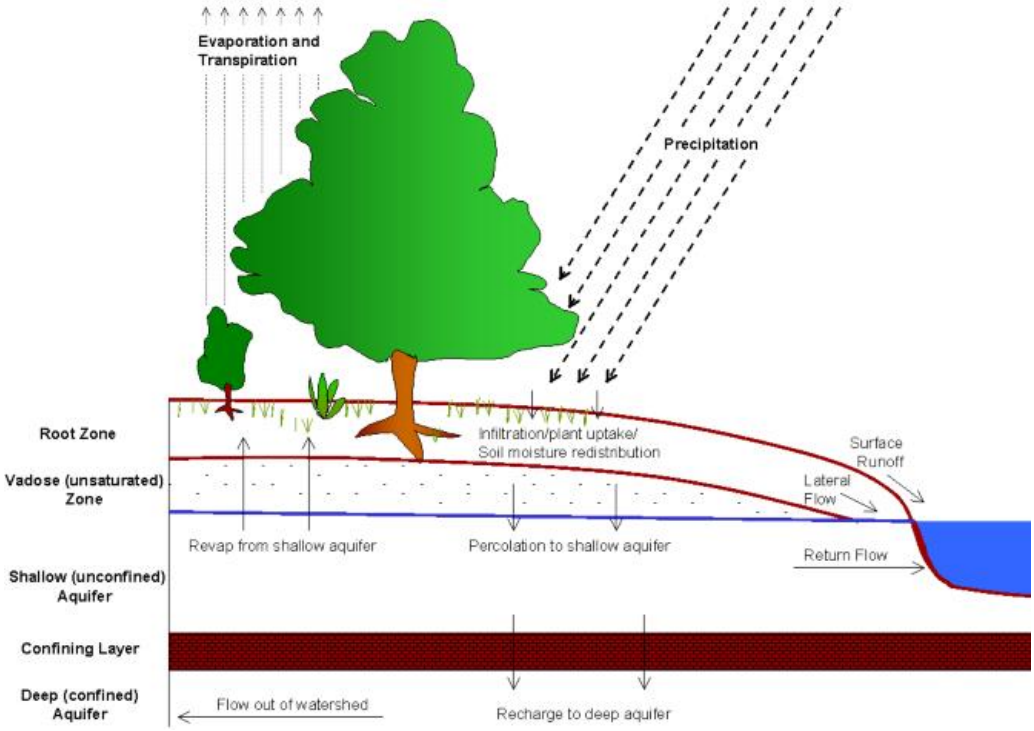

Figure 6-Schematic Representation of the Hydrologic Cycle.(Neitsch et al., 2011)

Hydrologic response units (HRUs) are areas within each sub-basin lumped together to comprise a single land cover, soil, and management combination. The hydrologic components of the SWAT model are based on water balance (Equation 5).

$$SW_t = SW_0 + \sum_{i=1}^{t}(R_{day} - Q_{surf} - E_a - w_{seep} - Q_{gw})$$

Equation 5

Where

SW_t= Final soil water content (mmH_2O),

SW_0= Initial soil water content on day i (mmH_2O),

t= Time (day),

R_{day}= Precipitation on day i (mmH_2O),

Q_{surf}= Surface runoff on day i (mmH_2O),

E_a= Evapotranspiration on day i (mmH_2O),

W_{seep}= Water entering the vadose zone from the soil profile on day i (mmH_2O),

Q_{gw}= Return flow on day i (mmH_2O),

The climate data provide soil moisture and energy inputs that control water balance. Climate information which is needed in SWAT is daily precipitation, maximum and minimum air temperature, solar radiation, wind speed and relative humidity.

surface runoff occurs when rate of water to the ground surface exceeds infiltration rate, at the beginning of precipitation soil, is dry so infiltration rate is high, but after a while with wetting soil, infiltration rate will decrease.

SWAT uses two methods for estimating surface runoff, the SCS curve number method (SCS, 1972), and the Green & Ampt infiltration method (1911). In the present research SCS Curve Number method has been applied to estimate surface runoff.

2.3.2. Upland Sediment Erosion in SWAT

In SWAT, erosion that occurred by rainfall and runoff is computed with the Modified Universal Soil Loss Equation (MUSLE) (Williams, 1975). MUSLE is a modified version of the Universal Soil Loss Equation (USLE) developed by (Wischmeier and Smith 1965, and 1978). In USLE rainfall energy is an effective factor at estimating average annual gross erosion while in MUSLE equation, runoff factor is important. Using runoff factor improves the sediment yield prediction, because of limiting the need for delivery ratio (the sediment yield at any spot along the channel divided by the source erosion above the spot), and the equation can be applied to the individual storm events. Equation 6 illustrates the modified universal soil loss equation.

$$sed = 11.8.(Q_{surf}.q_{peak}.area_{hru})^{.56}.k_{USLE}.C_{USLE}.P_{USLE}.LS_{USLE}.CFRG$$

Equation 6

where

Sed= Sediment yield on a given day (metric tons),

Q_{surf}= Surface runoff volume (mm H_2O/ha),

Q_{peak}= Peak runoff rate (m^3/s),

Area $_{hru}$= Area of the HRU (ha),

K_{USLE}= USLE soil Erodibility factor (0.013 metric ton m^2 hr. / (m^3-metric ton cm)),

C_{USLE}= USLE cover and management factor,

P_{USLE}= USLE support practice factor,

LS_{USLE}= Topographic factor,

CFRG= Coarse fragment factor,

2.3.3. Soil Erodibility Factor

Soil erodibility measures the tendency of soil particles to erode by rainfall, and runoff. Some kinds of soil erode more easily in comparison to other soil, although some of their characteristic are the same. This difference is caused by the soil characteristic, and termed soil erodibility. The soil erodibility factor is the rate of erosion per unit erosion index from a standard plot. A unit plot is 22.1 (m) long, with a length- wise slope of 9 percent. Soil texture us the influential factor at estimating soil erodibility factor, although other factors including, permeability, organic matter, and soil structure attribute at soil erodibility. For instance, with increasing silt fraction, soil becomes more erodible. Measurement of soil erodibility is costly and time consuming. (Wischemeier, 1971) developed an equation for estimating the soil erodibility equation.

$$K_{USLE} = \frac{0.00021.M^{1.14}.(12 - OM) + 3.25(C_{soilstr} - 2) + 2.5(C_{perm} - 3)}{100}$$

$$M = (m_{silt} + m_{vfs}).(100 - m_c)$$

Equation 7

Where

K_{USLE}= Soil erodibility factor

M= Particle- size parameter

OM= Percentage organic matter (%)

$C_{soilstr}$= Soil structure code used in soil classification

C_{perm}= Profile permeability class

m_{silt}= Silt content (0.002-0.05 mm diameter particle) (%)

m_{vfs}= Very fine sand content (0.05- 0.1 mm diameter particle) (%)

m_c= Clay content (<0.002 diameter particle) (%)

2.3.4. **Cover and Management Factor**

The ratio of soil loss from agricultural land under specified conditions to the corresponding loss from continuous fallow and clean- tilled (Wischemeier and Smith, 1978). Equation 8 shows the formula used for calculating cover and management factor.

$$C_{USLE} = \exp([\ln(0.8) - \ln(C_{usle,mn})].exp[-0.00115.rsd_{surf}] + ln[C_{USLE,mn}])$$

$$C_{USLE,mn} = 1.463\ ln[C_{USLE,aa}] + 0.1034$$

Equation 8

$C_{USLE, mn}$= Minimum C factor

rsd_{surf}= Amount of residue on the soil surface (kg/ha)

$C_{USLE, aa}$= Average annual C factor

2.3.5. **Support Practice Factor**

The ratio of soil loss with a specific support practice to the corresponding loss without any support practice (Wischemeier and Smith, 1978) is called practice factor. Support practice include, terrace system, counter tillage, strip cropping on the contour. Support practice varies from 0 to 1. In the no support practice farmland, the support practice factor is zero.

2.3.6. **Topographic Factor**

The ratio of the soil loss per unit area from a field slope to the soil loss from a 22.1 (m) length of 9% slope under the same condition is called topographic factor (LS_{USLE}). Equation 9 describe topographic factor.

$$LS_{USLE} = \left(\frac{L_{hill}}{22.1}\right)^{m} . (65.41 \times \sin^2(\alpha_{hill}) + 0.065)$$

$$m = 0.6(1 - \exp[-35.835. slp])$$

Equation 9

Where

L_{hill}= Slope length (m)

m=Exponential factor

α_{hill}=Slope angle

slp= Slope (m/m)

2.3.7. **Coarse Fragment Factor**

The coarse fragment factor explains the percentage of rock in the specific soil layer. Equation 10 shows the formula for estimating the coarse fragment factor.

$$\mathrm{CFRG} = \exp(-0.053.\mathrm{rock})$$

Equation 10

Where

CFRG= Coarse fragment factor

Rock= Percent of rock in the soil layer (%)

In SWAT, sediment transport consists of two components, upland component, and channel component. In the upland component, SWAT considers particle size distribution of eroded sediments from landscape and routes them into channels and surface water bodies. Channel sediment component considers deposition and degradation of sediment in the channels, which depends on the stream power, shear stress, and the composition of channel bank and bed sediment.

In the SWAT, for modeling sediment transport, bed and bank erosions there are four different equations including, Simplified Bagnold (default method), Kodatie, Molinas and Wu, Yang sand and gravel model (Neitsch et al., 2011). In this study, the default model (simplified equation) has been applied for modeling purpose.

SWAT has been widely utilized throughout the world, with applying SWATShare Tool, researchers can share their SWAT models with other researchers and also access different SWAT models (Rajin et al., 2015). SWAT is used to track nutrient and sediment load in watersheds (Yesuf et al., 2015)), and to evaluate the anthropogenic impacts on the sediment budget (Creech et al., 2015). SWAT also has been used to assess the impact of climate change and agricultural BMPs on sediment and nutrient yields (Schiefer et al. 2013; Bosch et al., 2014).

2.3.8. **Sediment within Impoundments in SWAT**

SWAT applies a simple mass balance equation to simulate the movement of sediment inflow and outflow within impoundments. Four different types of water bodies including reservoirs, potholes, wetlands, and ponds are defined by SWAT, and the sediment process in each of them are identical. SWAT assumes the impoundment is a completely mixed reactor, which means sediment inflow in to the impoundment distributed instantaneously throughout the volume. The mass balance equation for the sediment in a reservoir is (Neitsch et al., 2011):

$$\mathrm{sed}_{\mathrm{wb}} = \mathrm{sed}_{\mathrm{wb,i}} + \mathrm{sed}_{\mathrm{flowin}} - \mathrm{sed}_{\mathrm{stl}} - \mathrm{sed}_{\mathrm{flowout}}$$

Equation 11

Where

Sed_{wb}= Sediment load in the reservoir at the end of the day (metric tons)

$Sed_{wb,i}$= Sediment load in the reservoir at the beginning of the day (metric tons)

Sed_{flowin}=Sediment load added to the reservoir with inflow (metric tons)

Sed_{stl}= Sediment load settled in the reservoir (metric tons)

$Sed_{flowout}$= Sediment load delivered out of the reservoir with outflow (metric tons)

SWAT uses a modified overflow rate model for calculating the deposited incoming sediment load (Clar andBarfield, 2004). For each time step, the deposition routine starts with the calculation of the detention times, which is presented in Equation 12;

$$t_D = \frac{(C_t(1 - DS)vol)}{Qo}$$

Equation 12

Where

t_d= Detention time (s)

Vol= Average reservoir volume over the time step (ft^3)

Q_0= Average outflow rate over the time step (cfs)

C_t= Empirical factor for reservoir geometry, stratification of suspended sediment, and hydraulic response

DS= Dead storage (Griffin et al., 1985)

SWAT applies Equation 13 for estimating the initial concentration of suspended solids in the reservoir.

$$conc_{sed,i} = \frac{(sed_{wb,i} + sed_{flowin})}{(V_{stored} + V_{flowin})}$$

Equation 13

Where

$conc_{sed,i}$= Initial concentration of suspended sediment in the reservoir (Mg/m^3)

$sed_{wb,i}$= Sediment load in the reservoir at the beginning of the day (metric tons)

sed_{flowin}= Sediment load added to the reservoir with inflow (metric tons)

V_{stored}= Volume of stored water in the reservoir (m^3)

V_{flowin}= Volume of water inflow on given day (m^3)

Settling in the reservoir happened when the sediment concentration in the reservoir exceeds the equilibrium sediment concentration defined by the user. The following equations display the sediment concentration within the reservoir at the end of the day.

$$conc_{sed,f} = (conc_{sed,i} - conc_{sed,eq}).\exp[-k_s.t.d_{50}] + conc_{sed,eq}$$

If $conc_{sed,i} > conc_{sed,eq}$

$$conc_{sed,f} = (conc_{sed,i} - conc_{sed,eq})$$

If $conc_{sed,i} > conc_{sed,eq}$

Equation 14

Where

conc $_{sed,f}$= Final suspended sediment concentration within the reservoir (Mg/m^3)

conc $_{sed,i}$= Initial suspended sediment concentration within the reservoir (Mg/m^3)

conc $_{sed,eq}$= Equilibrium suspended sediment concentration in reservoir (Mg/m^3)

d_{50}=Median size of inflow sediment (μm)

t= Length of time step, which is assumed a day in this research.

k_s= Decay constant (1/ day). In our models this factor is equal 0.184, which means 99% of the 1 (μm) particle settle out within 25 days.

SWAT uses Equation 15 to determine the amount of deposited sediment within the reservoir.

$$sed_{stl} = (conc_{sed,i} - conc_{sed,f}).V$$

Equation 15

Where

Sed $_{stl}$= Amount of deposited sediment load (metric tons)

conc $_{sed,f}$= Final suspended sediment concentration within the reservoir (Mg/m^3)

conc $_{sed,i}$= Initial suspended sediment concentration within the reservoir (Mg/m^3)

V= Volume of water in the reservoir (m^3)

Following equation displays how SWAT estimate the amount of sediment transported out of the water body on a given day.

$$sed_{flowout} = conc_{sed,f}.V_{flowout}$$

Equation 16

Where

$Sed_{flowout}$= Amount of transported sediment load out of the reservoir (metric tons)

$conc_{sed,f}$= Final suspended sediment concentration within the reservoir (Mg/m^3)

$V_{flowout}$= Volume of outflow from the reservoir (m^3)

2.4. Calibration Tool

SWAT-CUP is a calibration and uncertainty program, which has been developed for the calibration of SWAT (Abbaspour et al., 2007). This program was created by Karim Abbaspour at Swiss Federal Institute for Environmental Science and Technology. This program links Sequential Uncertainty Fitting (SUFI2), Particle Swarm Optimization (PSO), Generalized Likelihood Uncertainty Estimation (GLUE), Parameter Solution (ParaSol), and Markov Chain Monte Carlo (MCMC) procedure to SWAT. It also enables sensitivity, calibration, validation, and uncertainty analysis of the SWAT models. In this present research, SUFI2 for model calibration and uncertainty analysis has been applied, because SUFI2 is pretty efficient for time-consuming large scale model (Abbaspour et al., 2015).

Calibration of a model can follow either a deterministic or stochastic approach. A deterministic approach uses a trial and error procedure; the user adjusts the calibration parameters until simulation and observation data get sufficiently close. The deterministic approach yields a single data as the solution. The stochastic approach has been developed to better mimic the uncertainty present in most natural systems. It is typically recommended that a stochastic approach should be used for calibration in natural systems (Abbaspour, 2015) due to the uncertainty in input data.

In SUFI2, uncertainty in parameters appear as uniform distribution ranges, reflecting uncertainty in the conceptual model, parameters, variables, and uncertainty in

the measured data. Therefore, in SUFI2 the model output is a propagation of the uncertainties in the parameters and is provided as the 95% probability distribution (95PPU) calculated at the 2.5% and 97.5% points of the cumulative distribution of output. A variety of factors are used as metrics to quantify the "goodness of fit" between observed data and the simulated output range. Such metrics include the p-factor and r-factor. The p-factor is the factor that shows the percentage of observation data falling within the 95 PPU region. The r-factor is the thickness of the 95PPU envelope divided by the standard deviation of the measured data. (Abbaspour, 2015) suggested that satisfactory values for discharge simulations are: p-factor > 70% and r-factor less than or equal to 1. However, for sediment calibration process, smaller p-factors and larger r-factors are acceptable.

Several other statistical parameters including the Nash-Sutcliffe Efficiency (NSE), R^2 and Percent Bias (PBIAS) (Moriasi et al., 2007) have been found to aid in the quantification of the goodness of fit between simulated and observed values. The NSE is an evaluation of how well a model predicts hydrologic or sediment behaviors better than the average of the observed data. The NSE formula for hydrologic behaviors is displayed in Equation 17.

$$NSE = 1 - \frac{\sum_{t=1}^{T}(Q_0^t - Q_m^t)^2}{\sum_{t=1}^{T}(Q_0^t - \overline{Q}_0)^2}$$

Equation 17

Where:

Q_0^t= Observed discharge at observation t

Q_m^t= Hydrologic model discharge at observation t

t= Time (day) of observations

T= Total number of observations

Q_0= Average of all observations

(Moriasi et al., 2007) recommended the following ranges for hydrologic moldes with a montly time- step:

Very good: 0.75<NS≤ 1.00

Good: 0.65<NS≤ 0.75

Satisfactory: 0.50<NS≤ 0.65

Unsatisfactory: NS≤ 0.50

However, (Moriasi et al., 2007) noted that the lower NSE are acceptable for a daily time- step calibration. Applying the NSE factor for determining the calibrating of the models, have been widely accepted by other researchers.

PBIAS is the statistical measurement of the average tendency of the simulated parameters (Hydrology, Sediment, Nutrients) to be bigger or smaller than the observtion value (Moriasi et al., 2007). In general, model simulation can be identified as satisfactory if PBIAS ± 25% for streamflow, PBIAS ± 55% for sediment, and PBIAS ± 70% for N and P.

$$\mathrm{PBIAS} = \left[\frac{\sum_{i=1}^{n}(Y_i^{obs} - Y_i^{sim}) \times 100}{\sum_{i=1}^{n}(Y_i^{obs})}\right]$$

Equation 18

Where:

Y_i^{obs}= Observed parameter at observation i

Y_i^{sim}= Simulated model parameter at observation i

i= Observation number

n= Total number of observations

(Moriasi et al., 2007) recommended the following ranges for a sediment model with a monthly time steps.

Very good:	PBIAS≤ ±15
Good:	±15 < PBIAS ≤ ±30
Satisfactory:	±30< PBIAS ≤ ±55
Unsatisfactory:	PBIAS ≤ ±55

CHAPTER 3 STUDY LOCATION DESCRIPTION

This research has been defined to estimate sediment accumulation rate within the reservoirs, and eventually forecasting the remaining storage capacity in the Great Lakes Basin. The study area consists of 12 reservoirs throughout the Great Lakes watershed, as shown in Figure 7.

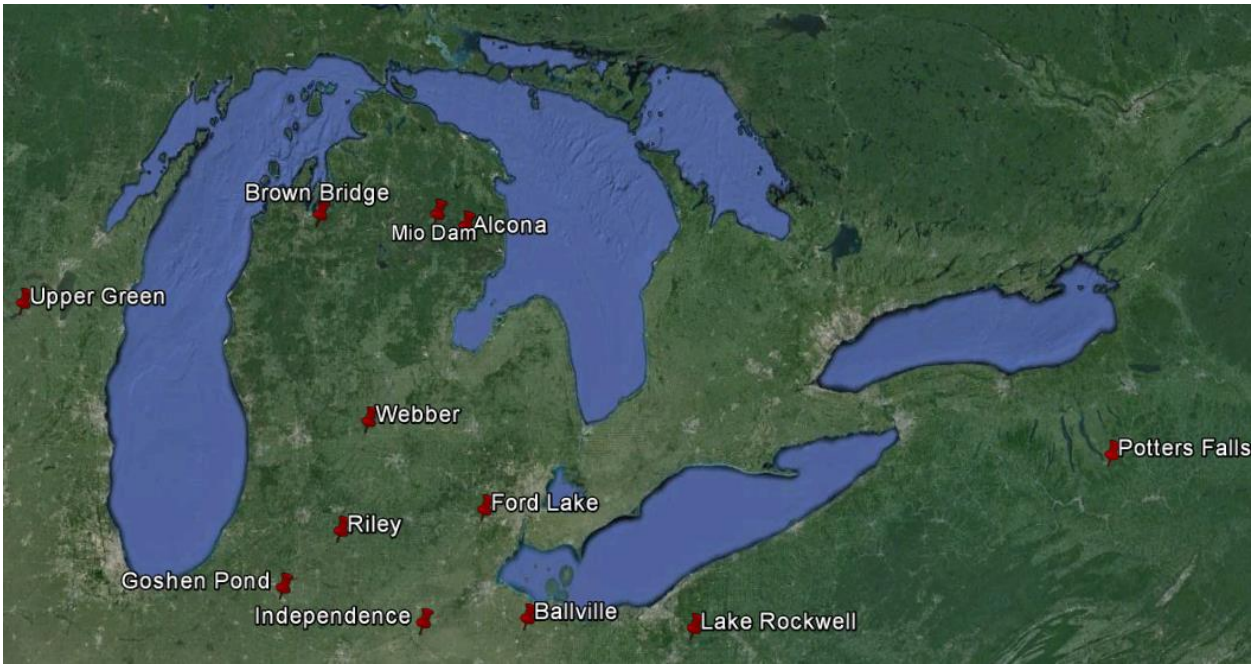

Figure 7- Map of All Selected Reservoir Sites

The emphasis was on reservoirs that drained the agricultural land and a few reservoirs that drained urban land and forest area. The name and location of study reservoirs, the name of rivers contains the study reservoir, and the land use of the study basins are listed in Table 1. Six of the study watersheds are in the state of Michigan, three of them are in the state of Ohio, the rest of three reservoirs are in the state of Indiana, Wisconsin, and New York.

Table 1- All Dams in Study

Dam Name	Location	Primary Land use of Drainage Area	River
Ballville	Fremont, Ohio	Agricultural	Sandusky River
Webber	Lyons, Michigan	Agricultural	Grand River
Riley	Sherwood, Michigan	Agricultural	Saint Joseph River
Upper Green Lake	Green Lake, Wisconsin	Agricultural	Puchyan River
Goshen Pond	Goshen, Indiana	Agricultural	Elkhart River
Independence	Columbus, Ohio	Agricultural	Maumee River
Lake Rockwell	Kent, Ohio	Urban/ Forested	Cuyahoga River
Ford Lake	Ballville, Michigan	Urban/ Forested	Huron River
Potters Falls	Ithaca, New York	Forested	Six-mile Creek
Brown Bridge Pond	Traverse City, Michigan	Forested	Boardman River
Mio	Comins Flats, Michigan	Forested	Au Sable River
Alcona	Oscoda, Michigan	Forested	Au Sable River

3.1. Ballville Dam

Ballville Dam is located along the Sandusky River in the state of Ohio. The dam was constructed in 1911 and has been used as the water supply for the City of Fremont since 1959. During a statewide flood of 1913, the original dam was heavily damaged and had to be enlarged to its present configuration. Ballville Dam is 15 mi (24 km) from the mouth of the Sandusky River, which flows from south to north. Ballville Dam is located on the outskirts of the city of Fremont, Ohio and is owned by the city. There was minor debris removal during the 1904s and 1950s near the penstock intakes (USACE, 1981). There was also a drawdown in 1969 to repair and modify the dam. Because the dam reservoir

is long (11,155 ft) and narrow (less than 490 ft), there is greater flooding and widening of the river upstream of the dam.

Table 2- Reservoir Dara from USACE NID Website

Year Built	Coordinate		Height (ft)	Max-Storage (ac. ft)	Normal-Storage (ac. ft)	Surface Area (ac)	Drainage Area (mi^2)
	Longitude	Latitude					
1911	-83.13615	41.32619	34	2,402	524	89	1,254

The region to the southeast of the watershed is the most elevated. Overland flow direction is from southeast to the southwest and then goes to the north and eventually drains into Ballville reservoir. The topographic slope average in the Ballville Dam watershed is about 2.30%. The steepest subbasins are in the middle and southeast of the watershed. However, the flattest subbasin is northwest and close to the watershed mouth. Knowledge of the watershed topography is required for evaluating sediment yield and transport details.

An additional key factor in investigating the sediment yield and transport is land use of the contributing watershed. Land cover type impacts runoff and soil erosion within a basin. Land use and topography layer (i.e., Digital Elevation map) are both important input features for predicting water and sediment yield in a watershed. Land use in the Ballville Dam watershed is mostly dominated by farmland. However, there are also some forest and urban lands in the study watershed. Figure 8 indicates the land use breakdown in the Ballville Dam watershed in 2001. Approximately 80% of the land is agricultural, with approximately 20% of the land defined as urban and forest. The most important developed areas (Tiffin and Upper Sandusky City) are in the center of the watershed.

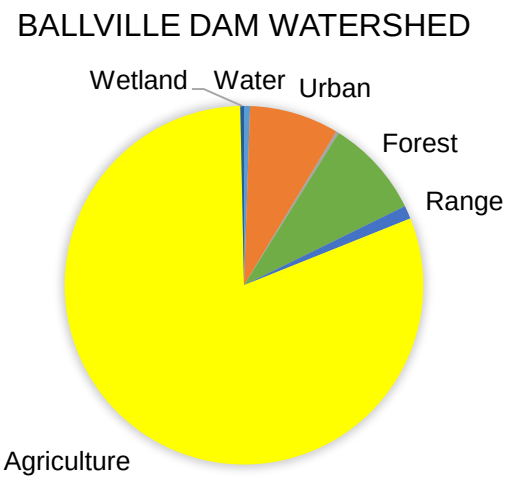

Figure 8- Land Use Breakdown in 2001, National Land Cover Database (Homer et al., 2007)

The United State Geology Survey (USGS) operates several gages on the Sandusky River that record the streamflow and sediment load. The nearest gage upstream of the Ballville Dam reservoir is Gage 04198000 which is about 2 mi (3.2 km) far from the dam, near Fermont City. The drainage area of Gage 04198000 is 1,251 mi^2 (3,240 km^2). Gage 04198000 has a collection history of suspended sediment concentrations from 1950 to 2002 and stream discharge since 1923. There is also another USGS gage upstream of the dam, at Melmore (Gage 04197100). Gage 04197100 has recorded stream discharge since 1927 and suspended sediment load between 1987 and 1989. Gage locations are highlighted in Figure 9.

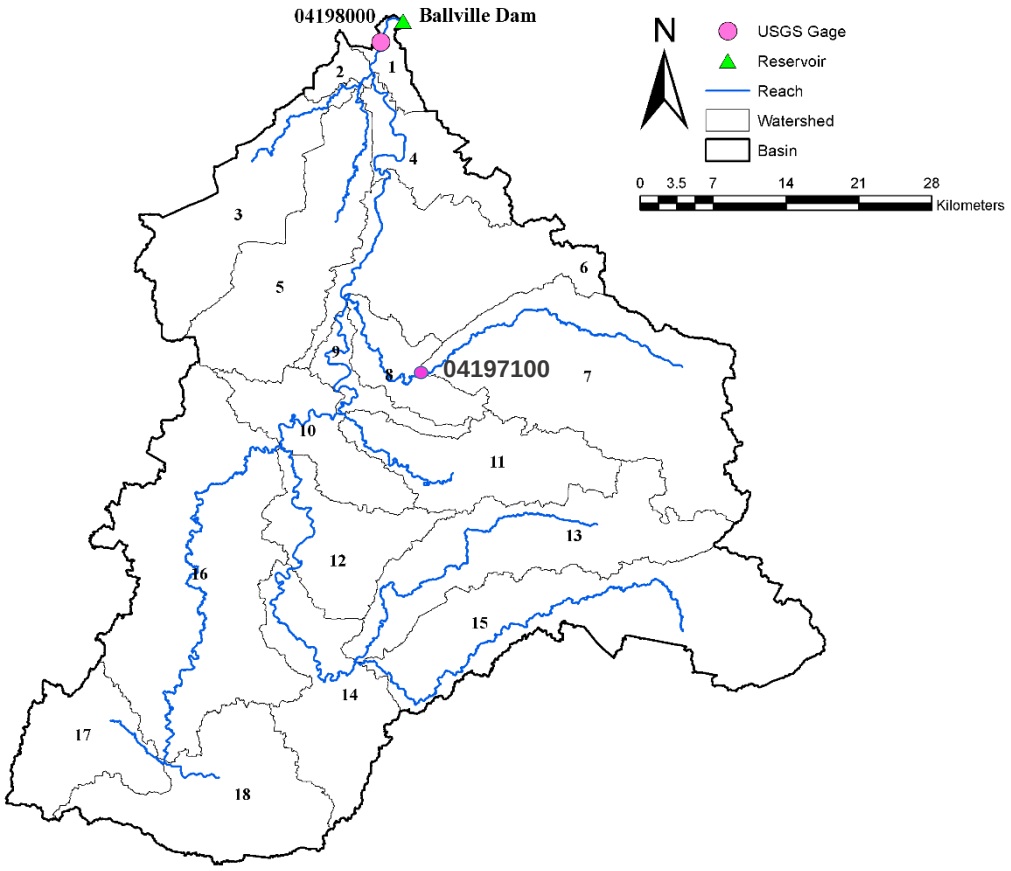

Figure 9- USGS Gages in the Sandusky River Watershed

An analysis was conducted for the gage upstream of the Ballville Dam to determine years when significant flooding occurred. The sediment load carried into a reservoir is at its highest value during floods. Typically, half of a river's annual sediment load is associated with just 5 to 10 days of flood discharge (McCully, 1996). The magnitude of transported sediment is related to the storm's duration, time, and magnitude (Rovira and Batalla, 2006). Several major floods have occurred at the Ballville Dam watershed since its construction. Figure 10 displays the annual peak streamflow at Gage 04198000 and 04197100.

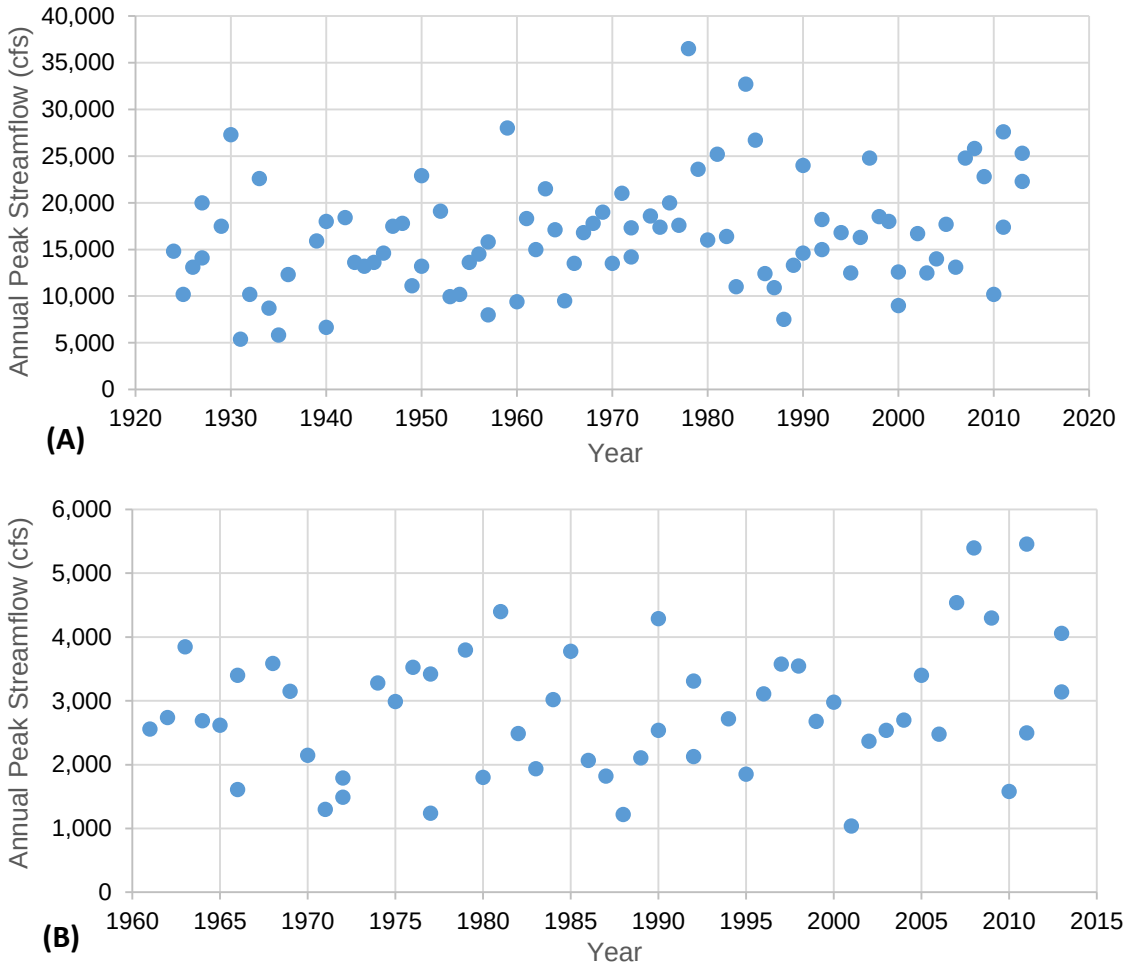

Figure 10- Annual Peak Streamflow for (A) Gage 04198000; near Fermont, (B) Gage 04197100; at Melmore

The highest record discharge was 36,500 cfs (1,033 cms) in 1978, although the peak stream discharge of 63,500 cfs (1,798 cms) happened in 1913 (Evans et al., 2002). The normal frequency analyses have been done on peak stream discharge at Gage 04198000 and 04197100. The corresponding stream discharge for each of the recurrence interval is provided in Table 3. The 500-year and 100-year recurrence interval events correspondent to 34,000 cfs (963 cms) and 30,000 cfs (849 cms), respectively. Therefore, the historically large flood events in 1913 and 1978 exceeded the 500-year flood event. Other significant floods occurred in 1927, 1930, 1933, 1950, 1959, 1963, 1971, 1979, 1981, 1984, 1985, 1990, and 1997 (USGS, 2002)."

Table 3- The Magnitude of Different Recurrence Interval

Recurrence	Stream Flow Discharge (cfs)	
	Gage 04198000	Gage 04197100
1.5- yr	13,793	2,420
5- yr	21,332	3,706
50- yr	30,605	4,926
100- yr	32,896	5,200
500- yr	37,708	5,758

The rating curves relate the suspended sediment load to the stream discharge, and they can describe the relationship between stream discharge, and suspended sediment discharge. Figure 11 and Figure 12 display the rating curve for Gage 04198000 and 04197100, respectively. Note that the R^2 value for both gages within the Ballville watershed is above 0.90, which suggests a good fit in the developed relationship to the observed stream and sediment discharge data.

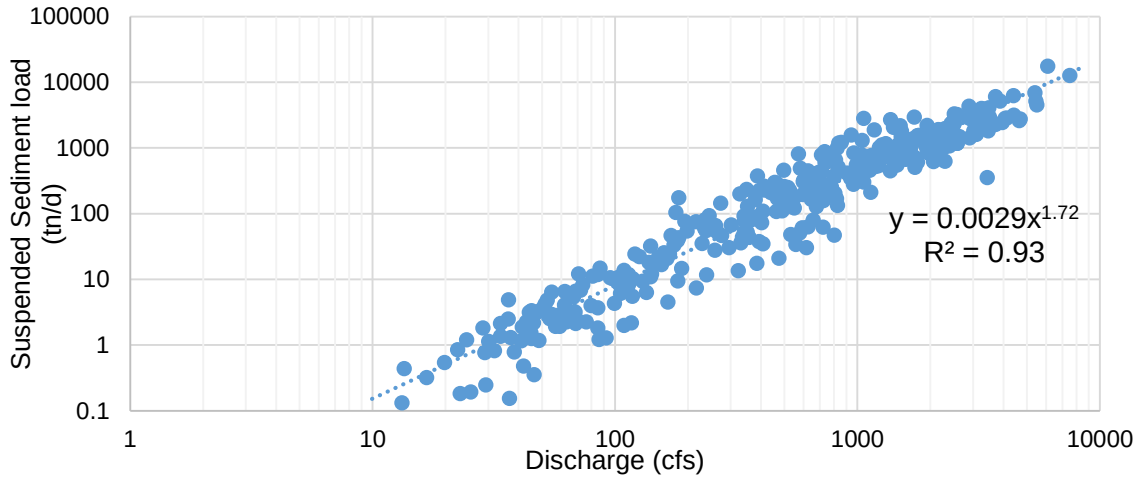

Figure 11- Rating Curve for Gage 04198000 from 1950 to 2002

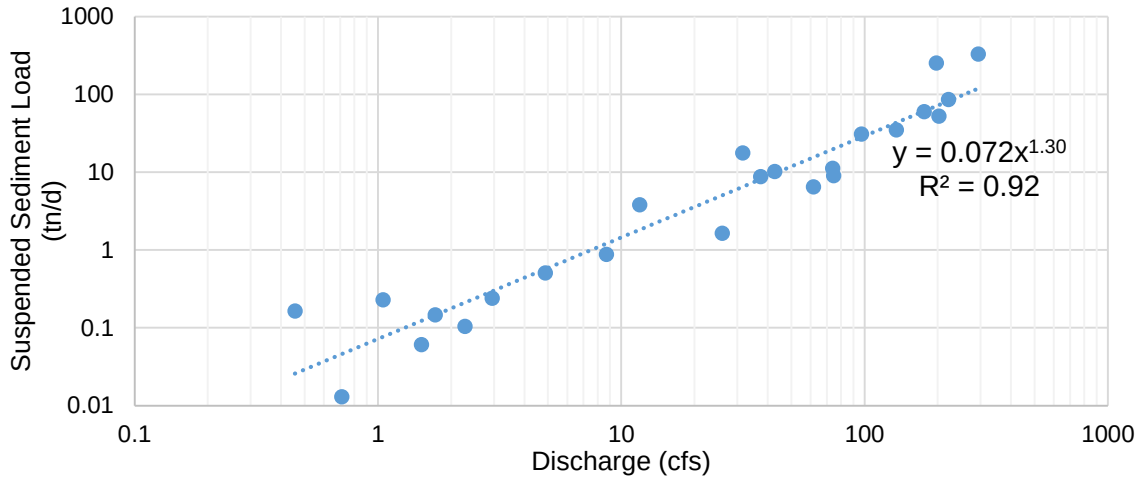

Figure 12- Rating Curve for Gage 04197100 from 1987 to 1989

3.2. Webber Dam

Webber Dam was built on the Grand River in Ionia County, the state of Michigan in 1907. Webber Dam operation began on March 12, 1907. The Webber Dam is an earth embankment dam with a concrete core wall. Dam is providing the generating stations to the Commonwealth Power Company. Grand River is the longest river in the state of Michigan; with some major and minor tributaries. Grand River watershed has the second largest drainage area in Michigan, and with 5,572 mi^2 (14,431 km^2) area, comprise 13% of the Lake Michigan basin. However, in this project, just a part of the Grand River watershed, which contains Webber Dam has been investigated. The drainage area of Webber Dam is 1,750 mi^2 (4,532 km^2) as reported by the National Inventory of Dams, and the impounded lake at its normal retention level is 660 ac (267 ha). Table 4 displays the characteristic of eleven reservoirs including Webber Dam, which are on Grand River as reported on the NID website.

Table 4- Reservoirs Data from USACE NID Website

Dam Name	Sub-Basin	Year Built	Height (ft)	Max Storage (ac. ft)	Normal Storage (ac. ft)	Surface Area (ac)
Grand Ledge	18	1900	8	1,200	1,200	1
Holton	30	1936	15	1,000	8	1
Hubbardston	4	1850	26	420	385	35
Lyons	12	1900	18	1,820	620	120
Michigan Center	31	1911	9	8,000	5,280	2,160
Minard Mill	29	1944	8	170	110	41
North Lansing	19	1936	20	1,810	500	92
Rainbow Lake	1	1962	46	5,400	4,000	238
Sterner	8	1921	13	85	65	4
Webber	13	1907	30	6,000	6,000	660
Wilson	24	1880	12	190	60	13

With respect to topography, the southern portion of the Webber Dam watershed is more elevated than north. The river flows from south to the north, then join to the other tributary that is coming from east to west, and eventually they drain out of the watershed. The Webber Dam watershed is pretty flat, with an average slope of about 3%.

Webber Dam watershed is an area dominated mostly by farmland, with some forest, urban, and wetland. Figure 13 indicates the land use breakdown in Webber Dam watershed in 2001. Approximately 60% of the land is farmland and the rest is developed, forest, and wetland. The southern part of the watershed is mostly covered by forest, while the north and middle part are mostly farmland. The Cities of Lansing and Jackson are two important urban areas in this watershed.

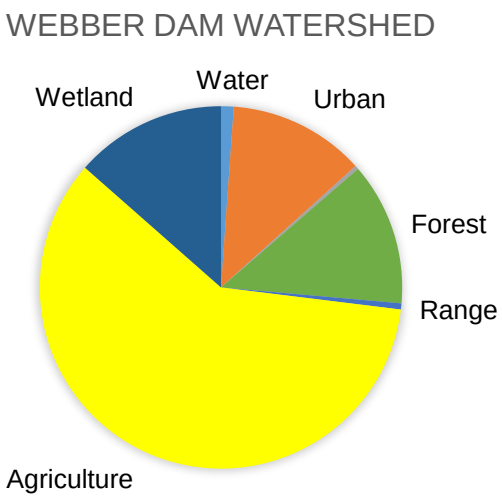

Figure 13- Land Use Breakdown in 2001, National Land Cover Database (Homer et al., 2007)

There are several USGS gages in the study watershed, but some of them are not active anymore. Three active gages have been selected for analysis in this research. The nearest gage upstream of the Webber Dam is at Portland, Ionia County (Gage 04114000). Gage 04114000 has recorded stream discharge since 1952; the further gage upstream of the dam is Gage 04113000 at Lansing, Ingham County, which has stream discharge records dating back to 1901. The gage downstream of the dam is Gage 04116000 at Ionia, Ionia County, and has recorded stream discharge since 1931. Unfortunately, no gage in the watershed has recorded suspended sediment load. The drainage area of Gage 04113000 is about 1,230 mi^2 (3,186 km^2) and Gage 04114000 is 1,385 mi^2 (3,587 km^2), and Gage 04116000 is about 2,840 mi^2 (7,356 km^2). The location of eleven reservoirs and three gages have been shown in Figure 14. Gage 0411600 is the closest to the outlet; this gage can provide good information about the flow that leaves the watershed.

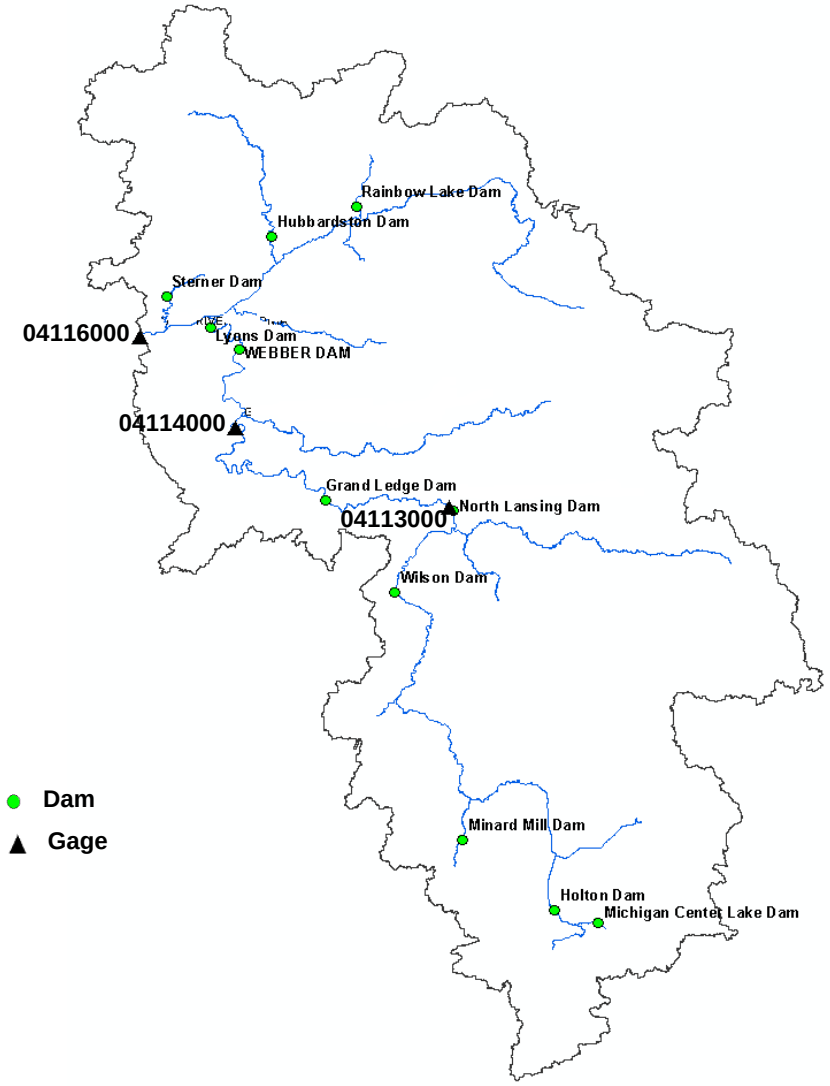

Figure 14- USGS Gages in the Grand River Watershed

A gage analysis was conducted to determine years when significant flooding occurred. Several major floods have occurred on the Grand River watershed. Figure 15 displays the annual peak streamflow at the three USGS gages used in the analysis. The highest record of discharge was about 25,000 cfs (708 cms) in 1904 before Webber Dam construction. There were also some other floods in 1947, 1975, and 2004.

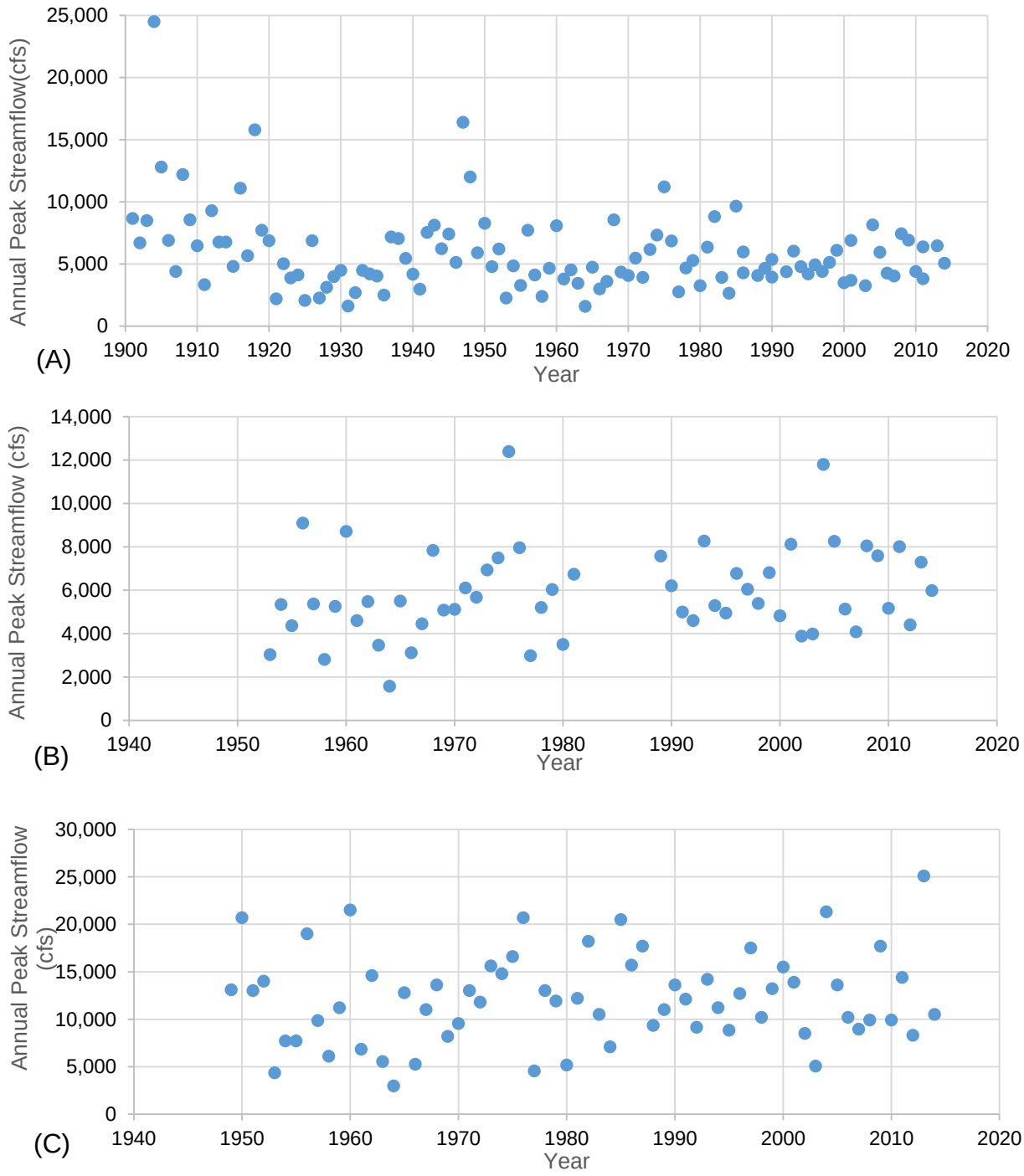

Figure 15- Annual Peak Streamflow for (A) Gage 04113000, at Lansing, (B) Gage 04114000, at Portland, and (C) Gage 04116000, at Ionia

The results of the frequency analysis are shown in Table 5. The highest recorded event at Gage 0411600 is 25,000 cfs in 1904 approaches the 500-year recurrence event.

Table 5- The Magnitude of Different Recurrence Interval

Storm Events	Stream Flow Discharge (cfs)		
	Gage 04113000	Gage 04114000	Gage 04116000
1.5- yr	4,463	5,017	10,143
5- yr	8,533	7,654	16,159
50- yr	12,395	10,156	21,868
100- yr	13,264	10,718	23,151
500- yr	15,029	11,862	25,760

3.3. Riley Dam

Riley Dam was constructed in 1923 in the state of Michigan, with the formation of Union Lake. Prior to 1923 the St. Joseph River meandered through the present impounded area on the north side of the Union Lake. Riley Dam impounds Union Lake in Branch County. The dam is located in the St. Joseph River basin on the main branch of the St. Joseph River, just downstream of Union City. Although it has been suggested that dam has caused a significant reduction in downstream delivery, this has not been documented (Creech et al., 2010). Previous studies have concluded that the Riley Dam sub-watershed area consisted primarily of forest, wetland, and savanna land uses prior to the construction of the dam (Comer and Albert, 1998). The sediment trapping efficiency of the dams upstream of the Riley Dam are unknown. However, the reduction in sediment delivery to downstream areas is significant (Creech et al., 2010). The drainage area of Riley Dam is 523 mi^2 (1,354 km^2). The impounded lake has a surface area of 518 acres (209 ha). Table 6 shows the characteristic of some reservoirs including Riley Dam built on St. Joseph River watershed as displayed on the NID website.

Table 6- Reservoirs Data from USACE NID

Dam	Sub-Basin	Year Built	Height (ft)	Normal Storage (ac. ft)	Max Storage (ac. ft)	Pond Area (ac)
Riley-3	9	1923	20	3,240	5,760	518
Marble Lake-2	26	1962	6	1,968	1,946	766

Riley Dam watershed is an area dominated by farmland, with some forest, urban and wetland. Figure 16 displays the land use breakdown in the Riley Dam watershed in 2001. About 60% of the land is farm, 15% wetland, 12% forest, 10% urban, and the rest of the land is rangeland and water.

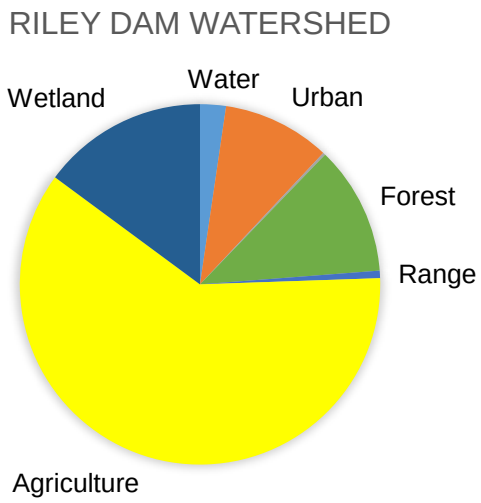

Figure 16- Land Use Breakdown in 2001, National Land Cover Database (Homer et al., 2007)

East part of the watershed is more elevated than the west and north- west, so the stream direction is from east to the west. Within this watershed, the maximum elevation is 390 (m) and the minimum is 261 (m). The study watershed is pretty flat, with an average slope of 2.1%. However, the eastern portions of the watershed are steeper than the west, and in some eastern areas, the slope exceeds 5%.

There are several USGS gages that have recorded stream discharge in the Riley Dam watershed. However, only Gage 04096405 records the recent stream discharge.

Others have data collection that ceased in the late 1970's and these are not especially useful for present-day calibration efforts. Therefore, the SWAT model was calibrated to the monthly average streamflow as measured at Gage 04096405. The gage is located at the upstream portion of the Riley Dam on St. Joseph River at Burlington. Gage 04096405 is pretty close to the watershed outlet, and its drainage area is 206 mi^2 (533 km^2). There is not any gage in the watershed that collects recent sediment load data. Figure 17 displays the gage and dams location.

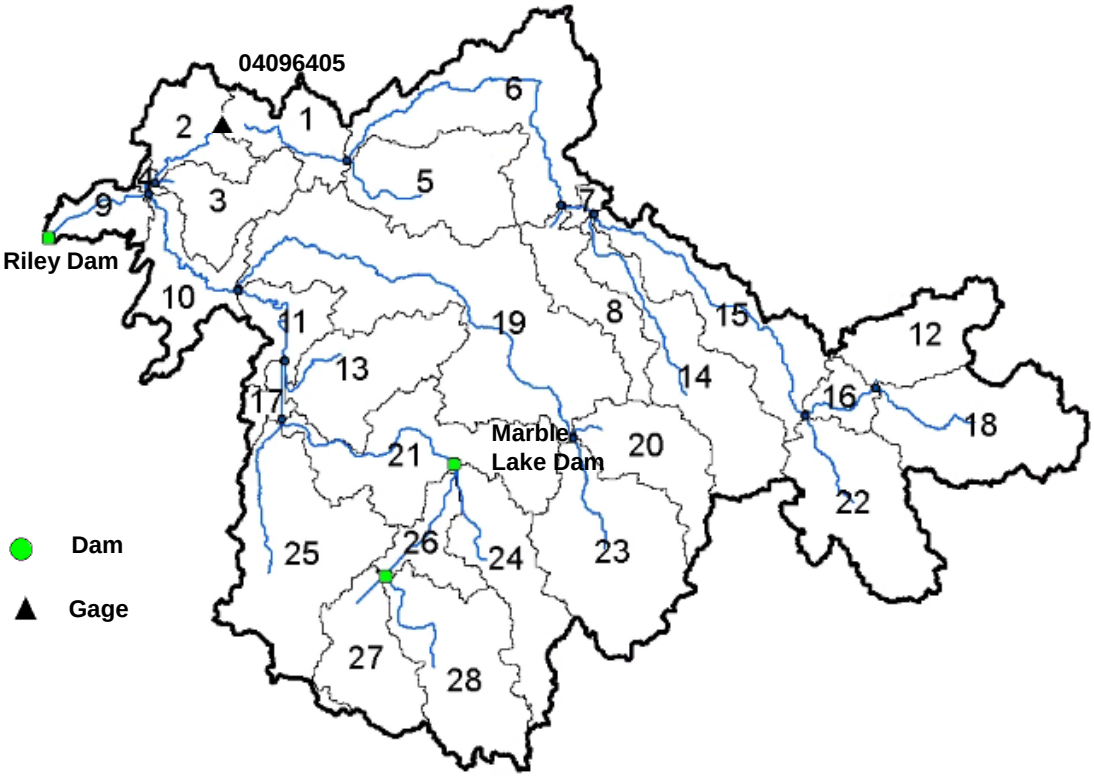

Figure 17- USGS Gage in the St. Joseph River Watershed

Figure 18 displays the peak streamflow at Gage 04096405; the highest record discharge was about 1,340 cfs (38 cms) in 1982 and 1,400 cfs (40 cms) in 1989.

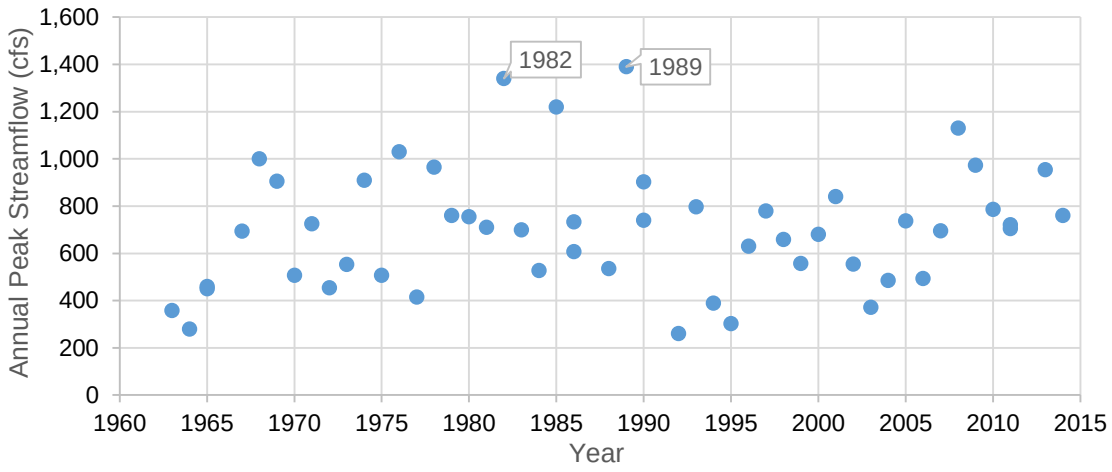

Figure 18- Annual Peak Streamflow for USGS 04096405; St. Joseph River at Burlington

Normal frequency analyses were conducted to the gage at the upstream of the dam to determine the stream discharges equivalent to different year recurrence interval. The results of normal frequency analyses are given in Table 7. As the results show the peak stream flow at Gage 04096405 exceeded to 100- year recurrent interval in 1982 and 1989.

Table 7- The Magnitude of Different Recurrence Interval

Storm Events	Stream Flow Discharge (cfs)
	Gage 04096405
1.5- yr	591
5- yr	914
50- yr	1,221
100- yr	1,290
500- yr	1,430

Four of the gages within Riley Dam watershed recorded suspended sediment load from 1974 to 1977. Figure 19 through Figure 22 display the sediment rating curve of each gage. The R^2 of the developed equation representing each gage varies between 0.41 to 0.80.

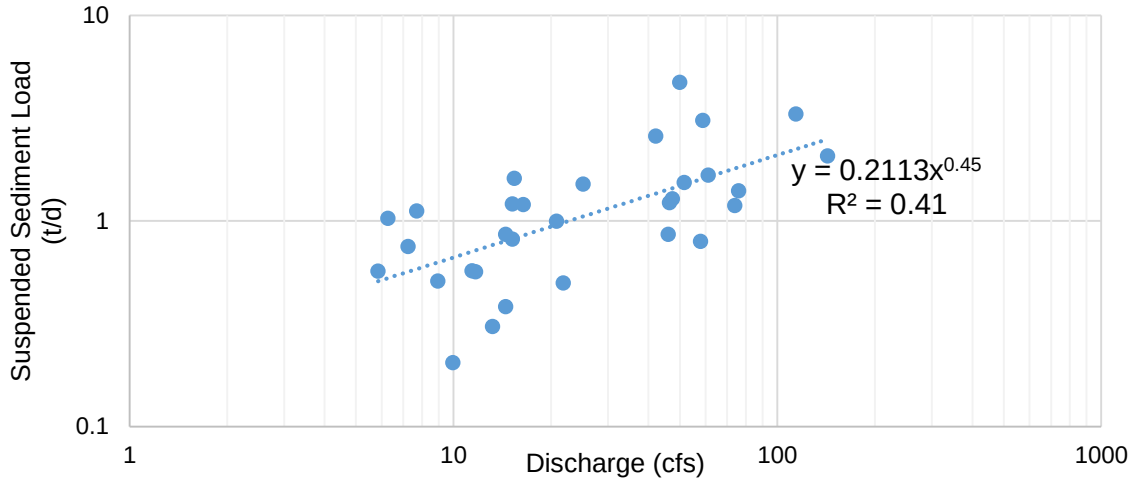

Figure 19- Rating Curve for Gage 04096272 from 1974 to 1977

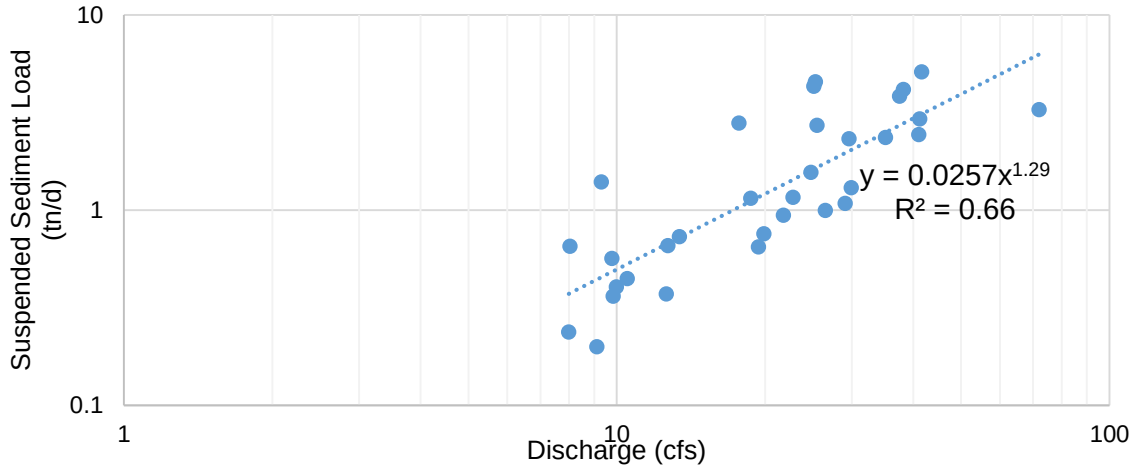

Figure 20- Rating Curve for Gage 04096312 from 1974 to 1977

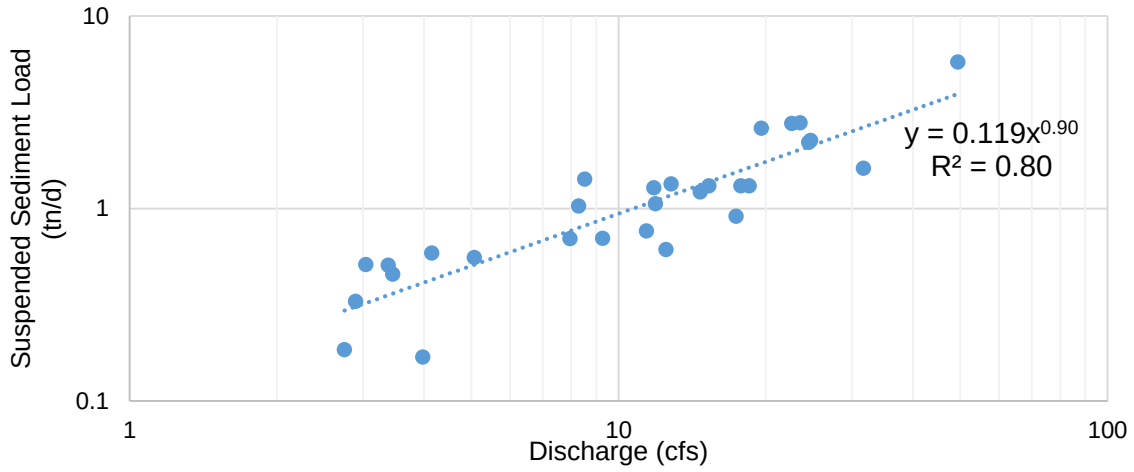

Figure 21- Rating Curve for Gage 04096325 from 1974 to 1977

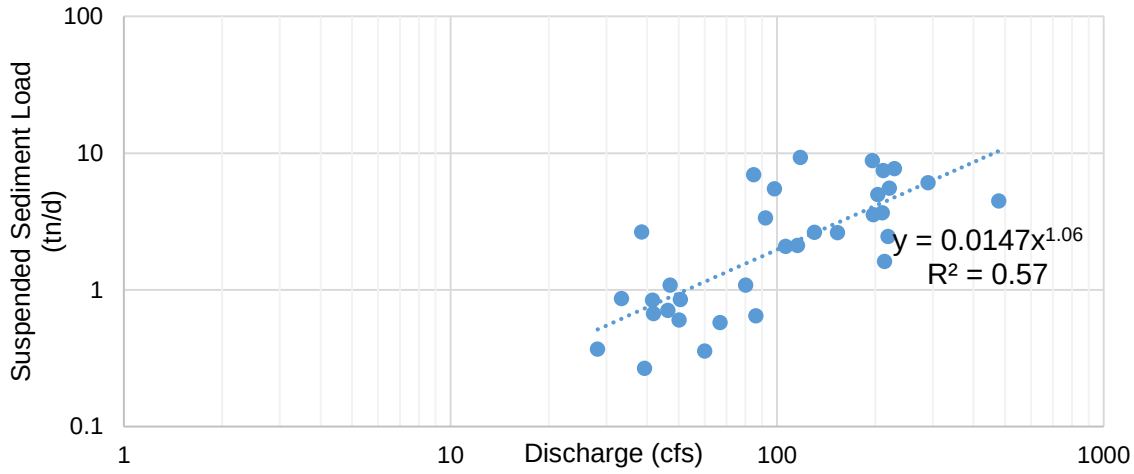

Figure 22- Rating Curve for Gage 04096340 from 1974 to 1977

3.4. Upper Green Lake Dam

Upper Green Lake Dam was constructed in 1869 in the state of Wisconsin and modified in 1994. Upper Green Lake Dam, which impounds Green Lake, is downstream of Ripon, Wisconsin. The dam is located on the Puchyan River which drains into the Fox River and ultimately into Lake Michigan at Green Bay. According to the Dartford Historical Society, the Green Lake area reported high water level that threatened the dam (Heiple and Heiple, 1977). In 1987, the bulk head on the dam was replaced and water levels returned to normal levels. The drainage area of Upper Green Dam is 115 mi^2 (298 km^2) as reported by the National Inventory of Dams and the impounded lake at its normal retention level is 7,346 ac (2,973 ha). Table 8 shows the characteristic of Upper Green Dam as displayed on the NID website.

Table 8- Reservoirs Data from USACE NID

Year Built	Height (ft)	Max Discharge cfs	Normal Storage (ac. ft)	Max Storage (ac. ft)	Drainage Area (mi^2)
1869	8	414	30,000	40,000	115

The Upper Green Dam watershed is a pretty flat watershed, and the average slope is about 3%. This study watershed is an area dominated mostly by agricultural land, with some forest, urban, and wetland. Figure 23 displays the land use breakdown in the Upper Green watershed in 2001. Over 60% of the watershed is farmland, 10% of the watershed is a wetland, the rest is developed and forest. In this watershed, the most important urban area is the City of Ripon with about five mi^2 (13 km^2) area.

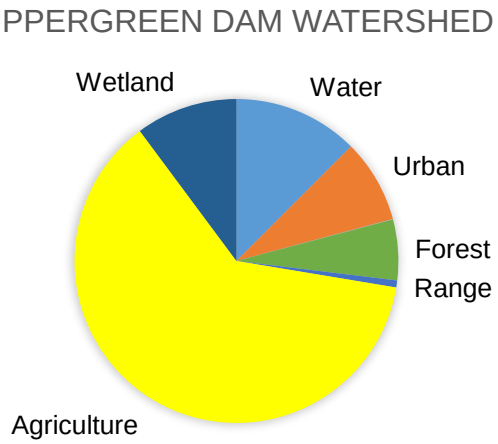

Figure 23- Land Use Breakdown in 2001, National Land Cover Database (Homer et al., 2007)

There are several USGS gages in the study watershed, but some of them are not active anymore, and they just contained very old data. The location of the reservoir and gages have been shown in Figure 24.

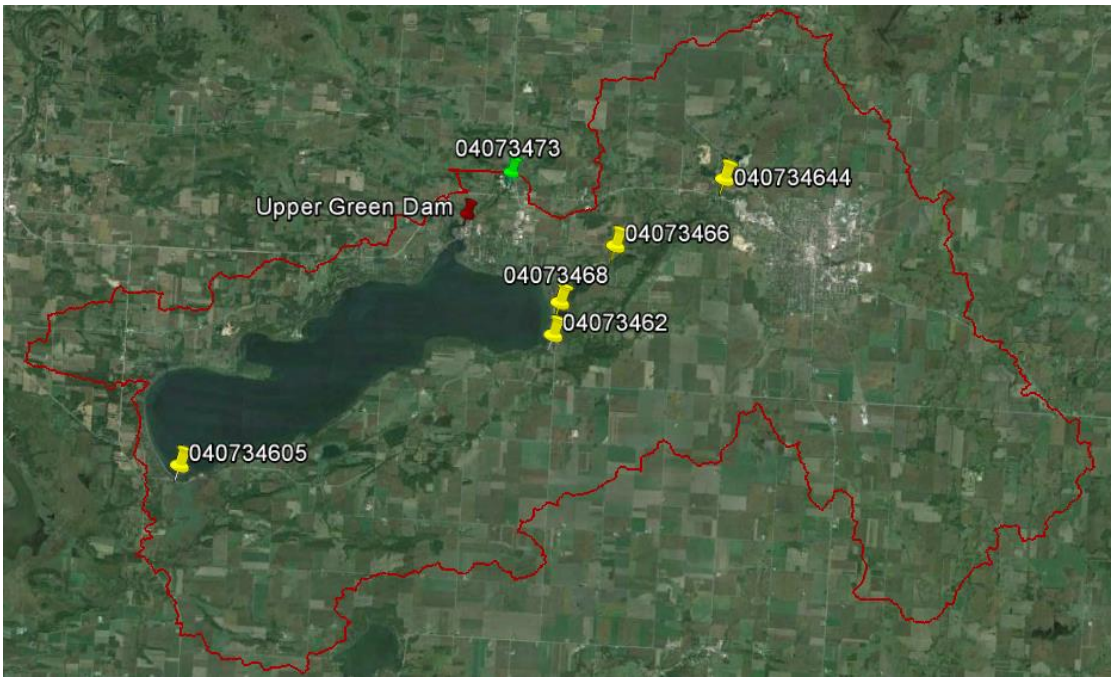

Figure 24- Upper Green Dam River Watershed

The nearest gage upstream of the Upper Green reservoir is gage 04073462, with a drainage area of 3.05 mi^2 (8 km^2) in Green Lake County, Wisconsin. Gage 04073462 recorded stream discharge from 1981 to 1988, and after some years off, it has started recording stream discharge since 1996. Gage 04073473, with a drainage area of 105 mi^2 (272 km^2) has been collecting stream flow since 1996. Gage 04073473 is located a mile northeast of the dam at the outlet of Green Lake. The average of monthly stream discharge at Gage 04073473 has been used for calibrating the study watershed. There is no gage in the watershed recorded recently suspended sediment load.

Some major floods have occurred within Upper Green Lake watershed since its construction. Flooding events can cause a considerable sediment yield. Therefore, a normal flood frequency analyses were conducted to the gages in the study watershed to determine years when the significant flood happened. Figure 25 displays the annual peak

streamflow at Gage 04073462 and 04073473, respectively. The big flood happened in 2008, which its flow exceeded 500-year recurrence interval.

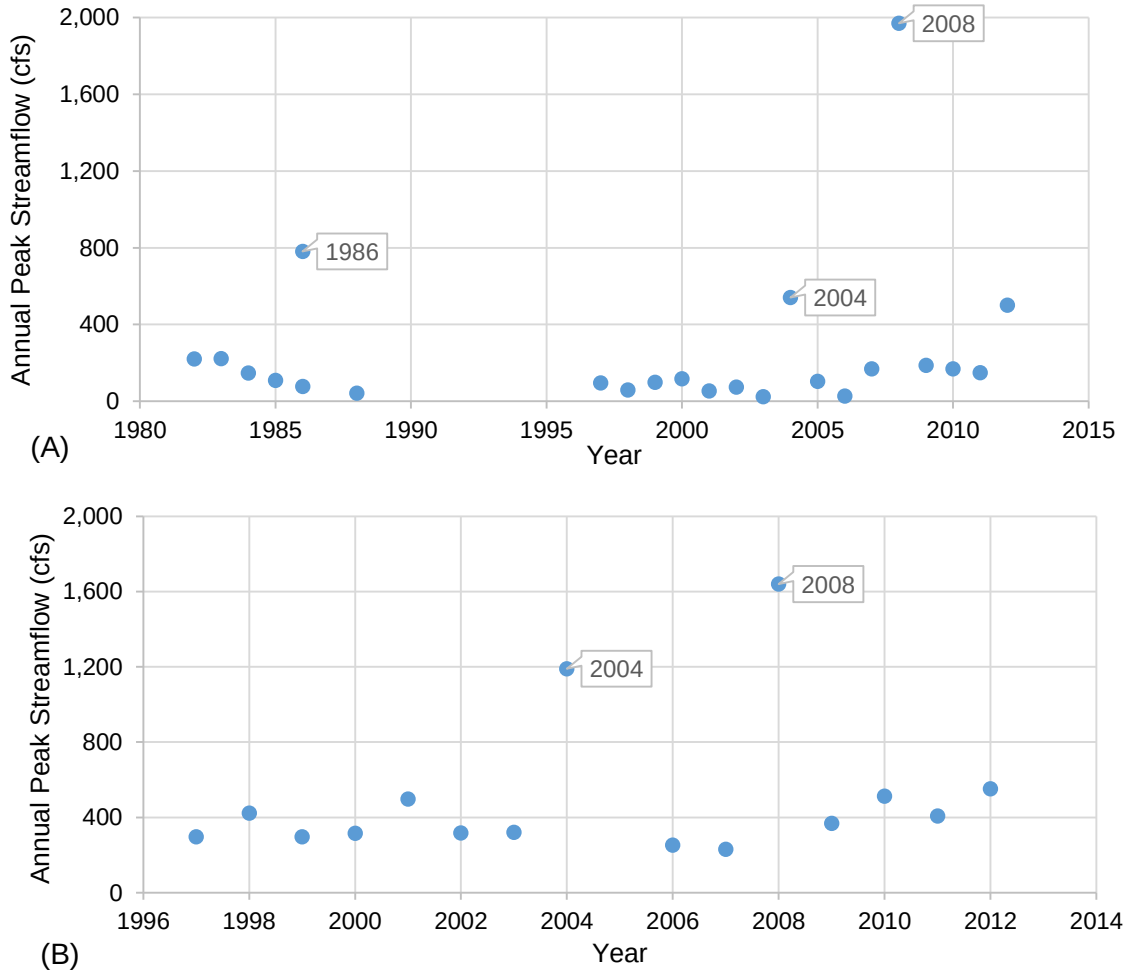

Figure 25- Annual Peak Streamflow for (A) Gage 04073462 and (B) Gage 04073473

The results of flood frequency analyses are given in Table 9. Except flood event which it's flood magnitude exceeded 500- year flood event, there was also another flood in 2004 but in two different months. For Gage 04073462, this peak occurred on May 23, 2004, at 540 cfs (15 cms), for Gage 04073473 this peak occurred on June 11th, 2004 at 1,640 cfs (46 cms). Dartford Historical Society reported the peak discharge of 781 cfs (22 cms) on September 10th in 1987 for the Gage 04073462, in this time the bulkhead on the dam was replaced, and water levels returned to normal levels.

Table 9- The Magnitude of Different Recurrence Interval

Storm Events	Stream Flow Discharge (cfs)	
	Gage 04073462	Gage 04073473
1.5- yr	83	347
5- yr	602	827
50- yr	1,094	1,282
100- yr	1,205	1,384
500- yr	1,430	1,592

Some gages within the Upper Green Watershed recorded suspended sediment concentration, suspended sediment discharge, and stream discharge. The sediment rating curve was developed for each gage. Figure 26 through Figure 30 display the observed data and sediment rating curve for each gage. The R^2 values corresponding to the sediment rating curves vary between 0.58 and 0.84.

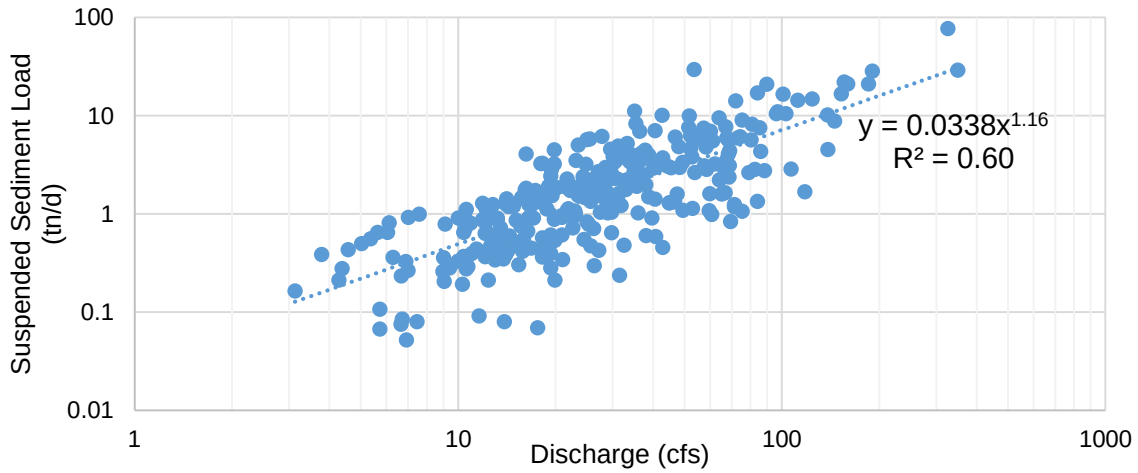

Figure 26- Rating Curve for Gage 04073468 from 1987 to 2012

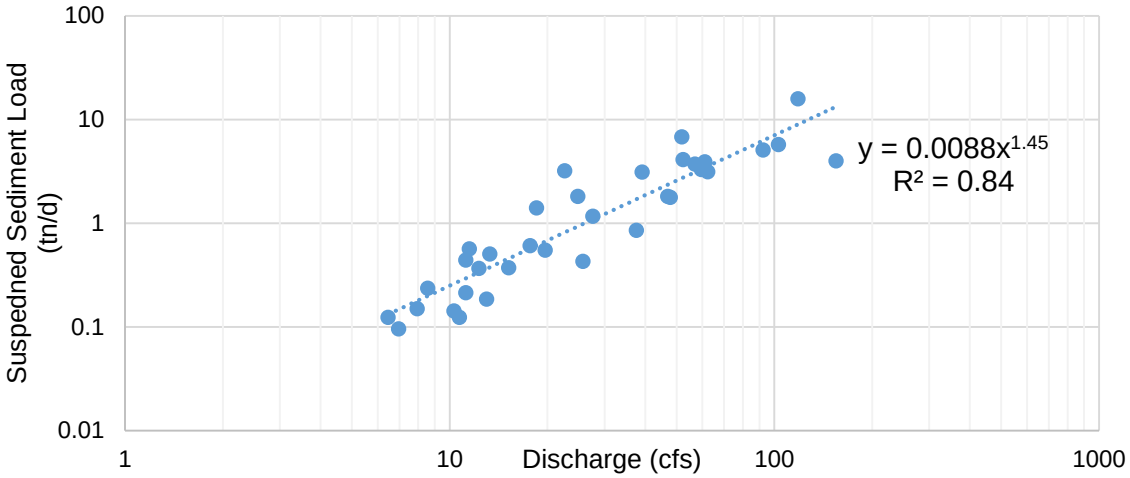

Figure 27- Rating Curve for Gage 04073466 from 2012 to 2014

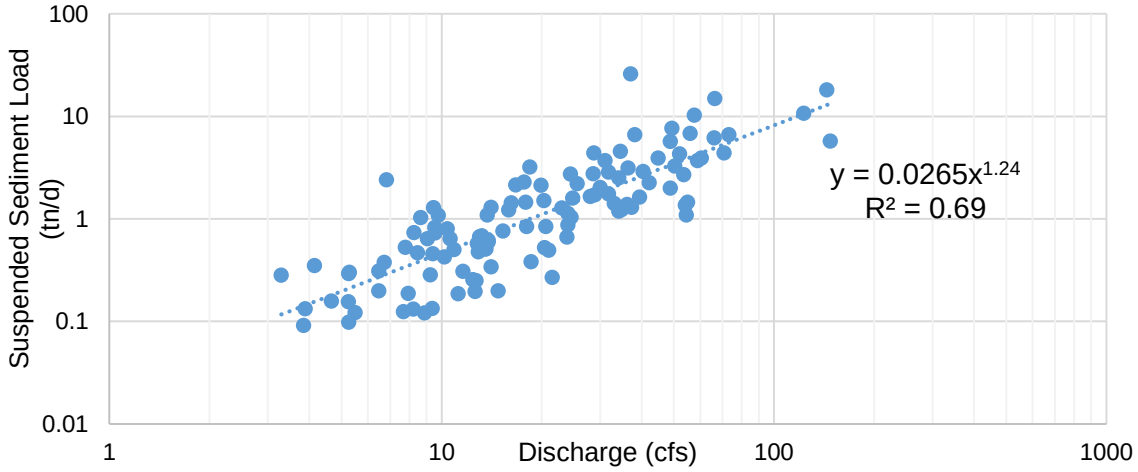

Figure 28- Rating Curve for Gage 040734644 from 1987 to 1996

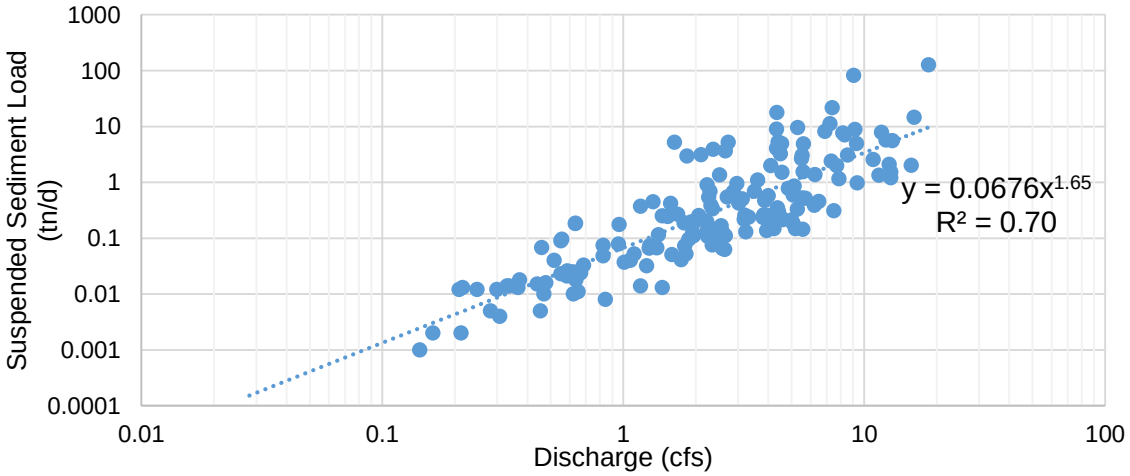

Figure 29- Rating Curve for Gage 04073462 from 1982 to 2003

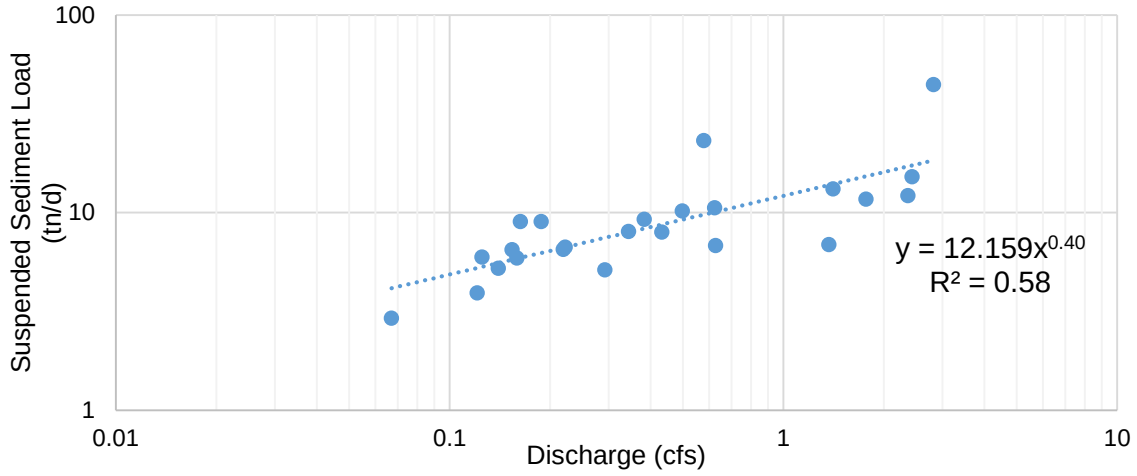

Figure 30- Rating Curve for Gage 040734605 from 2012 to 2014

3.5. Goshen Pond Dam

The Goshen Pond Dam began construction in 1866, and was completed in 1868 to supply power for milling and later hydroelectric power generation. Goshen Pond Dam is located in Elkhart County, Indiana and sits on the Elkhart River which drains into the St. Joseph River. The drainage area of Goshen Pond Dam is 590 mi^2 (1,528 km^2) as calculated by the National Inventory of Dams (NID 2010). The impounded lake is 122 ac (49 ha) in size. Several dams including Goshen Pound Dam have been built on the Elkhart River. Table 10 displays dams and their associated reservoir characteristic.

Table 10- Reservoirs Data from USACE NID Website

Dam	Sub-Basin	Year Built	Height (ft)	Pond Area (ac)	Normal Storage (ac. ft)	Max Storage (ac. ft)
Goshen Pond	1	1868	16	122	930	3,100
Sylvan Lake	4	1837	30	618	5,986	7,400
Lake Barbara	12	1979	11	69	613	886
Adams Lake	2	1952	7	269	942	942
Syracuse Lake	9		8	414	1,760	1,760

Goshen Pond Dam watershed is an area dominated by agricultural land with some urban, forest, and wetland area. Figure 31 indicates the land use breakdown in Goshen

Pond Dam watershed in 2001. Approximately 70% of the land is farmland and the rest of the land is urban, forest, and wetland.

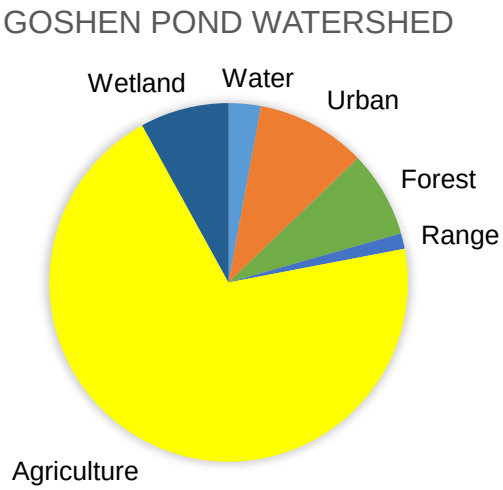

Figure 31- Land Use Breakdown in 2001, National Land Cover Database (Homer et al., 2007)

Some USGS gages are located on Goshen Pond Dam watershed, Gage 04100500 is located downstream of the Goshen Dam in Elkhart County, Indiana and records the recent stream flow. Figure 32 shows the gage and dams location in the study watershed. Within Goshen Pond Dam watershed, no gage has recorded the recent suspended sediment load.

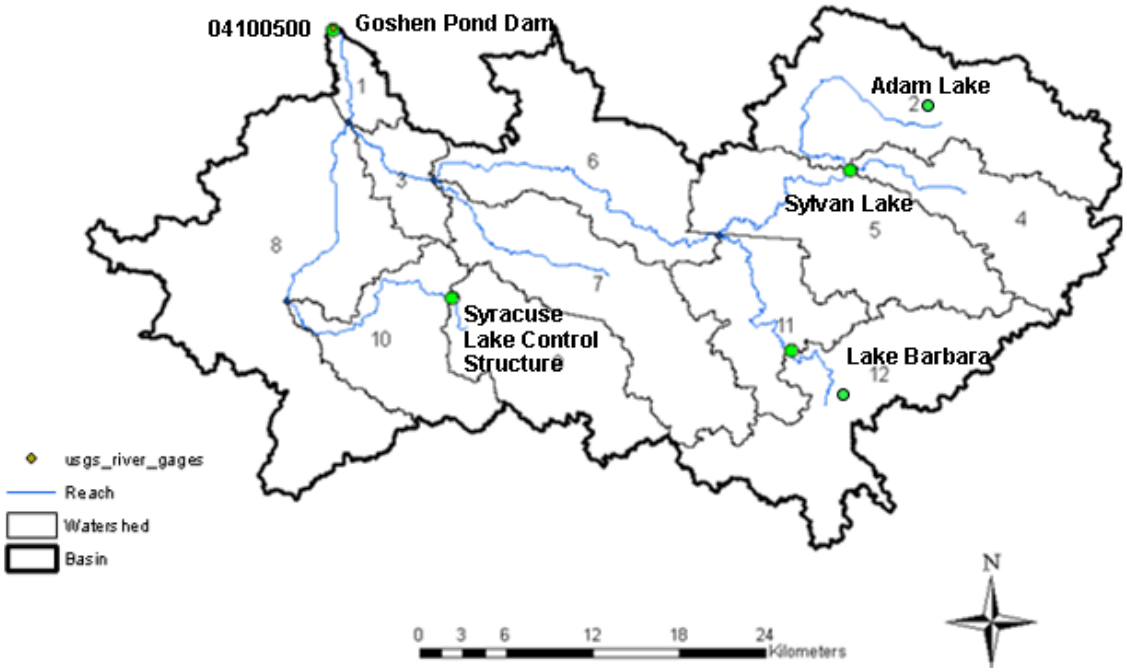

Figure 32- USGS Gage in the Elkhart River Watershed

Figure 33 displays the annual peak streamflow at Gage 04100500. The highest record discharge of 6,360 cfs (180 cms) and 6,189 cfs (175 cms) happened in 1982 and 1985, respectively.

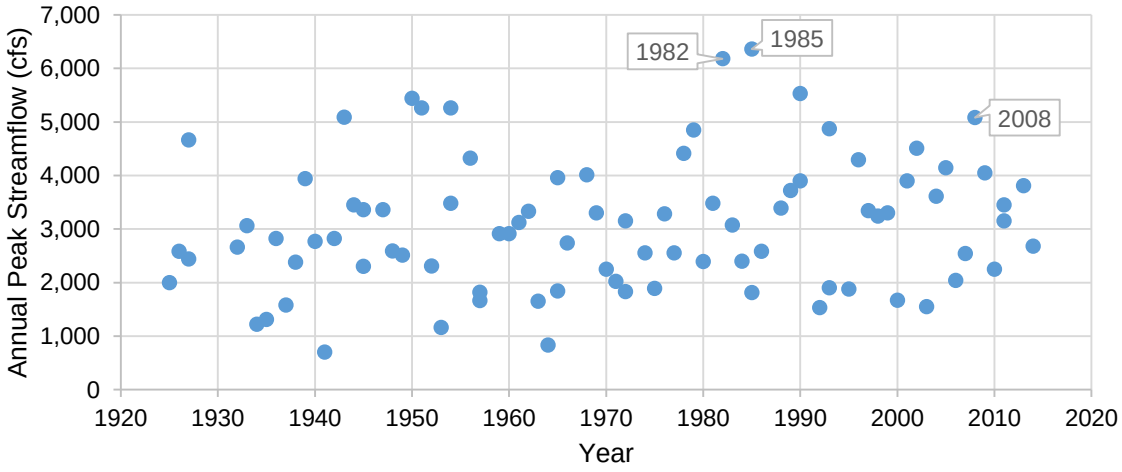

Figure 33- Annual Peak Streamflow for Gage 04100500; Elkhart River at Goshen,

Significant flood events are expected to provide the considerable loads of sediment to the dams and maybe reflected in the sediment accumulation. Several major floods

have occurred on Elkhart River watershed in Goshen Pond Dam watershed. The normal flood- frequency analyses have been conducted on Gage 04100500. The results of flood frequency are given in Table 11, the flood events in 1982 and 1985 exceeded the flood magnitude of 100- year recurrence interval.

Table 11- Stream Discharge Corresponding to Various Recurrence Levels

Recurrence	Stream Flow Discharge (cfs)
	Gage 04100500
1.5- yr	2,538
5- yr	4,098
50- yr	5,568
100- yr	5,898
500- yr	6,570

3.6. Independence Dam

Independence Dam is located near the city of Defiance, in the state of Ohio on the Maumee River. The River is located near Ft. Wayne, Indiana and flows towards Toledo, where the river spills into Lake Erie. Independence Dam is a low head dam owned by the Ohio Department of Natural Resources. According to the National Inventory of Dams Database, the Independence Dam serves a drainage area of 5,545 mi^2 (14,361 km^2) consisting primarily of agricultural land. There are not many trees located along the Maumee River. According to documentation obtained from the U.S Fish and Wildlife website, only 3 to 5 % of the Maumee River Basin remains wooded, which is due to agricultural purposes. The existing dam on the Maumee River was completed in 1924. This cement dam replaced the original wooden dam which was built in the 1800s for the canal system (Evans et al., 2002). Figure 34 displays the land use break down in the part of Maumee River watershed which contains the Independence Dam. Approximately 78%

of the study watershed is covered by agricultural land, about 11%, and 7% of the watershed are developed area and forest land, respectively.

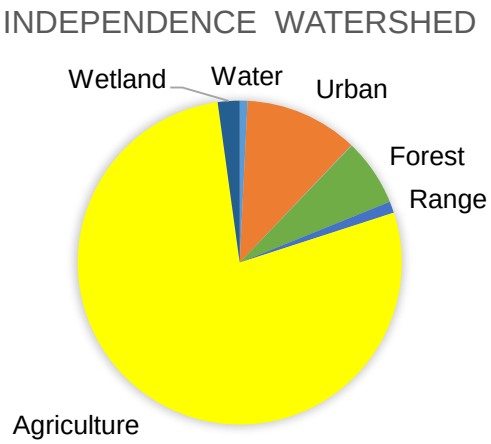

Figure 34- Land Use Breakdown in 2001, National Land Cover Database (Homer et al., 2007)

There are several gages within Independence Dam watershed, among these gages, Gage 04193500 and 04192500 have collected stream discharge and suspended sediment load. Figure 35 displays the location of the reservoirs and each gage within the Independence Dam watershed. Gage 04193500 with the drainage area of 6,330 mi^2 (10,187 km^2) located downstream of the dam, and Gage 04192500 with the drainage area of 5,545 mi^2 (16,394 km^2) located just upstream of the dam.

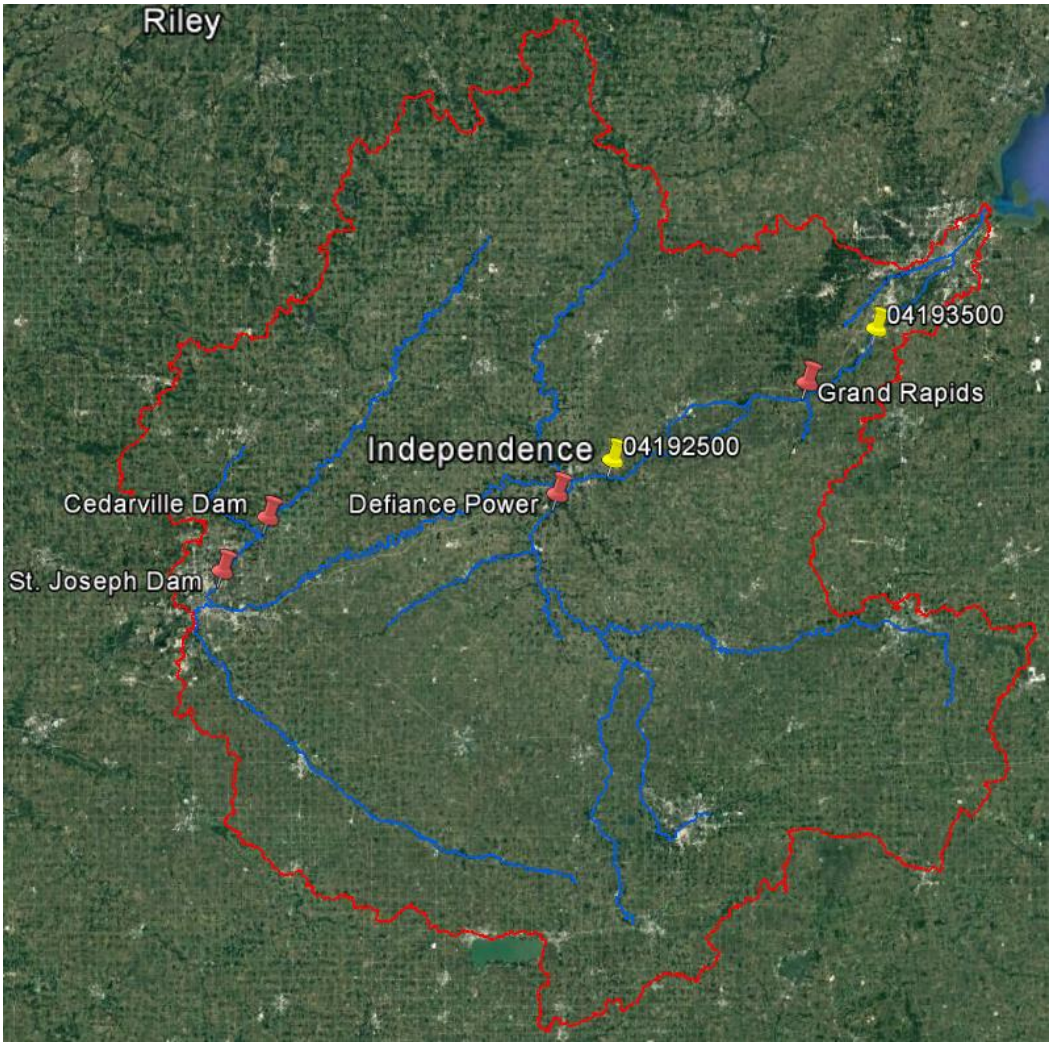

Figure 35- The Independence Dam Watershed

Figure 36 displays the annual peak streamflow at Gage 04193500 and 04192500. As the graphs show the flood events in 1913 and 1982 were significantly high. In 1913 the magnitude of the flood was 180,000 cfs (5,097 cms) at Gage 04193500. In 1982 the flood magnitude was 121,000 cfs (3,426 cms) and 104,000 cfs (2,945 cms) at Gage 04193500 and 04192500, respectively.

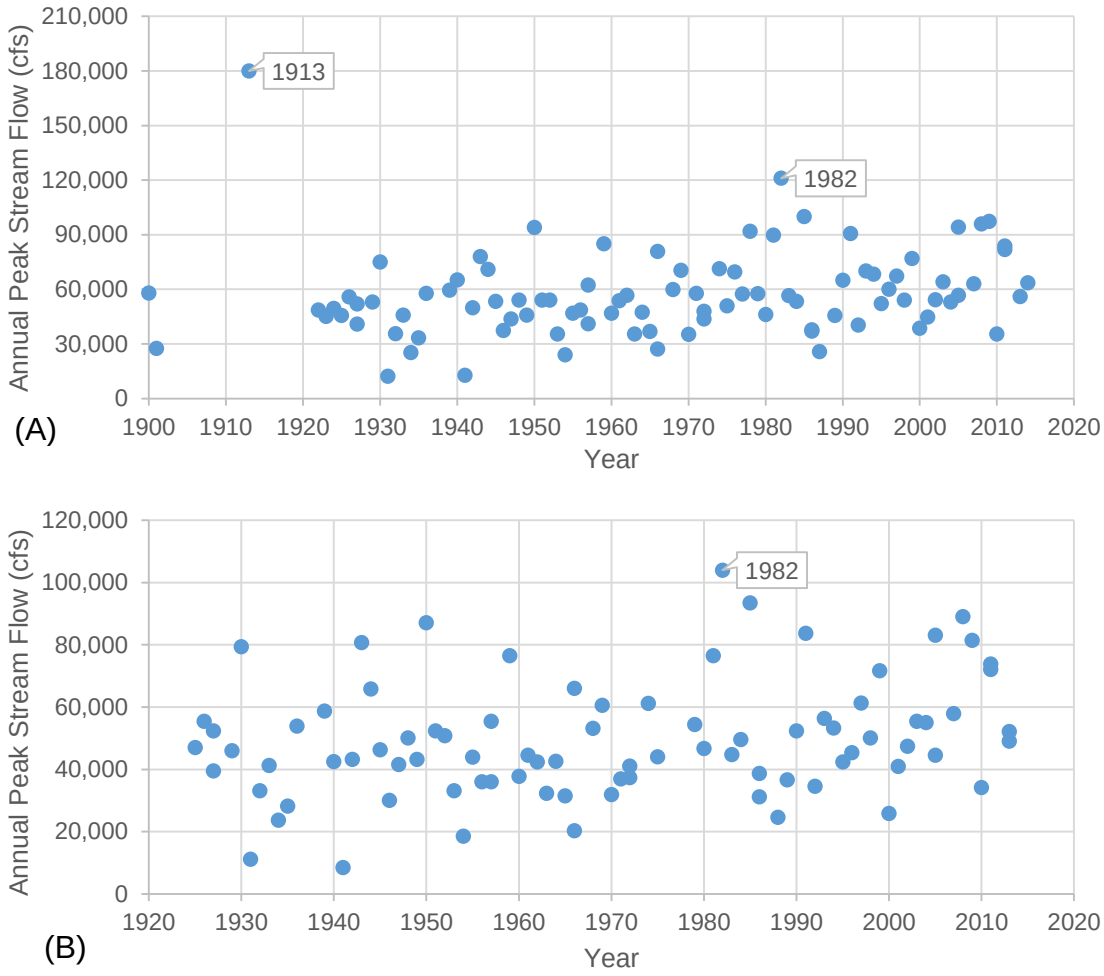

Figure 36- Annual Peak Streamflow for (A) Gage 04193500; Maumee River at Waterville, OH and (B) Gage 04192500; Maumee River at Defiance, OH

Normal Flood Frequency analyses was done on Gage 04193500 and 04192500. Table 12 displays the results of the frequency analyses at Gage 04193500 and 04192500. The flood in 1982 exceeded 100- year storm event, and in 1913 exceeded 500- year flood event.

Table 12- Stream Discharge Corresponding to Various Recurrence Levels

Recurrence	Stream Flow Discharge (cfs)	
	Gage 04193500	Gage 04192500
1.5- yr	47,290	41,564
5- yr	77,314	65,246
50- yr	105,806	87,721
100- yr	112,211	92,773
500- yr	125,233	103,044

The rating curve and observed data associated with the two gages (Gage 04193500 from 1950 to 2003; and Gage 04192500 from 1997 to 2000) are displayed in Figure 37 and Figure 38. The R^2 values corresponding to these curves are very good – in excess of 0.95 in both cases.

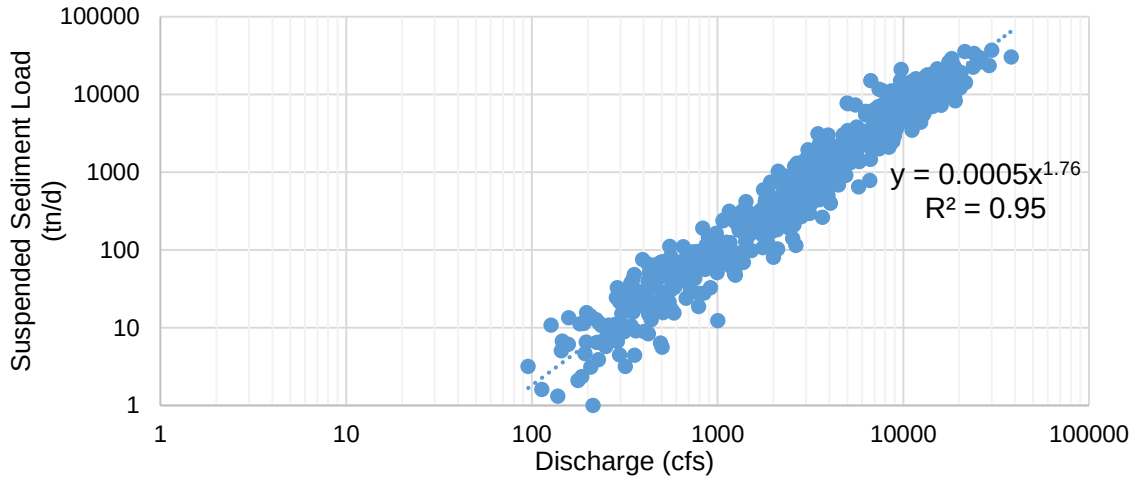

Figure 37- Rating Curve for Gage 04193500 from 1950 to 2003

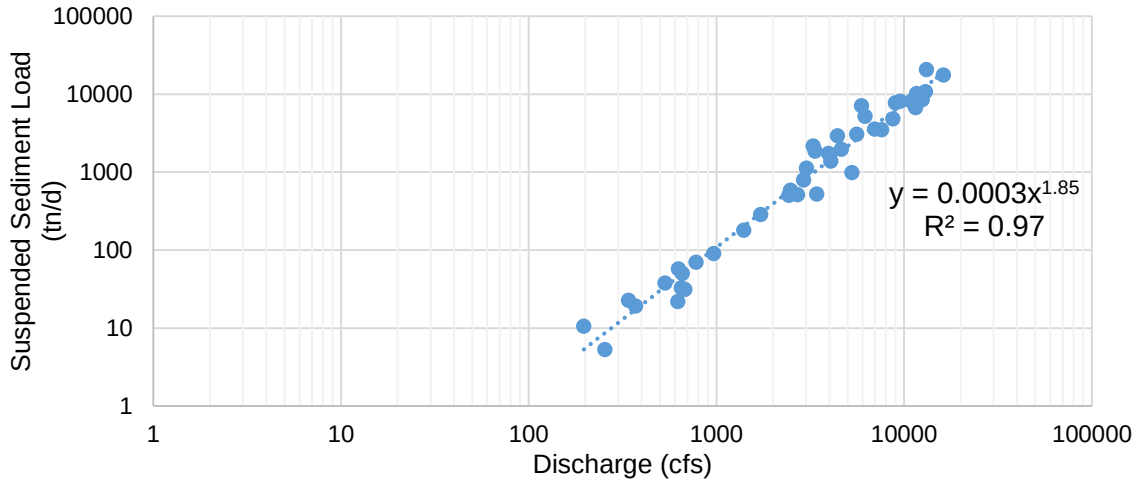

Figure 38- Rating Curve for Gage 04192500 from 1997 to 2000

3.7. Lake Rockwell Dam

Lake Rockwell Dam is located on the Cuyahoga River and is a part of the Upper Cuyahoga River watershed. Lake Rockwell Dam construction began in 1913 with operations commencing in May of 1915 in the state of Ohio. The reservoir was constructed as the primary water supply for the City of Akron. Prior to the reservoir, the City of Akron had experienced many major fires due to the lack of available water. Also, the increasing population during the 1800's created further demand for a more secure water supply. The growth in industry and population led to the pollution of the downstream river. Lake Rockwell Dam drainage area is 208 mi^2 (539 km^2) as reported by the National Inventory of Dams, and the impounded lake is 810 ac (328 ha). Table 13 shows the Rockwell reservoir data as displayed on the NID website.

Table 13- Reservoir Data from USACE NID

Dam Name	Year Built	Coordinate		Height (ft)	Max-Storage (ac. ft)	Normal-Storage (ac. ft)	Surface Area (ac)
		Longitude	Latitude				
Lake Rockwell	1913	-81.33111	41.18278	35	18,250	8,172	810

One of the significant factors in estimating soil erosion, sediment yield, and sediment transport is the topography of the watershed. In a steep basin, much more soil is eroded and delivered downstream in comparison to a flat area, because of the higher velocity of runoff in the steep basins. The northeast part of the Cuyahoga River watershed is more elevated than southwest, so the flow direction is from northeast to the southwest. Runoff with suspended sediment from the most upstream reaches of the river (northeast of the watershed) transfers into the downstream channels. Some of the suspended sediment accumulate behind dams and other portions pass through dams and delivers

into the downstream reaches. The average slope of the watershed is about 6%. However, the west part of the basin is the steepest, and the northeast is the flattest area.

Another important factor in sediment yield and transport is land use. The land cover in this watershed is a mostly developed area, forest, and some agricultural area. Figure 39 Indicates the land use breakdown in the Cuyahoga River watershed in 2001. Upstream of the dam is mostly forest and cropland. However, the largely developed area such as Cleveland and Akron are located downstream of the dam.

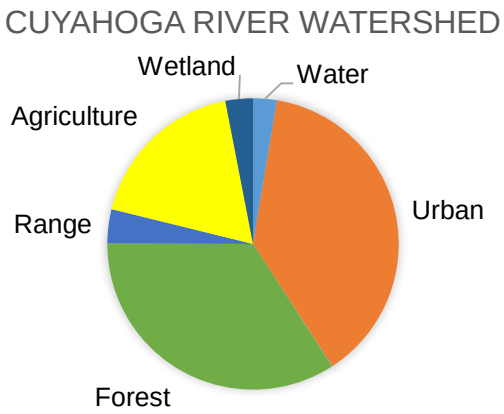

Figure 39- Land Use Breakdown in the Study Watershed in 2001, National Land Cover Database (Homer et al., 2007)

There are several USGS gages on the Cuyahoga River that illustrate how streamflow and sediment load in the river are changing over time. The nearest gage upstream of the Lake Rockwell reservoir is at Hiram Rapids, OH (Gage 04202000). The gage has recorded stream flow since 1927 and suspended sediment concentration from 1985 to 1986. The drainage area of the gage is 151 mi^2 (391 km^2). There are two other USGS gages downstream of Lake Rockwell Dam; the gages at Summit County (Gage 04206000) and Independence (Gage 04208000). Gage 04206000 has recorded streamflow discharge since 1927 and suspended sediment concentration from 1972 to 1981. Gage 04208000 has recorded the streamflow discharge since 1903 and suspended

sediment concentration from 1950 to 2002. The location of the reservoir and each gage are displayed in Figure 40.

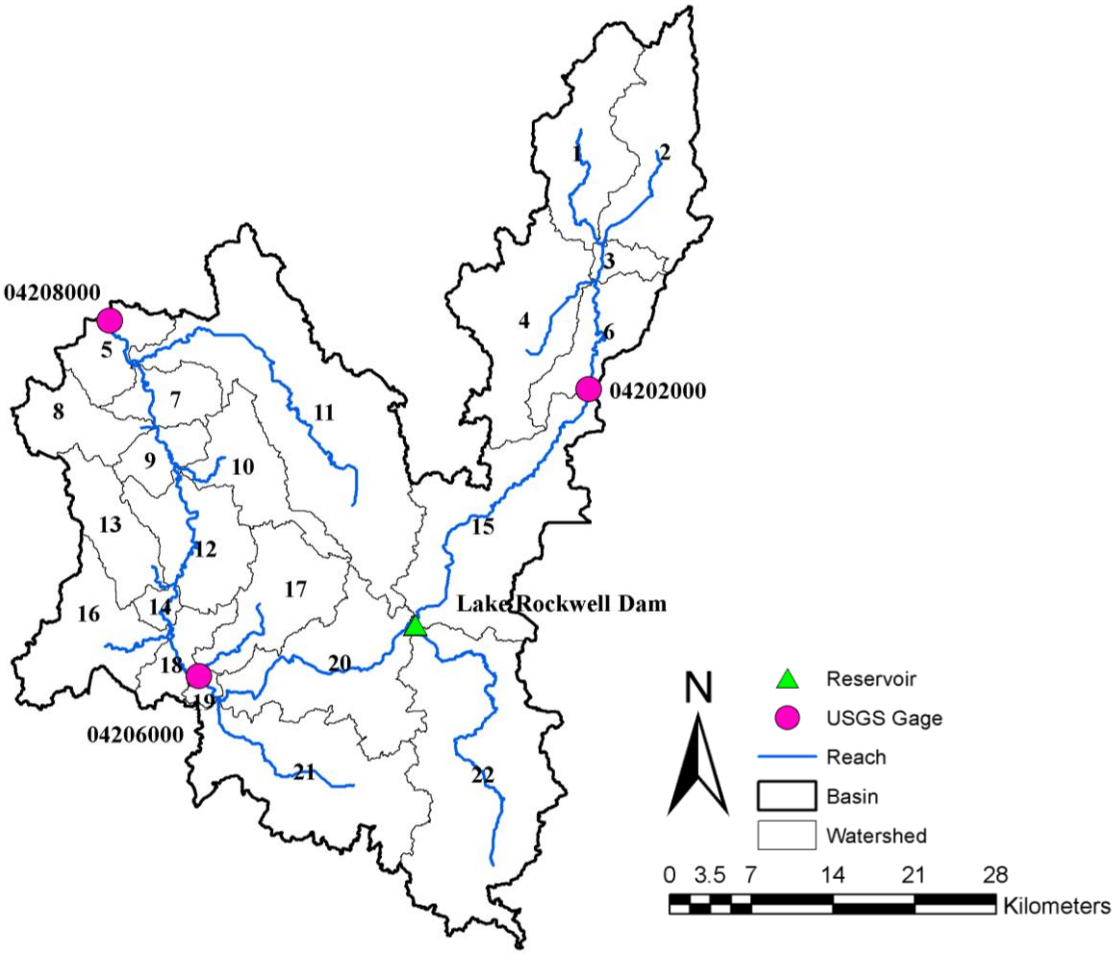

Figure 40- USGS Gages in the Cuyahoga River Watershed

Several major floods have occurred at the Lake Rockwell reservoir since its construction. The annual peak streamflow over time at three different USGS gages is displayed in Figure 41. For each of these three gages, there were major flood events in 1959, 1976 and 1979 that resulted in increased sediment yield.

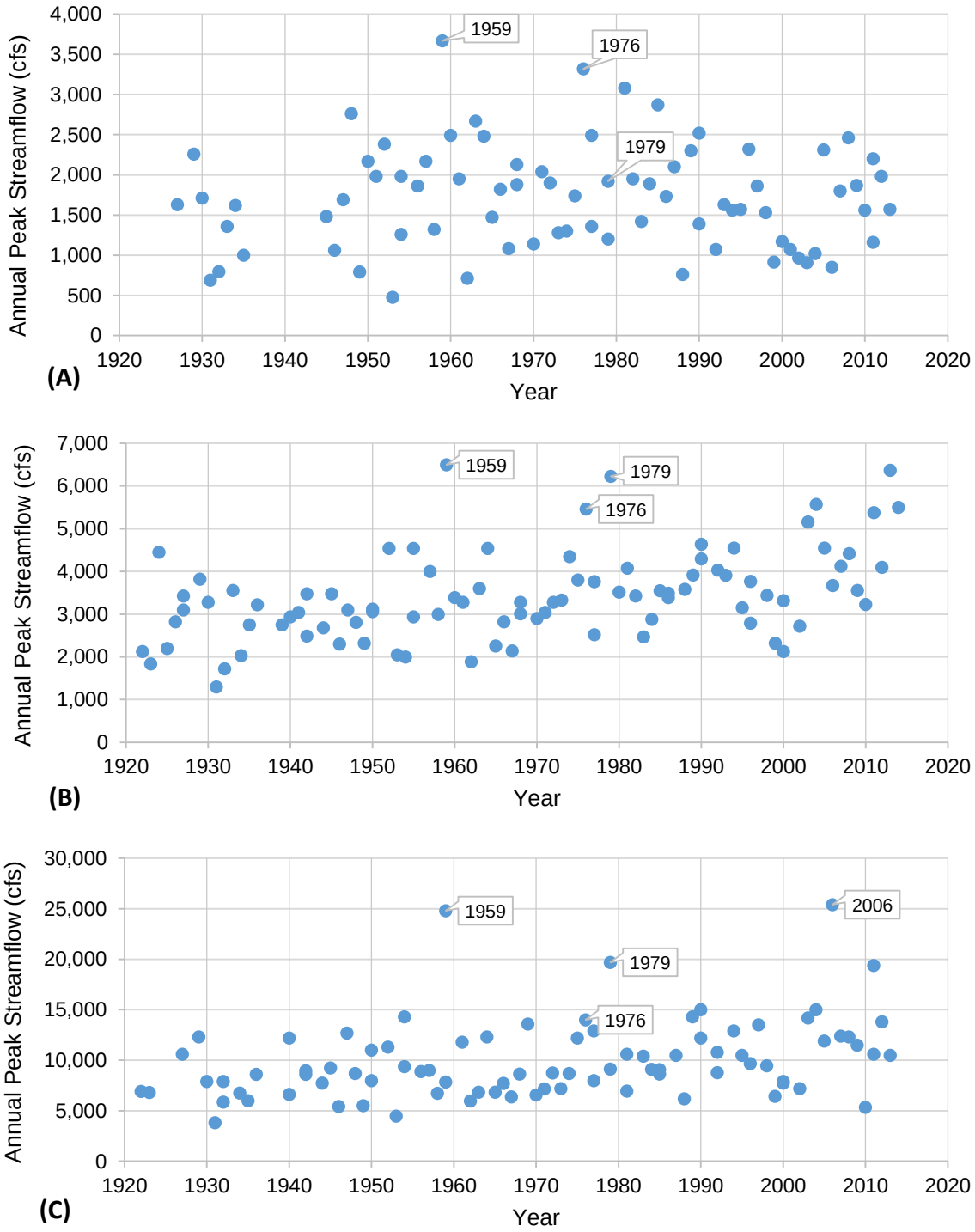

Figure 41- Annual Peak Streamflow for (A) Gage 04202000, 16 miles upstream of reservoir, (B) Gage 04206000, 16 miles downstream of reservoir, and (C) Gage 04208000, 35 miles downstream of reservoir

The statistical- frequency analyses were done for the three gaged locations to estimate the magnitude of stream discharge corresponded to different storm events. The

results of frequency analyses are given in Table 14. The flood- frequency analyses estimated the magnitude of the 500-year recurrence interval events at Gage 04202000, Gage 04206000, and Gage 04208000 are 3,500 cfs (99 cms), 6,400 cfs (181 cms), and 21,000 cfs (595 cms), respectively. As the graphs display, the flood events in 1959, 1976 and 2006 exceeded the 500-year flood event.

Table 14- Stream Discharge Corresponding to Various Recurrence Levels

Recurrence	Stream Flow Discharge (cfs)		
	Gage 04202000	Gage 04206000	Gage 04208000
5- yr	2,258	4,316	13,246
50- yr	3,035	5,577	17,905
100- yr	3,209	5,860	18,952
500- yr	3,564	6,436	21,082

The rating curve of Gage 04208000 from 1950 to 2000, Gage 04206000 from 1972 to 1981, Gage 04202000 from 1985 to 1986 and Gage 04207200 from 1972 to 1979 were displayed in Figure 42 through Figure 45. The R^2 of each rating curve varies from 0.61 to 0.85, which show the good fit between the suspended sediment load and stream discharge.

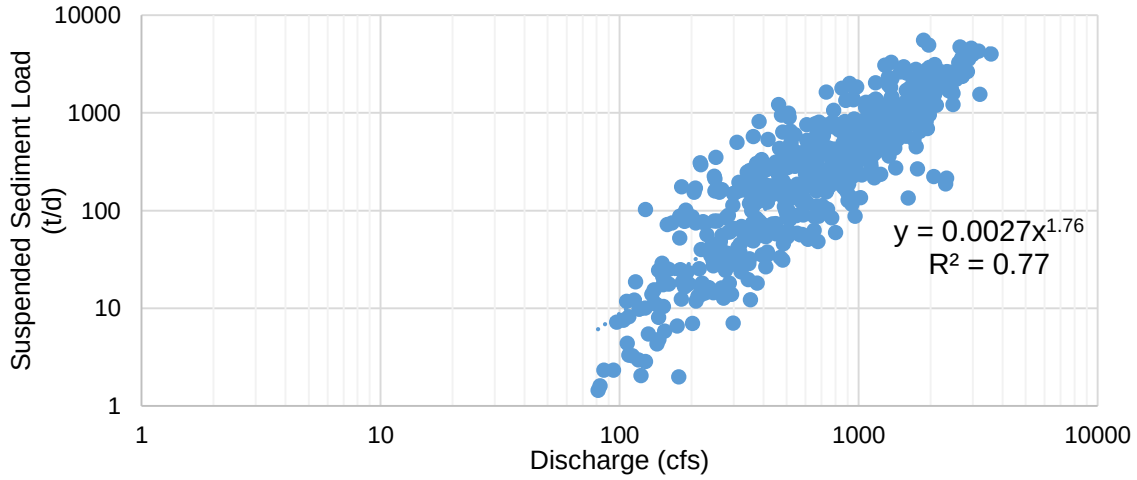

Figure 42- Rating Curve for Gage 04208000 from 1950 to 2000

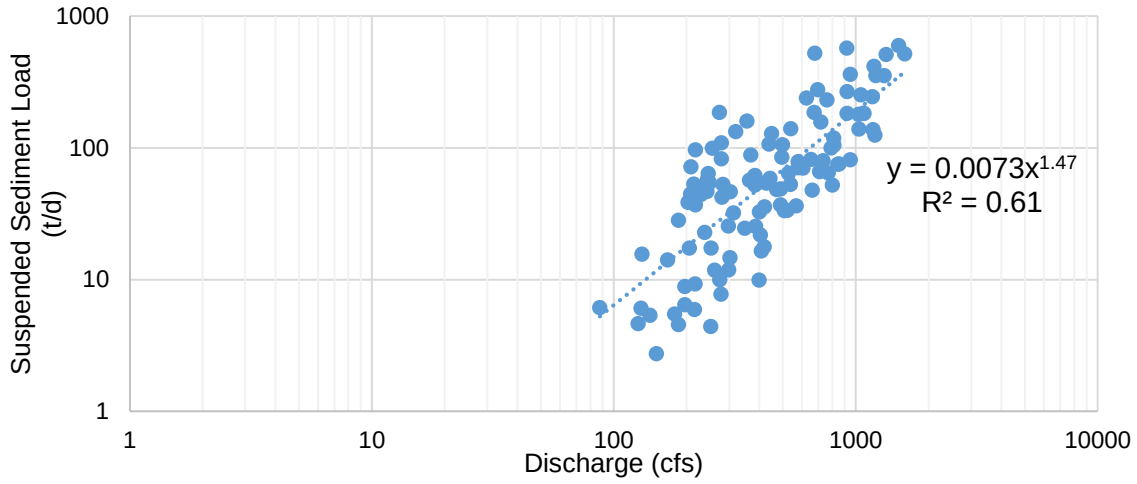

Figure 43- Rating Curve for Gage 04206000 from 1972 to 1981

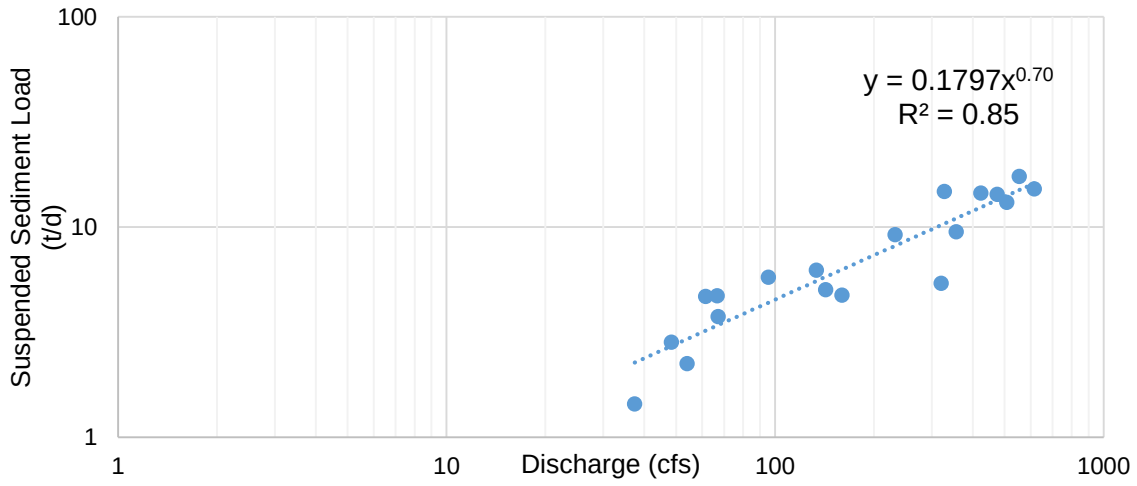

Figure 44- Rating Curve for Gage 04202000 from 1985 to 1986

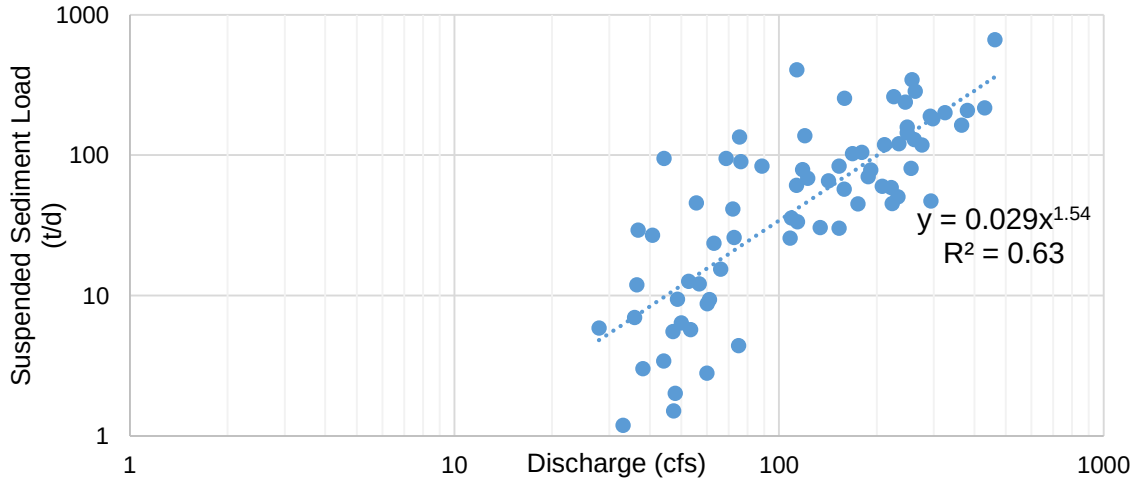

Figure 45- Rating Curve for Gage 04207200 from 1972 to 1979Ford Lake Dam

3.8. Ford Lake Dam

Ford Lake Dam is in Ypsilanti Township, Michigan. The dam is located on the Huron River and is a part of the Huron River watershed. Ford Lake Dam and powerhouse were constructed by Henry Ford in 1932 as a part of a program to develop rural industry in Michigan. The area surrounding the lake was bought out for agriculture as done by employees of the dam. The development of Interstate-94 in the late 1940's and early 1950's contributed to the current land use of the area which is primarily classified as developed and urbanized. The drainage area of Ford Lake Dam is 814 mi^2 (2,108 km^2) as calculated by the National Inventory of Dams (NID 2010). The impounded lake is roughly 987 ac (399 ha) in size. Table 15 shows the dams and their associated reservoirs characteristic in the study watershed.

Table 15- Reservoirs Data from USACE NID

Dam	Sub-Basin	Year Built	Height (ft)	Pond Area (ac)	Normal Storage (ac. ft)	Max Storage (ac. ft)
Kent Lake	1	1946	20	1,050	9,600	12,000
Flook	4	1965	13	769	4,000	6,000
Ford Lake	8	1932	45	987	17,770	18,000

The Ford Lake Dam watershed is an area dominated by agriculture, urban, forest, and some wetland area. Figure 46 indicates the land use breakdown in the Ford Lake Dam watershed in 2001. About 30% of the land is urban area, 25% farmland and 22% forest the rest of the land is wetland and water.

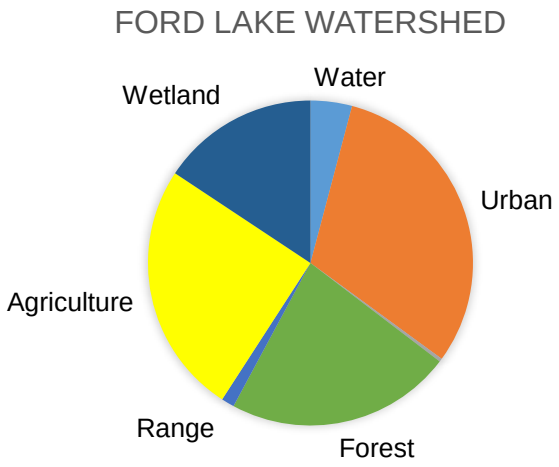

Figure 46- Land Use Breakdown in 2001, National Land Cover Database (Homer et al., 2007)

Some USGS gages are operated on Ford Lake Dam watershed, one of the gages (Gage 04174500) located upstream of Ford Lake Dam on Huron River, in Ann Arbor and records the recent stream discharge. Figure 47 displays the gages and dams location within Ford Lake Dam watershed; there is no gage that records recent sediment load data within this watershed.

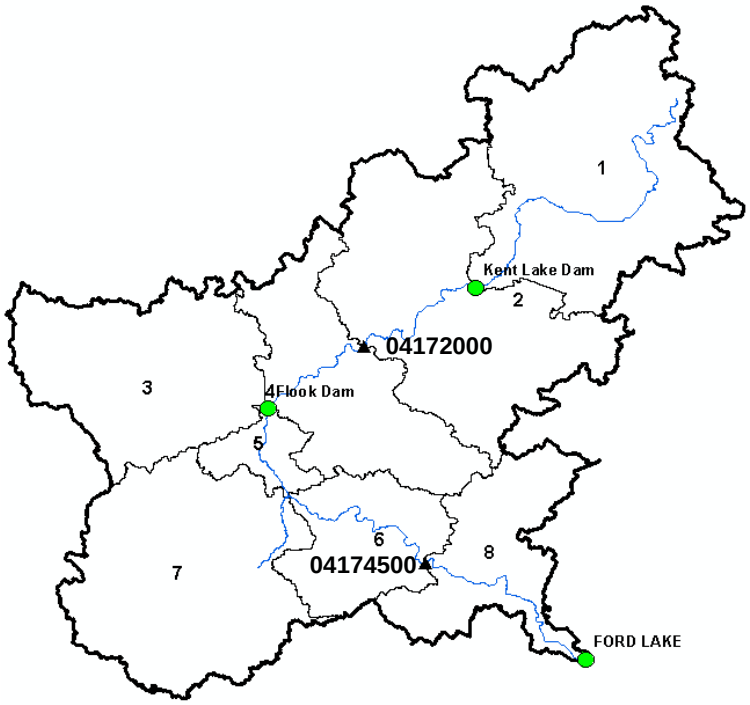

Figure 47- USGS Gages in the Huron River Watershed

Figure 48 displays the annual peak streamflow at Gage 04174500. The highest record of discharge happened in 1902, 1918, and 1947 which their magnitudes were 5,510 cfs (156 cms), 5,840 cfs (165 cm), and 5,170 cfs (146 cms).

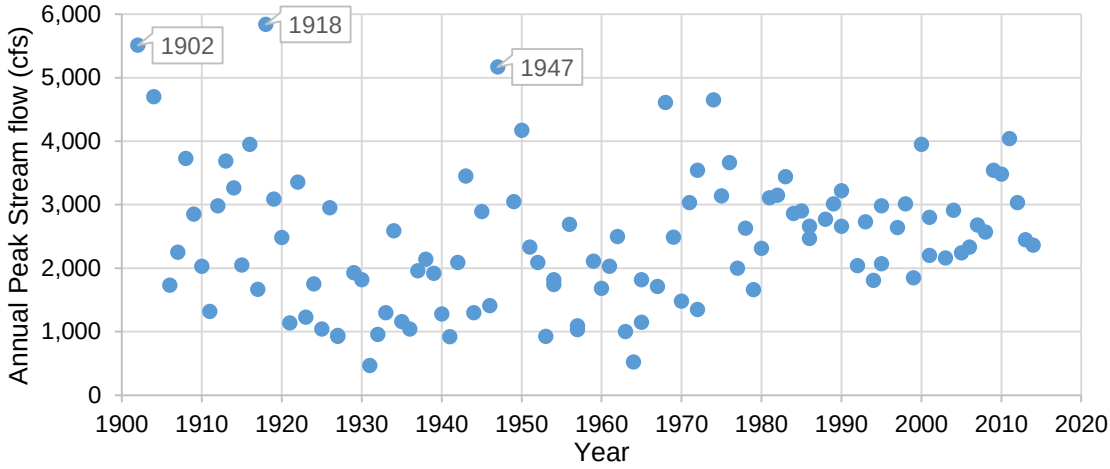

Figure 48- Annual Peak Streamflow for USGS 04174500; Huron River, IN

The normal frequency analyses were done on Gage 04174500, and their results were displayed in Table 16. The flood event in 1902 and 1918 exceeded the 500- year storm event, and the flood event in 1947 exceeded the 500- year flood event.

Table 16- Stream Discharge Corresponding to Various Recurrence Levels

Recurrence	Stream Flow Discharge (cfs)
	Gage 04174500
1.5- yr	1,985
5- yr	3,335
50- yr	4,616
100- yr	4,904
500- yr	5,490

3.9. Potter's Falls Dam

Potter's Falls Dam is located on the Oswego River in the state of New York, and is a part of the Six Mile Creek watershed. Downstream of the dam is Cayuga Lake. The dam is the water supply for the city of Ithaca. In 1911, Potters Falls Dam was completed,

and the Six Mile Creek Dam was no longer used except as a backup. Due to the geography and geology of the area, a small silt dam was constructed upstream of Potters Falls Dam in 1925 to help slow the sediment accumulation to the main reservoir (Tompkins Historical Society, 2012). In 1936, the silt dam was repaired, cleaned and enlarged. The silt dam is drained and dredged every few years. However, Potters Falls Dam still has much accumulation. Full-scale dredging of Potters Falls has not been done, but it was dredged by the opening of the low-level outlet gate through the 1950s (Tompkins Historical Society, 2012). The drainage area of Potter Fall's Dam is 45.6 mi^2 (118 km^2) as reported by the National Inventory of Dams, and the impounded lake is 47 ac (19 ha). Table 17 displays the Potter's Falls reservoir data as displayed on the NID website.

Table 17- Reservoir Data from USACE NID

Dam Name	Year Built	Coordinate		Height (ft)	Max Storage (ac. ft)	Normal Storage (ac. ft)	Surface Area (ac)
		Longitude	Latitude				
Potter's Fall	1911	-76.460577°	42.417339°	75	1,290	800	47

The Potter's Fall Dam watershed is an area dominated by forest, with some agricultural land and wetland. Figure 49 indicates the land use breakdown in the Potter's Falls Dam watershed in 2001. About 60% of the land is forest, 25% is formed land, and only 3% of the watershed is a developed area.

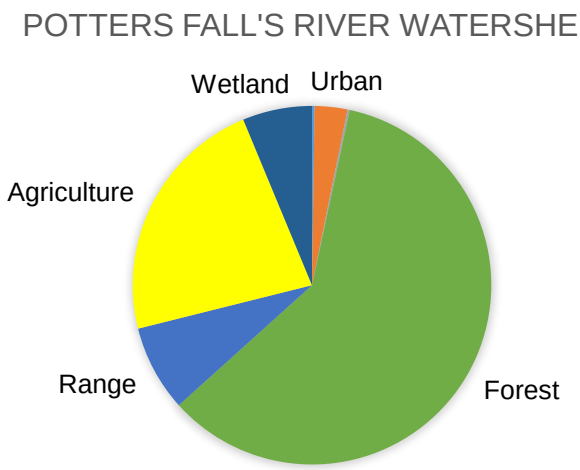

Figure 49- Land Use Breakdown in 2001, National Land Cover Database (Homer et al., 2007)

Eastern region of the watershed is elevated than west, and overland flow direction is from east to the west. Potter's Falls watershed is a steep watershed. The average of the topographic slope is about 13%, although, in some areas, the slope exceeds 25%, especially in southern boundary of the watershed. The middle part of the watershed is pretty flat, and its slope is between 0 and 5%.

Several USGS gages are operated in the study watershed. The nearest gage to the upstream of Potter's Falls reservoir is Gage 04233300. The Gage 04233300 is located on Six Mile Creek, in Bethel Grove, in the state of New York, and its drainage area is about 29 mi^2 (75 km^2). The gage has recorded stream discharge since 1995 and suspended sediment concentration from 1999 to 2013. The location of the Potter's Fall Dam and gage are displayed in Figure 50.

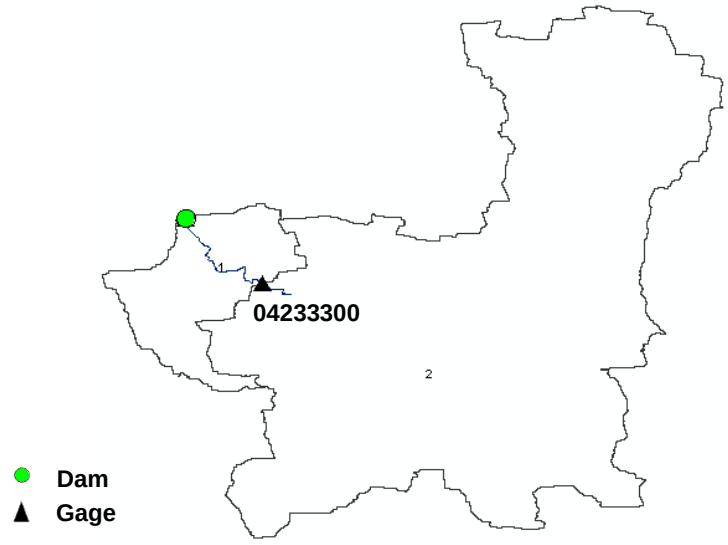

Figure 50- USGS Gages in the Six Mile Creek Watershed

The analysis was conducted for the gage upstream of the Potter's Falls Dam to determine years when significant flooding occurred. Several major floods have occurred at Potter's Falls Dam watershed since its construction. There were some floods in Jun 1972, May 1833, December 1901, Jun 1905, and August 1992, which were recorded by Tompkins County Historical Society. Figure 51 displays the annual peak streamflow at the gage location, the highest record discharge was more than 6,000 (cfs) which happened in 1996.

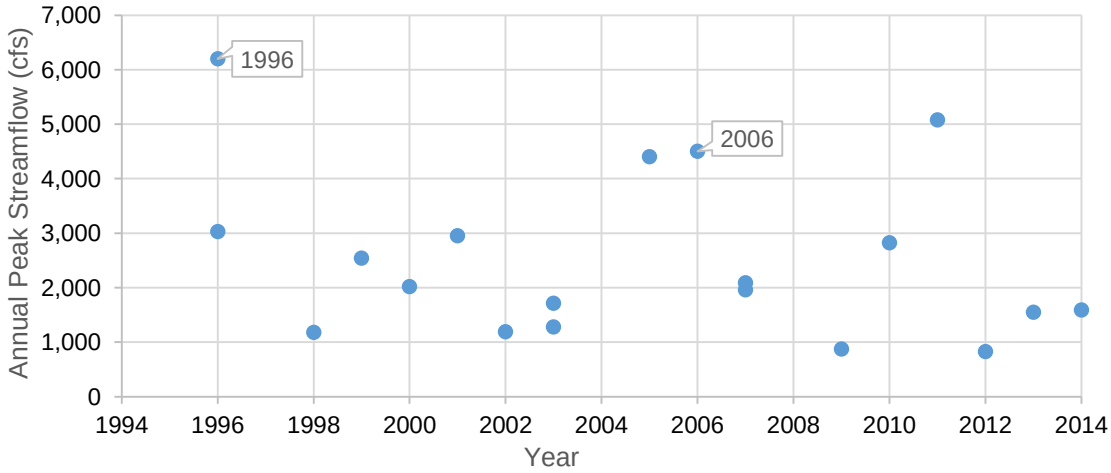

Figure 51- Annual Peak Streamflow for Gage 04233300; Six Mile Creek at Bethel Grove, NY

The normal frequency analyses of peak annual stream flow were done for Gage 04233300 to estimate the magnitude of different rainfall events. The results of frequency analyses are given in Table 18. The biggest flood at Gage 04233300, happened in 1996, and its magnitude exceeded the 100-year recurrence interval

Table 18- Stream Discharge Corresponding to Various Recurrence Levels

Recurrence	Stream Flow Discharge (cfs)
	Gage 04233300
1.5- yr	1,876
5- yr	3,771
50- yr	5,570
100- yr	5,974
500- yr	6,796

Gage 04233300 recorded suspended sediment discharge from 1999 to 2013. Figure 52 and Figure 53 display the rating curve for Gage 04233300 from 1999 to 2013, and Gage 042033286 from 2003 to 2013, respectively. The R^2 of the rating curves are higher than 0.68, which show the good fit between Streamflow and sediment discharge.

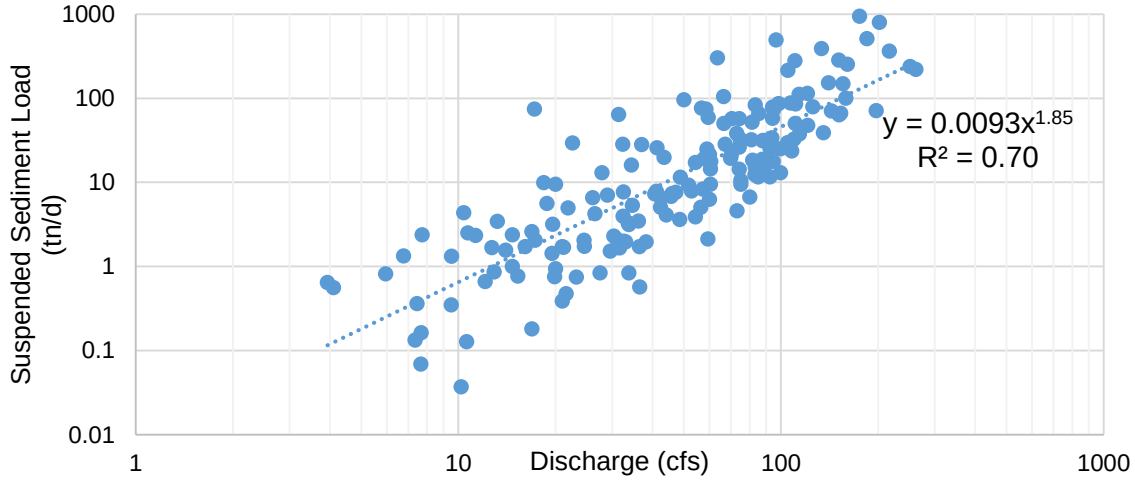

Figure 52- Rating Curve for Gage 04233300 from 1999 to 2013

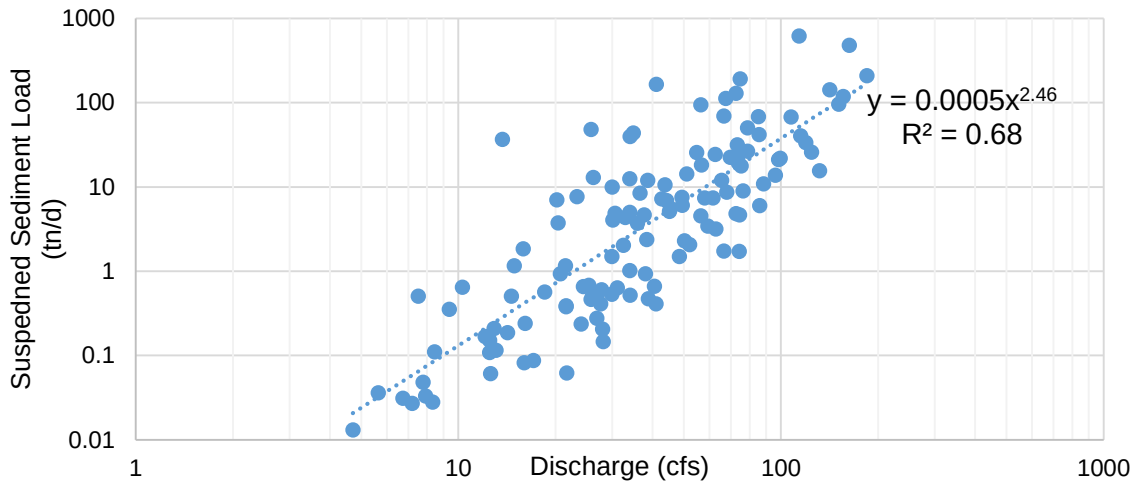

Figure 53- Rating Curve for Gage 042033286 from 2003 to 2013

3.10. Brown Bridge Dam

Brown Bridge Dam was located in Grand Traverse, Michigan. It was constructed and completed in 1922. Traverse City started to develop in the 1840's, and thus the city saw the construction of many dams from 1867 to 1922 along the Boardman River. On October 7th, 2012, there was a breach on the Boardman River which emptied Brown Bridge Pond. This occurred due to the Brown Bridge Pond Dam removal project (Puit et al., 2012). The dam has since been removed (Ellison, 2013). The dam was located on the Boardman River and was a part of the Boardman River watershed. The drainage area of Brown Bridge Pond Dam is 151 mi^2 (391 km^2) as calculated by the National Inventory of Dams (NID 2012). The impounded lake is 191 ac (77 ha) in size. The characteristic of Brown Bridge reservoir is displayed in Table 19.

Table 19- Reservoirs data from USACE NID

Dam	Sub-Basin	Year Built	Height (ft)	Pond Area (ac)	Normal Storage (ac. ft)	Max Storage (ac. ft)
Brown Bridge	16	1900	36	191	1,900	3,000

The Brown Bridge watershed is in a hilly area. The average of slope in this watershed is about 3.80%. The middle part of the watershed is pretty flat, the slope is between 0 to 1%, the southern and northern boundaries of the watershed are steep and in some regions the slope exceeded 5%. Eastern region of the watershed is more elevated than west and the stream direction is from east to the west.

The Brown Bridge Dam watershed is an area dominated by forest and rangeland. Figure 54 indicates the land use breakdown in the Brown Bridge Dam watershed in 2001. More than 50% of the land is forest, and 20% is rangeland, while agricultural and urban area take up only 5% and 8% of the entire watershed, respectively.

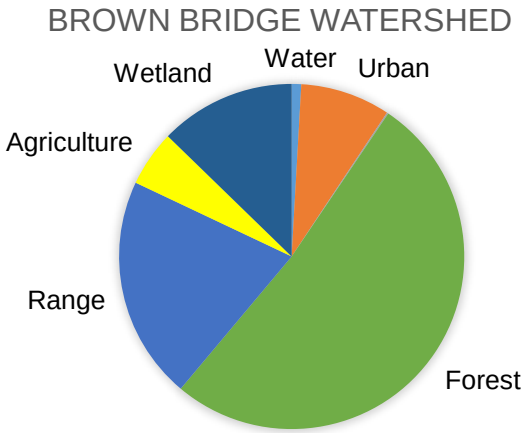

Figure 54- Land Use Breakdown in 2001, National Land Cover Database (Homer et al., 2007)

Some USGS gages are located on Brown Bridge Dam watershed, between these gages only Gage 04126970 records the recent stream flow. Gage 04126970 has collected stream discharge since September 1997. The Gage 04126970 is located at the upstream of the dam on Board Man River. In Figure 55 the gage and dam location have been shown. In this watershed, there is no gage that records recent sediment load data.

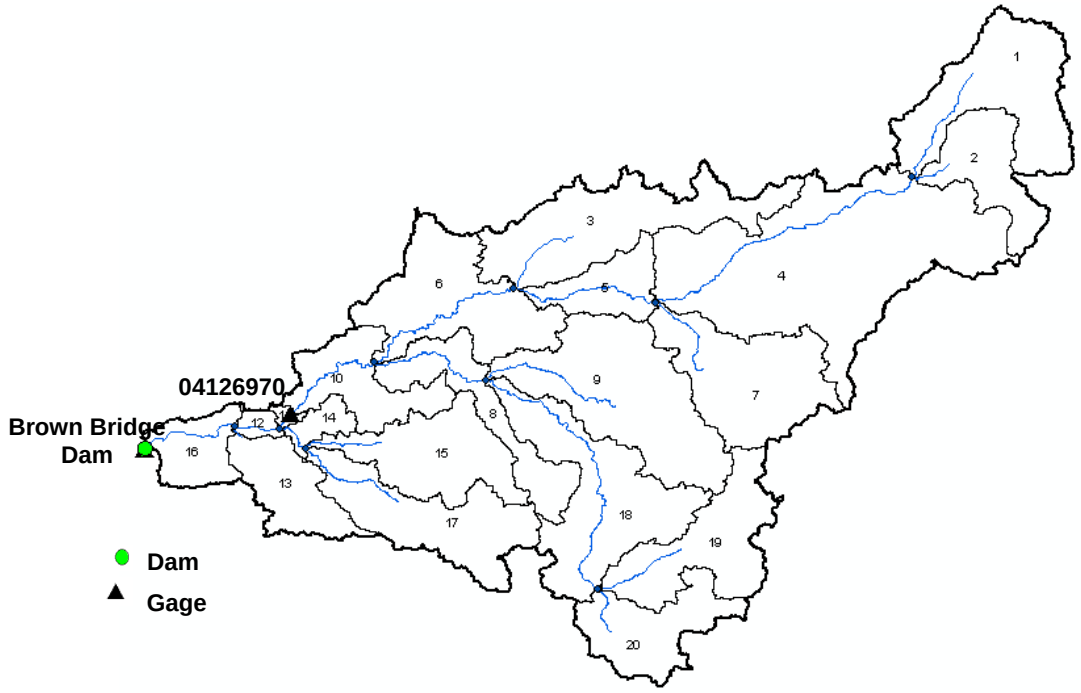

Figure 55- USGS Gage in the Board Man River Watershed

Flood events deliver a large amount of water into a river, and they also bring along lots of eroded soil from the surrounding landscape. Significant flood is expected to move the considerable loads of sediment along the river and eventually dump sediment into the harbors or some temporary storages such as reservoirs. Therefore, an analysis was conducted for the gages at the upstream of the dam to determine years when significant flooding occurred. Figure 56 displays the annual peak streamflow at Gage 04126970.

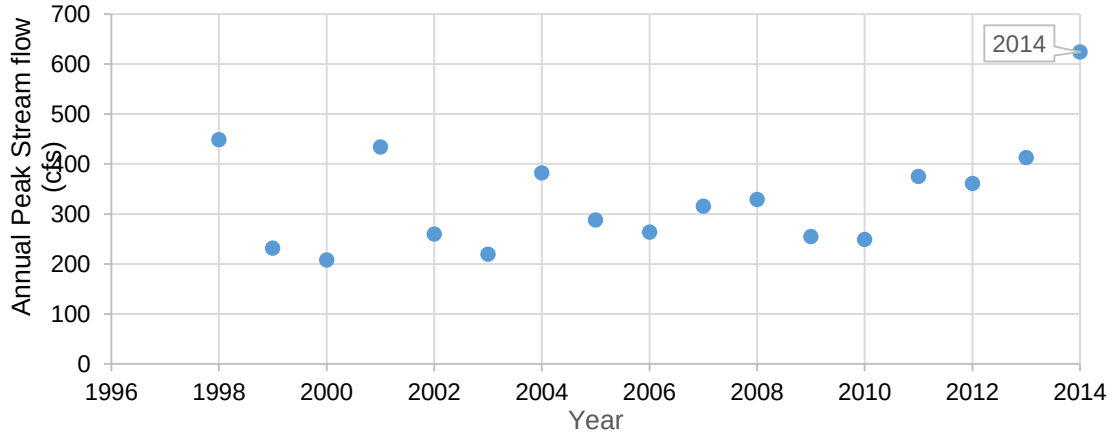

Figure 56- Annual Peak Streamflow for Gage 04126970, Grand Traverse County

The highest discharge which has been recorded by Gage 04126970 was more than 600 cfs (17cms), and happened in 2014 when the dam was removed. Frequency analysis of the annual peak stream flow (Table 20), which has been done by authors estimated 100-year recurrence interval event is equivalent to approximately 575 cfs (16 cms). Therefore, the flood in 2014 was more than 100-year recurrence interval.

Table 20- Stream Discharge Corresponding to Various Recurrence Levels

Recurrence	Stream Flow Discharge (cfs)
	Gage 04126970
1.5- yr	421
5- yr	547
50- yr	575
100- yr	632
500- yr	421

3.11. Mio and Alcona Dams

Mio Dam was constructed in 1917, while Alcona Dam construction began in 1916, and due to the financial issues, it was not completed until 1923. Mio Dam is located on Au Sable River in Oscoda County, Michigan. Alcona Dam is located on Au Sable River in Alcona County, Michigan. During the 1800s, the area surrounding these dams saw the development of lumber industries and logging railroad surrounding Au Sable River (Macdonald, 1942). The drainage area of Mio and Alcona dams is 1,100 mi^2 (2,849 km^2) and 1,469 mi^2 (3,805 km^2), respectively as calculated by the National Inventory of Dams (NID 2012). The information of some dams including the Mio and Alcona reservoirs are displayed in Table 21.

Table 21- Reservoirs Data from USACE NID

Dam	Sub-Basin	Year Built	Height (ft)	Pond Area (ac)	Normal Storage (ac. ft)	Max Storage (ac. ft)
Mio	6	1917	38	860	12,000	12,000
Alcona	11	1924	60	1,075	25,000	25,000
Loud	14	1913	40	790	12,600	12,600
Five Channels	15	1912	40	250	4,000	4,000
Cooke	16	1912	50	1,700	30,000	30,000
Foote	17	1918	47	1,800	30,000	30,000
Lake St Helen Lake Level Control	18	1930	8	2,400	3,360	7,700

Au Sable watershed is in a hilly area. The average of slope in this watershed is about 4.10%. This study watershed is an area dominated mostly by forest and rangeland. Figure 57 indicates the land use breakdown within this study watershed in 2001. More than 60% of the land is forest and about 14% is rangeland, while agricultural area takes up only 2%, wetland 11%, and urban area 8% of the watershed.

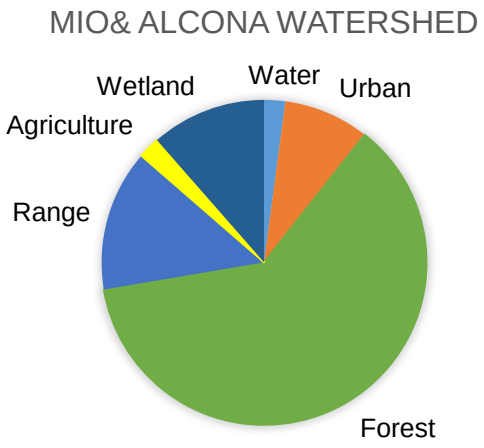

Figure 57- Land Use Breakdown in 2001, National Land Cover Database (Homer et al., 2007)

Some USGS gages including Gage 04136500 and 04137005 are located on the Au Sable River. Gage 04136500 has located downstream of Mio Dam and collected stream discharge since July 1996. Gage 0417005 is located at the downstream of the Alcona Dam and recorded stream flow discharge since September 1997. Au Sable model

was calibrated to the average monthly streamflow as measured at Gage 04136500 and 04137005. In Figure 58 the gages and dams location have been shown. Within this study watershed, there is no gage that records recent sediment load data.

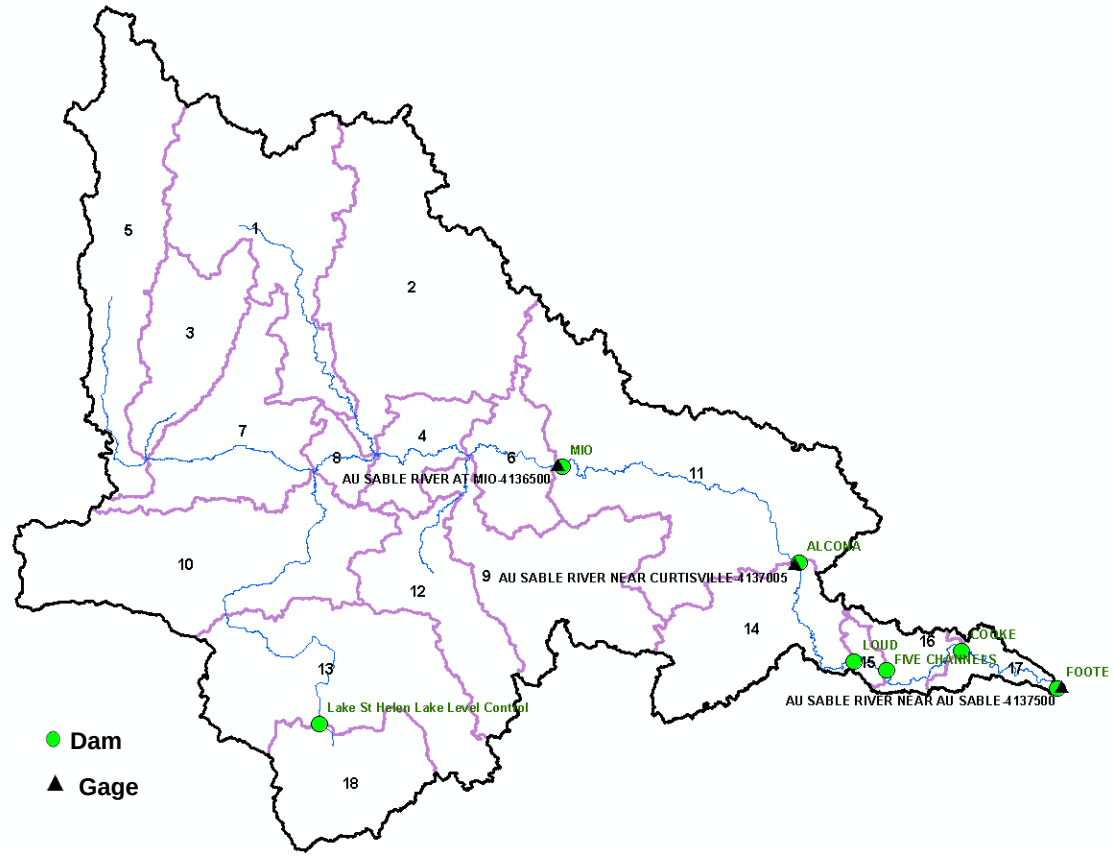

Figure 58- USGS Gages in the Au Sable River Watershed

Figure 59 displays the annual peak streamflow at Gage 04136500 and 0417005. Frequency analysis of the peak annual stream flow was done, and its results are given in Table 22.

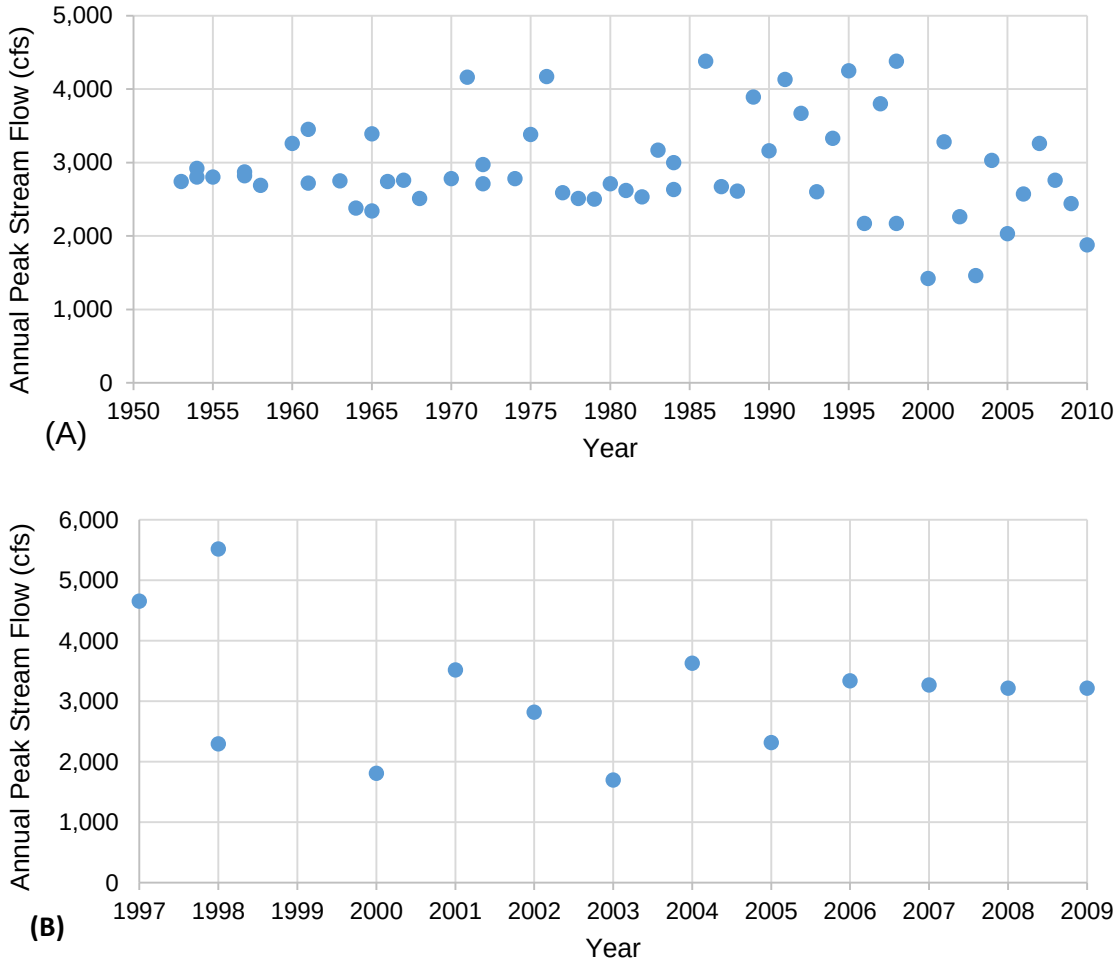

Figure 59- Annual Peak Streamflow for (A) Gage 04136500; Downstream of Mio Dam and (B) Gage 0417005; downstream of Alcona Reservoir

The stream discharge at Gage 04136500 were usually less than 4,000 cfs (113 cms) except in a couple of years. The frequency analysis estimated the 50-year recurrence interval event is equivalent to approximately 4,269 cfs (121 cms) at Gage 04136500 and 5,322 cfs (151cms) at Gage 04137005. So in a couple of years including 1998 the flow exceeded 50-year recurrence interval, and in other years from 1953 to 2010 the stream discharge is less than 50- year flood events.

Table 22- Stream Discharge Corresponding to Various Recurrence Levels

Recurrence	Stream Flow Discharge (cfs)	
	Gage 04136500	Gage 0417005
1.5- yr	2,638	2,858
5- yr	3,475	4,123
50- yr	4,269	5,322
100- yr	4,448	5,592
500- yr	4,811	6,140

CHAPTER 4 METHODOLOGY

In the present research, for simulating sediment dynamics in the watershed modeling framework, the Soil and Water Assessment Tool (SWAT) has been adopted. For sensitivity analysis, calibrating, and validating SWAT models, the SWATCUP tool has been applied. SWAT and SWATCUP tools were fully described in Chapter Two.

In this chapter, the input data and process of modeling, calibrating, and validating the study watersheds are described. The hydrologically calibrated SWAT models of all eleven study dams were provided by the US Army Corps of Engineers (USACE). Calibrating these models for sediment components and analyzing the model results are some parts of this research.

The primary input data for building a hydrology and sediment yield SWAT model include soils, land use, topography, reservoir dimension, and weather data. The soils, land use, topography layers were overlapped to parameterize the watershed model. The climate data (precipitation, temperature, humidity, wind speed, solar radiation) were input to estimate the hydrologic processes in the basin. Additional input data including the reservoir dimension, irrigation, and best management practices (BMPs) were added in the model.

In all of the study watersheds, topography or Digital Elevation Model (DEM) was determined using the USGS National Elevation Dataset1/3 Arc- Second (10 m) provided by USGS (http://nationalmap.gov/elevation.html). Land use data were obtained from National Land Cover Database (NLCD) provided by the USGS National Land Cover Institute (Homer et al., 2007). Soils data were retrieved from the Soil Survey Geographic (SSURGO) Database (Schwarz and Alexander, 2004), the SSURGO database collected

by the National Cooperative Soil Survey. The weather data required for SWAT models were obtained from United States Department of Agriculture Agricultural Research Service (USDA ARD) (http://ars.usda.gov/Research/docs.htm?docid=19388). The reservoir data required were obtained from the US Army Corps of Engineers National Inventory Dams (USACE NID) (http://nid.usace.army.mil/cm_apex/f?p=838:120).

For those study watersheds that have one or more USGS sediment gages (Ballville, Lake Rockwell, and Potter's Falls watershed) the sediment models have been calibrated to the recorded sediment data. However, in the un-gaged watersheds (Webber, Riley, Goshen Pond, Upper Green, Ford Lake, Brown Bridge, Mio and Alcona watersheds) another approach is used. All study dams are classified into one of three groups based on the land use, climate data, soil characteristic, and slope of each. Within each group, there is one gaged watershed. The calibrated parameters of the gaged watershed have been applied for calibrating the un-gaged watersheds which are in the same group.

The bar chart in Figure 60 indicates the land use breakdown in each study watershed. Ballville, Goshen, Upper Green Lake, Riley and Webber dams which are mostly dominated by agricultural land, are classified in group A, because they are similar in terms of land use, topography, soil structure, and climate data. Ford Lake and Lake Rockwell watersheds which have similar characteristics are in group B. Brown Bridge, Mio and Alcona (modeled together), and Potter's Falls are in group C, because they are all significantly covered by forest. In the following sections, the reason of these classification is discussed in detail. In each group there is one gagged watershed that is used to guide the calibration for the ungagged watersheds. After calibrating and validating

each study watershed, the sediment accumulation rate and sediment trapping efficiency within each study reservoir have been estimated. The estimated sediment trapping efficiency from SWAT is also compared with Brune Curve method (Brune, 1953).

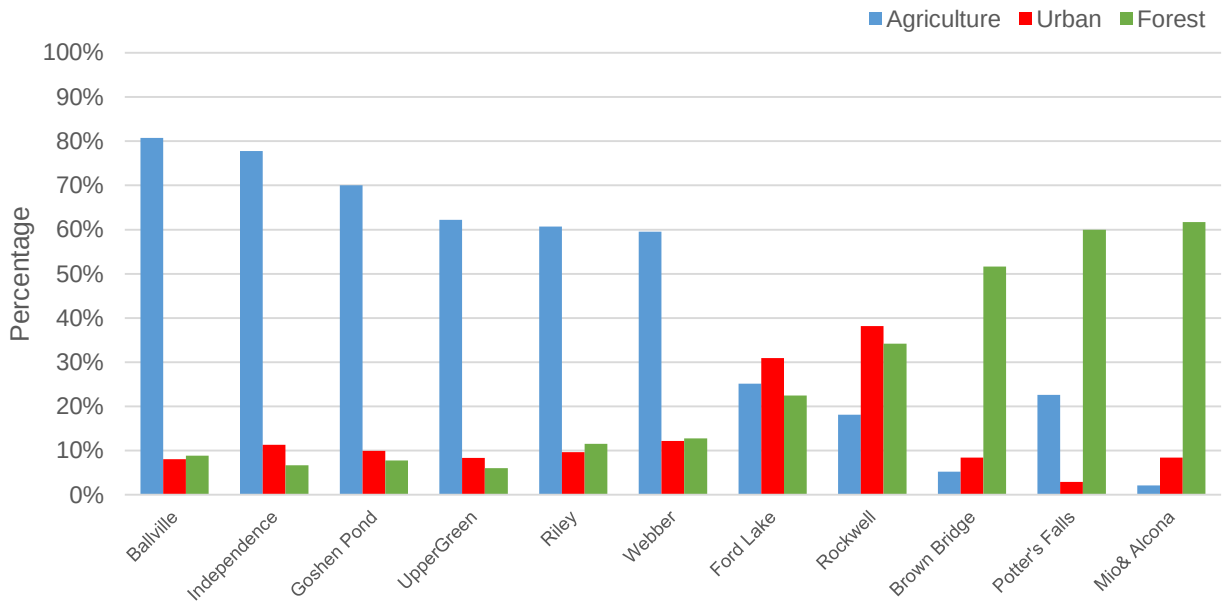

Figure 60- Land Use in Study Dam Watersheds

4.1. Ballville Dam

4.1.1. Calibration the Post- European Model

Refining many different parameters during the calibration process is complicated and time-consuming. A sensitivity analysis can be completed prior to calibration to identify parameters that have the greatest impact on model results. Parameter sensitivity is assessed, and the most important parameters are adjusted within their allowable ranges to provide the best match between observed and simulated results. Figure 61 shows the results of global sensitivity analysis in Ballville Dam watershed. Two factors; t-Stat, and P-Value are defined to determine the sensitivities of parameter. The parameters which

have smaller P-Value, and the larger t-State are more influential among other parameters. For instance, the SOL_ROCK (percent rock in soil layer) and SPCON (coefficient in sediment transport) with the largest t-Stat, are the most influential parameters. While the PRF (peak rate adjustment factor) and LAT_SED (sediment concentration in lateral and groundwater flow) with the least t-State are the least influential parameters among the calibration parameters.

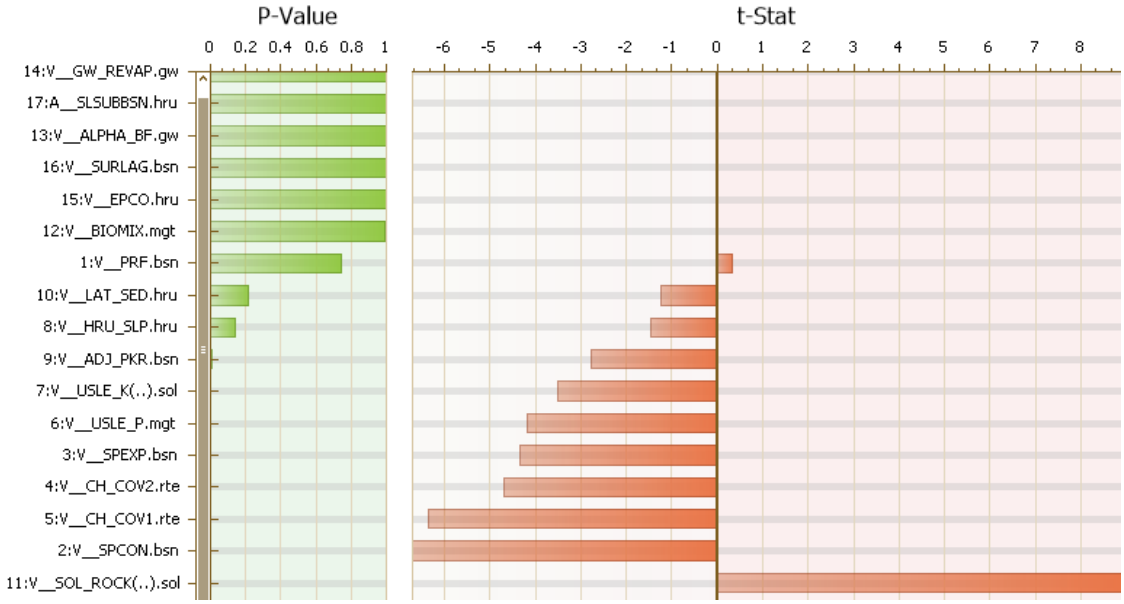

Figure 61- Global Sensitivity Analysis Results for Ballville Dam Model

The SWAT model was calibrated to the mean monthly sediment load as recorded by Gage 04198000. The calibration parameters and their final values are listed in Table 23. The parameters in the last five rows in Table 23 are from the hydrologic calibration process, completed by USACE.

Table 23- Calibrated Parameters and Final Values for Ballville Dam Model

Parameter	Table	Description	Method	Min	Max
PRF	.bsn	Peak rate adjustment factor	Replace	1.60	1.66
SPCON	.bsn	Coefficient in sediment transport	Replace	0.001	0.004
SPEXP	.bsn	Exponent in sediment transport	Replace	1.00	2.00
CH_COV2	.rte	Channel cover factor	Replace	0.30	0.90
CH_COV1	.rte	Channel erodibility factor	Replace	0.00	1.00
USLE_P	.mgt	USLE equation support practice factor	Replace	0.65	0.85
USLE_K	.sol	USLE equation soil erodibility factor	Replace	0.23	0.3
HRU_SLP	.hru	Average slope steepness (m/m)	Replace	0.002	0.035
ADJ_PKR	.bsn	Peak rate adjustment factor	Replace	0.50	1.00
LAT_SED	.hru	Sediment concentration in lateral and groundwater flow (ppm)	Replace	0.00	5.00
SOL_ROCK	.sol	Percent rock in soil layer (%)	Replace	8.00	20.00
BIOMIX	.mgt	Biological mixing efficiency	Replace	0.40	0.80
ALPHA_BF	.gw	Base flow alpha factor (days)	Replace	0.40	0.40
GW_REVAP	.gw	Groundwater "revap" coefficient	Replace	0.19	0.19
EPCO	.hru	Plant uptake compensation factor	Replace	0.88	0.88
SURLAG	.bsn	Surface Runoff lag coefficient	Replace	0.64	0.64
SLSUBBSN	.hru	Average slope length (m)	Absolute	24.12	24.12

In the Ballville Dam watershed, the five years from 1975 through 1980 have been considered a “warm up” period. The model was calibrated based on the recorded sediment from 1980 to 1989 and then validated from 1990 to 1999. Figure 62 and Figure 63 display the statistics comparing observed with simulated average monthly flow and sediment for calibration and the validation runs. The NSE is 0.63 and 0.66 for the calibration and validation runs, respectively - which is satisfactory. In the calibration simulation, p-factor and r-factor are 0.76 and 0.95, respectively. These represent very good correspondence. For the validation run, the p-factor remains 0.76 and the r-factor is 2.09, which is a bit higher than desired. However, if the range of calibration parameters is reduced to decrease the r-factor to about 1, the p-factor in the calibration run will decrease considerably below acceptable values. Hence, these values were accepted.

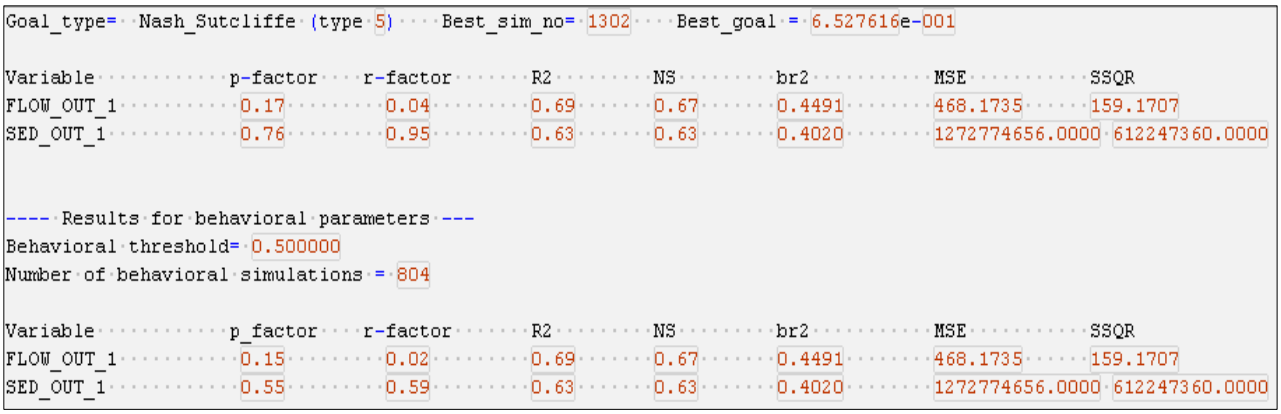

```
Goal_type= Nash_Sutcliffe (type 5)    Best_sim_no= 1302    Best_goal = 6.527616e-001

Variable          p-factor    r-factor      R2          NS          br2          MSE          SSQR
FLOW_OUT_1        0.17        0.04          0.69        0.67        0.4491       468.1735     159.1707
SED_OUT_1         0.76        0.95          0.63        0.63        0.4020       1272774656.0000 612247360.0000


---- Results for behavioral parameters ---
Behavioral threshold= 0.500000
Number of behavioral simulations = 804

Variable          p_factor    r-factor      R2          NS          br2          MSE          SSQR
FLOW_OUT_1        0.15        0.02          0.69        0.67        0.4491       468.1735     159.1707
SED_OUT_1         0.55        0.59          0.63        0.63        0.4020       1272774656.0000 612247360.0000
```

Figure 62- Statistics Comparing Observed Data with the Simulation Data in Calibration Period

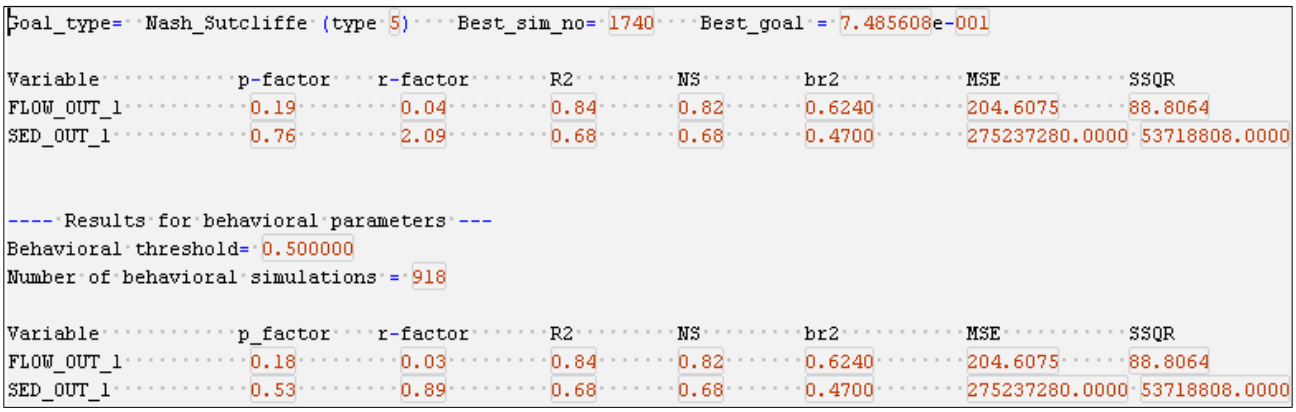

```
Goal_type= Nash_Sutcliffe (type 5)    Best_sim_no= 1740    Best_goal = 7.485608e-001

Variable          p-factor    r-factor      R2          NS          br2          MSE          SSQR
FLOW_OUT_1        0.19        0.04          0.84        0.82        0.6240       204.6075     88.8064
SED_OUT_1         0.76        2.09          0.68        0.68        0.4700       275237280.0000 53718808.0000


---- Results for behavioral parameters ---
Behavioral threshold= 0.500000
Number of behavioral simulations = 918

Variable          p_factor    r-factor      R2          NS          br2          MSE          SSQR
FLOW_OUT_1        0.18        0.03          0.84        0.82        0.6240       204.6075     88.8064
SED_OUT_1         0.53        0.89          0.68        0.68        0.4700       275237280.0000 53718808.0000
```

Figure 63- Statistics Comparing Observed Data with the Simulation Data in Validation Period

The SWAT model for Ballville Dam represented the watershed using 18 subbasins. The Ballville Dam and the Gage 04198000 (observation gage) are in Subbasin 1. The subbasins were further divided into a total of 158 Hydrologic Response Units (HRUs) based on land use, soils, and slope characteristic.

The model was calibrated based on the average monthly sediment load at Gage 0419800. The sediment load that leaves Subbasin 1 in the calibration and validation runs is presented in Figure 64 and 4-6. The green region (95 PPU envelop) shows the potential sediment load leaving Subbasin1, the blue line displays observation data, while the red line provides the best estimation. The observed sediment data fits within the simulated range in both calibration and validation runs. However, there are some spikes in sediment

yield at Subbasin 1 for the months of June 1981, February 1984, and December 1990. To assist in evaluation of the excessive sediment yield for those months, the suspended sediment concentration and stream discharge recorded by Gage 04198000 are depicted in Figure 66. The red and blue lines in Figure 66 represent the suspended sediment concentration and stream discharge recorded by this gage.

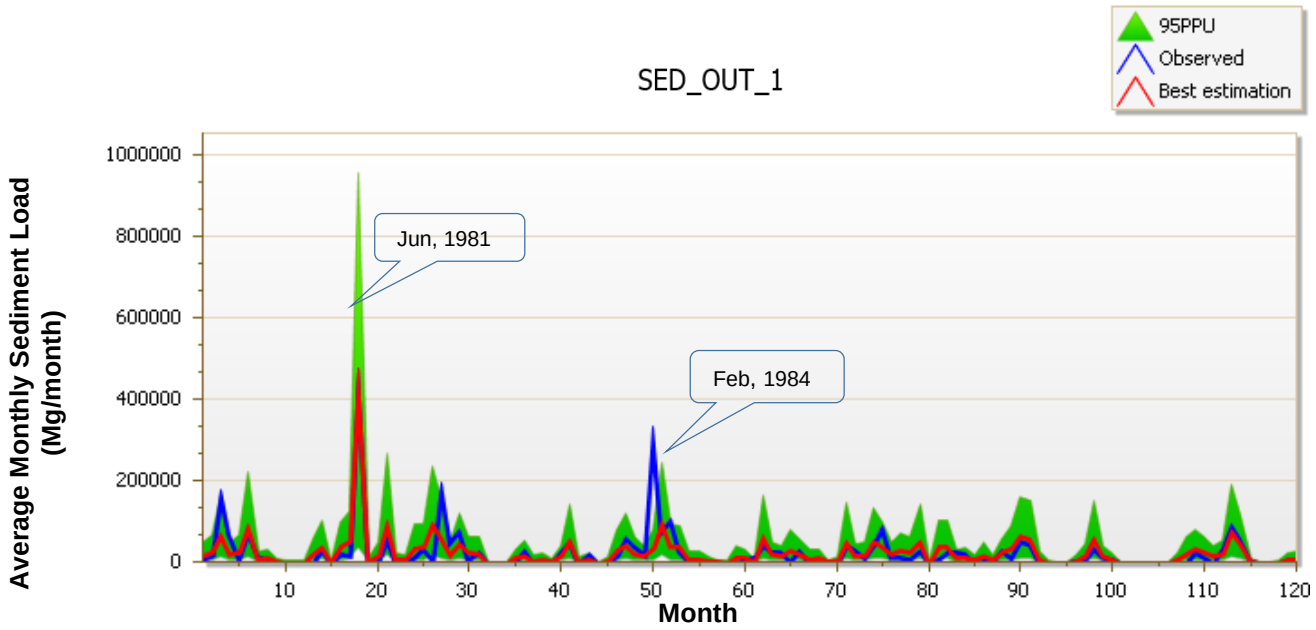

Figure 64- Calibration of Ballville Model at Gage 04198000, from 1980 to 1989

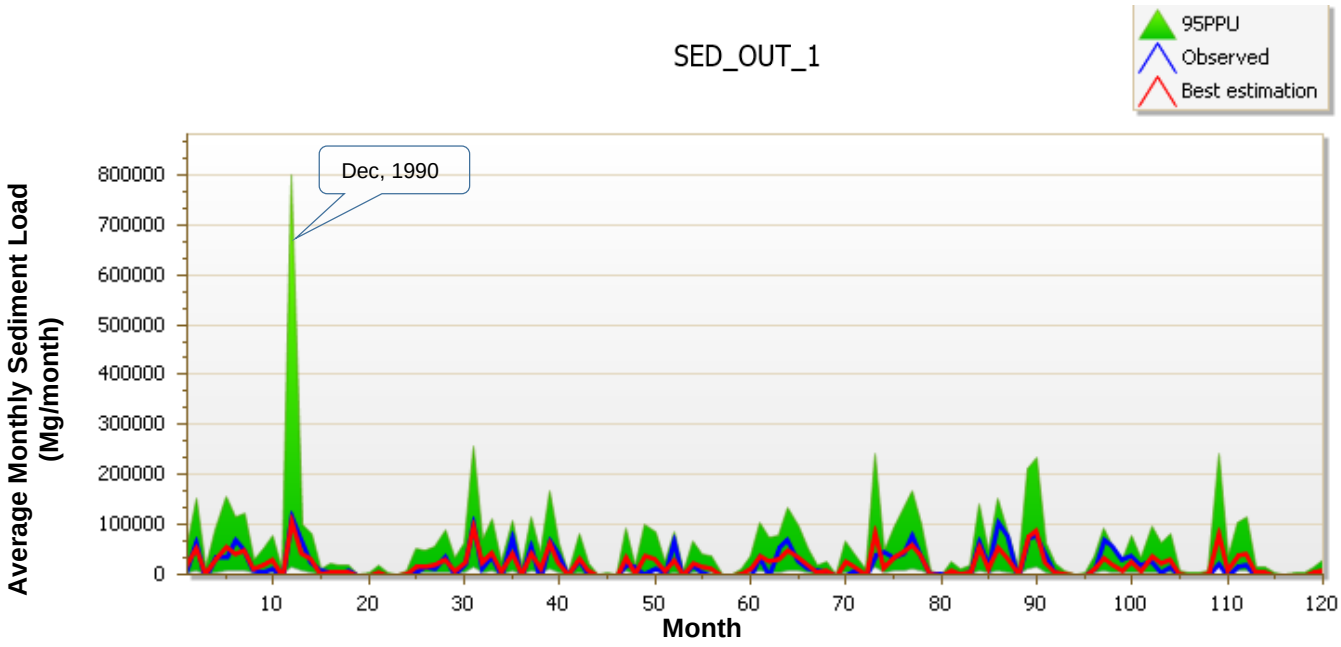

Figure 65- Validation of Ballville Model at Gage 04198000, from 1990 to 1999

The suspended sediment concentration is highest in June 1981 with a value about 600 (ppm). This can be a potential explaination for the large spike in SWAT result of Jun 1981. The stream discharge for the months of February 1984 and December 1990 was the highest. The stream discharge in February 1984 corresponds to 500-year recurrence interval. Therefore, the strong flood events in February can result in high sediment yield in the watershed.

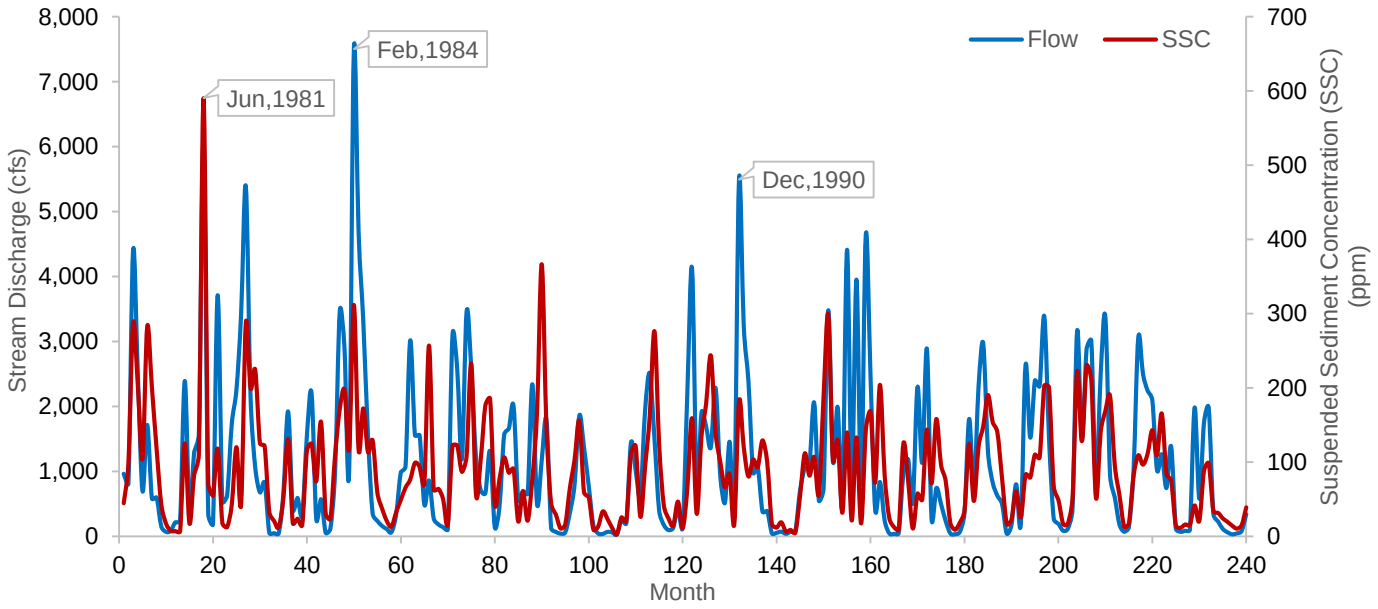

Figure 66- Comparing Stream Discharge and Suspended Sediment Concentration Recorded by Gage 04198000 from 1980 to 1999

The SWAT model for Ballville Dam represented the watershed using 18 subbasins. The Ballville Dam and the Gage 04198000 (observation gage) are in Subbasin One. The subbasins were further divided into a total of 158 Hydrologic Response Units (HRUs) based on land use, soils, and slope characteristic.

In evaluating sediment accumulation rate behind the dam, which is one of the objectives of this project, a SWAT analysis was completed to determine the sediment inflows and outflows in the reservoir. The difference between these loads provides an

estimate of the potential annual sediment loads that were trapped behind the dam. The result of this analysis are fully discussed in Chapter Five.

4.1.2. Developing and Calibrating the Pre- European Model

The other objective of this research, is estimating the natural sediment yield and evaluating the impact of human interfere on sediment yield. In this section, developing the SWAT model of pre- European settlement model are discussed. Oak savanna, prairie, wet prairie, riparian forest, and wetland originally covered the Ballville Dam watershed. In the early 1800s, European hunters and trappers settled around the Sandusky River. With European settlements in the region, some forest lands were removed for cultivating and farming. Figure 67 displays the natural land use within the Ballville Dam watershed (Ohio DNR, 2003).

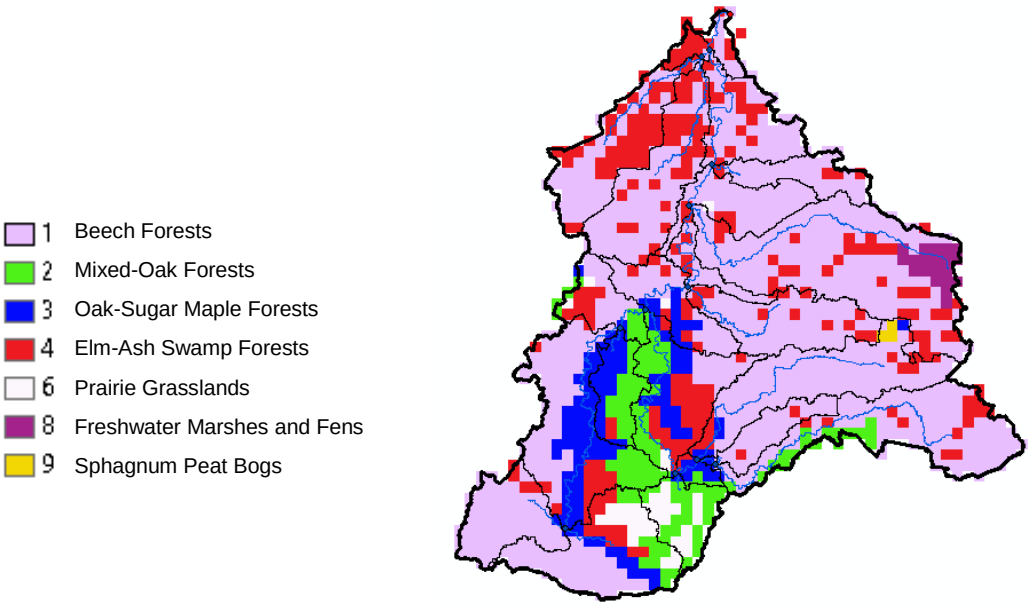

Figure 67- Land Use within Ballville Dam Watershed: Pre-European Settlement (Ohio DNR, 2003)

Natural sediment delivery is the sediment loading expected for pre-European conditions in the watershed. The natural sediment delivery has been estimated through revised/edited use of the calibrated SWAT model of the watershed. For the natural

sediment delivery simulations, the SWAT model was executed with the land use modified to reflect natural, pre-European conditions in the watershed. In addition, all man-made dams were removed from the watershed model. While it is acknowledged that climate change may have impacted the hydrologic portion of the SWAT calibration, those impacts are beyond the scope of the present investigations. Therefore, the natural sediment delivery simulations assumed the same climate conditions as used in the present-day simulations.

It is impossible to calibrate to any observed pre-European conditions, because of lack of observational data that pre-dates European settlement. The radionuclide dating used in this research does not extend back that far in history. Calibration parameters from the post-European period have been used for the pre-European simulation, with the exception that the USLE equation support practice factor (USLE-P) has been decreased by 70% for simulating natural vegetation. This follows the practice of Creech (2015) in simulating natural conditions. The results of running pre- European scenario are discussed in Chapter Five.

4.2. Webber Dam

4.2.1. Calibration the Post- European Model

To better understand the process of affecting the water and sediment yield within the Grand River watershed and evaluating the sediment accumulation rate behind the Webber Dam, the SWAT model of Webber Dam has been created. For matching up the modeled results with observed data the model has been calibrated to the monthly stream discharge. The second column in Table 24 is trapping efficiency from the Brune Curve; the third column represents sediment accumulation rate from radionuclide dating of

sediment layer. The fourth column is sediment load that delivers into the reservoir, which can be estimated by dividing sediment accumulation rate by trapping efficiency. Finally, the last column is sediment load that leaves the dam. This load has been estimated by subtracting the sediment load flows into the dam and sediment accumulation rate.

Table 24-- Sediment Loads from 1990 to 2009 for Webber Dam Watershed

Year	TE	SED_ACCU (tn/yr)	SED_IN (tn/yr)	SED_OUT (tn/yr)
1990	15%	22,703	151,352	128,650
1991	30%	22,703	75,677	52,974
1992	15%	26,709	178,062	151,352
1993	24%	21,367	89,029	67,662
1994	24%	21,367	89,029	67,662
1995	37%	21,367	57,750	36,382
1996	35%	21,367	61,049	39,682
1997	37%	21,367	57,750	36,382
1998	35%	28,045	80,128	52,083
1999	46%	20,032	43,548	23,516
2000	35%	18,696	53,419	34,722
2001	24%	20,032	83,466	63,434
2002	37%	20,032	54,140	34,108
2003	46%	20,032	43,548	23,516
2004	15%	26,042	173,613	147,571
2005	30%	26,042	86,805	60,764
2006	15%	7,545	50,302	42,757
2007	24%	8,681	36,169	27,488
2008	15%	19,364	129,095	109,731
2009	15%	13,355	89,031	75,676

Based on the radionuclide dating and natural mixing of sediments in cores, sediment accumulation rate is calculated as constant over approximately yearly time-scales and is not capture the variance associated with wetter or drier years. Therefore, this method is not recommended for calibrating this un-gagged watershed.

The other method is using the sediment parameters of the calibrated watershed models, which have pretty close characteristics including: land use, weather data, slope, and soil to the un-gaged watershed. For calibrating Webber Dam model, the sediment parameters of calibrated Ballville Dam model have been applied. Land cover in Ballville

and Webber watersheds are dominated by farmland. The Urban area is about 8% in Ballville watershed and about 12% in Webber. Around 9% of Ballville basin and 13% of Webber are a forest. Therefore, the land cover in these two watersheds is pretty close.

Webber and Ballville Dam watersheds are in two neighbor's state and their climate feature is pretty close. For instance, the average annual precipitation is about 840 (mm) in the Webber Dam and (935) mm in Ballville Dam watershed. Evapotranspiration is around 546 (mm) in Ballville and 552 (mm) in Webber Dam watershed. Table 25 compares some climate data from NOAA website and some SWAT outputs in both models.

Table 25- Annual Average Data for Ballville and Webber Dam Basins

Parameters	Ballville	Webber
Precipitation (mm)	935	843
Snow Fall (mm)	100	119
Snow Melt (mm)	100	121
Evapotranspiration (mm)	546	552
Potential Evapotranspiration (mm)	978	926
Percolation Out of Soil (mm)	140	142
Groundwater (Shallow Aquifer) (mm)	127	133

Ballville and Webber Dam watersheds are pretty flat, as it was described in the Chapter Three, the average slope is about 2.30% in Ballville and 2.00% in Webber Dam watershed. SWAT divided the Webber watershed into 32 subbasins, the Webber Dam (Dam 10) is in the Subbasin 13. For calculation purpose, the subbasins were further divided into 185 HRUs.

Sediment parameters of Ballville Dam model were applied into the Webber Dam model to calibrate the SWAT model, then a SWAT analysis was completed to determine the amount of the sediment that delivers into the reservoir and the sediment load that

exits the reservoir. The difference between these sediment loads represents the potential annual sediment accumulation rate within the Webber Dam reservoir. Chapter Five describes sediment accumulation rate in more detail.

4.2.2. Developing and Calibrating the Pre- European Model

Grand River is the longest river in the state of Michigan. More than 200 years ago, the Ottawa, Ojibwa, and Potawatomi tribes lived along the Grand River. Fishing and hunting were their way of life during the 1700s. The Grand River watershed in the 1800s was mostly forest (about 85% of the land). Also, about 8% of the land cover was rangeland, which was mostly in south of the watershed. Figure 68 shows the distribution of land uses during the pre- European period. The land use data was download from Michigan Department of Technology, Management and Budget website (*http://www.mcgi.state.mi.us/mgdl/?rel=ext&action=sext*, 2002).

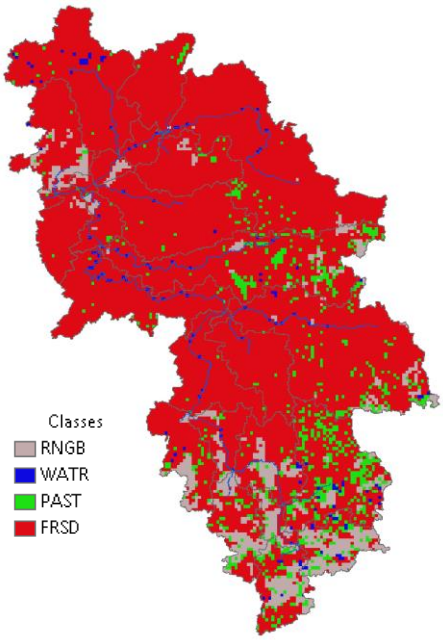

Figure 68- Land Use within Webber Dam Watershed: Pre-European Settlement (DTMB, 2002)

Natural sediment delivery is the sediment loading expected for pre-European conditions in the watershed. The natural sediment delivery has been estimated through revised/edited use of the calibrated SWAT model of the watershed. For the natural sediment delivery simulations, the SWAT model was executed with the land use modified to reflect natural, pre-European conditions in the watershed. In addition, all man-made dams were removed from the watershed model. While it is acknowledged that climate change may have impacted the hydrologic portion of the SWAT calibration, those impacts are beyond the scope of the present investigations. Therefore, the natural sediment delivery simulations assumed the same climate conditions as used in the present-day simulations, and as assumed in the USACE hydrologic calibrations.

It is impossible to calibrate to any observed pre-European conditions, as we have no observational data that pre-dates European settlement. The radionuclide dating used in this investigation does not extend back that far in history. Calibration parameters from the post-European period have been used for the pre-European simulation, with the exception that the USLE equation support practice factor (USLE-P) has been decreased by 70% for simulating natural vegetation. This follows the practice of Creech (2015) in simulating natural conditions. The results of pre- European scenario simulation are discussed in Chapter Five.

4.3. Riley Dam

4.3.1. Calibrating the Post- European Model

Riley Dam watershed is one of the un-gagged basins that do not have enough sediment observation data for calibrating the model. The sediment parameters of Ballville Dam have been used for calibrating this watershed because Ballville Dam and Riley Dam

watersheds have close characteristics regarding: land use, slope, climate data and soil characteristic. Both Riley and Ballville Dam watersheds are dominated by agricultural land use and less than 20% of their lands are developed and forested. Table 26 displays some of the climate data including precipitation and snowfall depth from NOAA website and SWAT outputs in both models. As the table shows the climate feature is pretty similar in both watersheds; for instance, the precipitation depth in Riley Watershed is only 0.85 % less than the Ballville Watershed.

Table 26- Average Annual Data for Ballville and Riley Dam Watersheds

Parameters	Ballville	Riley
Precipitation Depth (mm)	935	927
Snow Fall Depth (mm)	100	129
Snow Melt Depth (mm)	100	127
Evapotranspiration Depth (mm)	546	548
Potential Evapotranspiration Depth (mm)	978	907
Percolation Out of Soil Depth (mm)	140	190
Groundwater Depth (Shallow Aquifer) (mm)	127	171

Ballville and Riley Dam basins are pretty flat. As described in Chapter Three, the average slope is about 2.3% in the Ballville Dam basin and it is about 2.1% in Riley basin.

The SWAT model for Riley Dam represented the watershed using 28 subbasins; the Riley Dam is in the Subbasin 9. The subbasins were further divided into a total of 75 HRUs. In the Riley SWAT model, the “warm up” period was considered from 1986 through 1990, then model was simulated between 1991 and 2010.

4.3.2. Developing and Calibrating the Pre- European Model

Natural sediment delivery is the sediment loading expected for pre-European conditions in the watershed. The natural sediment delivery has been estimated through revised/edited use of the calibrated SWAT model of the watershed. For the natural sediment delivery simulations, the SWAT model was executed with the land use modified

to reflect natural, pre-European conditions in the watershed. In addition, all man-made dams were removed from the watershed model. While it is acknowledged that climate change may have impacted the hydrologic portion of the SWAT calibration, those impacts are beyond the scope of the present investigations. Therefore, the natural sediment delivery simulations assumed the same climate conditions as used in the present-day simulations, and as assumed in the USACE hydrologic calibrations.

It is impossible to calibrate to any observed pre-European conditions, as there is no observational data that pre-dates European settlement. The radionuclide dating used in this investigation does not extend back that far in history. Calibration parameters from the post-European period have been used for the pre-European simulation, with the exception that the USLE equation support practice factor (USLE-P) has been decreased by 70% for simulating natural vegetation. This follows the practice of Creech (2015) in simulating natural conditions.

The results of comparing the baseline scenario, with anthropogenic scenario are discussed in Chapter Five.

4.4. Upper Green Lake Dam

4.4.1. Calibrating the Post- European Model

For evaluating sediment accumulation rate behind the Upper Green Dam, the SWAT model of Upper Green Dam has been created. For matching up the modeled with the observed data, the model has been calibrated to the monthly stream discharge at Gage 04073473. Because of no active gage recorded recent sediment load in the watershed, the Upper Green model has been calibrated with applying the sediment calibrate parameters of Ballville Dam model. Upper Green and Ballville Dam watersheds

have some similar characteristics regarding land use, weather data, slope, and soil. In both watersheds, the land cover is dominated by farmland. Urban area covers 8% of the basin in both watersheds. About 6% of Upper Green watershed and 9% of Ballville basin are covered by forest. Upper Green and Ballville Dam watersheds have similar climate feature. For instance, the mean annual precipitation depth is about 773 (mm) in the Upper Green and 935 (mm) in Ballville watersheds. Evapotranspiration depth is around 546 (mm) in Ballville and 615 (mm) in Upper Green basin. Some climate data from NOAA website and SWAT outputs in both models are given in Table 27.

Table 27- Annual Average Data for Ballville and Upper Green Dam Basins

Parameters	Ballville	Upper Green
Precipitation (mm)	935	773
Snow Fall (mm)	100	86
Snow Melt (mm)	100	85
Evapotranspiration (mm)	546	615
Potential Evapotranspiration (mm)	978	1,018

Ballville and Upper Green Dam watersheds are pretty flat, as described in Chapter Three, the slope is about 2.30% in Ballville and 3% in Upper Green Dam watersheds.

The SWAT model of Upper Green contains one subbasin. For calculation purpose, the subbasin was further divided into 10 HRUs.

4.4.2. Developing and Calibrating the Pre- European Model

Before European settlement, the Upper Green Lake watershed was heavily forested as well as some subbasins were wetlands and grasslands. The first European settlers came to the township of Ripon (upstream of the dam) in 1844. Figure 69 shows pre- European settlement land use in this study watershed. Approximately 57% of the basin was forest, 28% range, and the rest of that was wetland and water.

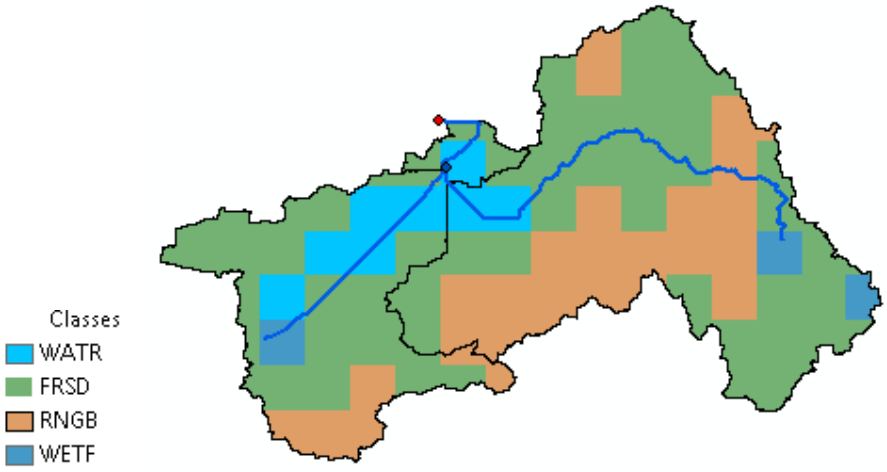

Figure 69- Land Use of Upper Green Dam Watershed; Pre-European Settlement (Wisconsin DNR, 2006)

Natural sediment delivery is the sediment loading expected for pre-European conditions in the watershed. The natural sediment delivery has been estimated through revised/edited use of the calibrated SWAT model of the watershed. For the natural sediment delivery simulations, the SWAT model was executed with the land use modified to reflect natural, pre-European conditions in the watershed. In addition, all man-made dams were removed from the watershed model. While it is acknowledged that climate change may have impacted the hydrologic portion of the SWAT calibration, those impacts are beyond the scope of the present investigations. Therefore, the natural sediment delivery simulations assumed the same climate conditions as used in the present-day simulations, and as assumed in the USACE hydrologic calibrations.

It is impossible to calibrate to any observed pre-European conditions, as there has no observational data that pre-dates European settlement. The radionuclide dating used in this investigation does not extend back that far in history. Calibration parameters from the post-European period have been used for the pre-European simulation, with the exception that the USLE equation support practice factor (USLE-P) has been decreased

by 70% for simulating natural vegetation. This follows the practice of Creech (2015) in simulating natural conditions.

4.5. Goshen Pond Dam

4.5.1. Calibrating the Post- European Model

Goshen Pond Dam watershed is the other basin that do not have enough sediment observation data for calibrating the model. For calibrating this watershed, the sediment calibrated parameters of Ballville Dam have been used. Goshen Pond and Ballville Dam watersheds are similar in terms of land use, soil, and topography characteristic. Table 28 shows the climate data in these two study watersheds, as the data show the climate features in these watersheds are similar. In Goshen Pond Dam watershed, the “warm up” period is from 1975 through 1980. The model simulation period is between 1980 and 2010. The Goshen Pond Dam watershed is divided into 12 subbasins for the analyzing purpose and the Goshen Pond Dam is in the Subbasin One. The subbasins are further divided into a total of 26 Hydrologic Response Units (HRUs).

Table 28- Average Annual Data for Ballville and Goshen Pond Basins

Parameters	Ballville	Goshen Pond
Precipitation (mm)	935	963
Snow Fall (mm)	100	108
Snow Melt (mm)	100	94
Evapotranspiration (mm)	546	517
Potential Evapotranspiration (mm)	978	880

4.5.2. Developing and Calibrating the Pre- European Model

The Goshen Pond watershed was heavily forested land, before European settlement. However, currently, just 8% of the watershed is a forest.

Natural sediment delivery is the sediment loading expected for pre-European conditions in the watershed. The natural sediment delivery has been estimated through revised/edited use of the calibrated SWAT model of the watershed. For the natural sediment delivery simulations, the SWAT model was executed with the land use modified to reflect natural, pre-European conditions in the watershed. In addition, all man-made dams were removed from the watershed model. While it is acknowledged that climate change may have impacted the hydrologic portion of the SWAT calibration, those impacts are beyond the scope of the present investigations. Therefore, the natural sediment delivery simulations assumed the same climate conditions as used in the present-day simulations, and as assumed in the USACE hydrologic calibrations.

It is impossible to calibrate to any observed pre-European conditions, as there has no observational data that pre-dates European settlement. The radionuclide dating used in this investigation does not extend back that far in history. Calibration parameters from the post-European period have been used for the pre-European simulation, with the exception that the USLE equation support practice factor (USLE-P) has been decreased by 70% for simulating natural vegetation. This follows the practice of Creech (2015) in simulating natural conditions.

4.6. Lake Rockwell Dam

4.6.1. Calibrating the Post- European Model

Sensitivity analysis was completed for the Lake Rockwell Dam model and the results were shown in Figure 70. The sensitivity result analysis showed that the sediment is sensitive to nine parameters. The SPCON (coefficient in sediment transport), which has the highest t-Stat is the most influential parameter and VCRIT (critical velocity), with the lowest t-Value is the least sensitive parameter.

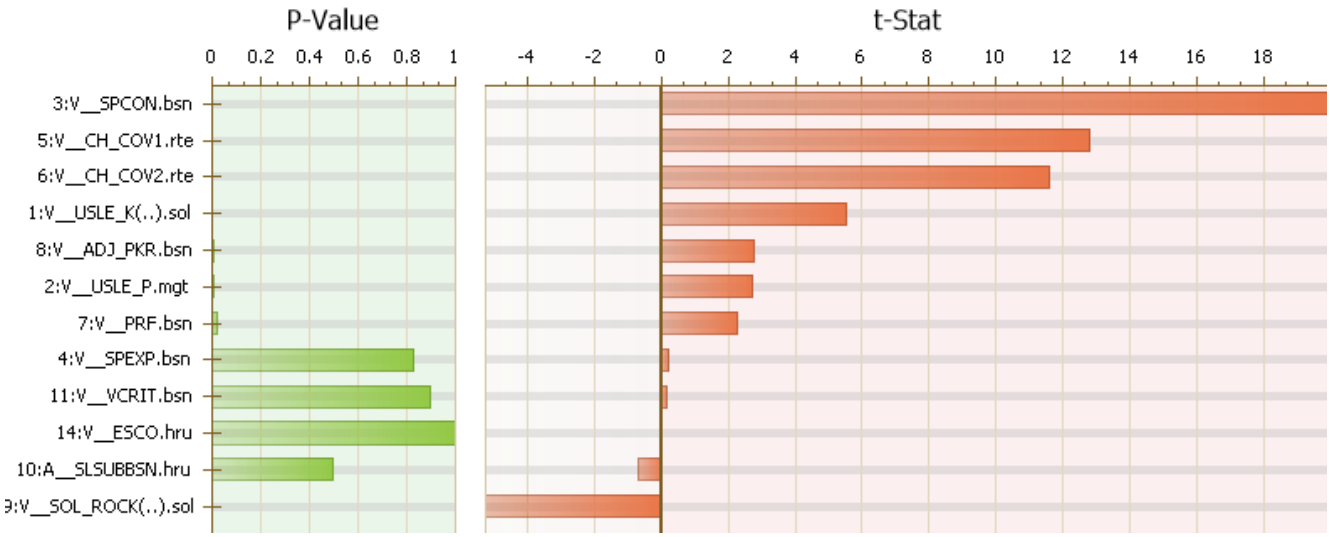

Figure 70- Global Sensitivity Analysis Results for Rockwell Dam Model

The influential parameters have been adjusted within their allowable range to achieve the best match between simulation and observation data. In this case, the model was calibrated to the recorded mean monthly sediment load at Gage 04208000, which is in Subbasin Five. The calibration parameters and their final calibrated values are given in Table 29. The last three parameters in Table 29 are from the hydrologic calibration model, so they are not adjusted here.

Table 29- Calibrated Parameters and Final Values for Rockwell Dam Model

Parameter	Table	Description	Method	Min	Max
USLE_K	.sol	Soil erodibility factor	Replace	0.20	0.30
USLE_P	.mgt	Support practice factor	Replace	0.65	0.85
SPCON	.bsn	Coefficient in sediment transport	Replace	0.00006	0.0006
SPEXP	.bsn	Exponent in sediment transport	Replace	1.00	1.20
CH_COV1	.rte	Channel erodibility factor	Replace	0.00	0.50
CH_COV2	.rte	Channel cover factor	Replace	0.00	0.50
PRF	.bsn	Peak rate adjustment factor	Replace	1.20	1.50
ADJ_PKR	.bsn	Peak rate adjustment factor	Replace	1.00	1.50
SOL_Rock	.sol	Percent rock in soil layer (%)	Replace	3.00	12.00
SLSUBBSN	HRU	Average slope length (m)	Absolute	0.00	-5.00
VCRIT	.bsn	Critical velocity (m/s)	Replace	0.35	2.11
ALPHA_BF	.gw	Base flow alpha factor (days)	Replace	0.96	0.96
GW_DELAY	.gw	Groundwater delay (days)	Replace	20.40	20.40
ESCO	.hru	Soil evap. compensation factor	Replace	0.89	0.89

In the Rockwell Dam watershed, the five years from 1983 through 1988 have been considered as a “warm up” period, which allowed the model to overcome the potential effects of the initial conditions. The model was calibrated to the recorded data from 1988 to 1997 and then validated from 1998 to 2007. Figure 71 displays the statistics comparing observed with simulation results for the calibration run and Figure 72 shows this comparison for the validation run. In the calibration run, the sediment p-factor and r-factor are 0.78 and 1.08, respectively, which are good. In the validation run, p-factor and r-factor are 0.84 and 1.60. The NSE in calibration and validation runs are 0.71 and 0.72, respectively, which represent very good correspondence.

```
Goal_type=  Nash_Sutcliffe (type 5)    Best_sim_no= 146    Best_goal = 7.284271e-001

Variable          p-factor    r-factor      R2          NS          br2          MSE          SSQR
FLOW_OUT_5        0.22        0.00          0.84        0.77        0.6713       76.2605      30.8828
FLOW_OUT_6        0.16        0.00          0.66        0.64        0.5148       7.7995       0.6556
FLOW_OUT_19       0.23        0.00          0.81        0.80        0.6332       20.5375      5.1147
SED_OUT_5         0.78        1.08          0.71        0.71        0.5030       155651792.0000 24640770.0000


---- Results for behavioral parameters ---
Behavioral threshold= 0.500000
Number of behavioral simulations = 1468

Variable          p_factor    r-factor      R2          NS          br2          MSE          SSQR
FLOW_OUT_5        0.22        0.00          0.84        0.77        0.6713       76.2605      30.8828
FLOW_OUT_6        0.16        0.00          0.66        0.64        0.5148       7.7995       0.6556
FLOW_OUT_19       0.23        0.00          0.81        0.80        0.6332       20.5375      5.1147
SED_OUT_5         0.74        0.97          0.71        0.71        0.5030       155651792.0000 24640770.0000
```

Figure 71- Statistics Comparing Observed Data with the Simulation Data in Calibration Period

Goal_type= Nash_Sutcliffe (type 5) Best_sim_no= 345 Best_goal = 7.217451e-001

Variable	p-factor	r-factor	R2	NS	br2	MSE	SSQR
FLOW_OUT_5	0.20	0.00	0.84	0.82	0.7592	64.7041	11.5357
FLOW_OUT_6	0.17	0.00	0.69	0.58	0.6349	7.9182	1.8434
FLOW_OUT_19	0.22	0.00	0.80	0.77	0.7522	25.7642	3.0172
SED_OUT_5	0.84	1.60	0.74	0.72	0.5132	52855580.0000	17839488.0000

--- Results for behavioral parameters ---
Behavioral threshold= 0.500000
Number of behavioral simulations = 1056

Variable	p_factor	r-factor	R2	NS	br2	MSE	SSQR
FLOW_OUT_5	0.20	0.00	0.84	0.82	0.7592	64.7041	11.5357
FLOW_OUT_6	0.17	0.00	0.69	0.58	0.6349	7.9182	1.8434
FLOW_OUT_19	0.22	0.00	0.80	0.77	0.7522	25.7642	3.0172
SED_OUT_5	0.79	1.08	0.74	0.72	0.5132	52855580.0000	17839488.0000

Figure 72- Statistics Comparing Observed Data with the Simulation Data in Validation Period

The average of sediment loads exiting the subbasin 5 (watershed outlet) in calibration and validation runs are shown in Figure 73 and Figure 74. The green region shows the potential sediment load data leaving the Subbasin 5. The blue line represents the observation data, while the red line is the best simulation in the green region. The best simulation is the set of sediment load data which is the closest to the observation data in the green region. Figure 73 and Figure 74 display the good fit between the observed and simulated range of data.

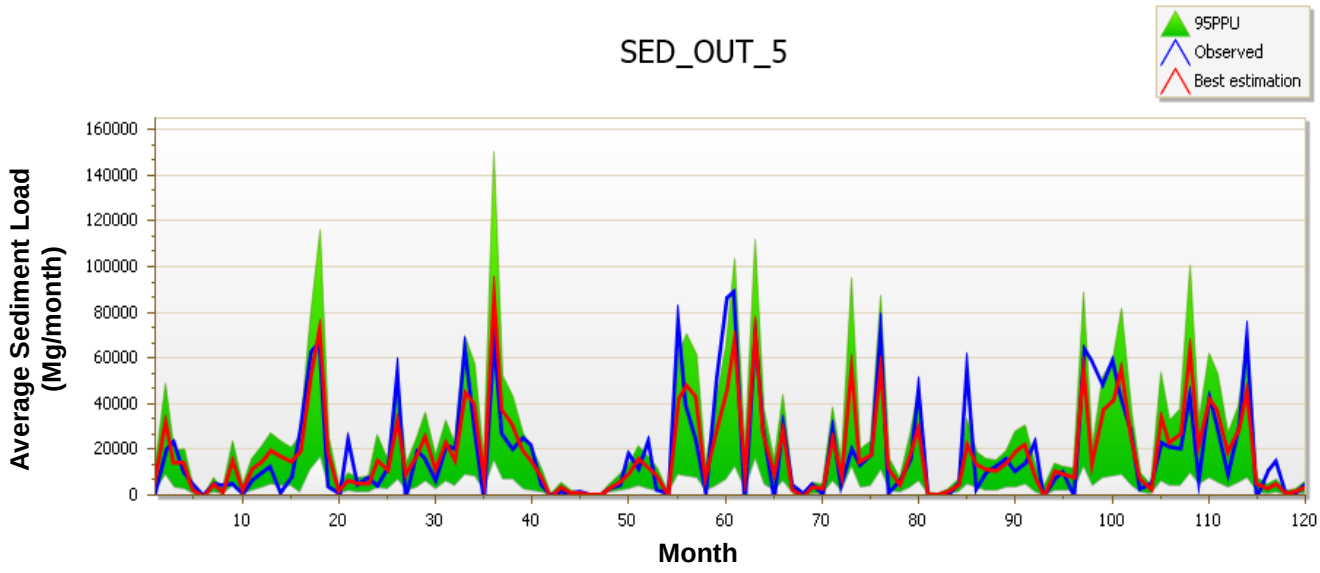

Figure 73- Calibration of Rockwell Model at Gage 04208000, from 1988 to 1997

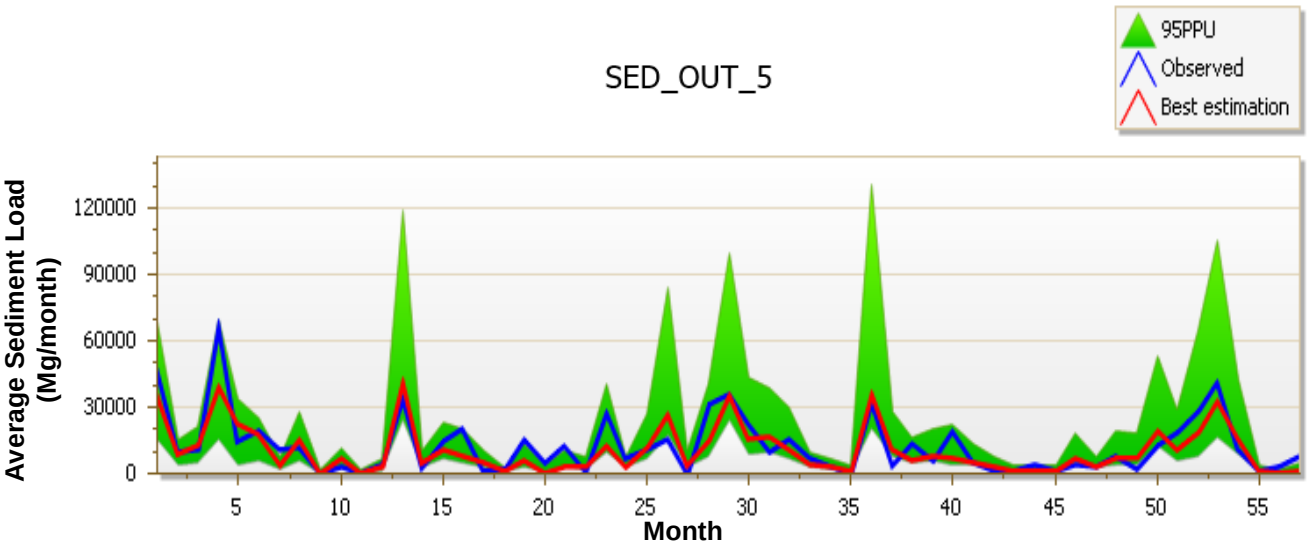

Figure 74- Validation of Rockwell Model at Gage 04208000, from 1998 to 2007

4.6.2. Developing and Calibrating the Pre- European Model

Before European settlement, Lake Rockwell watershed was defined as heavily forested. The Native American had little modified to the natural environment and just some disturbance into the natural ecology systems. However, in early 1800's with European settlement, most forests were cut down and they were gradually cleared for field crops, pasture, and timber products. Figure 75 depicts the natural vegetation in Lake Rockwell watershed; the natural vegetation GIS layer was downloaded from Ohio Department of Natural Resources website.

Natural sediment delivery is the sediment loading expected for pre-European conditions in the watershed. The natural sediment delivery has been estimated through revised/edited use of the calibrated SWAT model of the watershed. For the natural sediment delivery simulations, the SWAT model was executed with the land use modified to reflect natural, pre-European conditions in the watershed. In addition, all man-made dams were removed from the watershed model. While it is acknowledged that climate change may have impacted the hydrologic portion of the SWAT calibration, those impacts

are beyond the scope of the present investigations. Therefore, the natural sediment delivery simulations assumed the same climate conditions as used in the present-day simulations, and as assumed in the USACE hydrologic calibrations.

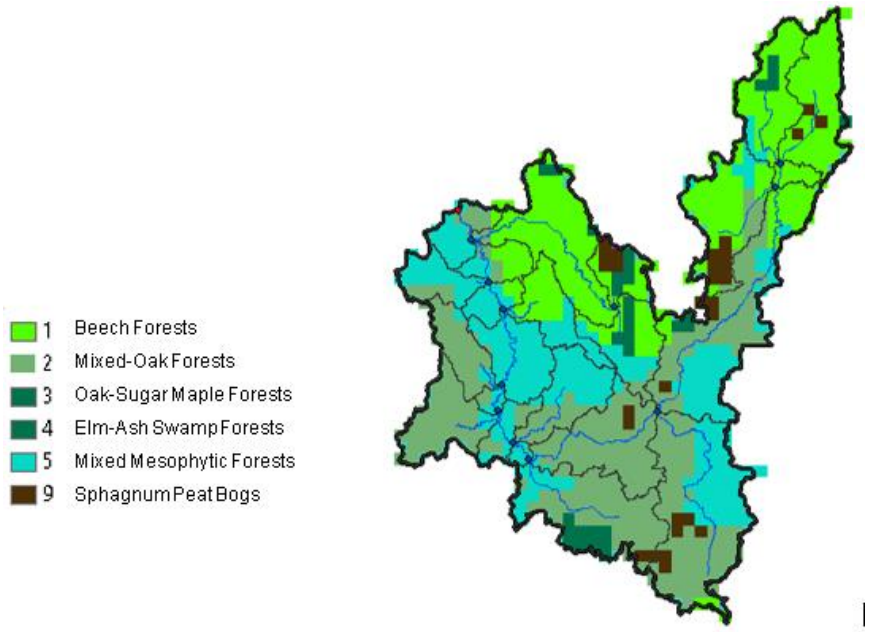

Figure 75- Land Use within Lake Rockwell Dam Watershed: Pre-European Settlement (Ohio DNR, 2003)

It is impossible to calibrate to any observed pre-European conditions, as the team has no observational data that pre-dates European settlement. The radionuclide dating used in this investigation does not extend back that far in history. Calibration parameters from the post-European period have been used for the pre-European simulation, with the exception that the USLE equation support practice factor (USLE-P) has been decreased by 70% for simulating natural vegetation. This follows the practice of Creech (2015) in simulating natural conditions. The results of this simulation are fully disscused in Chapter Five.

4.7. Ford Lake Dam

4.7.1. Calibrating the Post- European Model

There is not enough recorded sediment gage data within the Ford Lake watershed to be used for calibrating the model. So for calibrating this watershed, the method described in the first section of this chapter is used and the parameters from the sediment calibrated of Rockwell Dam have been applied into the Ford Lake model. The Rockwell and Ford Lake watersheds have similar land use, slope and soil characteristics. Table 30 shows the climate data for Rockwell and Ford Lake watersheds. Evapotranspiration is similar in both watersheds and their difference is less than 1%, but the precipitation depth in Rockwell watershed is about 25% higher than Ford Lake watershed. About one third of these two watersheds are developed area, about 25% of Ford Lake and 35% of Rockwell watersheds are forest, so the land use breaks down are pretty similar in these watersheds.

The five years from 1985 through 1990 have been considered a “warm up” period for the simulations, and model simulated from 1990 to 2009. The SWAT model of the Ford Lake Dam watershed utilizes eight subbasins. Ford Lake Dam is in Subbasin Eight. The subbasins were further divided into a total of 76 Hydrologic Response Units (HRUs).

Table 30- Annual Average Data for Rockwell and Ford Lake Dam Basins

Parameters	Rockwell	Ford Lake
Precipitation (mm)	1,071	797
Snow Fall (mm)	136	108
Snow Melt (mm)	135	110
Evapotranspiration (mm)	582	576
Potential Evapotranspiration (mm)	903	979

4.7.2. Developing and Calibrating the Pre- European Model

The watershed tributary to Ford Lake Dam was heavily forested prior to European settlement. Thereafter, most forest and pasture were removed, with an increase in urban development and farmland. Figure 76 displays the pre-European land use within the Ford Lake Dam watershed.

Natural sediment delivery is the sediment loading expected for pre-European conditions in the watershed. The natural sediment delivery has been estimated through revised/edited use of the calibrated SWAT model of the watershed. For the natural sediment delivery simulations, the SWAT model was executed with the land use modified to reflect natural, pre-European conditions in the watershed. In addition, all man-made dams were removed from the watershed model. While it is acknowledged that climate change may have impacted the hydrologic portion of the SWAT calibration, those impacts are beyond the scope of the present investigations. Therefore, the natural sediment delivery simulations assumed the same climate conditions as used in the present-day simulations, and as assumed in the USACE hydrologic calibrations.

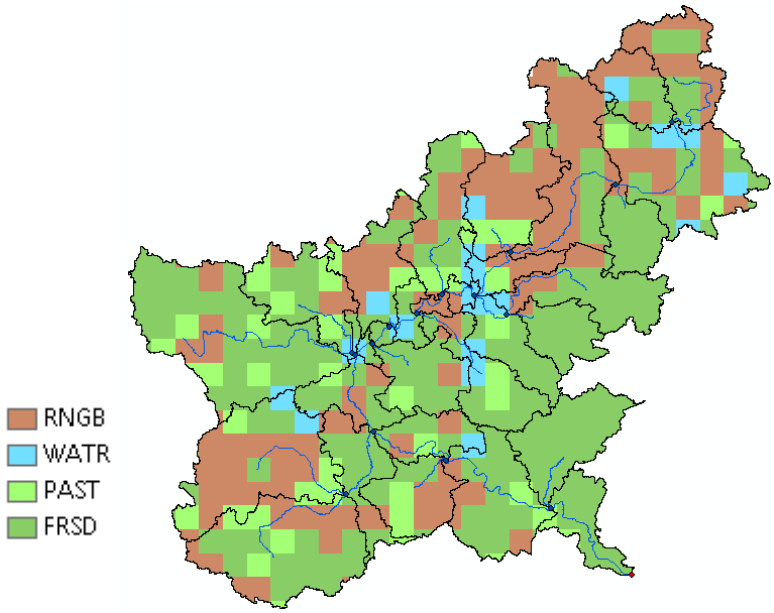

Figure 76- Land Use within Ford Lake Watershed: Pre-European Settlement (DTMB, 2002)

It is impossible to calibrate to any observed pre-European conditions, as the team has no observational data that pre-dates European settlement. The radionuclide dating used in this investigation does not extend back that far in history. Calibration parameters from the post-European period have been used for the pre-European simulation, with the exception that the USLE equation support practice factor (USLE-P) has been decreased by 70% for simulating natural vegetation. This follows the practice of Creech (2015) in simulating natural conditions.

4.8. Potter's Falls Dam

4.8.1. Calibrating the Post- European Model

A sensitivity analysis was completed of the independent variables/paramters in the Potter's Falls model. The sensitivity analysis found that five parameters are the most influential in impacting the sediment yield calculation. The global sensitivity results are provided in Figure 77. The HRU_SLP (average slope steepness) and SOL_ROCK

(percent rock in soil layer) with the highest t-State are the most influential parameters, while the USLE_K (soil erodibility factor) and USLE_P (support practice factor) are the least important among the sediment parameters. The importance of ADJ_PKR (peak rate adjustment factor) is medium among other parameters.

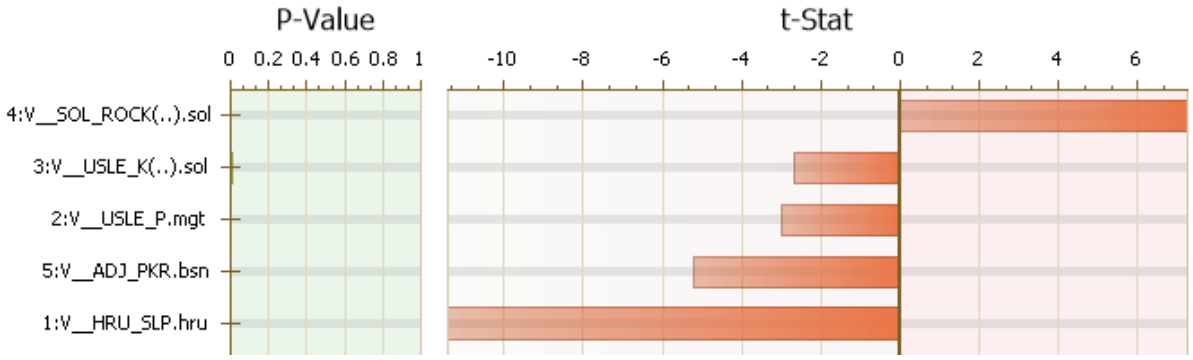

Figure 77- Global Sensitivity Analysis Results for Potter's Falls Model

Based on the sensitivity analysis, the five parameters were adjusted within their allowable ranges to provide the best match between modeled and observed sediment load. The model was calibrated to the observed values of mean monthly sediment load as measured at the Gage 04233300. The calibration parameters and their final calibrated value are given in Table 31. The final six last parameters listed in Table 31 were calibrated within the hydrologic simulation.

Table 31- Calibrated Parameters and Final Values for Potter's Falls Model

Parameter	Table	Description	Method	Min	Max
HRU_SLP	.bsn	Average slope steepness (m/m)	Replace	0.01	0.077
USLE_P	.mgt	USLE equation support practice	Replace	0.80	1.00
USLE_K	.sol	USLE equation soil erodibility factor	Replace	0.29	0.32
SOL_ROCK	.sol	Percent rock in soil layer (%)	Replace	24.50	33.50
ADJ_PKR	.bsn	Peak rate adjustment factor	Replace	0.56	0.85
SFTMP	.bsn	Mean air temperature (ºC)	Replace	1.43	1.43
SMTMP	.bsn	Threshold temperature for snow melt (ºC)	Replace	5.46	5.46
SOL_K	.sol	Saturated hydraulic conductivity (mm/hr.)	Replace	456.20	456.20
GW_DELAY	.gw	Delay time for aquifer recharge (days)	Replace	8.67	8.67
SLSUBBSN	.hru	Average slope length (m)	Replace	91.95	91.95
GW_REVAP	.gw	Groundwater "revap" coefficient	Replace	0.093	0.093

In the Potter's Falls model, five year period, from 1994 through 1999, was considered as a "warm up" period, reducing the potential influence of initial conditions on the simulation results. The model was calibrated to the recorded sediment load from 1999 to 2002, then validated from 2003 to 2010. Figure 78 and Figure 79 display the comparative statistics comparing observed with simulated results for the calibration and validation runs, respectively. For the calibration run, the p-factor is 0.76 and r-factor is 1.19. These are both within the acceptable range. The NSE for the calibration run is 0.59 which is satisfactory. For the validation run, the p-factor and r-factor are 0.61 and 0.79, respectively, which are acceptable. The NSE value for the validation run is 0.12, which is considered low. However, the simulated sediment accumulation rate within the reservoir matches well with radionuclide dating and bathymetric subtraction methods as explained more fully in Chapter Five.

Goal_type= Nash_Sutcliffe (type 5) Best_sim_no= 174 Best_goal = 5.975451e-001

Variable	p-factor	r-factor	R2	NS	br2	MSE	SSQR
FLOW_OUT_1	0.25	0.09	0.63	0.61	0.4276	0.6602	0.1357
SED_OUT_1	0.76	1.19	0.59	0.59	0.3441	2106023.2500	703914.5625

---- Results for behavioral parameters ---
Behavioral threshold= 0.100000
Number of behavioral simulations = 912

Variable	p_factor	r-factor	R2	NS	br2	MSE	SSQR
FLOW_OUT_1	0.25	0.09	0.63	0.61	0.4276	0.6602	0.1357
SED_OUT_1	0.73	0.94	0.59	0.59	0.3441	2106023.2500	703914.5625

Figure 78- Statistics Comparing Observed Data with the Simulation Data in Calibration Period

Goal_type= Nash_Sutcliffe (type 5) Best_sim_no= 193 Best_goal = 3.744164e-001

Variable	p-factor	r-factor	R2	NS	br2	MSE	SSQR
FLOW_OUT_1	0.30	0.13	0.69	0.63	0.6142	0.6301	0.0308
SED_OUT_1	0.61	0.79	0.14	0.12	0.0235	11335208.0000	4980842.0000

---- Results for behavioral parameters ---
Behavioral threshold= 0.100000
Number of behavioral simulations = 866

Variable	p_factor	r-factor	R2	NS	br2	MSE	SSQR
FLOW_OUT_1	0.28	0.13	0.69	0.63	0.6142	0.6301	0.0308
SED_OUT_1	0.59	0.59	0.14	0.12	0.0235	11335208.0000	4980842.0000

Figure 79- Statistics Comparing Observed Data with the Simulation Data in Validation Period

The average sediment load at Gage 04233300 for calibration and validation runs are shown in Figure 80 and Figure 81, respectively. The green region represents the potential sediment load leaving Subbasin One, the blue line shows the observation sediment load, while the red line represents the best simulation.

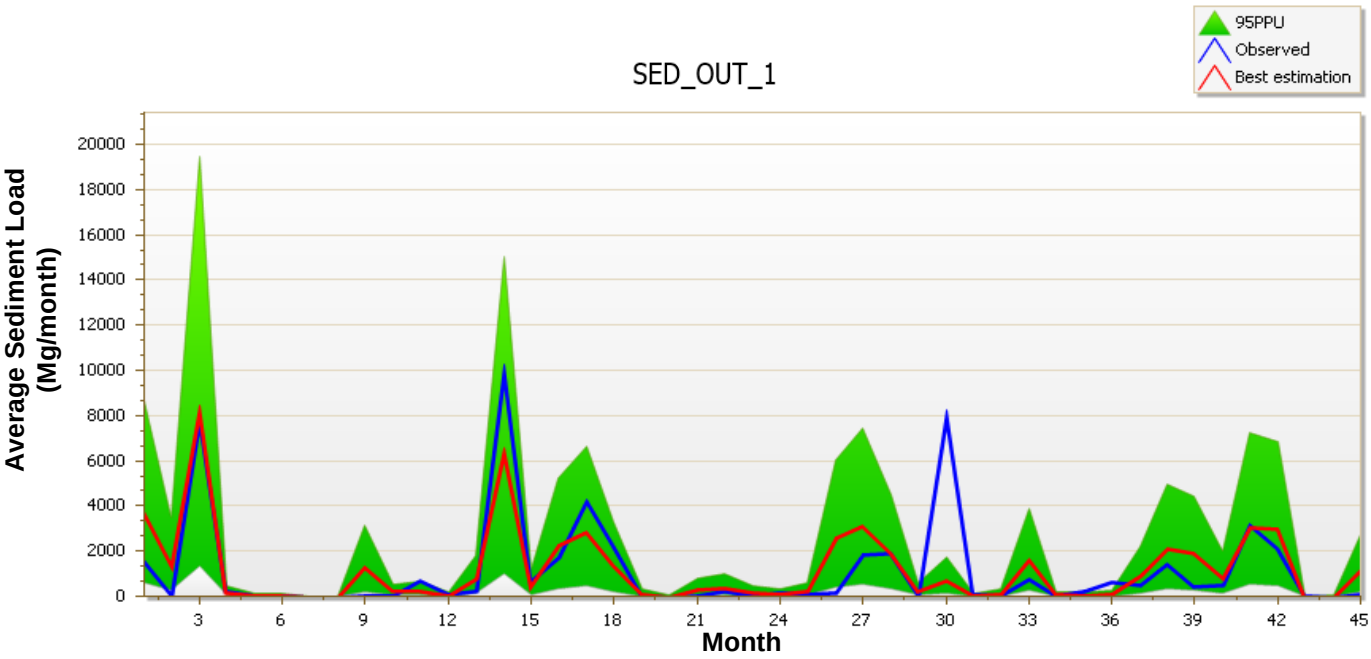

Figure 80- Calibration of Potter's Falls Model, at Gage 04233300, from 1999 to 2002

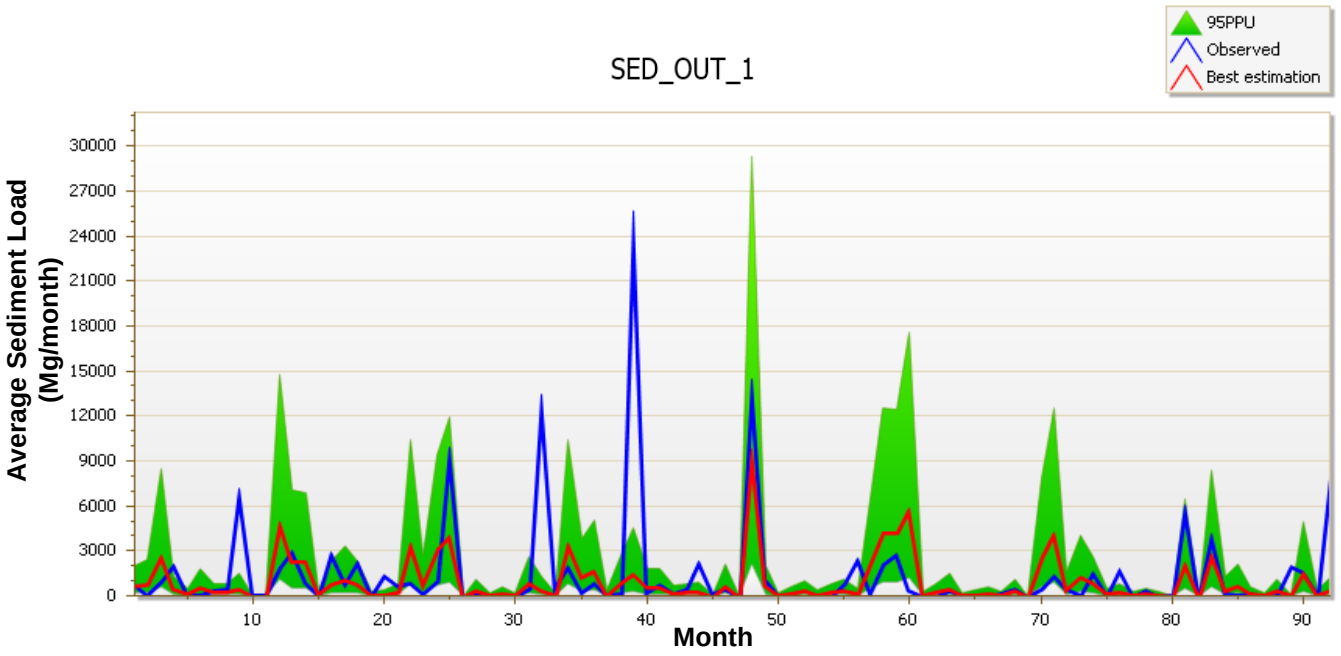

Figure 81- Validation of Potter's Falls Model at Gage 04233300, from 2003 to 2010

Figure 82 shows the recorded stream discharge and suspended sediment concentration by Gage 04233300 from 1999 to 2010. The suspended sediment concentration follows a similar trend as the stream discharge.

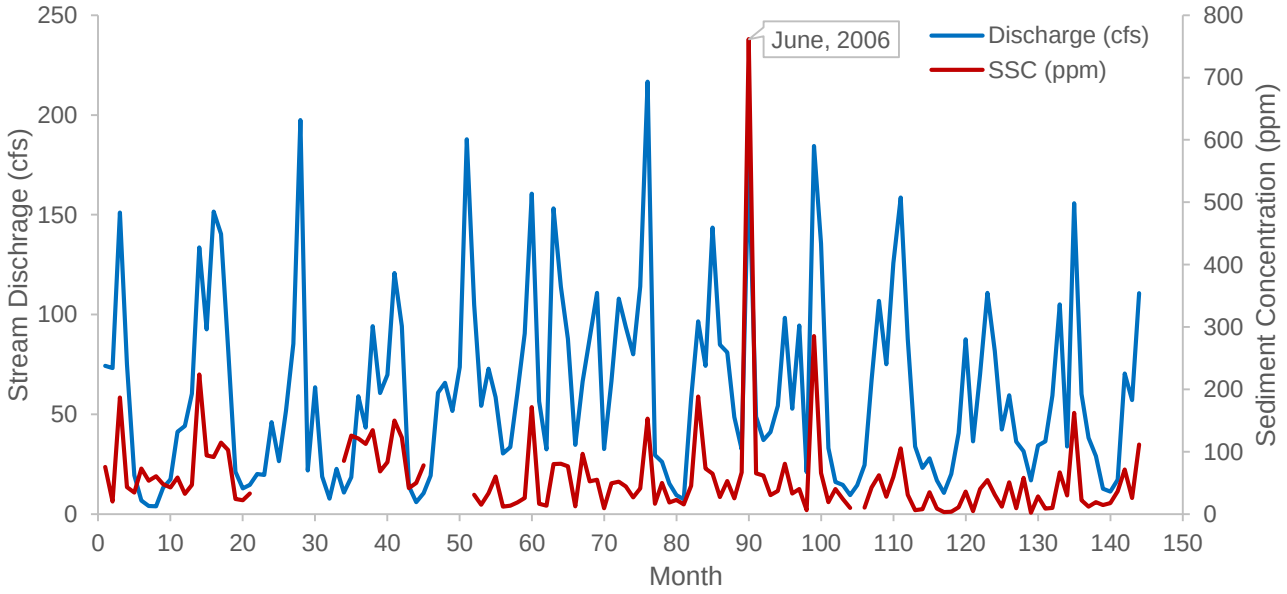

Figure 82- Comparing Recorded Stream Discharge and Sediment Concentration by Gage 04233300 from 1999 to 2010

4.8.2. Developing and Calibrating the Pre- European Model

For determining the natural sediment delivery in Potter's Fall watershed, the new scenario has been defined, which is called pre- European scenario. In the new scenario, the natural vegetation land use data (GIS based) has been input into the SWAT model and the existing dam was removed. The GIS layer of natural vegetation with high resolution, specifically for this watershed does not exist. (Ellis et al., 2010) developed the natural vegetation land use for the entire US, so its resolution is too low for the smaller watershed like Potter's Falls watershed. The natural vegetation (Ellis et al., 2010) showed that the entire study watershed was covered by forest before European settlements.

Natural sediment delivery is the sediment loading expected for pre-European conditions in the watershed. The natural sediment delivery has been estimated through revised/edited use of the calibrated SWAT model of the watershed. For the natural sediment delivery simulations, the SWAT model was executed with the land use modified to reflect natural, pre-European conditions in the watershed. In addition, all man-made dams were removed from the watershed model. While it is acknowledged that climate change may have impacted the hydrologic portion of the SWAT calibration, those impacts are beyond the scope of the present investigations. Therefore, the natural sediment delivery simulations assumed the same climate conditions as used in the present-day simulations, and as assumed in the USACE hydrologic calibrations.

It is impossible to calibrate to any observed pre-European conditions, as the team has no observational data that pre-dates European settlement. The radionuclide dating used in this investigation does not extend back that far in history. Calibration parameters from the post-European period have been used for the pre-European simulation, with the

exception that the USLE equation support practice factor (USLE-P) has been decreased by 70% for simulating natural vegetation. This follows the practice of Creech (2015) in simulating natural conditions. The results of comparing between pre- and post- European scenarios are discussed in Chapter Five.

4.9. Brown Bridge Dam

4.9.1. Calibrating the Post- European Model

There is not enough recorded sediment gage data within the Brown Bridge Dam watershed to be used for calibrating and validating the model. Therefore, for calibrating this watershed, the method described at the beginning of this chapter is used, and the sediment calibrated parameters of Potter's Falls model have been applied. The Potter's Falls and Brown Bridge watersheds have similar land use and weather data characteristics. Table 32 displays some climate data from NOAA website and SWAT outputs for both models. Weather data including snow fall, snow melt, and potential evaporation are pretty similar in two basins. However, precipitation depth in Brown Bridge watershed is about 18% less than Potter's Falls.

Table 32- Average Annual Data for Potter's Falls and Brown Bridge Watersheds

Parameters	Potter's Falls	Brown Bridge
Precipitation (mm)	996	816
Snow Fall (mm)	160	167
Snow Melt (mm)	150	163
Evapotranspiration (mm)	498	500
Potential Evapotranspiration (mm)	808	711
Percolation Out of Soil (mm)	205	275

In Brown Bridge watershed, the biggest part of the soil is sand and less than 10% of the soil is rock, while in Potter's Falls watershed, soil is mostly silt, and about 25% of the soil is rock. Because of these differences between soil structure in these two

watersheds, soil parameters value including the SOL_ROCK (the percentage of rock in the soil) and USLE_K (soil erodibility factor) for Potter's Fall model have not been applied for calibrating the Brown Bridge watershed.

Because of soil characteristic in the Brown Bridge watershed, the biggest portion of water budget is the groundwater discharge, while surface runoff forms just small portion of it. The Brown Bridge SWAT model contain 20 subbasins and 77 HRUs, and the Brown Bridge Dam is in Subbasin One.

4.9.2. Developing and Calibrating the Pre- European Model

For evaluating the natural sediment delivery within Brown Bridge Watershed, the new scenario called pre- European scenario has been defined. In the new scenario, the natural vegetation land use data (GIS based) has been input into the SWAT model and the existing dam was removed. The same climatic period of record, soil layer and topography map (digital elevation map) have been applied to the SWAT model for the pre- European scenario. Any impacts associated with climate change due to the anthropogenic sources is outside the scope of this research. As shown in Figure 83, prior to European settlement, the study watershed was primarily forest (95% of the watershed) and some rangeland (5% of the watershed).

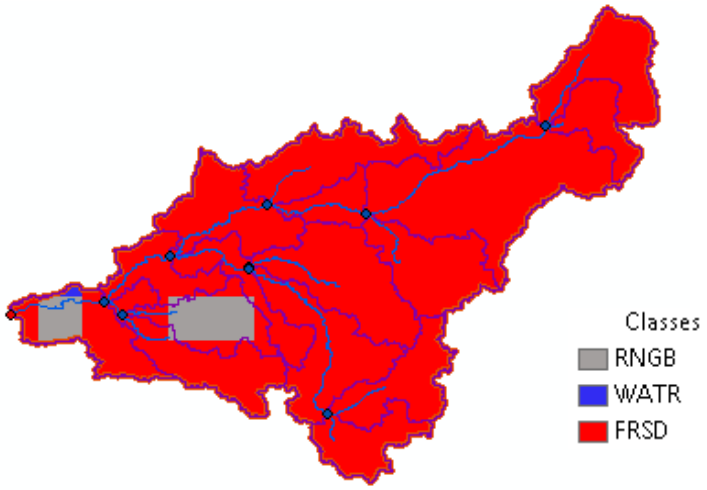

Figure 83- Land use within the Brown Bridge Watershed: Pre-European Settlement (DTMB website)

The land within the Boardman River watershed consists of glaciated topography and sandy soils, so many agricultural activities have not been done in this watershed. The SWAT model of the anthropogenic scenario consists of 17 subbasins and 147 HRUs. The model was run from 1993 to 2010, with considering five years as a "warm up" period. There is no observation sediment data in the 1800's to be used for calibrating the new SWAT model. However, the calibrated SWAT model of baseline scenario can guide us at calibrating the pre- European scenario. All calibrated parameters from baseline scenario have been kept in the pre- European scenario, except USLE_P (support practice) factor. The USLE-P decreased by 70% to simulate the natural vegetation.

4.10. Mio and Alcona Dams

4.10.1. Calibrating the Post- European Model

For evaluating sediment accumulation rate within the Mio and Alcona reservoirs, SWAT model of the Mio and Alcona Dams has been developed and calibrated to the monthly stream discharge at Gage 04136500 (downstream of Mio Reservoir) and 04137005 (downstream of Alcona Reservoir). Gage 04136500 and 04137005 have not

recorded any recent sediment data. Therefore, for calibrating Mio and Alcona watershed, sediment parameters of the other calibrated watershed which has the similar characteristics to the Mio and Alcona basin have been applied.

For calibrating this watershed, the method described at the beginning of this chapter is used and the sediment calibrated parameters of Potter's Falls model have been applied. The two watersheds have similar land use and weather data. **Error! Reference source not found.** displays some climate data from NOAA website and SWAT outputs for both models. Weather data including snowfall, snow melt, and evaporation are similar in two basins. However, precipitation depth in Brown Bridge watershed is about 17% less than Potter's Falls watershed.

Table 33- Average Annual Data for Potter's Fall and Mio& Alcona Dams Watershed

Parameters	Potter's Falls	Mio& Alcona
Precipitation (mm)	996	826
Snow Fall (mm)	160	180
Snow Melt (mm)	150	172
Evapotranspiration (mm)	498	493
Potential Evapotranspiration (mm)	808	688
Percolation Out of Soil (mm)	205	250

In this watershed, soil is mostly sand and less than 5% of it is rock. While in Potter's Falls watershed, soil is mostly silt and about 25% of the soil is rock. Because of the difference between soil structure in these two watersheds, soil parameter value including the SOL_ROCK (the percentage of rock in the soil) and USLE_K (soil erodibility factor) for Potter's Falls model have not been applied for calibrating the Brown Bridge watershed. Because of soil characteristic in the Mio and Alcona watershed, the biggest portion of water budget is the groundwater discharge and surface runoff forms just small portion.

4.10.2. Developing and Calibrating the Pre- European Model

For evaluating the natural sediment delivery within Au Sable watershed, the new scenario called pre- European scenario has been defined. In the pre- European scenario, the same climatic period of record, soil layer and topography map (digital elevation map) have been applied to the SWAT model for the pre- European land use scenario as was used in the present-day scenario (no climate change influences included). The current land use layer has been replaced by the natural vegetation and All man-made dams have been removed. Before European settlement, the study watershed was primarily forest (86% of watershed) and some rangeland (12% of watershed) as shown in Figure 84. The land within the Au Sable River watershed consists of glaciated topography and sandy soils, so many agricultural activities have not been done in this watershed. The results of comparison are discussed in Chapter Five

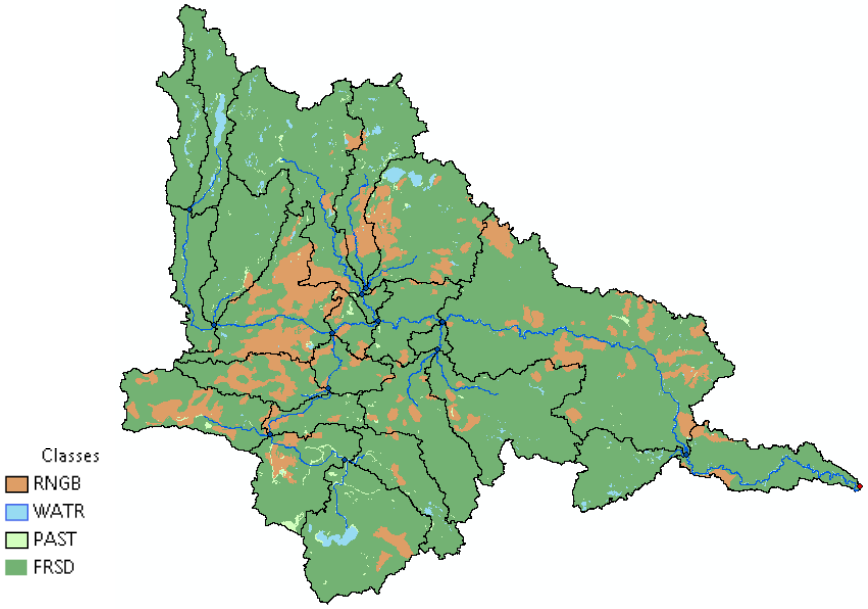

Figure 84- Land Use within the Mio and Alcona Watershed: Pre-European Settlement (DTMB, 2002)

CHAPTER 5 RESULTS AND DISCUSSIONS

The results of all simulations explained in Chapter Four, are discussed in this chapter. Section One, Two, and Three of this chapter explain the three scenarios which have been defined in this dissertation.

- **Post- European Settlement Scenario (Baseline Scenario)**

  In this scenario, all current input data such as current land use, soil data, topography, and weather data were added into each study SWAT model.

- **Pre- European Settlement Scenario (Natural Sediment Scenario)**

  For the natural sediment delivery simulations, the SWAT model was executed with the land use modified to reflect natural, pre-European conditions in the watershed. In addition, all man-made dams were removed from the watershed model. In this scenario, any impacts associated with the climate change due to anthropogenic sources are out of the scope of this research. The same climatic period of record, soil layer, and topography map (digital elevation map) have been applied to the SWAT model for the pre- European settlement scenario as was used in the present-day scenario.

- **Removing Impoundments Scenario**

  For evaluating the effect of man- made impoundments on the sediment yield this scenario was defined. In this scenario, all existing dams were removed, while other input data are similar to the post- European scenario.

In this research, to better understand how well the SWAT predicts the sediment components within a watershed, the results of SWAT simulations were compared with

both historic and new data collected on the study reservoirs. The comparison results are discussed in Section Four.

With the knowledge of sediment accumulation rate within the study reservoirs, which is estimated through the post- European scenario, the remaining reservoirs capacity are forecasted. The reservoir capacity is discussed in Section Five of this chapter.

Based on the sediment yield results from the SWAT models of the study watersheds, a linear regression mathematical model is developed to predict the current sediment yield, natural sediment yield, and sediment storage in un-modeled watersheds. The mathematical model is applied to each 8- digit HUC to estimate the current and pre-European sediment yield to each lake including, Lake Superior, Huron, Michigan, Erie, and Ontario. Section Six and Seven explained the process of developing mathematical models, and the results of applying the models within the Great Lakes Basin.

5.1. Post- European Settlement Scenario (Baseline Scenario)

5.1.1. Ballville Dam

In evaluating sediment accumulation rate behind the dam, a SWAT analysis was completed to determine the sediment inflows, and outflows in the reservoir. The difference between these loads provides an estimate of the potential annual sediment loads that are trapped behind the dam. Table 34 and Figure 85 depict the predicted annual sediment accumulation rates within Ballville Reservoir by SWAT from 1980 to 1999.

L95 PPU represents the lower boundary of 95 PPU region, and U95 PPU is the upper boundary, so any point between the L95PPU and U95PPU is a potential sediment accumulation rate within the reservoir. L95PPU, M95PPU, and U95PPU correspond to

2.5%, 50%, and 97.5% probability, respectively. In other words, they are calculated at the 2.5%, 50%, and 97.5% levels of the cumulative distribution of an output variable generated by the propagation of the parameter uncertainties using Latin hypercube sampling.

Table 34- Sediment Accumulation Rate (tn/yr) within Ballville Dam

Year	L95PPU	M95PPU	U95PPU
1980	12,777	34,531	63,328
1981	38,837	92,207	234,952
1982	15,687	56,900	113,660
1983	4,604	10,326	15,406
1984	17,850	68,771	144,907
1985	10,636	36,082	70,198
1986	7,494	16,378	23,522
1987	6,819	10,457	23,522
1988	7,670	34,491	70,642
1989	10,818	30,026	51,882
1990	48,110	74,561	169,798
1991	5,571	23,677	59,636
1992	11,461	38,430	71,546
1993	8,484	34,484	65,757
1994	6,079	12,581	16,713
1995	8,236	20,413	30,130
1996	12,269	35,832	61,660
1997	18,191	61,135	122,221
1998	6,562	15,470	21,684
1999	10,512	30,075	44,380
Min	4,604	10,326	15,406
Ave	13,433	36,841	73,777
Max	48,110	92,207	234,952

A high uncertainty in the sediment accumulation rate within the Ballville reservoir in some months appears as a large difference between the upper boundary and lower boundary in Table 34. Therefore, in this research, we mostly concentrated on the 50% probability of sediment accumulation rates (or M 95PPU results) throughout all reservoirs. The Ballville SWAT model predicted that the average of sediment accumulation rate within the Ballville reservoir varies between about 10,000 and 92,000 (tn/yr) from 1980 to

1999, and the average annual rate for the entire simulation period is approximately 37,000 (tn/yr).

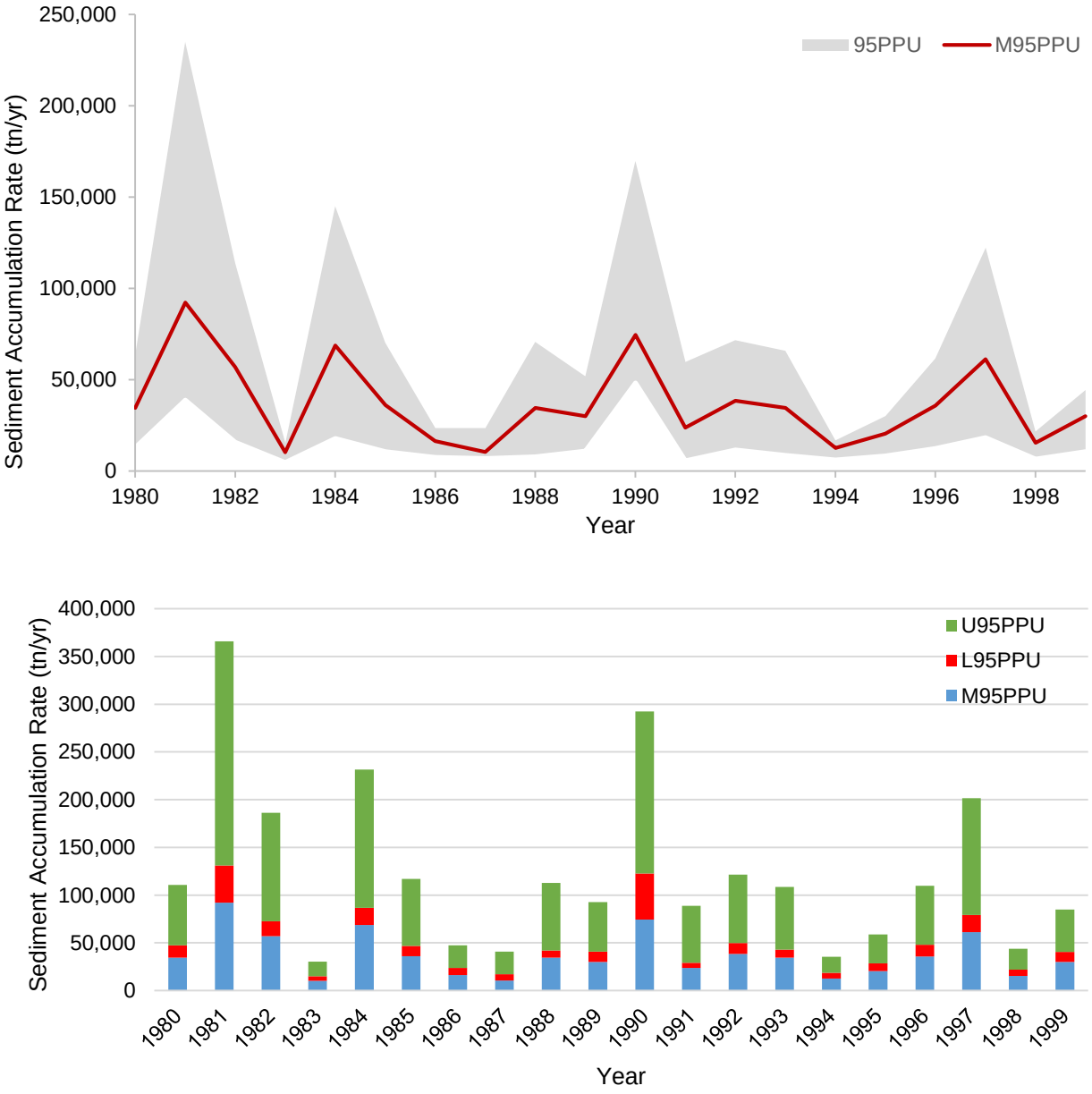

Figure 85- Sediment Accumulation Rate (tn/yr) within Ballville Reservoir Estimated by SWAT

Evan and colleagues (Evan et al., 2002) have evaluated sediment accumulation rate within the Ballville as part of dam removal efforts. They concluded the sediment accumulation rate within the reservoir peaked during years of significant flooding (1981,

1984, 1990, 1992, and 1997), which show the consistent result with the estimated accumulation rate by SWAT.

Brune Curve relates the trapping efficiency of suspended sediments to the average residence time of water within the reservoir. The normal reservoir capacity of Ballville Dam is about 524 ac. ft (0.65 Mm^3), and maximum capacity is 2,402 ac. ft (2.96 Mm^3). The reservoir capacity varies between the normal and maximum capacity over time. The average of annual stream flow recorded at Gage 04198000 from 1980 to 1999 was 1,197 cfs (33.90 cms). This gage is located upstream of the dam. The average residence time in the Ballville Dam reservoir is about one day. Using the Brune Curve the average trapping efficiency for the medium size particle is about 15% in this reservoir. The residence time can also be estimated in each year by taking the reservoir capacity and inflow data from the calibrated SWAT model. The second column in Table 35 represents the volume of the reservoir for each year from 1980 to 1999, and the third column shows the inflow into the reservoir. The fourth column represents the residence time which has been estimated by dividing the volume by the flow. Finally, with having the residence time and applying Brune Curve, trapping efficiency can have been estimated.

Table 35- Trapping Efficiency at Ballville Dam from 1980 to 1999 (Brune Curve)

Year	Volume V from SWAT (m^3)	Flow Q from SWAT (m/s)	V/Q (yr)	Trapping Efficiency from Brune Curve		
				Fine SED	Med SED	Coarse SED
1980	2,355,000	36.68	0.002	0%	4%	21%
1981	2,355,000	53.93	0.001	0%	0%	0%
1982	2,355,000	40.12	0.002	0%	4%	21%
1983	2,355,000	37.14	0.002	0%	4%	21%
1984	2,355,000	40.51	0.002	0%	4%	21%
1985	2,355,000	45.42	0.002	0%	4%	21%
1986	2,355,000	52.26	0.001	0%	0%	0%
1987	2,355,000	28.43	0.003	0%	15%	31%
1988	2,355,000	17.34	0.004	4%	24%	39%
1989	2,355,000	29.57	0.003	0%	15%	31%
1990	2,355,000	53.00	0.001	0%	0%	0%
1991	2,355,000	22.84	0.003	0%	15%	31%
1992	2,355,000	46.12	0.002	0%	4%	21%
1993	2,355,000	39.33	0.002	0%	4%	21%
1994	2,355,000	27.35	0.003	0%	15%	31%
1995	2,355,000	36.68	0.002	0%	4%	21%
1996	2,355,000	46.53	0.002	0%	4%	21%
1997	2,355,000	40.99	0.002	0%	4%	21%
1998	2,355,000	35.27	0.002	0%	4%	21%
1999	2,355,000	23.53	0.003	0%	15%	31%
Average				0%	7%	21%

Based on the Brune Curve method, the average trapping efficiency for medium sized sediment is about 7%. Table 36 displays the calculated average sediment trapping efficiency within the Ballville reservoir using SWAT results. The average trapping efficiency according to this approach is 12%.

Table 36- Trapping Efficiency at Ballville Dam from 1980 to 1999 (SWAT)

Year	Trapping Efficiency		
	L95PPU	M95PPU	U95PPU
1980	23%	10%	8%
1981	39%	12%	12%
1982	23%	13%	12%
1983	12%	4%	3%
1984	30%	20%	18%
1985	20%	11%	9%
1986	11%	4%	2%
1987	15%	4%	2%
1988	31%	21%	19%
1989	22%	10%	8%
1990	60%	25%	4%
1991	22%	16%	18%
1992	16%	9%	7%
1993	18%	11%	9%
1994	17%	5%	3%
1995	17%	6%	4%
1996	16%	7%	6%
1997	26%	15%	12%
1998	28%	17%	15%
1999	24%	11%	7%
Average	23%	12%	9%

The current version of SWAT cannot track particle sizes from the landscape to the stream and the reservoir. However, the assumption of constant D50 for a reservoir is not realistic, the D50 of the sediment inflow is modified by changing inflows. Therefore, the SWAT model may overestimate the sediment trapping rate during the lower flow years and underestimate during the higher flow years. In order to better mimic reality, different D50s were defined based on the annual incoming stream discharge and sediment inflow to the reservoir. The assumed D50 for years with greater peak inflows is larger, and the assumed D50 for the years with smaller inflows peaks is the smaller. Table 37 displays the selected D50 for each year of the simulation.

Table 37- Median Particle Size of the Sediment Inflow (μm) in Different Years

Year	1980	1981	1982	1983	1984	1985	1986	1987	1988	1989
D50	10	13	10	8	10	9	9	9	8	9
Year	1990	1991	1992	1993	1994	1995	1996	1997	1998	1999
D50	13	10	9	9	8	8	9	11	9	10

5.1.2. Webber Dam

For evaluating the sediment accumulation rate within the reservoir, uncertainty analysis on the sediment load that flows into the dam (Figure 86), and exits the dam (Figure 87) have been done. Then the difference of these loads has been calculated to assess the potential sediment rate that trapped behind the dam.

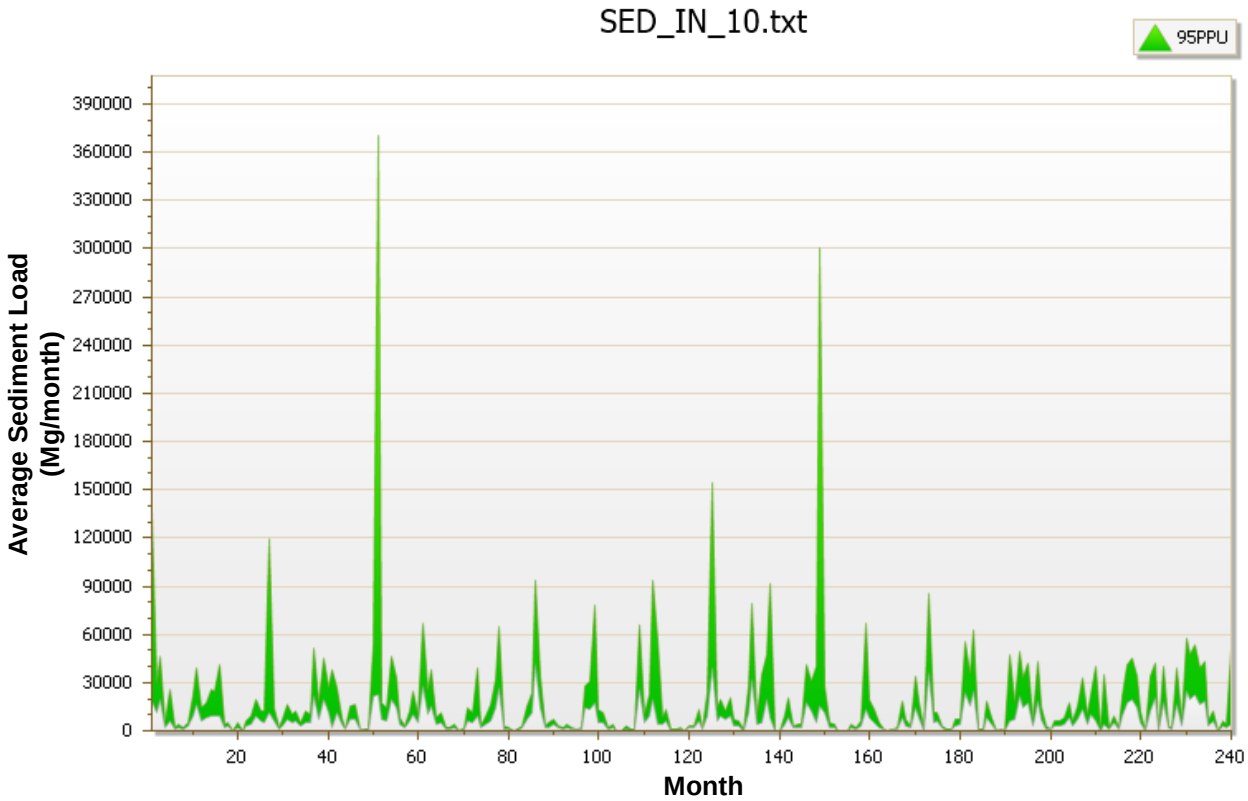

Figure 86- The Simulated Average Sediment Load Flows into Webber Dam, from 1990 to 2009

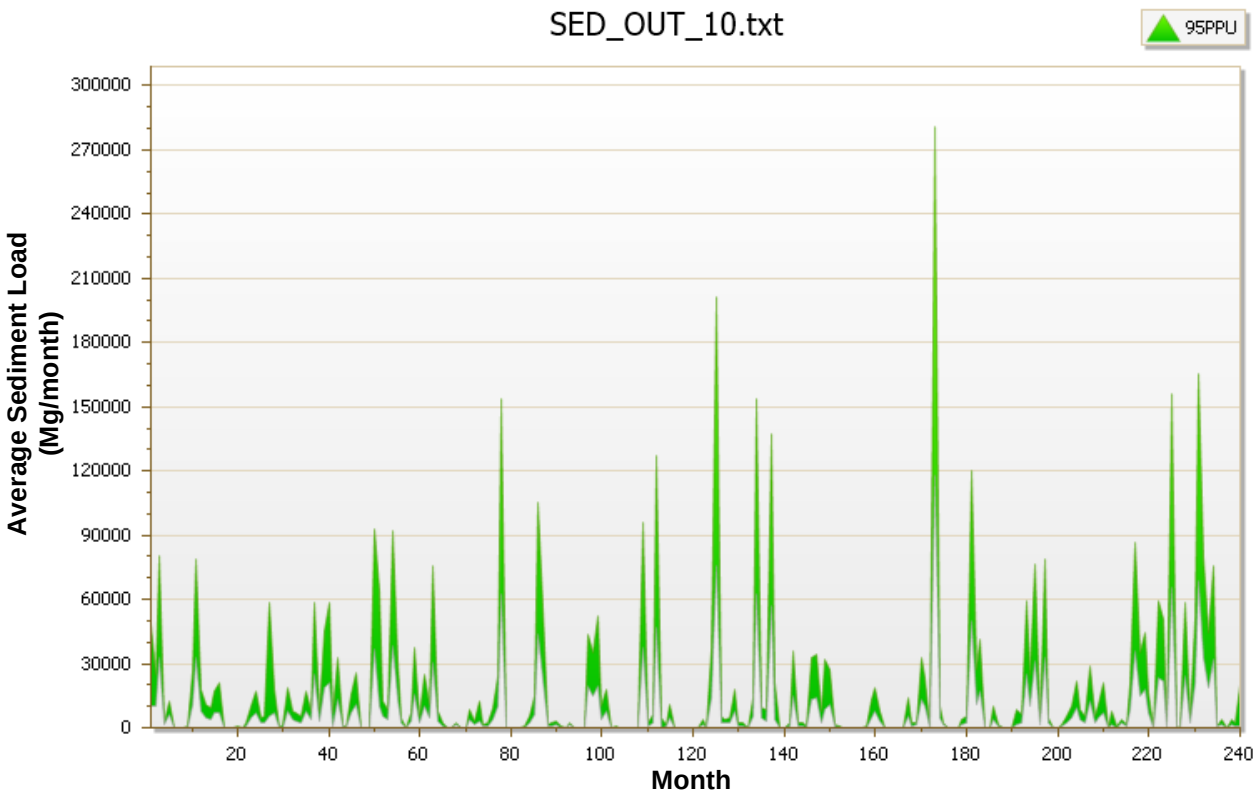

Figure 87- The Simulated Average Sediment Load Exits Webber Dam, from 1990 to 2009.

Table 38 and Figure 88 show the annual sediment accumulation rates within the Webber Dam reservoir from 1990 to 2009. L95 PPU represents the lower boundary, and U95 PPU is the upper boundary of potential sediment accumulation rate. Any point inside the 95PPU envelope is the potential sediment accumulation rate.

Table 38- Sediment Accumulation Rate (tn/yr) within Webber Dam

Year	L95PPU	M95PPU	U95PPU
1990	14,983	25,067	31,889
1991	14,216	24,719	35,222
1992	20,153	36,744	53,335
1993	21,257	35,039	44,289
1994	16,986	59,677	92,866
1995	27,703	39,665	51,626
1996	11,859	24,774	34,192
1997	26,195	35,901	41,374
1998	10,256	20,241	27,421
1999	16,599	36,325	74,325
2000	27,672	60,371	84,432
2001	23,587	48,498	73,408
2002	4,154	20,421	36,687
2003	17,800	28,620	39,440
2004	49,359	79,126	108,892
2005	27,708	46,561	59,342
2006	11,951	13,461	13,581
2007	6,786	14,021	21,256
2008	33,477	48,823	64,168
2009	42,997	84,548	126,099
Min	4,154	13,461	13,581
Ave	21,285	39,130	55,692
Max	49,359	84,548	126,099

The 50% probability of sediment accumulation rate (M 95PPU solutions) is between 13,000 (tn/yr) and 84,000 (tn/yr). The average of upper boundary sediment accumulation rate (U 95PPU) is about 56,000 (tn/yr), and the average of lower boundary sediment accumulation rate (L 95PPU) is above 21,000 (tn/yr).

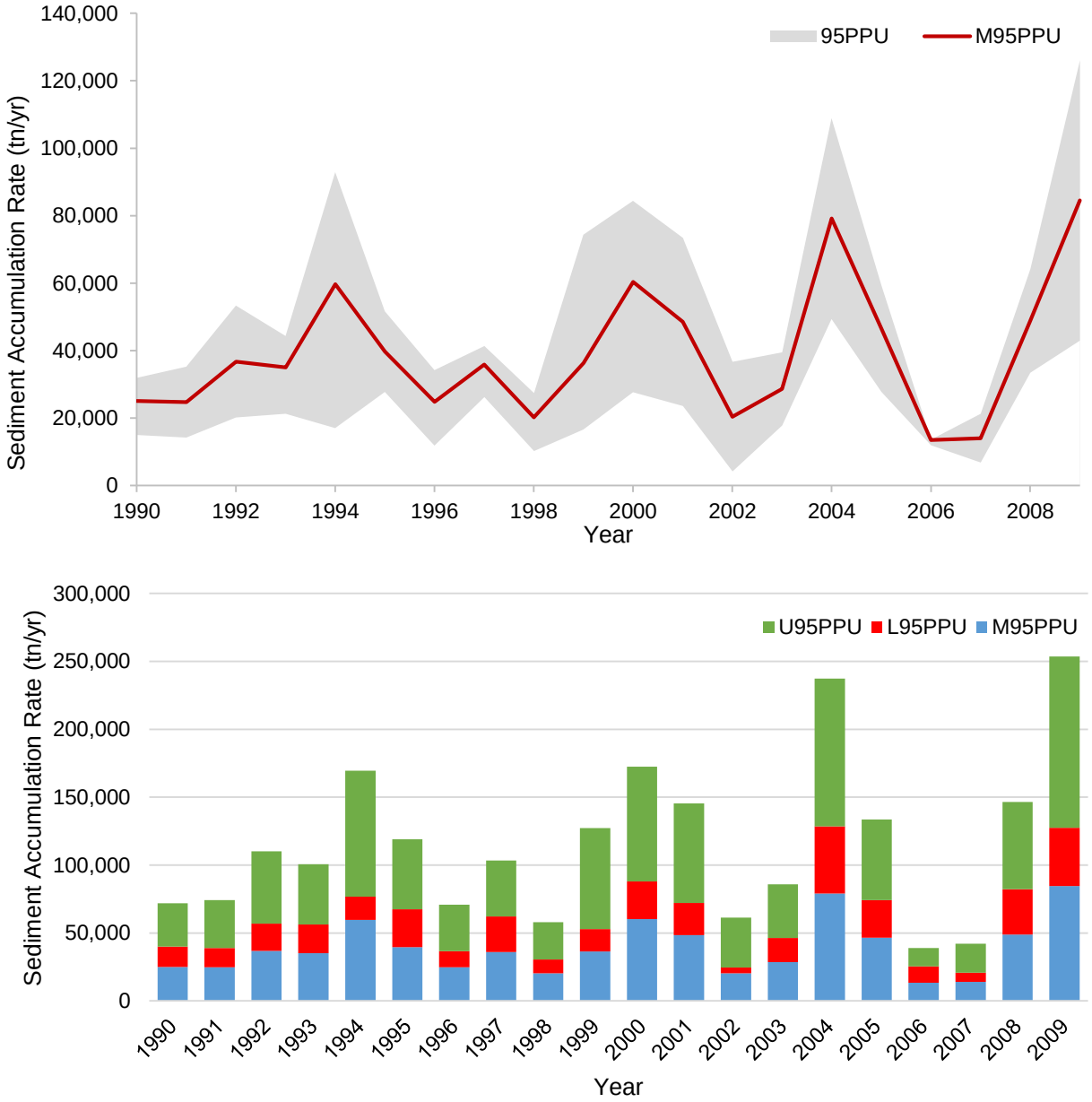

Figure 88- Sediment Accumulation Rate (tn/yr) within Webber Dam

For estimating trapping efficiency with using Brune Curve, knowledge of the reservoir capacity and average annual inflow are required. Reservoir capacity of Webber Dam is about 6,000 ac. ft (7.4 Mm^3), and Gage 04114000 at the upstream of the Webber Dam has recorded inflow into the reservoir from 1990 to 2009. Therefore, by dividing the capacity of the reservoir by the average annual inflow, the residence time can be

estimated. The reservoir capacity and inflow rate into the reservoir over time as presented in the hydrologically calibrated SWAT models can be used for calculating the residence time. With the estimated residence time and using Brune Curve, the trapping efficiency can be determined. Table 39 provides the trapping efficiency using this approach.

Table 39- Trapping Efficiency at Webber Dam from 1990 to 2009 (Brune Curve)

Year	Volume or V (m^3)	Flow or Q (m/s)	V/Q (yr)	Trapping Efficiency from Brune Curve		
				Fine SED	Medium SED	Coarse SED
1990	4,809,000	44.64	0.003	0%	15%	31%
1991	5,733,000	35.05	0.005	10%	30%	42%
1992	4,809,000	45.33	0.003	0%	15%	31%
1993	6,055,000	51.13	0.004	4%	24%	39%
1994	6,112,000	48.04	0.004	4%	24%	39%
1995	6,653,000	29.92	0.007	20%	37%	51%
1996	5,663,000	28.04	0.006	16%	35%	48%
1997	7,285,000	34.70	0.007	20%	37%	51%
1998	7,285,000	36.52	0.006	16%	35%	48%
1999	7,138,000	24.39	0.009	28%	46%	58%
2000	6,667,000	33.89	0.006	16%	35%	48%
2001	6,568,000	52.22	0.004	4%	24%	39%
2002	5,968,000	27.85	0.007	20%	37%	51%
2003	5,230,000	18.70	0.009	28%	46%	58%
2004	4,809,000	44.98	0.003	0%	15%	31%
2005	4,809,000	31.09	0.005	10%	30%	42%
2006	4,809,000	50.45	0.003	0%	15%	31%
2007	5,456,000	38.86	0.004	4%	24%	39%
2008	4,809,000	59.64	0.003	0%	15%	31%
2009	5,714,000	56.08	0.003	0%	15%	31%
Average				10%	28%	42%

As part of this project, the trapping efficiency estimated by SWAT is compared with Brune Curve approach. Table 40 displays the trapping efficiency within the Webber Dam reservoir for the SWAT simulation. The average of sediment trapping efficiency using the SWAT result is 23%, and average trapping efficiency for medium sized-particles using Brune Curve is 28%. The trapping efficiency estimated by the two methods differ by only 5%.

Table 40- Trapping Efficiency at Webber Dam from 1990 to 2009 (SWAT)

Year	Trapping Efficiency		
	L95PPU	M95PPU	U95PPU
1990	13%	13%	13%
1991	21%	21%	21%
1992	29%	29%	29%
1993	20%	19%	19%
1994	13%	24%	27%
1995	31%	27%	25%
1996	15%	16%	17%
1997	29%	24%	22%
1998	16%	18%	18%
1999	21%	24%	25%
2000	24%	26%	27%
2001	22%	26%	27%
2002	6%	13%	15%
2003	35%	33%	32%
2004	54%	53%	53%
2005	28%	27%	27%
2006	11%	7%	6%
2007	9%	11%	11%
2008	23%	20%	19%
2009	31%	34%	35%
Average	23%	23%	30%

The current version of SWAT uses a single particle size for the range of terrain - from the landscape to the stream and the reservoir. However, it is not realistic that the sediment size distribution would remain constant over this route. Even within a reservoir, it is unrealistic to assume a constant D50. The D50 of the sediment inflow is changing year to year as the inflow varies. Therefore, the model may overestimate sediment trapping rate during the dry years and underestimate during the wet years. To allow consideration of different conditions, variable D50s were defined based on the annual incoming stream discharge, and sediment inflow to the reservoir. Table 41 displays the selected D50 for each year of the simulation.

Table 41- Median Particle Size of the Inflow Sediment (µm) in Different Years

Year	1990	1991	1992	1993	1994	1995	1996	1997	1998	1999
D50	7	5	6	7	7	6	7	7	7	8
Year	2000	2001	2002	2003	2004	2005	2006	2007	2008	2009
D50	7	9	5	5	12	7	7	5	9	9

5.1.3. Riley Dam

In Riley SWAT model, the “warm up” period was considered from 1986 through 1990, then model was simulated between 1991 and 2010. For evaluating the sediment accumulation rate behind the dam, SWAT analysis was completed to estimate the sediment load that flows into the dam, and exits the dam, then the difference of these loads has been calculated to assess the potential sediment load that trapped behind the dam. Figure 89 shows the potential sediment load that flows into the dam and Figure 90 indicates the sediment load leaves the dam.

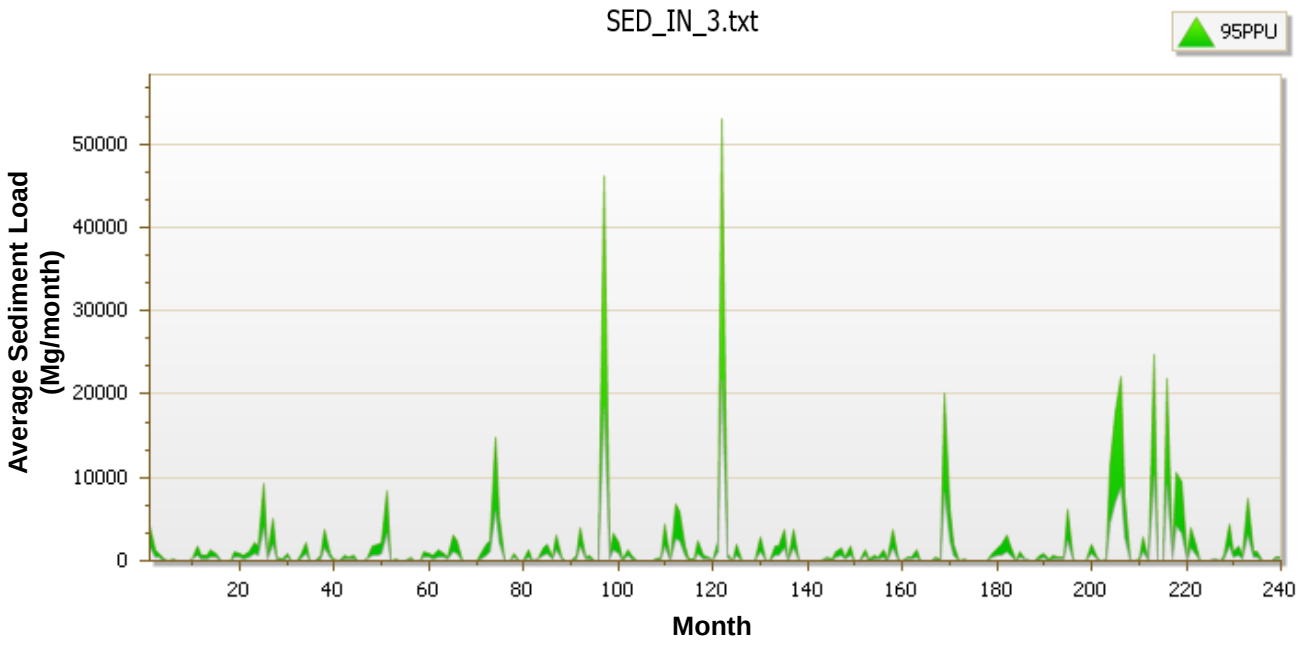

Figure 89- The Simulated Average Sediment Load Flows into Riley Dam, from 1991 to 2010.

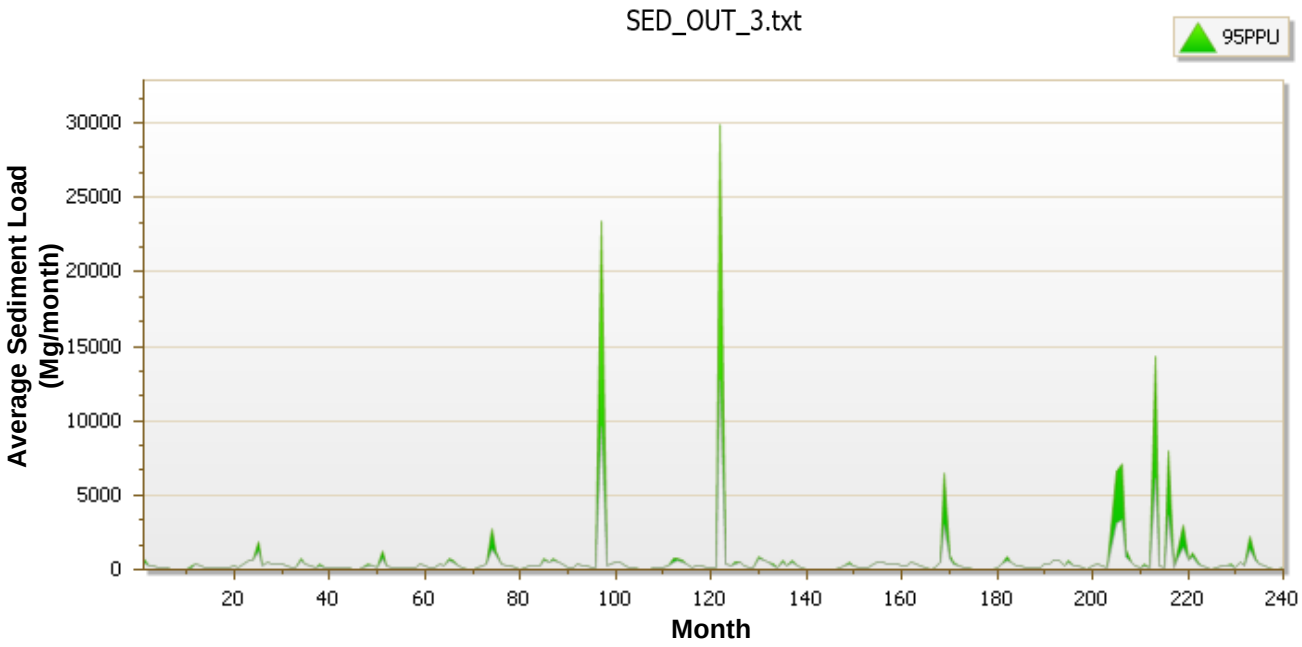

Figure 90- The Simulated Average Sediment Load Exits Riley Dam, from 1991 to 2010.

Table 42, and Figure 91 display the potential of annual sediment accumulation rate within Riley reservoir. L 95 PPU is the lower boundary, and U 95 PPU is the upper boundary of potential sediment accumulation rate envelope, so any point inside of the 95PPU boundary is the potential sediment accumulation.

Table 42- Sediment Accumulation Rate (tn/yr) within Riley Dam

Year	L95PPU	M95PPU	U95PPU
1991	1,950	4,811	8,041
1992	1,320	4,558	8,015
1993	3,527	9,153	14,967
1994	2,125	4,952	7,888
1995	3,963	8,495	13,650
1996	1,766	5,259	9,155
1997	6,828	14,163	22,249
1998	1,105	4,716	8,440
1999	11,003	20,708	32,216
2000	6,399	13,398	21,373
2001	9,347	19,202	30,332
2002	2,631	6,077	10,055
2003	976	3,759	6,816
2004	319	2,461	4,746
2005	8,376	15,966	24,518
2006	264	3,527	7,116
2007	4,271	10,352	16,868
2008	22,563	42,866	64,835
2009	5,985	13,658	22,054
2010	3,962	9,318	15,105
Min	264	2,461	4,746
Ave	4,934	10,870	17,422
Max	22,563	42,866	64,835

The 50% probability of sediment accumulation rate within the Riley reservoir varies from the minimum of 2,000 (tn/yr) to the maximum of 43,000 (tn/yr) between 1991 and 2010. The lowest value of sediment accumulation rate was 264 (tn/yr) which goes back to 2006, and the highest rate goes back to 2008, with the value of 64,000 (tn/yr). The potential reason for high sediment accumulation rate in 2008 is the high amount of inflow that discharges into the reservoir in this specific year.

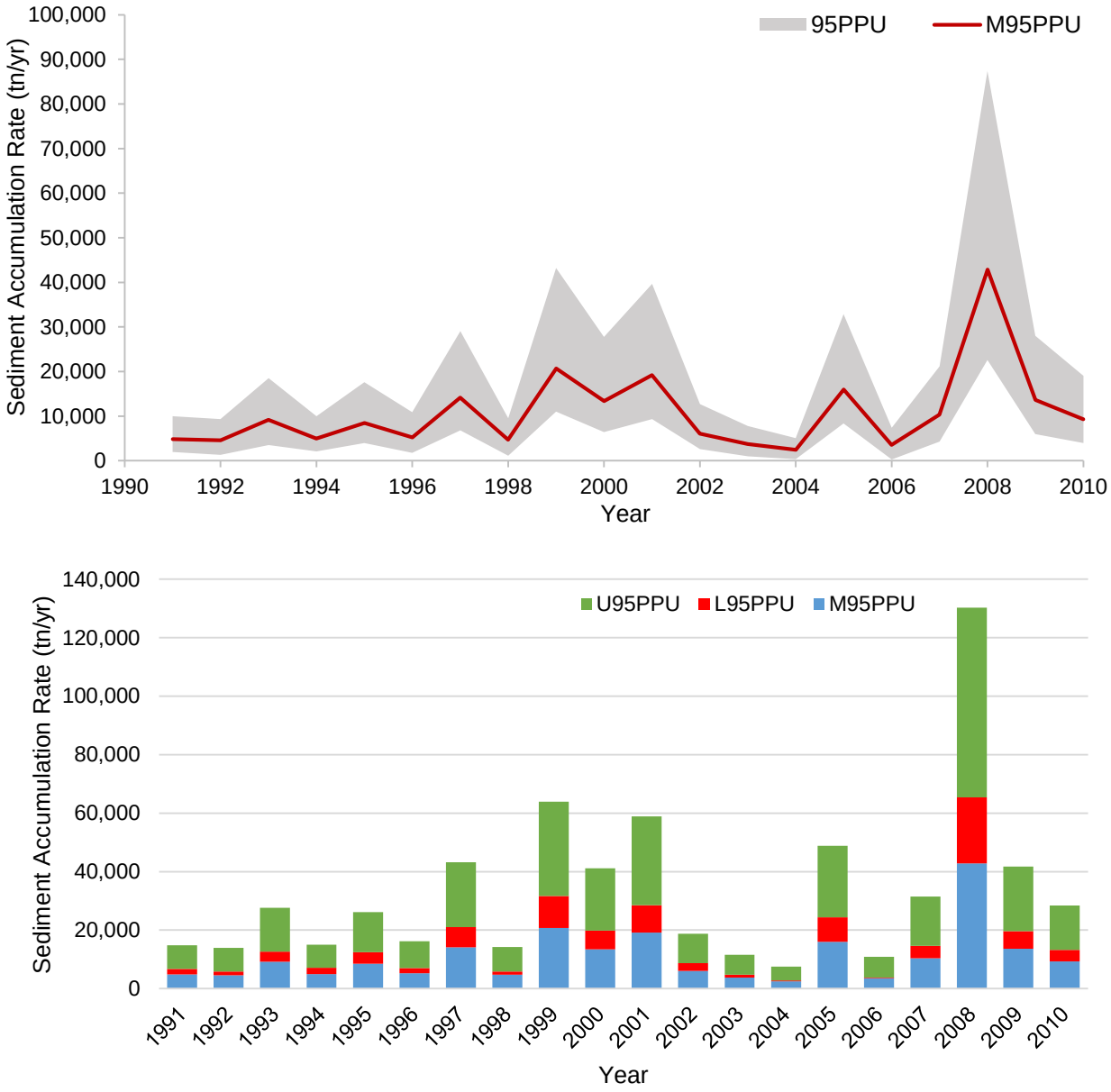

Figure 91- Sediment Accumulation Rate (tn/yr) within Riley Reservoir, Estimated by SWAT

For estimating trapping efficiency with applying the Brune Curve, knowledge of the reservoir capacity and volume of inflow is needed. The storage capacity of Riley reservoir is 7 (Mm^3). However, the reservoir volume is fluctuating over time. The residence time calculation has used the capacity of the reservoir and average annual inflow from the

SWAT simulation. Table 43 displays the trapping efficiency as calculated using the Brune Curve between 1991 and 2010.

Table 43- Trapping Efficiency at Riley Dam from 1991 to 2010 (Brune Curve)

Year	Volume or V (m^3)	Flow or Q (m/s)	V/Q (yr)	Trapping Efficiency from Brune Curve		
				Fine SED	Medium SED	Coarse SED
1991	6,136,000	9.16	0.021	51%	67%	77%
1992	6,136,000	13.82	0.014	43%	60%	70%
1993	6,105,000	19.36	0.010	31%	48%	60%
1994	6,136,000	8.97	0.022	54%	69%	78%
1995	5,174,000	10.75	0.015	44%	58%	69%
1996	6,136,000	12.93	0.015	44%	58%	69%
1997	6,136,000	16.70	0.012	35%	52%	64%
1998	4,000,000	17.26	0.007	20%	37%	51%
1999	4,000,000	13.03	0.010	31%	48%	60%
2000	4,000,000	14.82	0.009	28%	45%	55%
2001	6,136,000	21.86	0.009	28%	45%	55%
2002	4,000,000	9.47	0.013	39%	55%	65%
2003	6,136,000	13.74	0.014	43%	60%	70%
2004	6,136,000	16.35	0.012	35%	52%	64%
2005	6,136,000	11.24	0.017	45%	63%	72%
2006	6,136,000	18.07	0.011	36%	52%	64%
2007	6,136,000	16.42	0.012	35%	52%	64%
2008	6,136,000	23.37	0.008	26%	42%	56%
2009	6,136,000	20.06	0.010	31%	48%	60%
2010	4,295,000	15.83	0.009	28%	45%	55%
Average				36%	53%	64%

Brune Curve predicted the average trapping efficiency for medium sized sediment is 53%. As part of this research, the sediment trapping efficiency estimated by SWAT has been compared with Brune Curve approach. The sediment trapping efficiencies estimated by SWAT are listed in

Table 44.

Table 44- Trapping Efficiency at Riley Dam from 1991 to 2010 (SWAT)

Year	Trapping Efficiency		
	L95PPU	M95PPU	U95PPU
1991	47%	67%	77%
1992	28%	57%	69%
1993	40%	61%	70%
1994	52%	71%	80%
1995	58%	73%	79%
1996	35%	61%	72%
1997	57%	70%	76%
1998	20%	51%	64%
1999	46%	51%	53%
2000	62%	77%	83%
2001	34%	41%	45%
2002	52%	70%	79%
2003	24%	55%	68%
2004	10%	46%	61%
2005	61%	68%	72%
2006	6%	44%	61%
2007	46%	64%	71%
2008	52%	58%	60%
2009	51%	66%	73%
2010	47%	65%	73%
Average	41%	61%	69%

The average of estimated sediment trapping efficiency by SWAT is about 61%, which its difference with Brune Curve approach is only less than 10%.

5.1.4. Upper Green Dam

Upper Green model contains one subbasin. For calculation purpose, the subbasin was further divided into 10 HRUs. As described in Chapter Four, for calibrating the SWAT model, the sediment parameters of the Ballville Dam have been input in the Upper Green Model. For evaluating the sediment accumulation rate behind the dam, the potential sediment load that exits the dam (Figure 93) was subtracted from the sediment load that

delivers into the dam (Figure 92). The difference of the sediment inflow and outflow represents the sediment trapping rate.

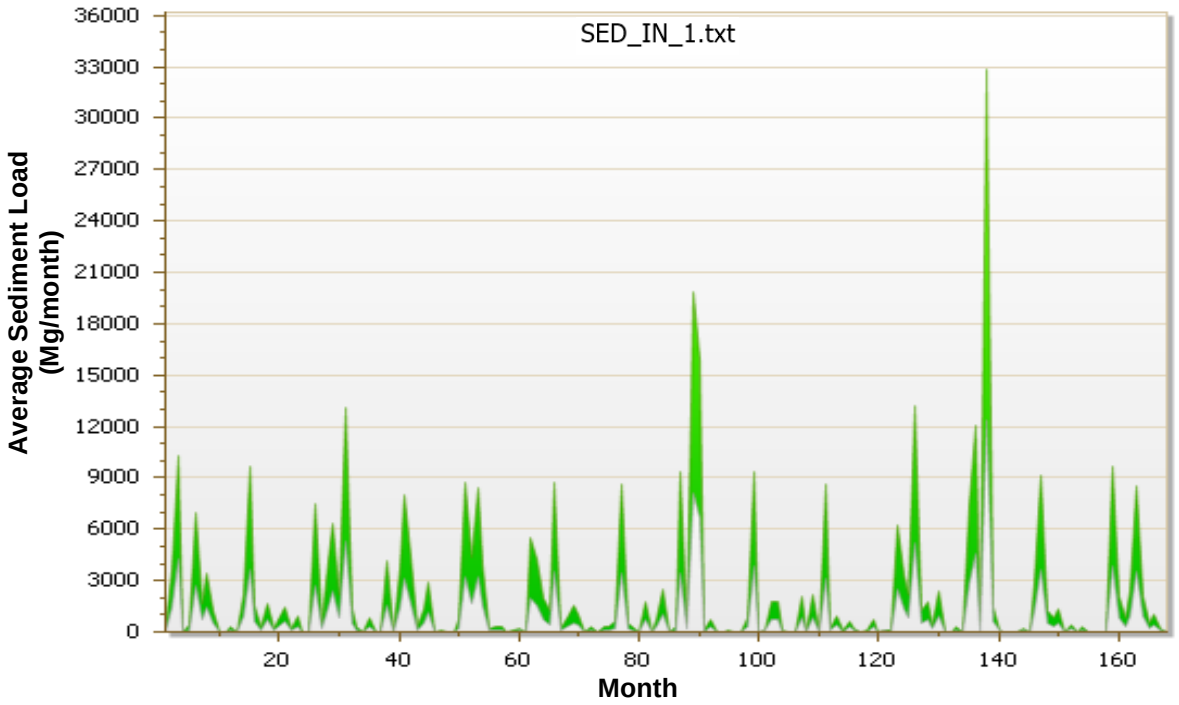

Figure 92- The Simulated Average Sediment Load Flows into Upper Green Lake, from 1997 to 2010.

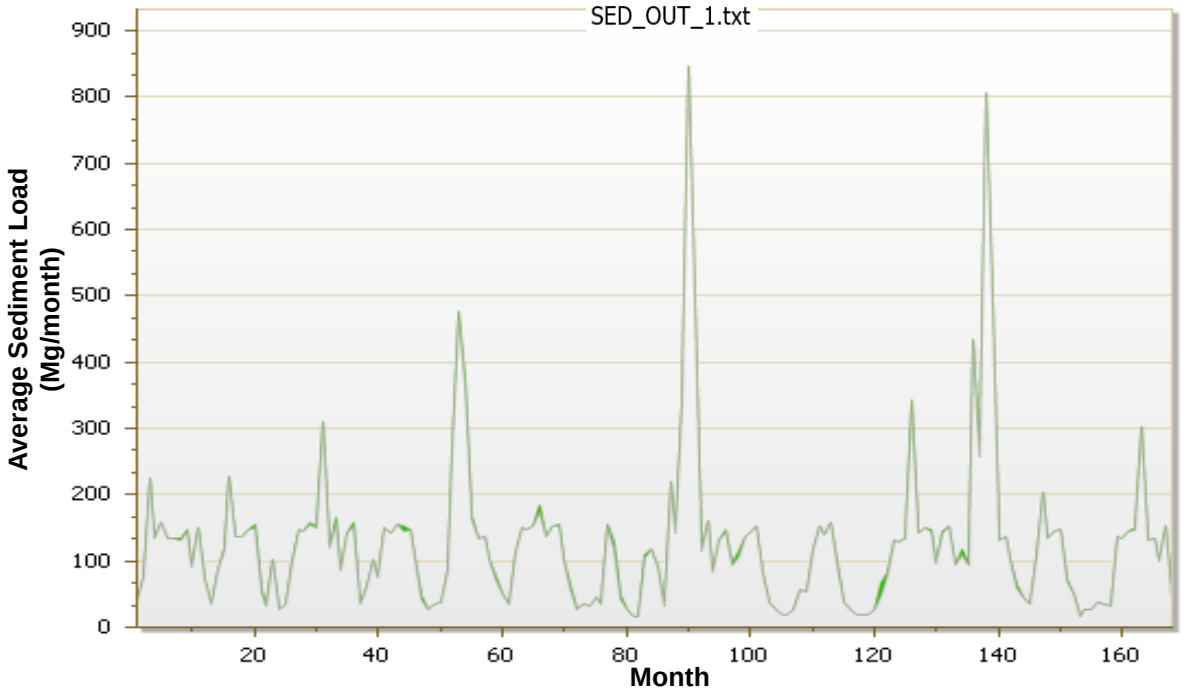

Figure 93- The Simulated Average Sediment Load Exits Upper Green Lake from 1997 to2010

Table 45 and Figure 94 display the annual sediment accumulation rate within Upper Green reservoir. L95 PPU is the lower boundary and U95 PPU is the upper boundary of the annual potential sediment accumulation rate. Any point inside of the 95PPU region is the potential sediment accumulation rate within Upper Green reservoir. M95 PPU represents the median of sediment accumulation rate in each month.

Table 45- Sediment Accumulation Rate (tn/yr) within Upper Green Dam (SWAT)

Year	L95PPU	M95PPU	U95PPU
1997	11,389	20,116	29,454
1998	6,868	12,854	19,453
1999	13,867	25,695	38,302
2000	9,589	17,839	26,565
2001	9,692	18,347	28,062
2002	9,312	17,550	26,643
2003	6,190	11,329	16,675
2004	18,818	33,563	49,540
2005	6,842	11,851	17,169
2006	4,922	9,285	14,309
2007	12,078	22,277	32,771
2008	20,529	38,140	57,816
2009	6,307	11,475	16,988
2010	10,777	19,436	28,719
Min	4,922	9,285	14,309
Ave	10,513	19,268	28,748
Max	20,529	38,140	57,816

The 50% probability of sediment accumulation rate (M 95PPU) varies between the minimum of 9,000 and the maximum of 38,000 (tn/yr) from 1997 to 2010, and the average rate in 19,000 (tn/yr).

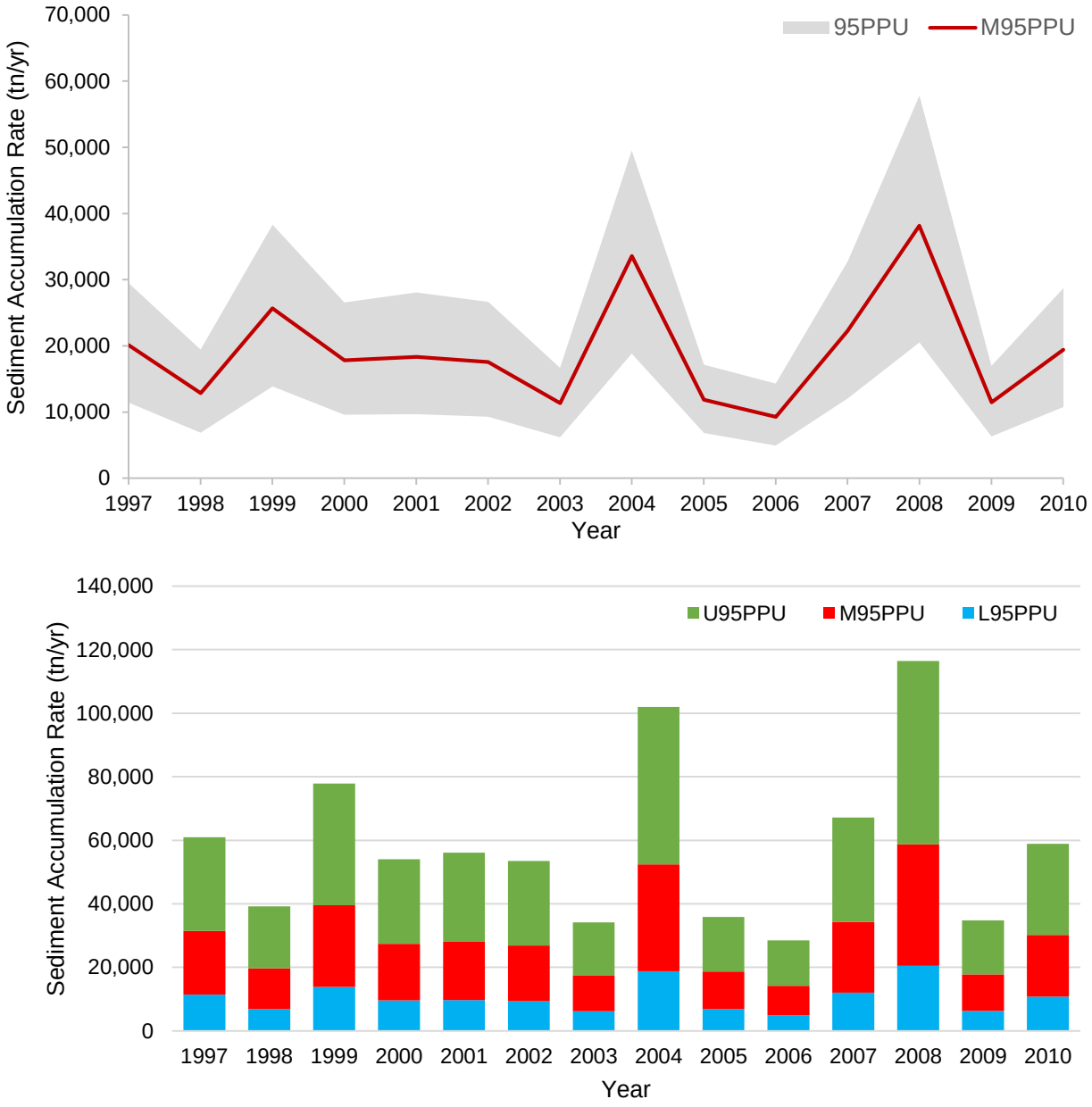

Figure 94- Sediment Accumulation Rate (tn/yr) within Upper Green Lake

There are two spikes in sediment accumulation rate in Jun 2004 and in July 2008. These peaks in sediment accumulation rate were occurred because of flood events in 2004 and 2008, which were explained in Chapter Three.

For estimating trapping efficiency with applying Brune Curve, knowledge of the reservoir capacity and average annual volume of inflow is required. Reservoir capacity of

Upper Green Dam is about 40,000 ac. ft (49 Mm^2), and there is a gage (Gage 04073473) close to the dam recorded stream discharge from 1997 to 2010. The residence time estimation has used the annual storage capacity and the amount of inflow into the reservoir from hydrologically calibrated SWAT model. Table 46 shows estimated trapping efficiency using Brune Curve between 1997 and 2010.

Table 46- Trapping Efficiency at Upper Green Dam from 1997 to 2010 (Brune Curve)

Year	Volume or V(m^3)	Flow or Q (m/s)	V/Q (yr)	Trapping Efficiency from Brune Curve		
				Fine SED	Medium SED	Coarse SED
1997	36,600,000	1.66	0.7	95%	98%	100%
1998	35,830,000	1.39	0.8	96%	99%	100%
1999	37,280,000	1.98	0.6	94%	97%	100%
2000	36,800,000	1.16	1.01	96%	100%	100%
2001	36,520,000	2.29	0.5	93%	96%	100%
2002	36,360,000	1.51	0.8	96%	99%	100%
2003	39,430,000	0.81	1.54	96%	100%	100%
2004	40,620,000	4.05	0.3	91%	96%	100%
2005	36,420,000	0.88	1.31	96%	100%	100%
2006	37,000,000	0.90	1.31	96%	100%	100%
2007	40,470,000	1.99	0.6	94%	97%	100%
2008	37,000,000	3.53	0.3	91%	96%	100%
2009	36,940,000	1.09	1.08	96%	100%	100%
2010	36,370,000	1.73	0.7	95%	98%	100%
Average				95%	98%	100%

Part of this research is comparing the estimated trapping efficiency by SWAT with Brune Curve approach. Table 47 displays the sediment trapping efficiency within Upper Green Dam reservoir as predicted by SWAT. The estimated average of sediment trapping efficiency by SWAT is about 93%, and by Brune Curve for medium sized sediment is 98%. The trapping efficiency estimated by these two approaches differ by only 5%.

Table 47- Trapping Efficiency at Upper Green Dam from 1997 to 2010 (SWAT)

Year	Trapping Efficiency		
	L95PPU	M95PPU	U95PPU
1990	91%	94%	96%
1991	85%	91%	94%
1992	90%	94%	96%
1993	91%	95%	96%
1994	84%	91%	93%
1995	87%	92%	95%
1996	89%	94%	95%
1997	90%	94%	96%
1998	93%	95%	96%
1999	88%	92%	95%
2000	89%	93%	95%
2001	90%	94%	96%
2002	87%	93%	95%
2003	88%	93%	95%
2004	91%	94%	96%
2005	85%	91%	94%
2006	90%	94%	96%
2007	91%	95%	96%
2008	84%	91%	93%
2009	87%	92%	95%
Average	89%	93%	95%

5.1.5. Goshen Pond Dam

For assessing the potential sediment accumulation rate that trapped behind the dam, a SWAT analysis has been done on the sediment load that flows into the reservoir and exits the reservoir have been estimated. Figure 95 shows the potential sediment load that flows into the dam and Figure 96 indicates sediment load leaves the dam.

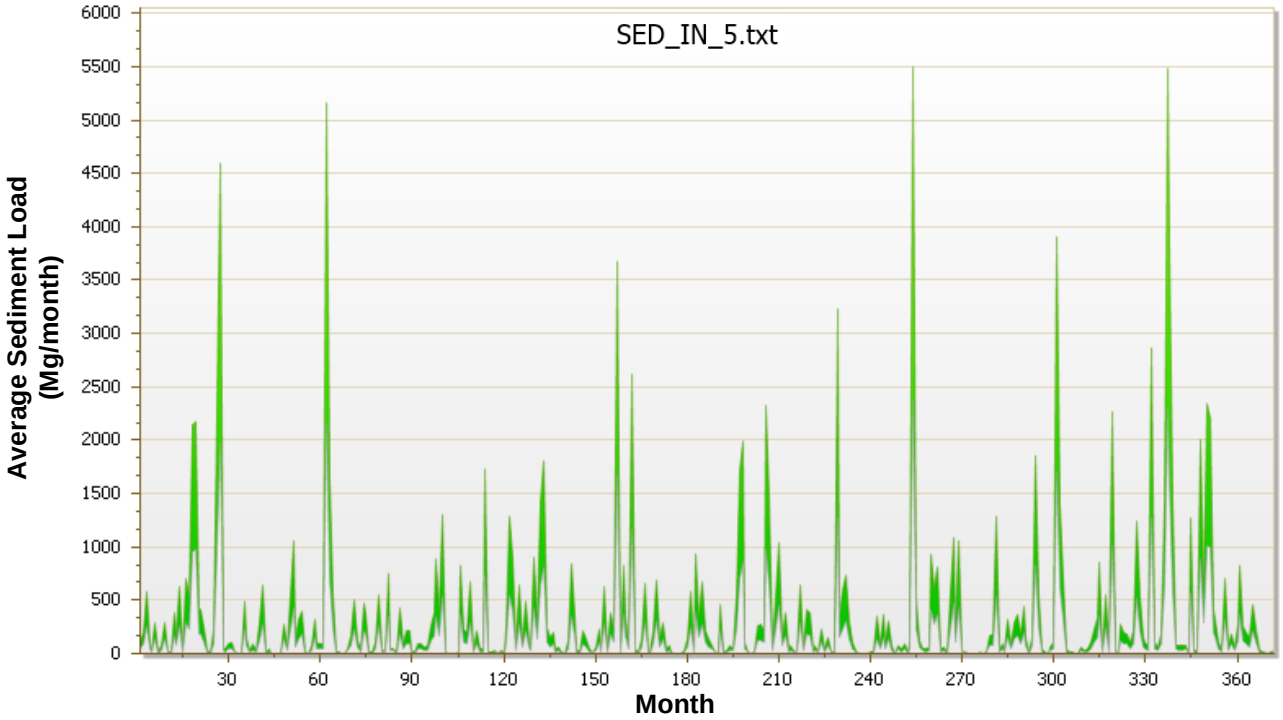

Figure 95- The Simulated Average Sediment Load Flows into Goshen Pond, from 1980 to 2010.

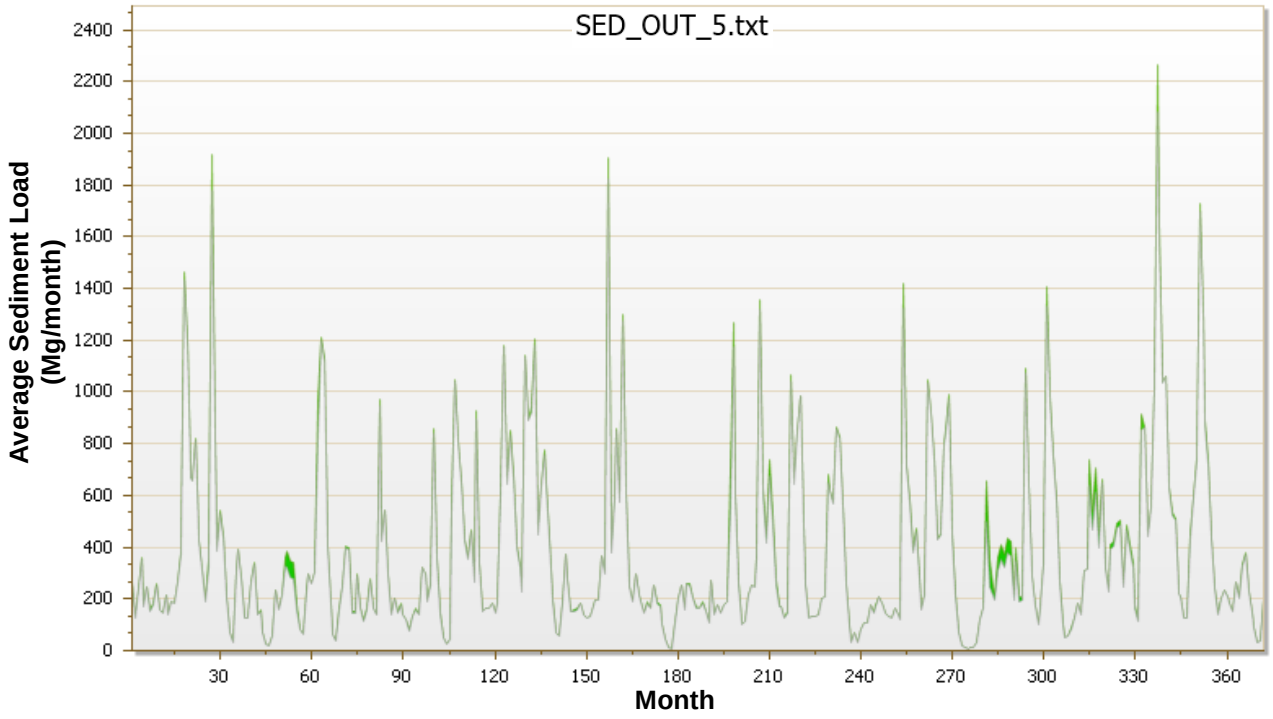

Figure 96- The Simulated Average Sediment Load Exits Goshen Pond, from 1990 to 2009.

Table 48 shows the annual sediment accumulation rate (the difference between sediment inflow, and outflow) within Goshen Pond reservoir. L95 PPU shows the lower

boundary and U95 PPU represents the upper boundary of potential sediment accumulation, so any point between the L95PPU and U95PPU is the potential sediment accumulation rate bind the dam.

Table 48- Sediment Accumulation Rate (tn/yr) within Goshen Pond

Year	L95PPU	M95PPU	U95PPU
1980	263	845	1,445
1981	1,859	3,692	5,651
1982	3,187	5,806	8,611
1983	130	534	974
1984	676	1,575	2,549
1985	1,606	3,238	4,987
1986	449	1,142	1,864
1987	235	695	1,184
1988	1,038	2,206	3,471
1989	616	1,392	2,231
1990	1,550	3,146	4,848
1991	795	1,756	2,800
1992	328	898	1,499
1993	2,092	3,971	5,970
1994	394	866	1,361
1995	901	1,902	2,976
1996	1,367	2,733	4,192
1997	1,753	3,395	5,130
1998	287	844	1,424
1999	1,420	2,835	4,412
2000	294	771	1,282
2001	2,353	4,423	6,592
2002	763	1,615	2,535
2003	661	1,475	2,350
2004	800	1,715	2,675
2005	1,583	3,020	4,532
2006	1,201	2,523	3,932
2007	2,069	3,963	6,024
2008	3,918	7,064	10,500
2009	1,931	3,768	5,725
2010	452	1,079	1,733
Min	130	534	974
Ave	1,193	2,416	3,724
Max	3,918	7,064	10,500

The 50% probability of annual sediment accumulation rate (M 95 PPU) varies between the minimum of 500 (tn/yr) in 1983 and maximum of 7,000 (tn/yr) in 2008. From 1980 to 2010 the average of sediment accumulation rate is 2,000 (tn/yr).

Table 49 displays the trapping efficiency as estimated using Brune Curve. The residence time estimation has used the reservoir volume and inflow from SWAT simulation. The Brune Curve predicted the average trapping efficiency of 32% within the Goshen Pond reservoir, for the medium sized sediment. The input data including the storage capacity and annual inflow can also be retrieved directly from NID website and Gage 04100500 (located just upstream of the reservoir), respectively. The residence time is calculated as 2.5 (days), using the storage capacity of 3,100 ac. ft (4 Mm^3) and the mean annual flow of 17.39 (cms) recorded by Gage 04100500. The Brune Curve predicted the average trapping efficiency of 37% for the medium sized sediment.

Table 49- Trapping Efficiency at Goshen Pond Dam from 1980 to 2010 (Brune Curve)

Year	Volume or V (m^3)	Flow or Q (m/s)	V/Q (yr)	Trapping Efficiency from Brune Curve		
				Fine SED	Medium SED	Coarse SED
1980	3,392,000	18.59	0.006	16%	34%	48%
1981	3,392,000	26.86	0.004	3%	25%	40%
1982	3,392,000	21.35	0.005	10%	30%	42%
1983	3,392,000	13.24	0.008	24%	42%	55%
1984	3,392,000	18.15	0.006	16%	34%	48%
1985	3,392,000	23.13	0.005	10%	30%	42%
1986	3,392,000	18.36	0.006	16%	34%	48%
1987	3,392,000	13.66	0.008	24%	42%	55%
1988	3,392,000	18.96	0.006	16%	34%	48%
1989	3,392,000	14.61	0.007	20%	37%	51%
1990	3,392,000	27.61	0.004	3%	25%	40%
1991	3,392,000	20.20	0.005	10%	30%	42%
1992	3,392,000	16.49	0.007	20%	37%	51%
1993	3,392,000	26.7	0.004	3%	25%	40%
1994	3,392,000	9.956	0.011	35%	52%	64%
1995	3,392,000	16.51	0.007	20%	37%	51%
1996	3,392,000	18.04	0.006	16%	34%	48%
1997	3,392,000	20.60	0.005	10%	30%	42%
1998	3,392,000	17.11	0.006	16%	34%	48%
1999	1,147,000	14.69	0.002	0%	4%	21%
2000	3,392,000	12.27	0.009	28%	45%	57%
2001	3,392,000	24.14	0.004	3%	25%	40%
2002	1,147,000	13.49	0.003	0%	17%	32%
2003	3,392,000	16.54	0.007	20%	37%	51%
2004	3,392,000	18.47	0.006	16%	34%	48%
2005	3,392,000	16.73	0.006	16%	34%	48%
2006	3,392,000	25.46	0.004	3%	25%	40%
2007	3,392,000	25.04	0.004	3%	25%	40%
2008	3,392,000	29.01	0.004	3%	25%	40%
2009	3,392,000	27.68	0.004	3%	25%	40%
2010	3,392,000	15.58	0.007	20%	37%	51%
Average				13%	32%	46%

Table 50 displays the sediment trapping efficiency estimated by SWAT. SWAT predicted that average of annual sediment trapping efficiency is 61%, which is about 30% higher than Brune Curve method.

Table 50- Trapping Efficiency at Goshen Pond Dam from 1990 to 2009 (SWAT)

Year	Trapping Efficiency		
	L95PPU	M95PPU	U95PPU
1980	27%	54%	65%
1981	52%	63%	68%
1982	50%	54%	56%
1983	20%	49%	62%
1984	48%	66%	74%
1985	41%	49%	53%
1986	38%	58%	68%
1987	32%	58%	70%
1988	54%	68%	74%
1989	48%	64%	71%
1990	48%	60%	65%
1991	42%	56%	63%
1992	35%	58%	69%
1993	47%	55%	59%
1994	51%	68%	76%
1995	56%	71%	78%
1996	58%	69%	74%
1997	57%	67%	71%
1998	29%	52%	63%
1999	59%	68%	72%
2000	40%	62%	73%
2001	54%	61%	65%
2002	55%	69%	75%
2003	49%	66%	73%
2004	46%	61%	68%
2005	52%	60%	63%
2006	50%	64%	71%
2007	53%	62%	66%
2008	47%	53%	55%
2009	54%	64%	69%
2010	43%	62%	71%
Average	46%	61%	68%

For matching up, the estimated trapping efficiency by these two approaches, the median size of sediment inflow (D50) reduced from 10 µm to 9 µm. Table 51 displays the estimated sediment trapping efficiency by SWAT after reducing D50.

Table 51- Trapping Efficiency at Goshen Pond Dam from 1990 to 2009 from (SWAT)

Year	Trapping Efficiency		
	L95PPU	M95PPU	U95PPU
1980	22%	51%	63%
1981	45%	56%	61%
1982	38%	42%	44%
1983	15%	46%	59%
1984	43%	63%	70%
1985	30%	38%	42%
1986	32%	55%	64%
1987	29%	56%	68%
1988	49%	63%	69%
1989	42%	59%	66%
1990	41%	53%	58%
1991	33%	49%	55%
1992	30%	56%	67%
1993	37%	46%	49%
1994	47%	66%	73%
1995	52%	68%	74%
1996	53%	64%	69%
1997	51%	60%	64%
1998	22%	48%	59%
1999	53%	62%	66%
2000	36%	60%	71%
2001	45%	53%	56%
2002	50%	65%	71%
2003	44%	62%	70%
2004	40%	55%	62%
2005	43%	51%	54%
2006	43%	60%	66%
2007	45%	54%	58%
2008	35%	41%	43%
2009	46%	58%	63%
2010	38%	59%	68%
Average	40%	55%	62%

The sediment trapping efficiency for the medium sized sediment decreased to 55% with decreasing D50 to 9 µm. The estimated sediment trapping efficiency by SWAT is still higher than Brune Curve approach, but their difference is less than 20%. Table 52 and Figure 97 show the annual sediment accumulation rate after reducing D50 from 10 to 9 µm.

Table 52- Sediment Accumulation Rate (tn/yr) within Goshen Pond

Year	L95PPU	M95PPU	U95PPU
1980	207	803	1,398
1981	1,560	3,298	5,074
1982	2,650	5,087	7,645
1983	93	496	913
1984	604	1,499	2,432
1985	1,143	2,528	3,963
1986	373	1,071	1,757
1987	200	677	1,153
1988	920	2,064	3,232
1989	534	1,292	2,074
1990	1,287	2,817	4,384
1991	612	1,551	2,491
1992	271	862	1,444
1993	1,597	3,359	5,076
1994	355	837	1,320
1995	823	1,811	2,806
1996	1,217	2,529	3,889
1997	1,528	3,103	4,718
1998	215	780	1,329
1999	1,264	2,588	4,024
2000	265	748	1,239
2001	1,938	3,880	5,840
2002	684	1,517	2,377
2003	581	1,396	2,219
2004	668	1,562	2,453
2005	1,288	2,600	3,954
2006	995	2,335	3,653
2007	1,741	3,605	5,485
2008	2,939	5,770	8,581
2009	1,619	3,411	5,221
2010	388	1,027	1,663
Min	93	496	913
Ave	986	2,158	3,349
Max	2,939	5,770	8,581

The median of sediment accumulation rate (M 95PPU) varies from the minimum of 500 (tn/yr) to the maximum of 6,000 (tn/yr). The minimum, and maximum sediment accumulation rate happened in 1983 and 2008. In 1982, and 1985 when the stream discharge exceeded 100- year recurrence interval, the sediment accumulation rate spiked.

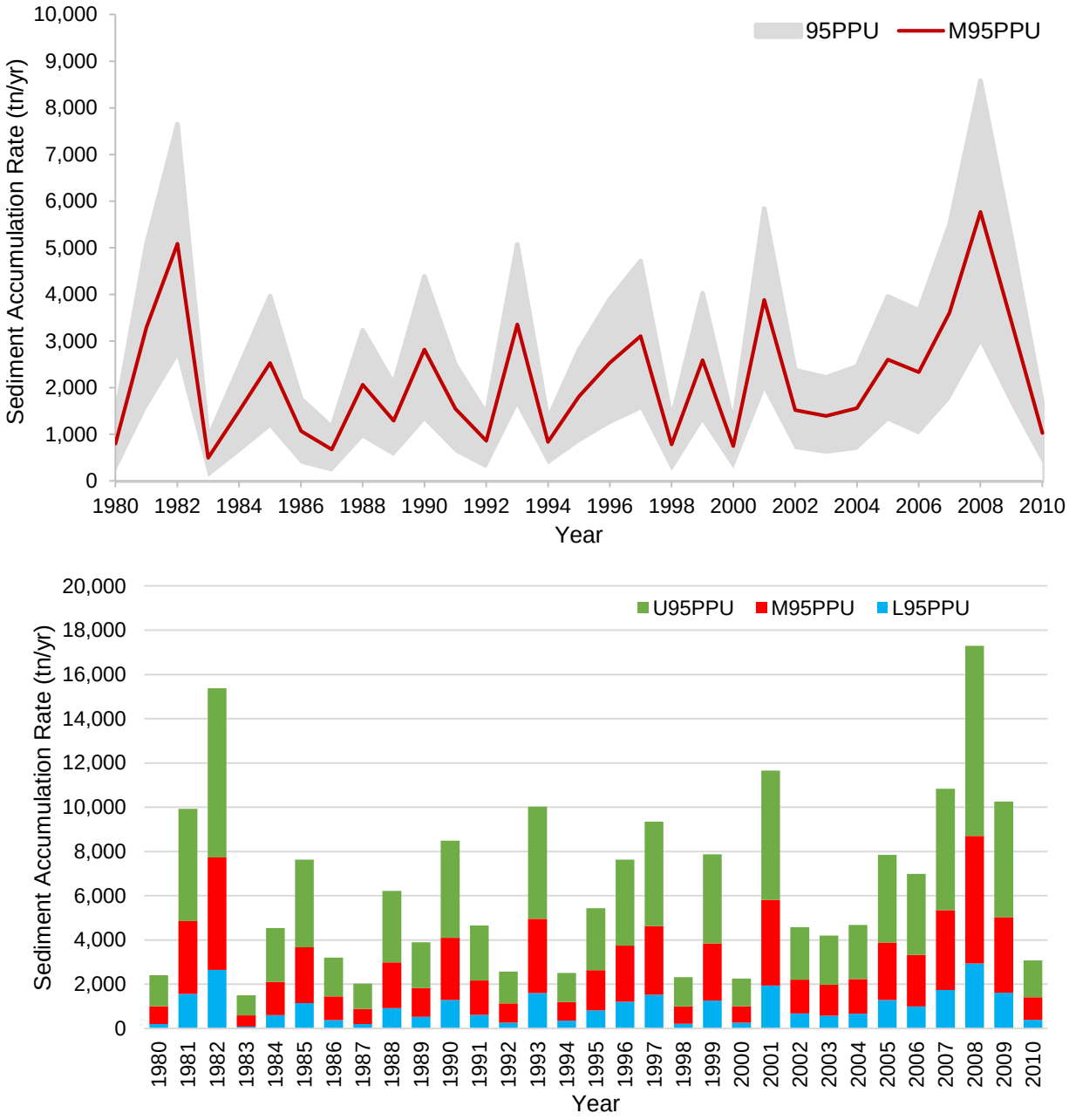

Figure 97- Sediment Accumulation Rate (tn/yr) within Goshen Pond

5.1.6. Lake Rockwell Dam

The SWAT analysis was completed for the sediment load that enters and exits the dam, then the difference of these loads was calculated to evaluate the potential sediment load trapped within the study reservoir. The potential sediment accumulation rates within Lake Rockwell reservoir, from 1988 to 2007 are displayed in Table 53 and Figure 98.

L95PPU and U95PPU represent the lower and upper boundaries of sediment accumulation rate, and M95PPU is the median sediment accumulation rate behind the dam.

Table 53- Sediment Accumulation Rate (tn/yr) within Lake Rockwell Dam

Year	L95PPU	M95PPU	U95PPU
1988	19,170	94,773	165,983
1989	27,017	135,835	247,914
1990	31,747	171,769	331,275
1991	12,971	70,900	129,776
1992	29,950	148,627	264,016
1993	25,814	125,622	230,265
1994	25,340	126,609	240,018
1995	19,380	107,951	201,000
1996	43,158	202,839	372,832
1997	21,571	113,750	205,391
1998	15,957	81,134	157,819
1999	23,372	122,350	233,539
2000	31,573	166,517	322,294
2001	13,453	78,510	139,956
2002	25,594	123,139	213,380
2003	41,424	204,166	367,089
2004	30,033	146,367	253,330
2005	37,398	178,627	337,417
2006	30,018	150,809	281,986
2007	37,557	168,714	313,558
Min	12,971	70,900	129,776
Ave	27,125	135,950	250,442
Max	43,158	204,166	372,832

The median of sediment accumulation rate (M95PPU) within Rockwell reservoir varies between the minimum of 71,000 (tn/yr) and the maximum of 204,000 (tn/yr) from 1988 to 2007, with the average rate of 136,000 (tn/yr).

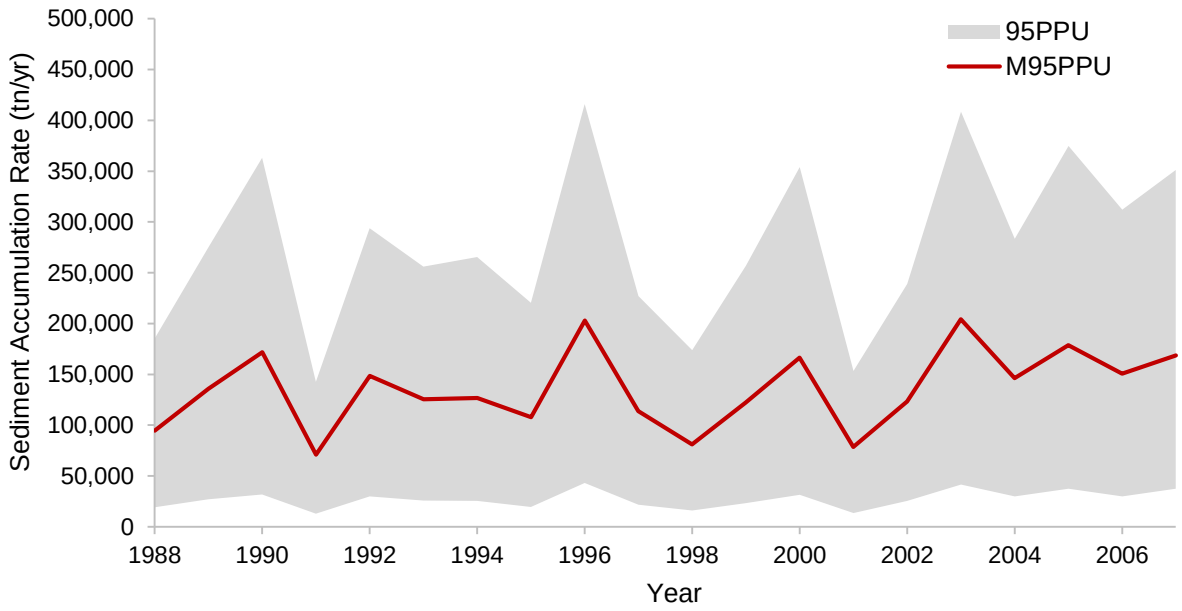

Figure 98- Sediment Accumulation Rate (tn/yr)

Brune developed a curve which relates the efficiency of the reservoir in trapping suspended sediments to the capacity of the reservoir and average annual volume of inflow. Brune evaluated data from 44 reservoirs, of which 40 were normally ponded reservoirs, two of them were desilting basins, and the remaining two were semi-dry reservoirs. To estimate the trapping efficiency with applying Brune Curve, knowledge of the reservoir capacity and average annual flow is required. The normal storage capacity of Rockwell reservoir is about 8,172 ac. ft (10.08 Mm^3), and the maximum capacity is 18,250 ac. ft (22.51 Mm^3). The reservoir capacity varies between the normal and maximum capacity over time. The residence time has been estimated by using the capacity of the reservoir and average annual inflow from the SWAT simulation. Table 54 shows the trapping efficiency as calculated with the Brune Curve. The average trapping efficiency for medium sized sediment is 83%.

Table 54- Trapping Efficiency at Lake Rockwell Dam from 1988 to 2007 (Brune)

Year	Volume or V(m^3)	Flow or Q (m/s)	V/Q (yrs)	Trapping Efficiency from Brune Curve		
				Fine SED	Medium SED	Coarse SED
1988	19,910,000	5.90	0.11	85%	92%	97%
1989	21,640,000	8.57	0.08	77%	88%	94%
1990	21,640,000	11.09	0.06	71%	83%	90%
1991	10,080,000	4.87	0.07	74%	84%	91%
1992	21,640,000	10.36	0.07	74%	84%	91%
1993	10,080,000	8.21	0.04	64%	78%	85%
1994	10,080,000	7.13	0.04	64%	78%	85%
1995	10,530,000	6.49	0.05	68%	80%	88%
1996	21,210,000	12.96	0.05	68%	80%	88%
1997	17,220,000	8.57	0.06	71%	83%	90%
1998	10,080,000	6.26	0.05	68%	80%	88%
1999	11,160,000	6.16	0.06	71%	83%	90%
2000	12,420,000	9.16	0.04	64%	78%	85%
2001	12,180,000	5.28	0.07	74%	84%	91%
2002	21,640,000	7.79	0.09	78%	88%	94%
2003	21,200,000	13.24	0.05	68%	80%	88%
2004	21,640,000	10.38	0.07	74%	84%	91%
2005	19,690,000	10.77	0.06	71%	83%	90%
2006	17,150,000	11.95	0.05	68%	80%	88%
2007	19,120,000	11.20	0.05	68%	80%	88%
Average				71%	83%	90%

Table 55 displays the sediment trapping efficiency within the Lake Rockwell reservoir estimated by SWAT from 1988 to 2007. The average of estimated sediment trapping efficiency by SWAT is 92%, while Brune Curve predicted the trapping efficiency of 83% for Lake Rockwell reservoir. Adjusting some parameters including the equilibrium concentration (SSC_{eq}), decay constant. and median size of sediment particle (D50) can be helpful for matching up the predicted trapping efficiency from Brune Curve with SWAT.

Table 55- Trapping Efficiency at Rockwell Dam from 1988 to 2007 (SWAT)

Year	Trapping Efficiency		
	L95PPU	M95PPU	U95PPU
1988	72%	93%	96%
1989	69%	90%	94%
1990	65%	89%	93%
1991	62%	89%	93%
1992	67%	90%	93%
1993	67%	89%	93%
1994	71%	92%	95%
1995	66%	91%	95%
1996	67%	89%	93%
1997	61%	88%	92%
1998	64%	89%	93%
1999	69%	91%	94%
2000	70%	91%	94%
2001	66%	92%	95%
2002	69%	90%	94%
2003	65%	89%	92%
2004	63%	88%	92%
2005	67%	89%	92%
2006	63%	87%	91%
2007	66%	88%	92%
Average	66%	90%	93%

In Rockwell Dam watershed for matching up the trapping efficiency from Brune Curve with SWAT, the median size of sediment in the reservoir has been reduced from 10 to 7 µm. Table 56 displays the average of sediment trapping efficiency from the SWAT result after changing D50. For medium sized particles, the average sediment trapping efficiency is about 85%, which is only 5% less than the trapping efficiency from the Brune Curve.

Table 56- Trapping Efficiency at Rockwell Reservoir from 1988 to 2007 from (SWAT)

Year	Trapping Efficiency		
	L95PPU	M95PPU	U95PPU
1988	69%	91%	94%
1989	65%	87%	91%
1990	60%	85%	89%
1991	57%	85%	90%
1992	61%	85%	90%
1993	63%	84%	89%
1994	67%	88%	92%
1995	65%	90%	94%
1996	63%	85%	89%
1997	56%	83%	88%
1998	57%	84%	90%
1999	65%	87%	90%
2000	67%	87%	90%
2001	60%	89%	93%
2002	64%	86%	90%
2003	60%	83%	87%
2004	59%	84%	89%
2005	61%	83%	87%
2006	57%	82%	86%
2007	61%	82%	86%
Average	62%	85%	90%

Table 57 and Figure 99, display the new sediment accumulation rate after reducing the median size of sediment particle (D50) in the SWATCUP.

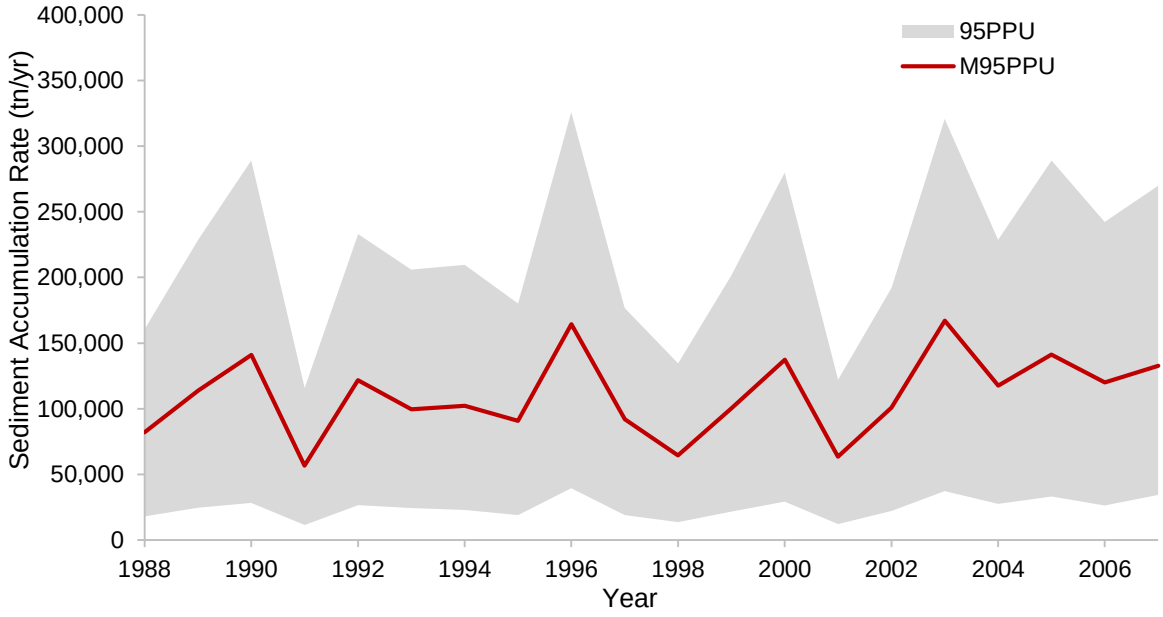

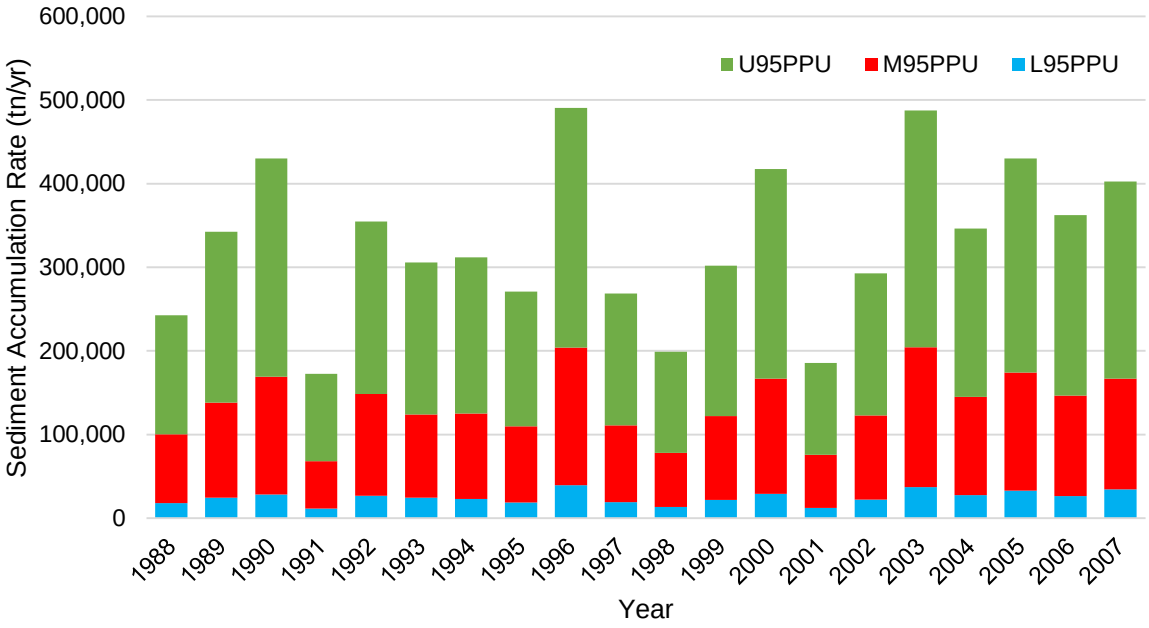

Figure 99- Sediment Accumulation Rate (tn/yr), Reduced D50

Table 57- Sediment Accumulation Rate within Lake Rockwell Dam (tn/yr), Reduced D50

Year	L95PPU	M95PPU	U95PPU
1988	17,977	82,080	142,732
1989	24,505	113,651	204,215
1990	28,243	141,027	260,836
1991	11,362	56,744	104,312
1992	26,645	121,798	206,254
1993	24,403	99,630	181,658
1994	22,844	102,307	186,721
1995	18,898	90,827	161,182
1996	39,459	164,437	286,538
1997	19,006	92,018	157,672
1998	13,528	64,557	120,990
1999	21,781	100,176	180,148
2000	29,245	137,450	250,684
2001	12,174	63,401	109,872
2002	22,203	100,758	169,812
2003	37,271	166,966	283,463
2004	27,501	117,657	201,120
2005	33,018	141,173	255,978
2006	26,395	120,027	215,975
2007	34,301	132,652	235,649
Min	11,362	56,744	104,312
Ave	24,538	110,467	195,791
Max	39,459	166,966	286,538

The average of sediment accumulation rate (M 95PPU) varies from 57,000 (tn/yr) to 167,000 (tn/yr), with an average rate of 110,000 (tn/yr).

5.1.7. Ford Lake Dam

The SWAT model of Ford Lake Dam watershed utilizes eight subbasins. Ford Lake Dam is in Subbasin Eight. The subbasins were further divided into a total of 76 Hydrologic Response Units (HRUs). The SWAT analysis was completed for the sediment load that flows into the dam and leaves the dam. The difference of these loads is an estimate of the sediment load trapped behind the dam. Figure 100 shows the potential sediment load that flows into the Ford Lake and Figure 101 indicates the sediment load exiting the dam.

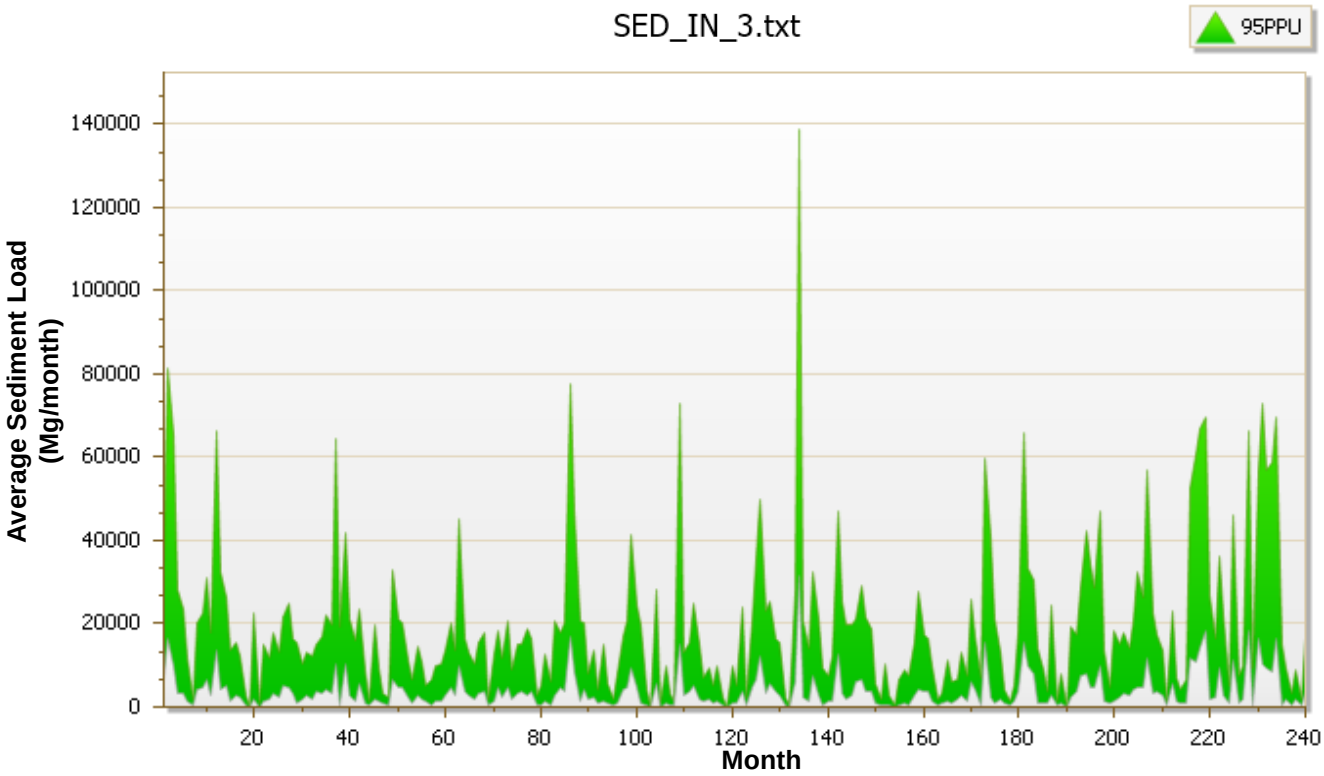

Figure 100- The Simulated Average Sediment Load Flows into Ford Lake, from 1990 to 2009.

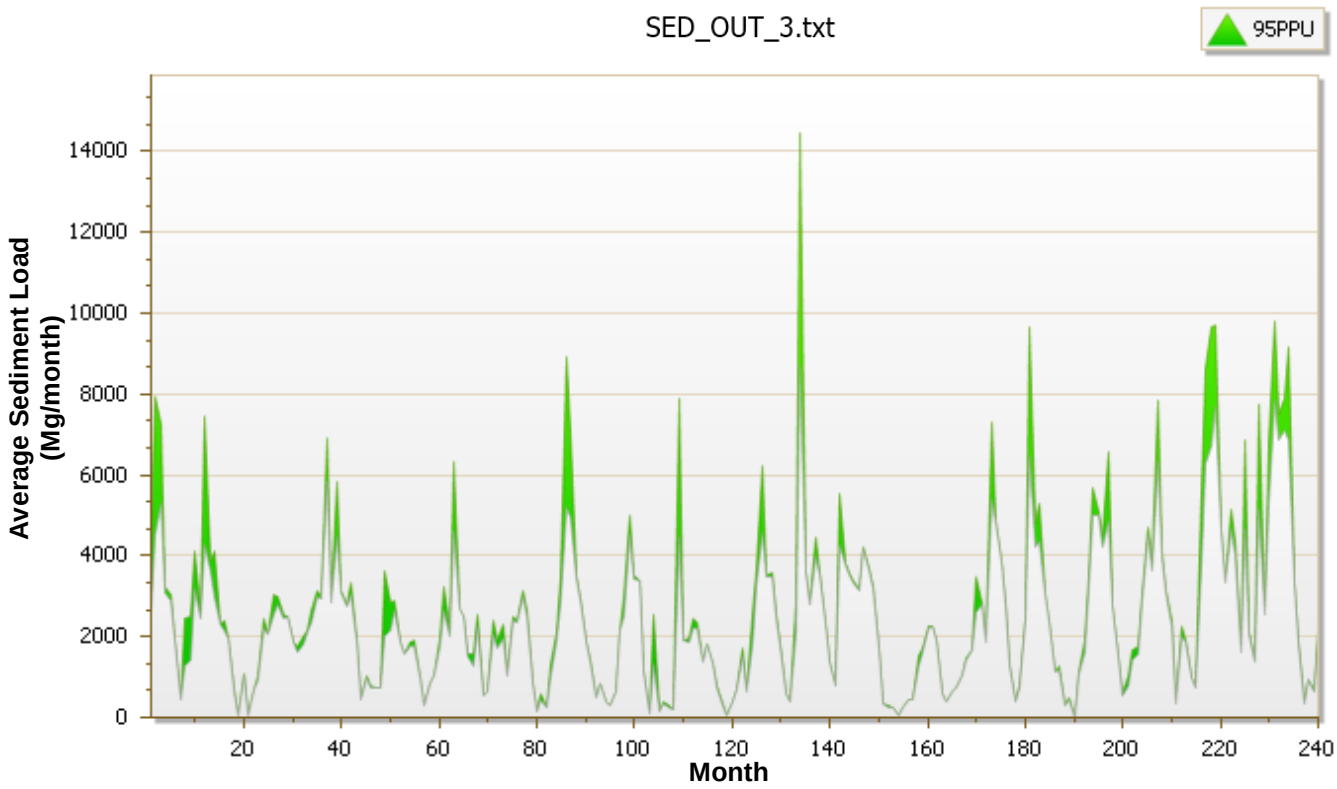

Figure 101- The Simulated Average Sediment Load Exits Ford Lake, from 1990 to 2009.

Table 58 and Figure 102 display the annual sediment accumulation rate within Ford Lake reservoir. L95 PPU and U95 PPU represent the lower boundary and upper boundaries of sediment accumulation rate. Any point inside the L 95PPU and U 95PPU boundaries have some probability of reflecting the actual sediment accumulation within the reservoir.

Table 58- Sediment Accumulation Rate (tn/yr) within Ford Lake estimated by SWAT

Year	L95PPU	M95PPU	U95PPU
1990	45,567	212,050	395,392
1991	8,740	78,058	165,989
1992	12,019	94,075	189,941
1993	16,055	98,256	221,420
1994	15,571	86,147	155,829
1995	18,855	98,428	186,274
1996	14,346	81,472	155,805
1997	22,767	120,364	232,147
1998	17,284	82,440	165,461
1999	19,839	100,115	179,579
2000	23,334	119,096	212,793
2001	43,596	171,725	359,581
2002	8,950	61,513	138,745
2003	12,161	72,074	134,578
2004	18,588	85,263	206,963
2005	26,695	107,098	216,878
2006	21,519	128,993	273,842
2007	21,627	120,729	249,239
2008	52,271	207,904	405,765
2009	33,023	167,492	360,521
Min	8,740	61,513	134,578
Ave	22,640	114,665	230,337
Max	52,271	212,050	405,765

The median of annual sediment trapping rate varies between the minimum of 61,000 and the maximum of 212,000 (tn/yr).

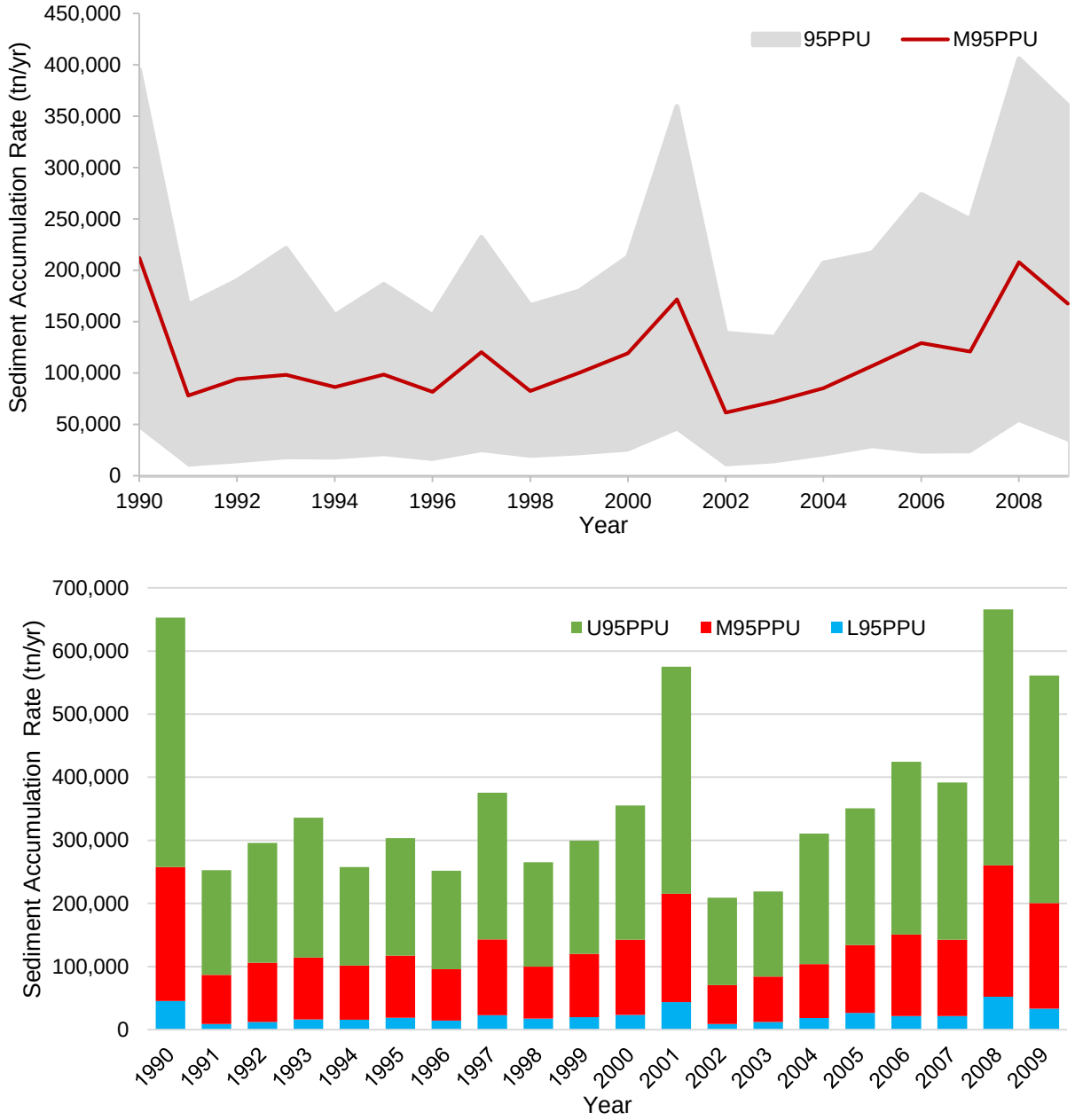

Figure 102- Sediment Accumulation Rate (tn/yr) within Ford Lake

Table 59 displays the calculated sediment trapping efficiency within Ford Lake reservoir using the Brune Curve. The average of sediment trapping efficiency within Ford Lake reservoir as calculated by Brune Curve approach is 79%.

Table 59- Trapping Efficiency at Ford Lake from 1990 to 2009 (Brune Curve)

Year	Volume or C (m3)	Flow or Q (m/s)	C/Q (yr)	Trapping Efficiency from Brune Curve		
				Fine SED	Medium SDE	Coarse SED
1990	21,360,000	19.32	0.04	65%	78%	85%
1991	21,870,000	11.64	0.06	71%	83%	90%
1992	21,640,000	17.55	0.04	65%	78%	85%
1993	21,910,000	17.03	0.04	65%	78%	85%
1994	21,870,000	11.41	0.06	71%	83%	90%
1995	21,900,000	14.94	0.05	68%	80%	88%
1996	21,830,000	11.09	0.06	71%	83%	90%
1997	21,920,000	15.03	0.05	68%	80%	88%
1998	21,920,000	12.02	0.06	71%	83%	90%
1999	21,910,000	11.15	0.06	71%	83%	90%
2000	21,920,000	15.08	0.05	68%	80%	88%
2001	21,800,000	24.51	0.03	58%	73%	81%
2002	21,890,000	13.11	0.05	68%	80%	88%
2003	21,860,000	9.16	0.08	76%	88%	92%
2004	21,710,000	18.92	0.04	65%	78%	85%
2005	21,870,000	15.75	0.04	65%	78%	85%
2006	21,700,000	20.85	0.03	58%	73%	81%
2007	21,850,000	20.62	0.03	58%	73%	81%
2008	21,740,000	30.57	0.02	50%	65%	75%
2009	21,880,000	27.52	0.03	58%	73%	81%
Average				66%	79%	86%

The estimated trapping efficiency by SWAT is provided in Table 60. The SWAT estimated the average trapping efficiency of 78%, which is pretty close to Brune Curve method, and their difference is only 1%.

Table 60- Trapping Efficiency at Ford Lake Dam from 1990 to 2009 (SWAT)

Year	Trapping Efficiency		
	L95PPU	M95PPU	U95PPU
1990	56%	83%	88%
1991	31%	78%	88%
1992	29%	75%	85%
1993	39%	76%	87%
1994	44%	79%	87%
1995	41%	77%	86%
1996	43%	80%	88%
1997	47%	79%	87%
1998	49%	78%	87%
1999	50%	81%	88%
2000	47%	80%	87%
2001	54%	78%	87%
2002	30%	73%	86%
2003	45%	82%	89%
2004	43%	71%	85%
2005	52%	77%	86%
2006	38%	77%	87%
2007	38%	75%	86%
2008	51%	76%	85%
2009	42%	75%	86%
Average	43%	78%	87%

5.1.8. Potter's Falls Dam

Potter's Fall SWAT model contains two subbasins. Potter's Falls Dam and Gage 04233300 are both within Subbasin One. The subbasins were further divided into a total of 45 Hydrologic Response Units (HRUs). The SWAT analysis was completed for the sediment load that flows into the dam and exits the dam. The difference of these loads is an estimate of the sediment load trapped behind the dam. Table 61 and Figure 103 display the sediment accumulation rates within Potter's Falls reservoir from 1999 to 2010. The L95 PPU and U95 PPU represent the lower, and upper boundaries of potential sediment accumulation rate, respectively. Any point inside the L95 PPU and U95 PPU boundaries have some probabilities of reflecting the actual sediment accumulation within

the reservoir. M95 PPU displays the 50% probability of sediment accumulation rate within Potter's Falls reservoir.

Table 61- Sediment Accumulation Rate (Mg/yr) within Potter's Falls Dam

Year	L95PPU	M95PPU	U95PPU
1999	542	11,196	26,152
2000	213	11,708	28,599
2001	339	8,403	20,373
2002	376	11,298	27,175
2003	126	11,734	29,821
2004	143	10,161	26,392
2005	264	10,844	26,865
2006	431	12,142	30,070
2007	284	10,260	25,209
2008	839	17,727	42,277
2009	831	13,544	31,886
2010	177	8,014	20,356
Min	126	8,014	20,356
Ave	380	11,419	27,931
Max	839	17,727	42,277

The median of sediment accumulation rate (M 95PPU) within Potter's Falls reservoir varies between 8,000 (tn/yr) and 18,000 (tn/yr) from 1999 to 2010. Figure 103 displays the sediment accumulation rate which is following the pretty smooth trend. However, there is a spike in 2008. The sediment accumulation rate is lowest in 2001 and 2003 among other months.

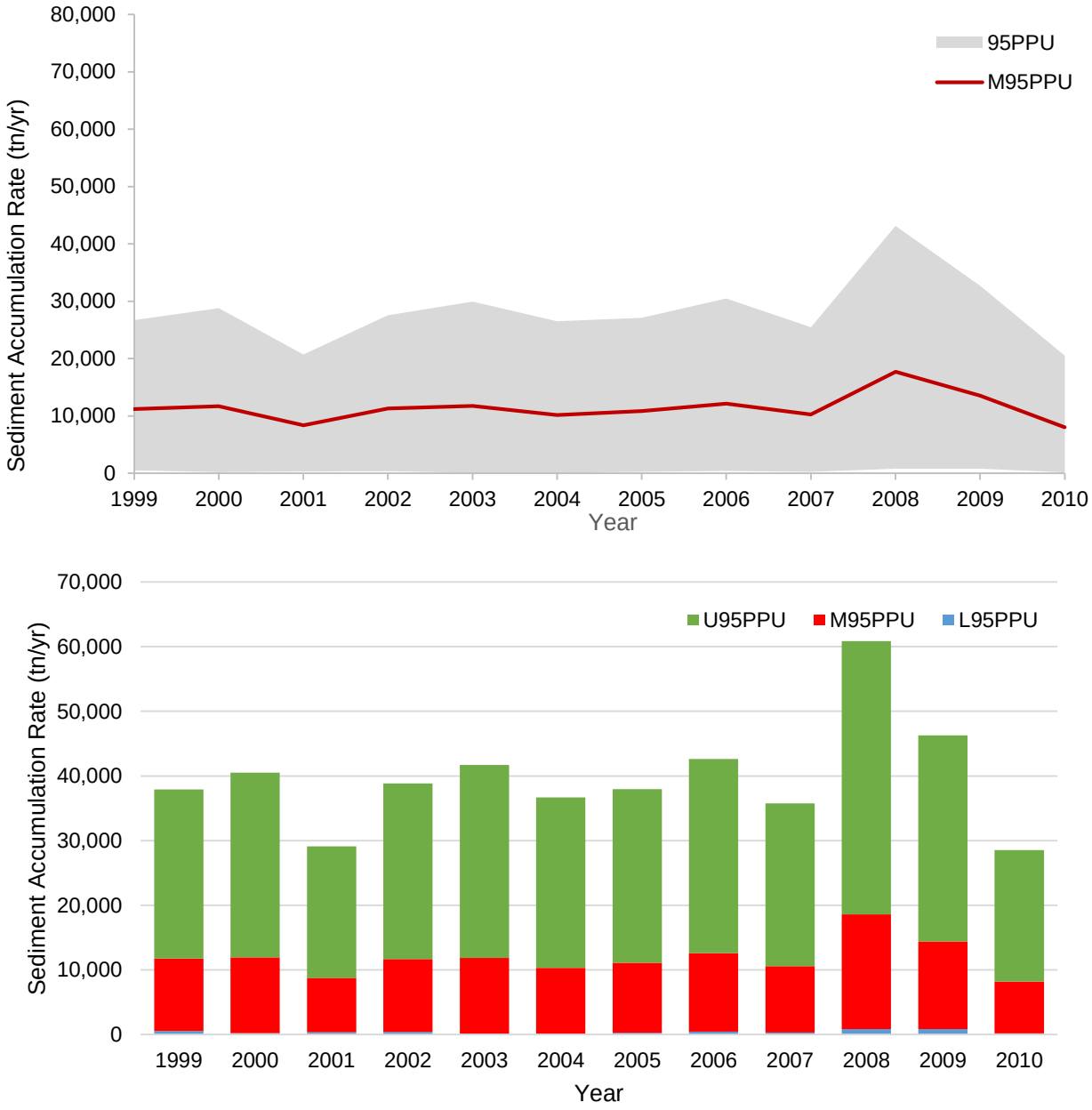

Figure 103- Sediment Accumulation Rate (tn/yr) within Potter's Falls Reservoir

In this research, we intend to compare trapping efficiency from SWAT output with Brune Curve. Brune Curve relates the residence time of water inflow in the reservoir with sediment trapping efficiency. Residence time can be estimated by dividing the volume of the reservoir by inflow rate. Table 62 displays the sediment trapping efficiency in Potter's Falls reservoir based on the Brune Curve.

Table 62- Trapping Efficiency at Potter's Falls Dam from 1999 to 2010 (Brune Curve)

Year	Volume or V (m^3)	Flow or Q (m/s)	V/Q (yrs)	Trapping Efficiency from Brune Curve		
				Fine SED	Medium SED	Coarse SED
1999	1,170,000	1.11	0.03	50%	65%	75%
2000	1,000,000	1.65	0.02	50%	65%	75%
2001	1,000,000	1.31	0.02	50%	65%	75%
2002	1,000,000	1.58	0.02	50%	65%	75%
2003	1,000,000	2.25	0.02	31%	48%	60%
2004	1,000,000	2.34	0.01	50%	65%	75%
2005	1,000,000	2.06	0.02	50%	65%	75%
2006	1,066,000	2.08	0.02	50%	65%	75%
2007	1,010,000	1.67	0.02	50%	65%	75%
2008	1,289,000	1.94	0.02	50%	65%	75%
2009	1,000,000	1.38	0.02	50%	65%	75%
2010	1,000,000	1.75	0.02	50%	65%	75%
Average				49%	64%	74%

The average of sediment trapping efficiency for medium size sediment is 64%. For coarse, and fine are 74% and 49%, respectively. Table 63 indicates sediment trapping efficiency from SWAT result. Average of sediment trapping efficiency is 64%, which is the same with Brune Curve.

Table 63- Trapping Efficiency at Potter's Falls Dam from 1999 to 2010 (SWAT)

Year	Trapping Efficiency		
	L95PPU	M95PPU	U95PPU
1999	21%	61%	66%
2000	8%	66%	73%
2001	18%	65%	73%
2002	16%	71%	79%
2003	4%	59%	69%
2004	6%	62%	74%
2005	10%	59%	68%
2006	17%	72%	82%
2007	10%	53%	60%
2008	22%	66%	72%
2009	32%	75%	80%
2010	9%	57%	67%
Average	14%	64%	72%

5.1.9. Brown Bridge Dam

The Brown Bridge SWAT model contain 20 subbasins and 77 HRUs, the dam is in Subbasin One. For evaluating the sediment accumulation rate behind the dam, a SWAT analysis is completed for the sediment load that flows into and exits the dam from 1998 to 2010. The difference of these loads is an estimate of the potential sediment load that trapped behind the dam. Green regions in Figure 104 and Figure 105 display the potential monthly sediment load that enters and exits the dam, respectively.

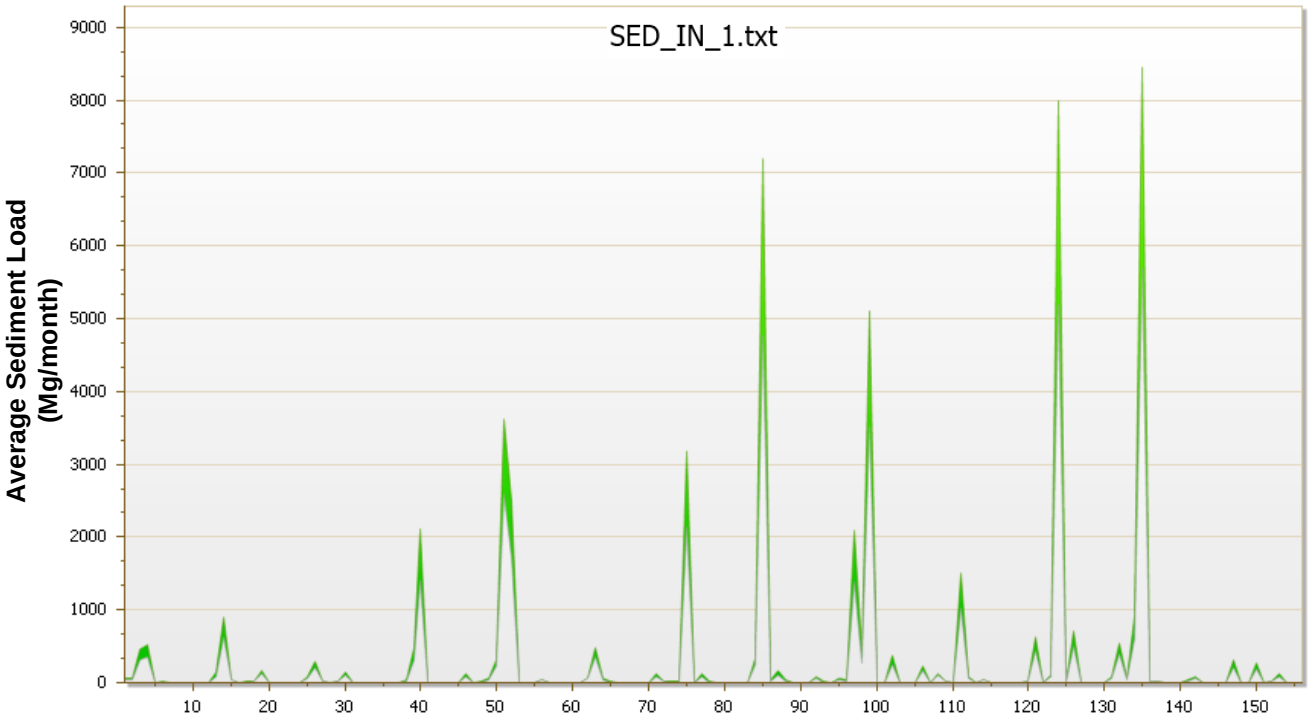

Figure 104- The Simulated Average Sediment Load Flows into Brown Bridge reservoir, from 1998 to 2010.

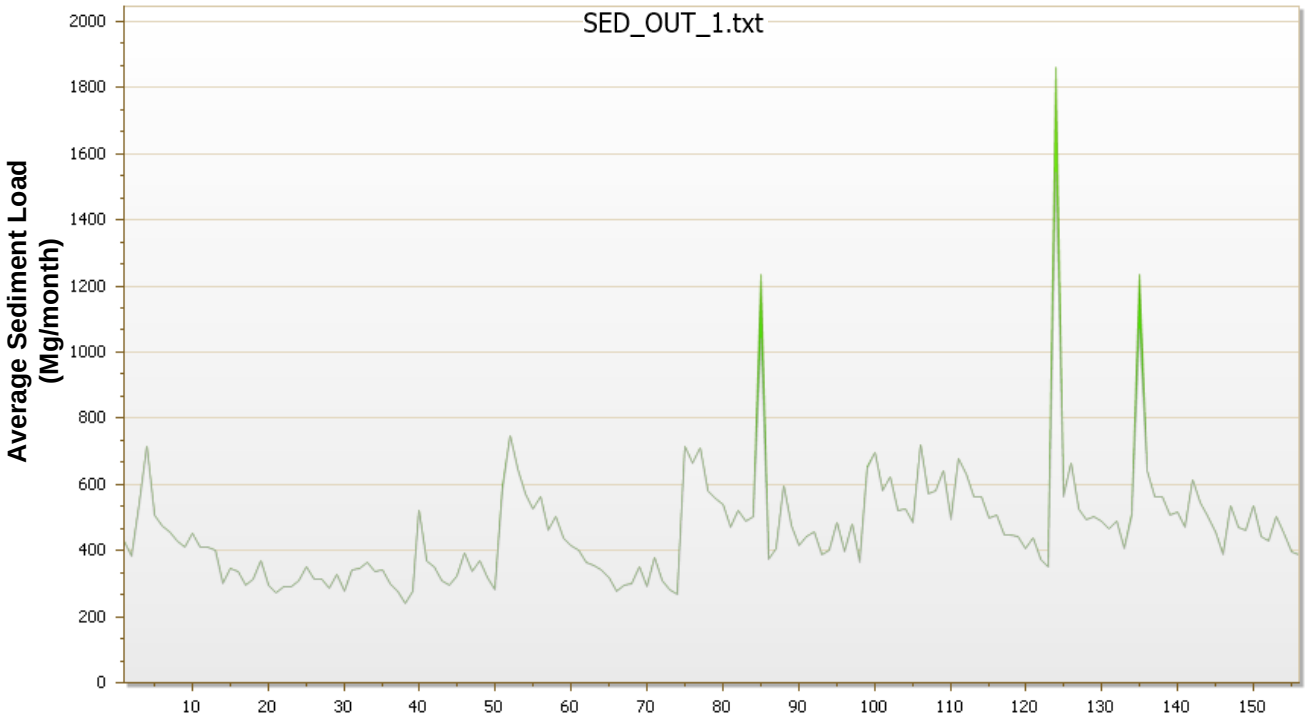

Figure 105- The Simulated Average Sediment Load Exits Brown Bridge reservoir, from 1998 to 2010.

Table 64 and Figure 106 display the annual sediment accumulation rates within the Brown Bridge reservoir. The 95PPU (95% prediction uncertainty) is the potential sediment accumulation rate envelope, which means any rate inside the 95PPU region has some probability of reflecting the actual sediment accumulation rate. The L95 PPU represents the lower boundary, and U95 PPU shows the upper boundary of the 95PPU region.

Table 64- Sediment Accumulation Rate (tn/yr) within the Brown Bridge Dam

Year	L95PPU	M95PPU	U95PPU
1998	355	560	745
1999	666	887	1,089
2000	116	210	290
2001	1,732	2,251	2,720
2002	4,588	5,697	6,669
2003	284	414	527
2004	2,245	2,924	3,537
2005	4,799	6,146	7,357
2006	5,780	7,301	8,661
2007	740	1,056	1,339
2008	6,277	8,033	9,620
2009	6,311	8,012	9,537
2010	96	231	351
Min	96	210	290
Ave	2,615	3,363	4,034
Max	6,311	8,033	9,620

SWAT predicted the 50% probability of sediment accumulation rate within Brown Bridge reservoir varies between the minimum of 210 (tn/yr) and the maximum of 8,000 (tn/yr). The dashed line in Figure 106 displays the annual stream discharge that flows into the dam, and the solid line represents the average of annual sediment accumulation rate. As Figure 106 displays both solid, and dashed lines follow a similar trend. As stream discharge into the reservoir decreases, the sediment accumulation rate reduces. The potential reason for high sediment accumulation rate in some months is because of the high amount of inflow discharge.

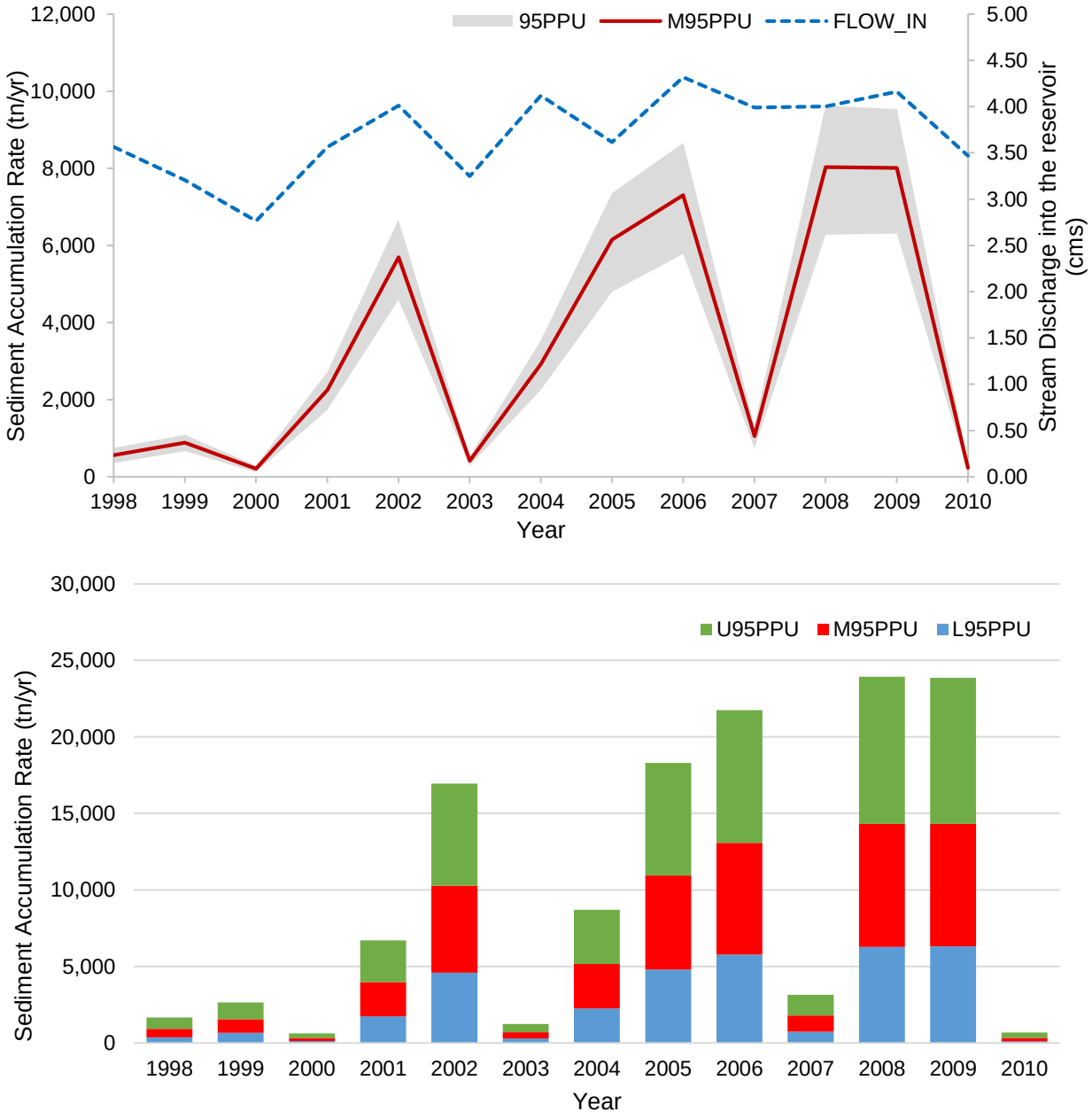

Figure 106- Estimated Sediment Accumulation Rate (tn/yr) within Brown Bridge Reservoir

The mean annual volume of inflow and the reservoir capacity can be estimated by SWAT. Table 65 displays the reservoir volume and inflow discharge estimated by SWAT, and predicted trapping efficiency using the Brune Curve.

Table 65- Trapping Efficiency at Brown Bridge Dam from 1998 to 2010 (Brune Curve)

Year	Reservoir Volume V (m^3)	Inflow Discharge Q (m/s)	V/Q (yr)	Trapping Efficiency from Brune Curve		
				Fine SED	Medium SED	Coarse SED
1998	3,329,000	3.54	0.03	57%	74%	81%
1999	3,053,000	3.18	0.03	57%	74%	81%
2000	2,350,000	2.76	0.03	57%	74%	81%
2001	3,441,000	3.51	0.03	57%	74%	81%
2002	3,441,000	4.01	0.03	57%	74%	81%
2003	3,441,000	3.21	0.03	57%	74%	81%
2004	3,441,000	4.10	0.03	57%	74%	81%
2005	3,441,000	3.62	0.03	57%	74%	81%
2006	3,441,000	4.19	0.03	57%	74%	81%
2007	3,296,000	3.89	0.03	57%	74%	81%
2008	3,441,000	3.96	0.03	57%	74%	81%
2009	3,441,000	4.18	0.03	57%	74%	81%
2010	3,422,000	3.52	0.03	57%	74%	81%
Average				57%	74%	81%

The average efficiency of the Brown Bridge reservoir in trapping medium sized sediment sediments is 74%. As displayed in Table 66, the average of sediment trapping efficiency from SWAT is about 71%, which is only 5% less than Brune Curve method.

Table 66- Estimated Trapping Efficiency at Brown Bridge Dam from 1998 to 2010 (SWAT)

Year	Trapping Efficiency		
	L95PPU	M95PPU	U95PPU
1998	42%	53%	60%
1999	66%	72%	76%
2000	25%	38%	46%
2001	83%	86%	88%
2002	89%	91%	92%
2003	45%	54%	60%
2004	80%	84%	86%
2005	84%	86%	87%
2006	90%	92%	93%
2007	57%	65%	71%
2008	84%	85%	86%
2009	87%	88%	89%
2010	17%	32%	42%
Average	65%	71%	75%

5.1.10. Mio and Alcona Dams

The SWAT model of Mio and Alcona Dams watershed utilizes18 subbasins, Mio Dam is in the Subbasin Six, Alcona Dam is in Subbasin 11. The subbasins were further divided into a total of 98 Hydrologic Response Units (HRUs). The SWAT analysis was completed for the sediment load that flows into the dam and leaves the dam. The difference of these loads is an estimate of the sediment load trapped behind the dam. Figure 107, and Figure 108 display sediment loads that flow into Mio reservoir and exits the reservoir.

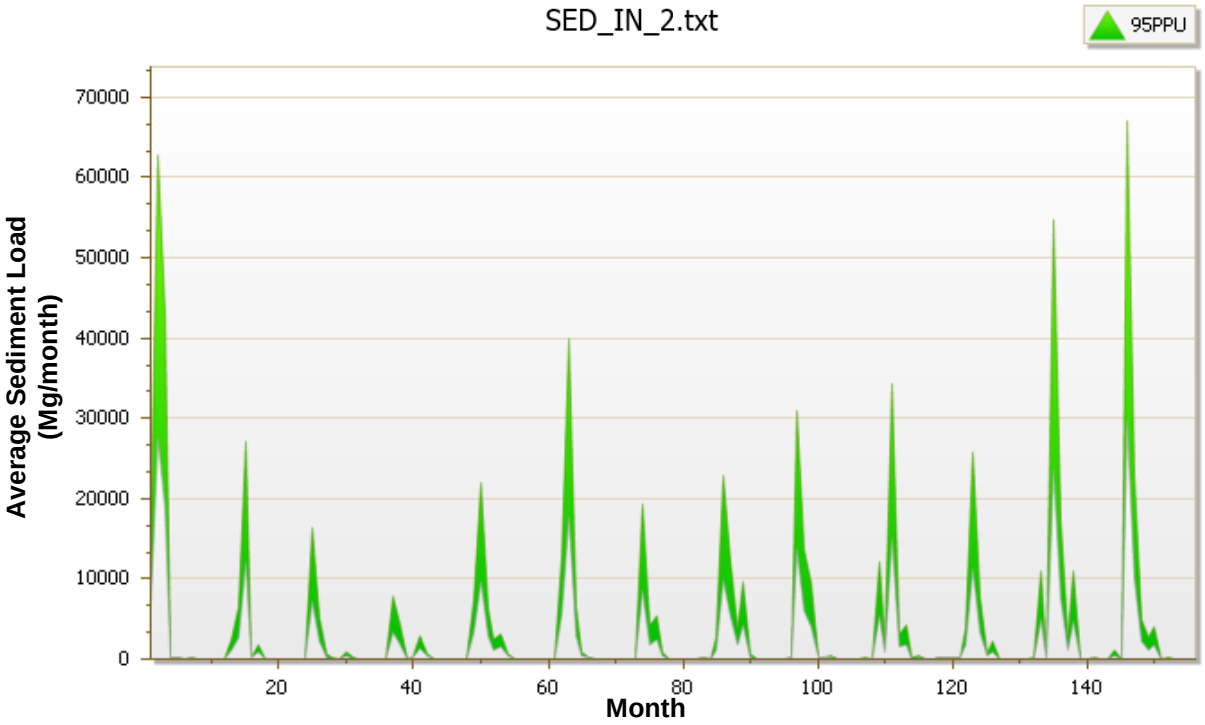

Figure 107- The Simulated Average Sediment Load Flows into Mio Reservoir, from 1997 to 2009.

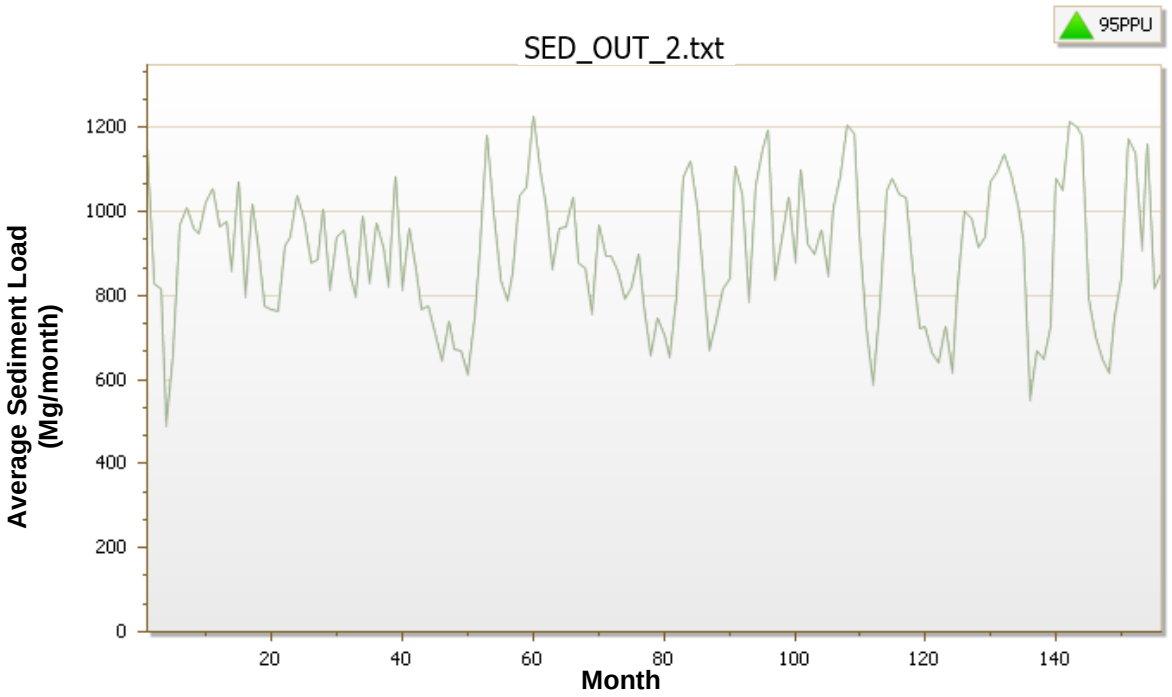

Figure 108- The Simulated Average Sediment Load Exits Mio Reservoir, from 1997 to 2009.

Figure 109, and Figure 110 show the sediment load that flows into the Alcona reservoir and exits the reservoir.

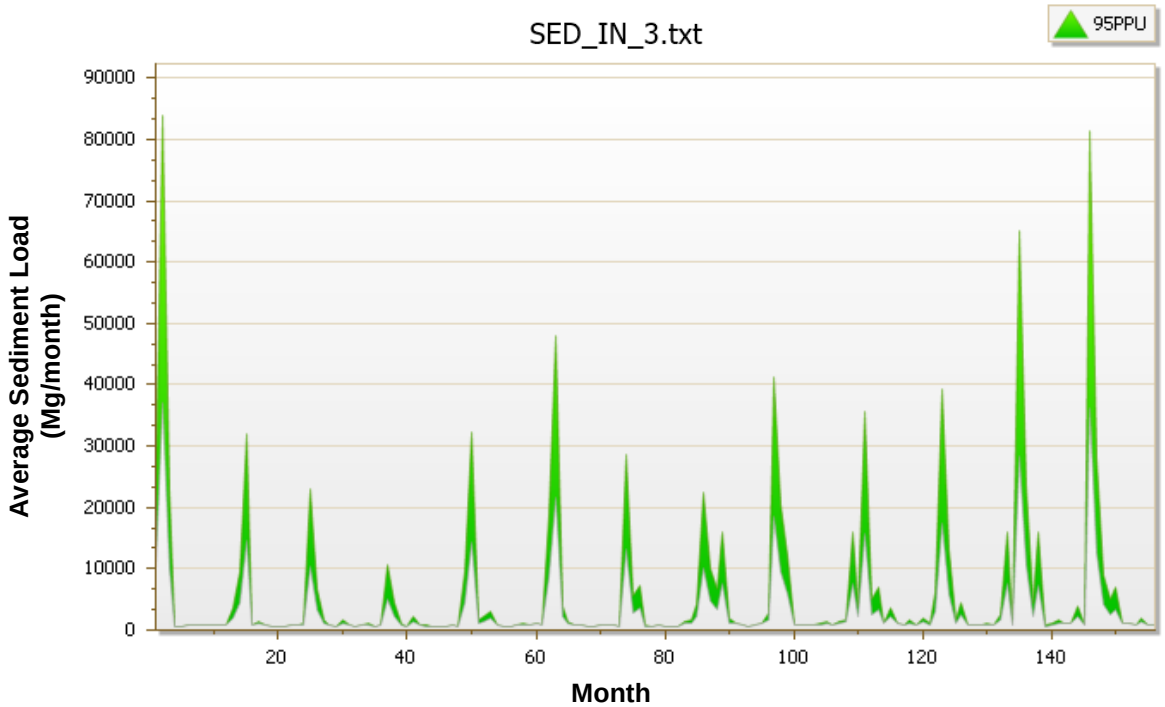

Figure 109- The Simulated Average Sediment Load Flows into Alcona Reservoir, from 1997 to 2009.

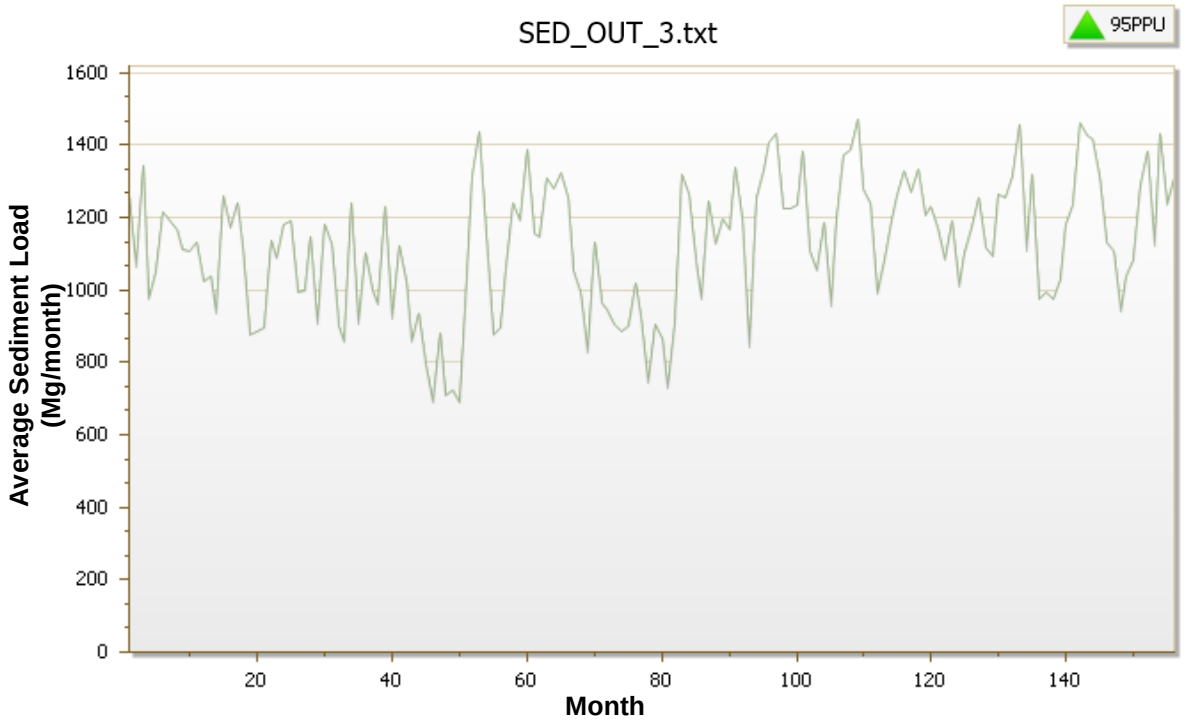

Figure 110- The Simulated Average Sediment Load Exits Alcona Reservoir, from 1997 to 2009.

Table 67 and Table 68 display the annual sediment accumulation rates within Mio and Alcona reservoirs, respectively. The 95PPU (95% prediction uncertainty) provides the potential sediment accumulation rate region. Any point inside the L95PPU and U95PPU boundaries have some probability of reflecting the actual sediment accumulation rate within the reservoir.

Table 67- Sediment Accumulation Rate (tn/yr) within Mio Dam

Year	L95PPU	M95PPU	U95PPU
1997	47,486	86,715	121,946
1998	7,194	19,512	30,863
1999	2,649	7,184	14,123
2000	935	2,535	7,208
2001	8,907	22,478	34,792
2002	17,364	36,774	54,347
2003	4,069	13,608	22,363
2004	13,172	29,875	45,133
2005	14,517	32,301	48,395
2006	16,373	34,757	51,499
2007	8,312	21,510	33,480
2008	34,836	66,667	95,497
2009	38,849	71,367	100,916
Min	935	2,535	7,208
Ave	16,513	34,253	50,812
Max	47,486	86,715	121,946

SWAT predicted the average of sediment accumulation rate within Mio reservoir varies between the minimum of 2,500 (tn/yr) and the maximum of 86,700 (tn/yr), with the average rate of 34,200 (tn/yr).

Table 68- Sediment Accumulation Rate (tn/yr) within Alcona Dam

Year	L95PPU	M95PPU	U95PPU
1997	56,205	97,584	134,990
1998	16,971	31,095	44,020
1999	10,428	20,421	29,473
2000	4,081	9,391	14,205
2001	17,494	32,388	45,993
2002	28,923	51,288	71,550
2003	16,381	29,565	41,711
2004	23,446	42,621	60,055
2005	30,417	54,374	75,868
2006	27,551	50,342	70,917
2007	24,970	45,916	64,903
2008	54,777	95,993	133,209
2009	56,596	98,187	135,875
Min	4,081	9,391	14,205
Ave	28,326	50,705	70,982
Max	56,596	98,187	135,875

Sediment accumulation rate within Alcona reservoir changing from the minimum of 9,400 (tn/yr) to the maximum of 98,100 (tn/yr), with the average of 50,700 (tn/yr). The dashed lines in Figure 111 and Figure 112 display the annual stream discharge that flows into the dam, and the solid lines represent the average of annual sediment accumulation rate. As stream discharge into the reservoir increases, the sediment accumulation rate increases.

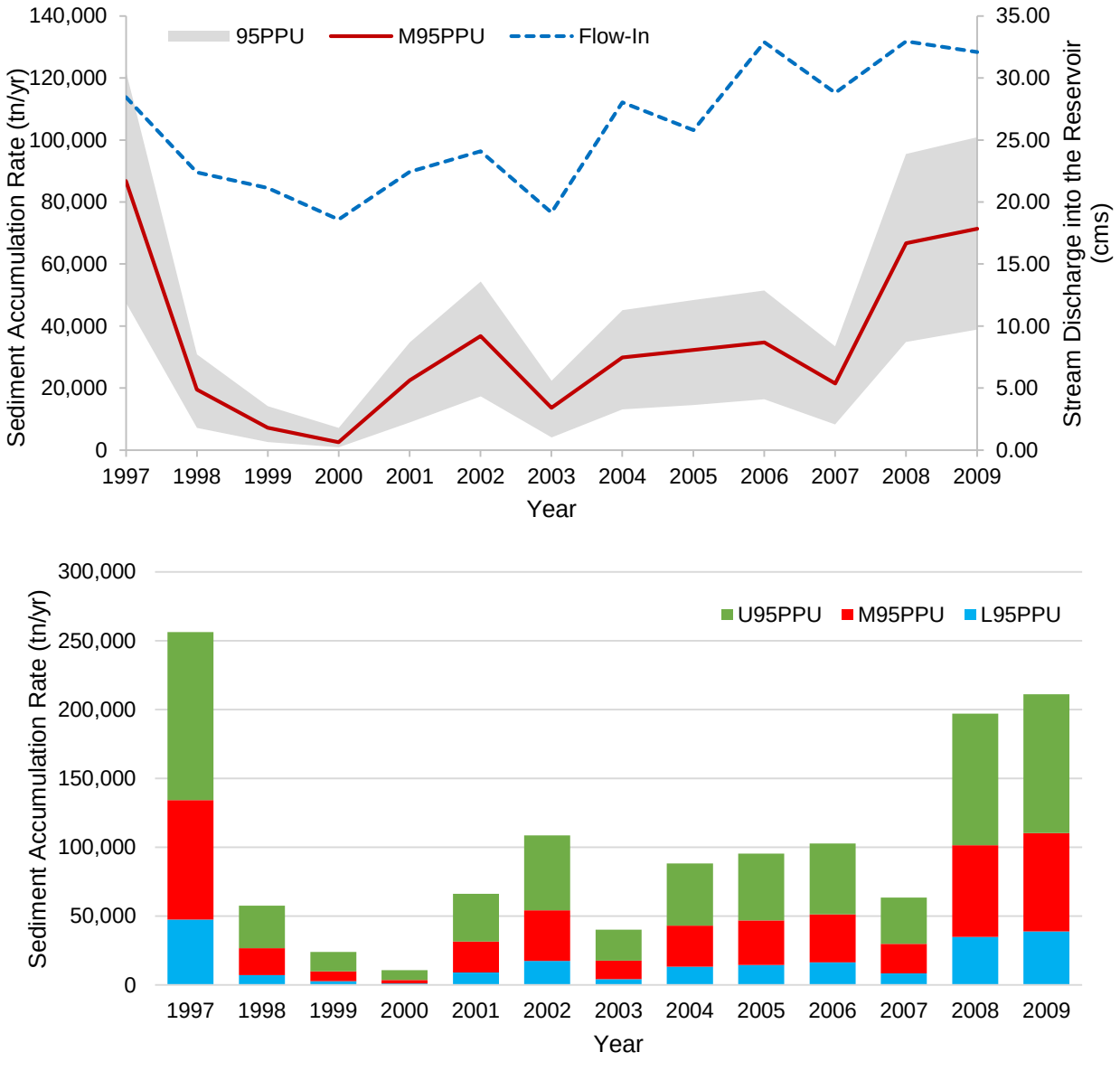

Figure 111- Sediment Accumulation Rate (tn/yr) within Mio Reservoir

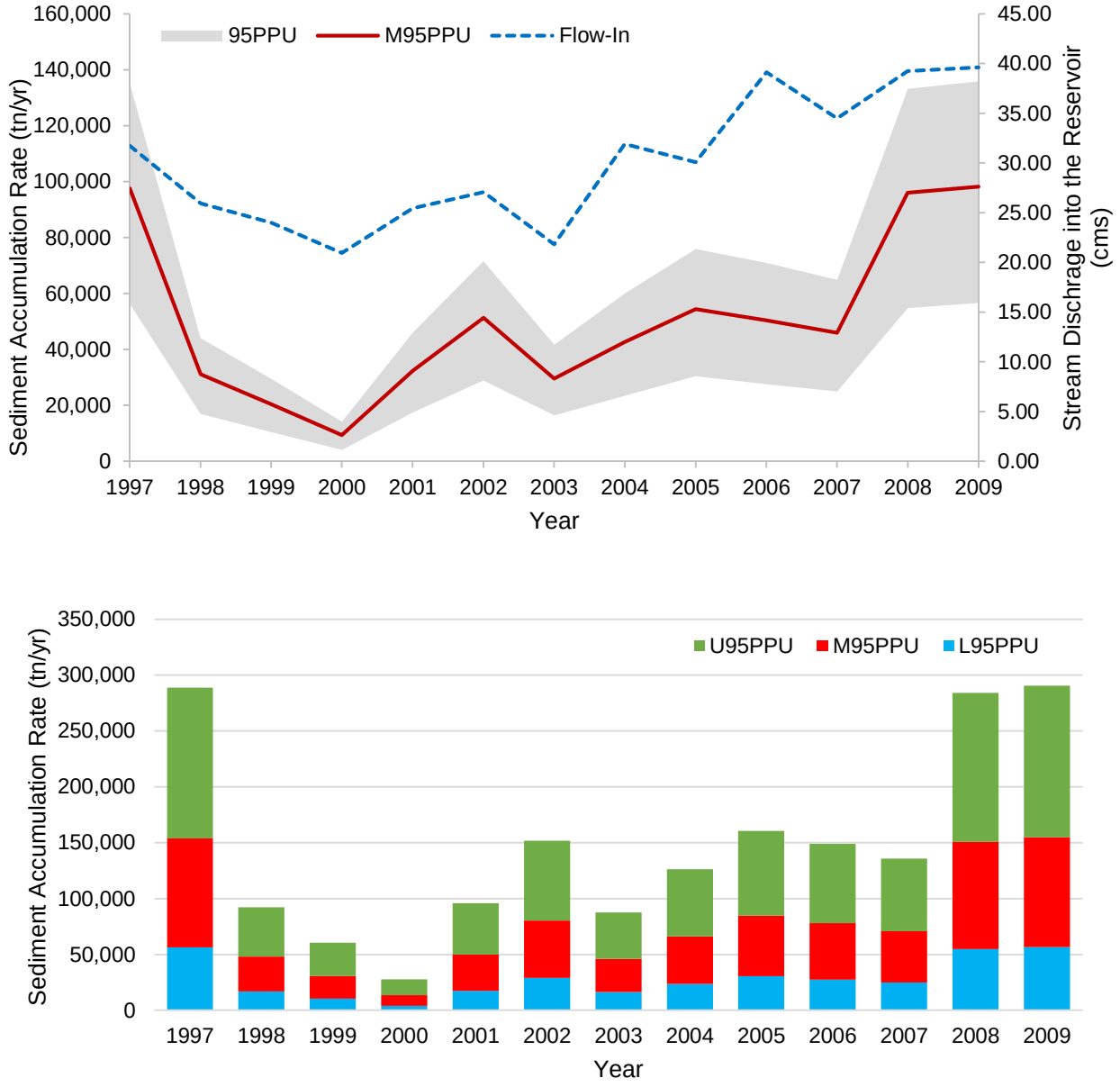

Figure 112- Sediment Accumulation Rate (tn/yr) within Alcona Reservoir

The normal capacity of Mio reservoir is about 12,000 ac. ft (15 Mm^3), and the recorded mean annual volume of inflow by Gage 04136500 is 26.59 (cms). So the sediment trapping efficiency for Mio Dam is 65%, using the Brune Curve approach. The normal storage of Alcona Dam is 25,000 ac. ft (31 m^3), and the recorded average of annual volume of inflow by Gage 04137005 is 32.74 (cms). Therefore, the sediment

trapping efficiency for Alcona Dam is 73%. The trapping efficiency within the Mio and Alcona reservoirs are listed in Table 69. As the results show the estimated sediment trapping efficiencies for Mio and Alcona by SWAT are pretty similar to the Brune Curve approach.

Table 69- Estimated Trapping Efficiency at Mio and Alcona reservoirs (SWAT)

Year	Mio			Alcona		
	L95PPU	M95PPU	U95PPU	L95PPU	M95PPU	U95PPU
1998	50%	65%	75%	58%	73%	81%
1999	50%	65%	75%	64%	78%	85%
2000	50%	65%	75%	64%	78%	85%
2001	58%	73%	81%	68%	80%	88%
2002	50%	65%	75%	64%	78%	85%
2003	50%	65%	75%	64%	78%	85%
2004	50%	65%	75%	64%	78%	85%
2005	58%	73%	81%	58%	73%	81%
2006	50%	65%	75%	58%	73%	81%
2007	58%	73%	81%	64%	78%	85%
2008	50%	65%	75%	58%	73%	81%
2009	64%	78%	85%	58%	73%	81%
2010	50%	65%	75%	58%	73%	81%
Average	53%	68%	77%	62%	76%	83%

5.2. Pre- European Settlement Scenario

5.2.1. Ballville Dam

The comparison of the pre- European results with post- European results for sediment delivery appear in Table 70. The following settlement has increased sediment yield by a factor of 8.5 at the watershed outlet (just downstream of the Ballville reservoir), and 9 at the dam location.

Table 70- Natural and Current Sediment Load at Ballville Dam Location

Scenarios	Sediment Load at Dam Location (tn/yr)	Sediment Load Just Downstream of Dam (tn/yr)	Number of Dams
Pre- European	33,153		0
Post- European	310,802	279,132	1

As explained in Chapter Two, there are two excessively large peaks in sediment yield in 1981 and 1990, which may skew the comparison between the pre- European and post- European scenario. Therefore, for comparing the natural sediment yield in this watershed the results of 1981 and 1990 were not included.

5.2.2. Webber Dam

Comparing the pre- European and post- European scenarios shows since pre-European settlement the sediment yield has increased by a factor of 11 at dam location, while just downstream of the Webber Dam sediment delivery increased by a factor of 9. The reason for this difference is sediment trapping within the dam, which reduces sediment delivery to the downstream reaches.

Table 71- Natural and Current Sediment Load at Webber Dam Location

Scenarios	Sediment Load at Dam Location (tn/yr)	Sediment Load Just Downstream of Dam (tn/yr)	Number of Dams
Pre- European	14,791	14,791	0
Post- European	168,748	129,619	10

5.2.3. Riley Dam

The comparison of the pre- European with post- European results for sediment delivery appear in Table 72. The following settlement, sediment has increased by a factor of 12 at the watershed outlet (just downstream of Riley reservoir), and increased by a factor of 29 just upstream of the Riley Dam.

Table 72- Natural and Current Sediment Load at Riley Dam Location

Scenarios	Sediment Load at Dam Location (tn/yr)	Sediment Load Just Downstream of Dam (tn/yr)	Number of Dams
Pre- European	634	634	0
Post- European	18,469	7,656	3

5.2.4. Upper Green Dam

The comparison of the pre- European with post- European results for sediment delivery appear in Table 73. The SWAT predicted sediment yield at Upper Green Dam location has increased by a factor of 4 since pre- European settlement. However, sediment yield increased by a factor of 52 at Upper Green reservoir location. The reason for such high difference is the trapping efficiency of Upper Green reservoir which is 98%.

Table 73- Natural and Current Sediment Load at Upper Green Dam Location

Scenarios	Sediment Load at Dam Location (tn/yr)	Sediment Load Just Downstream of Dam (tn/yr)	Number of Dams
Pre- European	398	398	0
Post- European	20,642	1,674	1

5.2.5. Goshen Pond Dam

The SWAT estimated that sediment delivery to the outlet of the watershed (just downstream of the dam) has increased by a factor of 2 since pre- European settlement, however, it increased by a factor of 3 at Goshen reservoir location (Table 74). In this specific watershed, although land use change can increase soil erosion, there are four more dams trapped some sediment loads and decreased the sediment delivery to the watershed outlet.

Table 74- Natural and Current Sediment Load at Goshen Pond Dam Location

Scenarios	Sediment Load at Dam Location (tn/yr)	Sediment Load Just Downstream of Dam (tn/yr)	Number of Dams
Pre- European	1,098	1,098	0
Post- European	4,134	1,975	5

5.2.6. Lake Rockwell Dam

The average of sediment yield at Lake Rockwell Dam location for the pre-European settlement scenario is about 5,500 (tn/year), while for the post- European scenario it is about 19,000 (tn/year). This simulation suggests that in the years following the 1800's, the sediment yield in the Rockwell Dam watershed has increased by a factor of 3.5 at the dam location; by a factor of 23 just upstream of the dam; and by a factor of 2 at the watershed outlet.

Table 75- Natural and Current Sediment Load at Lake Rockwell Dam Location

Scenarios	Sediment Load at Dam Location (tn/yr)	Sediment Load Just Downstream of Dam (tn/yr)	Sediment Load at Watershed outlet (tn/yr)	Number of Dams
Pre- European	5,556	5,556	92,168	0
Post- European	129,765	19,340	176,284	1

5.2.7. Ford Lake Dam

The SWAT model predicted that sediment yield has increased by a factor of 2 at Ford Lake Dam location since pre- European settlement. Although, in the years following the1800's some forest was replaced by the agricultural land use which increases sediment yield, but the sediment yield has decreased by half at the watershed outlet. Three dams with high trapping efficiency can be a reason of reduction in the sediment

yield since pre- European settlement. A considerable portion of the sediment load has been trapped behind these dams, so existing dams can result in sediment yield reduction although, more soil is eroding because of land use change.

Table 76- Natural and Current Sediment Load at Ford Dam Location

Scenarios	Sediment Load at Dam Location (tn/yr)	Sediment Load Just Downstream of Dam (tn/yr)	Number of Dams
Pre- European	90,700	90,700	0
Post- European	147,682	33,041	3

5.2.8. Potter's Falls Dam

The results of comparison between pre- and post- European scenarios show that the sediment yield has increased by 38 times at the watershed outlet (just downstream of the reservoir), and increased by a factor of 107 at dam location since pre- European settlement (Table 77). The high trapping efficiency of 64% within the Potter's Falls reservoir resulted in noticeable difference between the sediment yield at the watershed outlet (downstream of the dam), and upstream of the dam.

Table 77- Natural and Current Sediment Load at Potter's Falls Dam Location

Scenarios	Sediment Load at Dam Location (tn/yr)	Sediment Load Just Downstream of Dam (tn/yr)	Number of Dams
Pre- European	168	168	0
Post- European	17,883	6,546	1

5.2.9. Brown Bridge Dam

The SWAT simulation (Table 78) suggests that in the years following the 1800's, the sediment yield in Brown Bridge Dam watershed has increased by a factor of 2 at the watershed outlet (just downstream of the dam); by a factor of 10 at the dam location.

Table 78- Natural and Current Sediment Load at Brown Bridge Dam Location

Scenarios	Sediment Load at Dam Location (tn/yr)	Sediment Load Just Downstream of Dam (tn/yr)	Number of Dams
Pre- European	410	410	0
Post- European	3,989	626	1

5.2.10. Mio and Alcona Dams

The sediment yields in the pre-European scenario have been compared with the present-day scenario to estimate the total anthropogenic impacts within this study watershed. The results of running SWAT shows the sediment yield at the watershed outlet increased by a factor of 3 since pre- European settlement (Table 79).

Table 79- Natural and Current Sediment Load at Mio& Alcona Dams Location

Scenarios	Sediment Load at watershed outlet (tn/yr)	Number of Dams
Pre- European	6,369	0
Post- European	17,390	7

5.3. Un- Impoundment Scenario

For evaluating the effect of dam construction on the sediment yield, all existing reservoirs were removed, and the models were rerun. In some of the study reservoirs including Ballville, Upper Green, Lake Rockwell, Potter's Falls, and Brown Bridge, only

one reservoir has been modeled, and the reservoir located at the outlet of the watershed. With removing the reservoir from these models, sediment yield at the watershed outlet will increase as the same magnitude as accumulated sediment load within the reservoir. In this section of this dissertation, the results of running SWAT models for those reservoirs which have more than one reservoirs are described.

5.3.1. Webber Dam

Ten reservoirs (Figure 113) have been described in Webber Dam model, in the Removing Impoundment Scenario, all ten reservoirs were removed to evaluate how much sediment load delivers into the downstream reach within the un impoundment watershed.

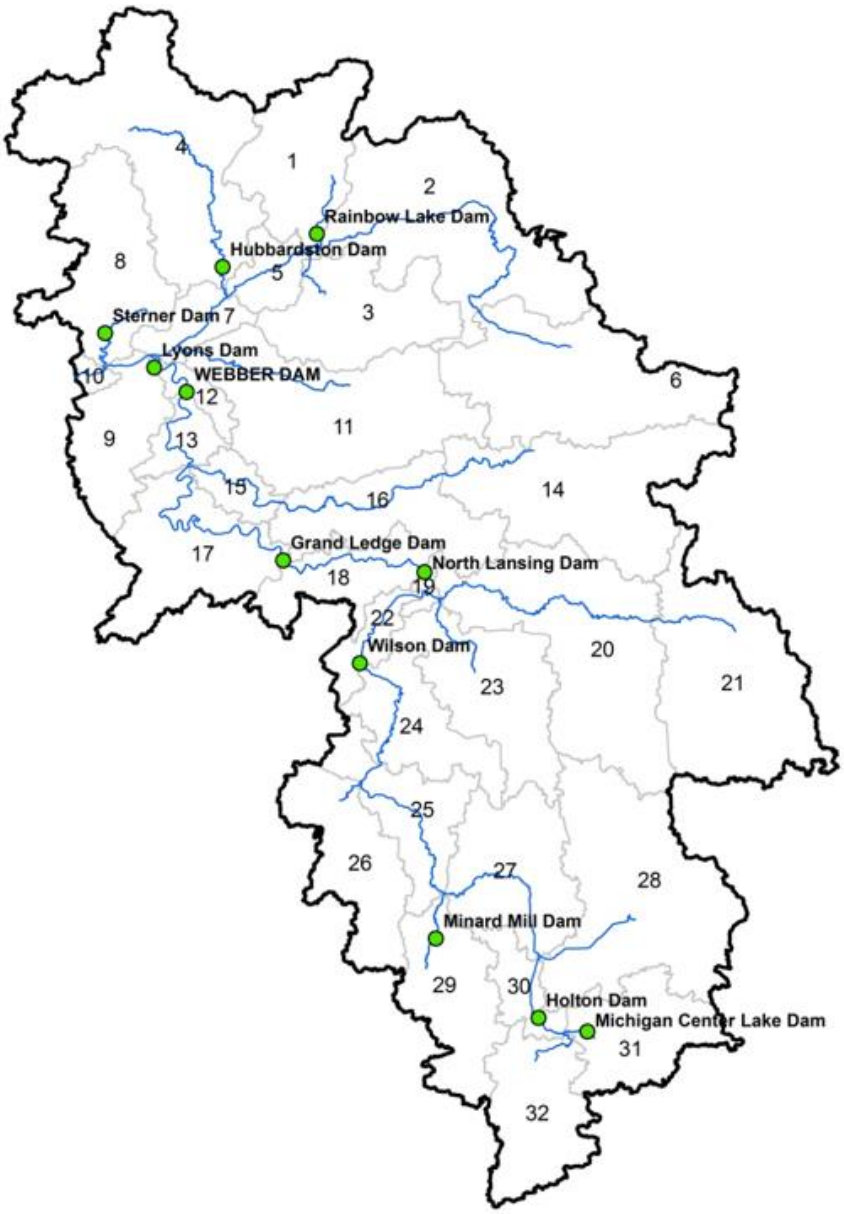

Figure 113- Dams Location Included in Webber Dam SWAT Model

The amount of sediment yields at Webber Dam watershed outlet for Baseline, and No Impoundment scenarios are presented in Table 80. The average of sediment yield leaving the watershed outlet is 385,325 (tn/yr) for baseline scenario, and 798,392 (tn/yr) for un-impoundment scenario. Therefore, with removing the reservoirs from Webber Dam model the sediment yield increases by a factor of two.

Table 80- Comparing Baseline, and Un- Impoundments Scenarios for Webber Dam Watershed

Year	Baseline			Un- Impoundment		
	SED_OUT_10 (tn/yr)			SED_OUT_10 (tn/yr)		
	L95PPU	M95PPU	U95PPU	L95PPU	M95PPU	U95PPU
1990	228,223	388,273	566,154	513,065	870,416	1,274,997
1991	209,350	358,121	505,811	381,096	651,856	965,679
1992	164,462	276,704	412,859	324,061	554,030	819,728
1993	283,675	472,575	676,498	533,003	903,873	1,326,251
1994	419,587	698,725	999,474	774,022	1,302,216	1,904,424
1995	160,504	285,654	385,075	321,085	546,994	802,405
1996	176,148	294,193	412,998	372,291	635,800	934,318
1997	202,359	369,057	564,914	414,791	703,233	1,030,876
1998	177,726	304,431	444,293	365,438	622,447	915,237
1999	193,397	338,474	482,737	437,595	754,278	1,121,613
2000	263,967	458,277	646,919	545,955	933,375	1,381,191
2001	310,867	544,993	781,987	611,877	1,057,311	1,574,994
2002	148,450	257,826	361,955	329,243	568,481	847,681
2003	101,656	176,335	278,578	216,894	370,803	548,849
2004	236,030	410,694	568,470	491,914	838,808	1,232,626
2005	221,766	380,618	545,324	465,762	793,674	1,171,489
2006	280,663	479,213	677,933	614,769	1,057,319	1,572,061
2007	166,608	285,905	407,519	352,279	610,175	910,133
2008	296,025	504,113	726,413	705,776	1,204,025	1,777,190
2009	247,552	422,327	592,837	577,787	988,726	1,458,324
Min	101,656	176,335	278,578	216,894	370,803	548,849
Ave	224,451	**385,325**	551,937	467,435	**798,392**	1,178,503
Max	419,587	698,725	999,474	774,022	1,302,216	1,904,424

The reason of increased sediment yield in un-impoundment scenario, is the sediment trapping efficiency within the reservoirs. Table 81 shows the volume, and inflow rate of each reservoir in the Webber Dam model, and the last column represents the sediment trapping efficiency of each reservoir.

Table 81- Sediment Trapping Efficiency within the Reservoirs in Webber Dam Model

Reservoir Number	Reservoir Name	Subbasin Number	Volume	Inflow	Retention Time	TE (Brune Curve)
			10^4 m^3	cms	yr	
1	Rainbow Lake	1	666	2.31	0.091	89%
2	Hubbardston	4	52	5.34	0.003	15%
3	Sterner	8	11`	2.60	0.001	0%
4	Minard Mill	29	21	1.27	0.005	30%
5	Michigan Center	31	987	2.10	0.149	93%
6	Holton	30	123	4.35	0.009	46%
7	Wilson	24	23	19.02	0.000	0%
8	North Lansing	19	223	29.38	0.002	15%
9	Grand Ledge	18	148	30.65	0.002	15%
10	Webber	13	740	39.56	0.004	28%
11	Lyons	12	225	39.97	0.002	15%

5.3.2. Riley Dam

Three reservoirs for the Riley Dam watershed as displayed in Figure 114 are modeled. For evaluating the effect of the impoundments on the sediment delivery to the downstream reaches, all three reservoirs were removed from the model.

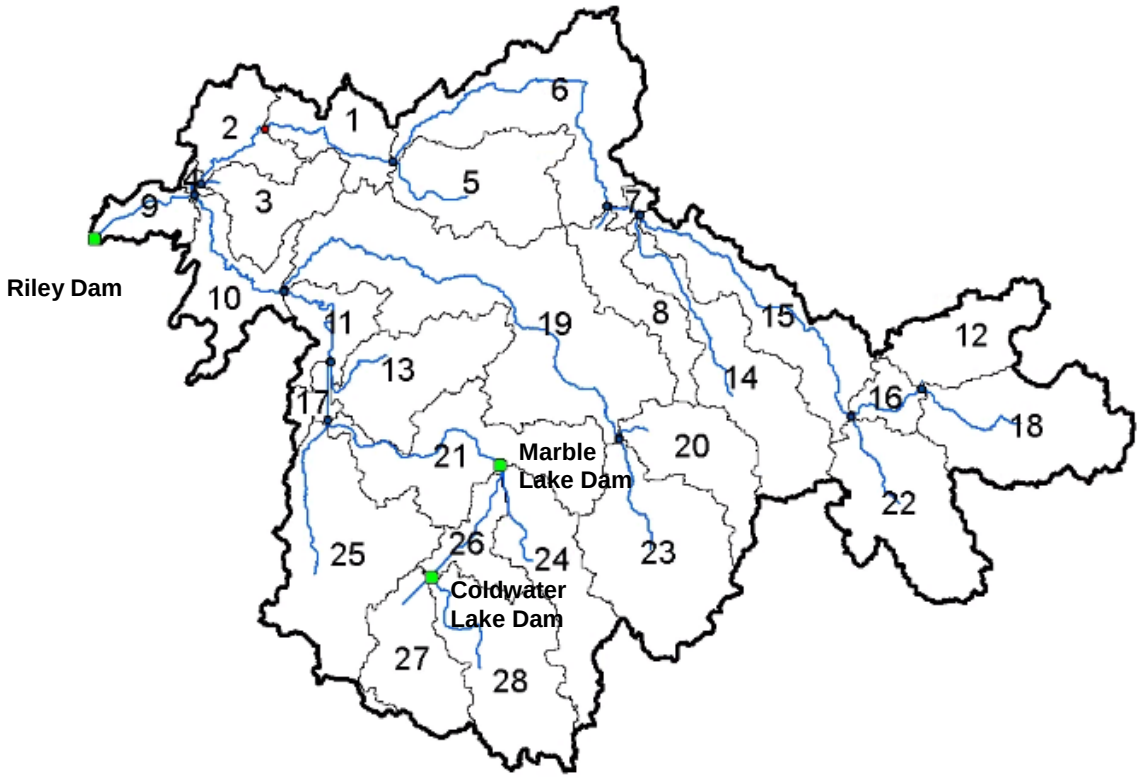

Figure 114- Dams Location Included in Riley Dam SWAT Model

Table 82 displays the sediment loads at Riley Dam watershed outlet for baseline, and un-impoundment scenarios. With removing dams from the model, the sediment load increases by a factor of two at the watershed outlet.

Table 82- Comparing Baseline, and Un-Impoundments Scenario for Riley Dam Watershed

Year	Baseline			Un- Impoundment		
	SED_OUT_3 (tn/yr)			SED_OUT_9 (tn/yr)		
	L95PPU	M95PPU	U95PPU	L95PPU	M95PPU	U95PPU
1991	2,195	2,332	2,455	4,481	7,729	11,234
1992	3,339	3,433	3,529	4,603	7,917	11,459
1993	5,349	5,854	6,369	8,953	15,093	21,615
1994	1,928	1,979	2,033	4,075	6,972	10,101
1995	2,906	3,201	3,541	6,839	11,646	16,805
1996	3,237	3,368	3,511	5,086	8,754	12,770
1997	5,187	6,108	7,114	11,806	20,351	29,813
1998	4,385	4,524	4,668	5,444	9,192	13,189
1999	13,159	20,075	28,411	24,425	41,509	59,754
2000	3,857	4,115	4,406	10,279	17,548	25,531
2001	18,329	27,331	37,428	27,352	46,752	68,278
2002	2,424	2,549	2,686	4,995	8,508	12,334
2003	3,055	3,115	3,172	4,046	6,944	10,084
2004	3,960	4,026	4,087	3,181	5,402	7,728
2005	5,452	7,353	9,585	13,843	23,261	33,336
2006	4,273	4,413	4,571	4,547	8,002	11,759
2007	5,026	5,864	6,738	9,282	16,108	23,753
2008	20,628	31,451	43,012	43,448	74,282	108,104
2009	5,833	7,070	8,358	11,853	20,821	30,675
2010	4,428	4,946	5,499	8,348	14,343	20,871
Min	1,928	1,979	2,033	3,181	5,402	7,728
Ave	5,947	**7,655**	9,559	10,844	**18,557**	26,960
Max	20,628	31,451	43,012	43,448	74,282	108,104

The sediment trapping efficiency for each reservoir with applying the Brune Curve are given in Table 83.The reservoirs volume, and their inflow rates are taken from hydrology calibrated SWAT model.

Table 83- Sediment Trapping Efficiency within the Reservoirs for Riley Dam Watershed

Reservoir Number	Reservoir Name	Subbasin Number	Volume	Inflow	Retention	TE (Brune Curve)
			10^4 m^3	cms	yr	
1	Coldwater Lake	27	395	0.51	0.25	91%
2	Marble Lake	26	240	1.73	0.04	78%
3	Riley	9	700	15.08	0.01	53%

5.3.3. Goshen Pond Dam

Five Dams have been modeled in Goshen Pond model, location of each dam is given in Figure 115. For evaluating the sediment yield in the un-impoundment watershed, all five dams were removed from the model, and the SWAT model was rerun.

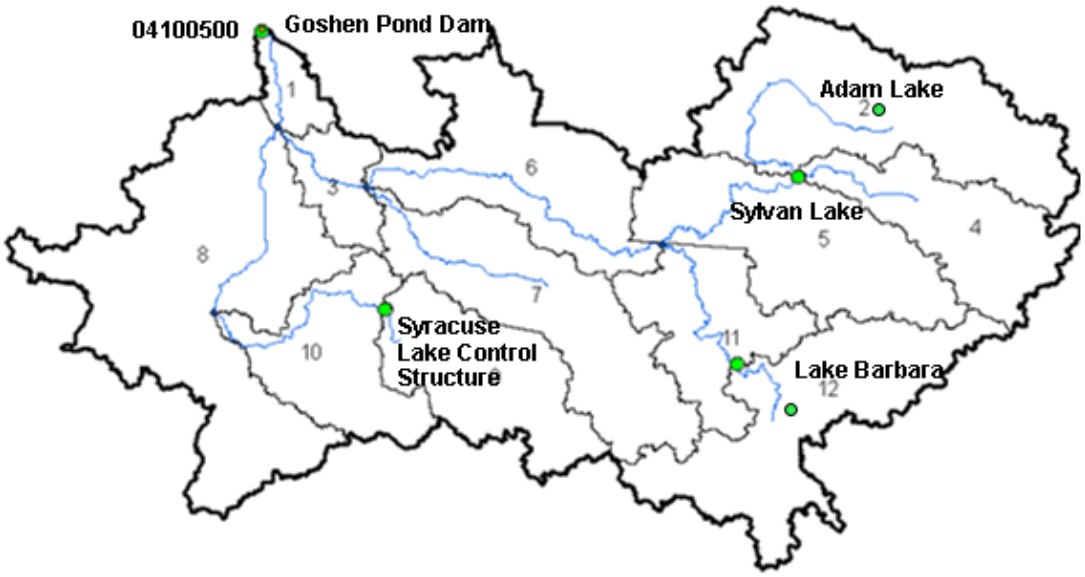

Figure 115- Dams Location Included in Goshen Pond SWAT Model

Table 84 shows the sediment yield at Goshen Pond watershed outlet for two scenarios; baseline scenario (post- European scenario), and un-impoundment scenario. The average of sediment yield at the watershed outlet is 1,796 (tn/yr) for baseline scenario, and 4,498 (tn/yr) for un-impoundment scenario. Therefore, constructing dams within this watershed results in increasing sediment yield by a factor of two.

Table 84- Comparing Baseline, and Un-Impoundments Scenario for Goshen Pond Dam Watershed

Year	Baseline			Un- Impoundment		
	SED_OUT_5 (tn/yr)			SED_OUT_1 (tn/yr)		
	L95PPU	M95PPU	U95PPU	L95PPU	M95PPU	U95PPU
1980	725	780	834	1,150	1,898	2,662
1981	1,924	2,617	3,308	4,099	6,853	9,759
1982	4,362	6,993	9,710	4,933	8,171	11,667
1983	534	588	645	707	1,223	1,756
1984	786	899	1,019	1,683	2,872	4,125
1985	2,729	4,116	5,561	4,722	7,913	11,398
1986	784	887	987	1,439	2,384	3,341
1987	501	521	540	790	1,319	1,863
1988	969	1,193	1,422	2,195	3,751	5,382
1989	731	892	1,056	1,529	2,595	3,748
1990	1,868	2,498	3,137	3,747	6,206	8,775
1991	1,239	1,619	1,999	2,238	3,717	5,209
1992	639	682	725	1,039	1,727	2,410
1993	2,754	4,022	5,288	5,061	8,382	11,706
1994	401	440	482	968	1,595	2,255
1995	747	871	999	1,955	3,271	4,685
1996	1,098	1,430	1,772	2,597	4,371	6,269
1997	1,495	2,042	2,618	3,645	6,051	8,649
1998	741	841	941	1,179	1,965	2,754
1999	1,136	1,598	2,109	2,889	5,003	7,336
2000	462	489	515	856	1,435	2,037
2001	2,361	3,430	4,533	5,063	8,379	11,883
2002	676	824	980	1,608	2,729	3,941
2003	734	852	972	1,507	2,525	3,597
2004	1,010	1,259	1,504	1,950	3,207	4,499
2005	1,714	2,524	3,360	3,701	6,147	8,778
2006	1,295	1,584	1,870	2,628	4,392	6,180
2007	2,160	3,098	4,009	3,761	6,313	8,909
2008	5,429	8,462	11,492	8,253	13,873	20,062
2009	1,869	2,484	3,118	4,333	7,152	10,117
2010	639	708	775	1,193	2,030	2,872
Min	401	440	482	707	1,223	1,756
Ave	1,436	**1,976**	2,525	2,691	**4,498**	6,407
Max	5,429	8,462	11,492	8,253	13,873	20,062

Table 85 presents the sediment trapping efficiency of each reservoir in the Goshen Pond watershed.

Table 85- Sediment Trapping Efficiency within the Reservoirs for the Goshen Pond Watershed

Reservoir Number	Reservoir Name	Subbasin Number	Volume	Inflow	Retention	TE (Brune Curve)
			10^4 m^3	cms	yr	
1	Adam Lake	2	116	2.39	0.02	58%
2	Sylvan Lake	4	738	1.39	0.17	92%
3	Syracuse	9	217	1.34	0.05	80%
4	Lake Barbara	12	109	2.14	0.02	58%
5	Goshen Pond	1	382.4	19.28	0.01	50%

5.3.4. Ford Lake Dam

Three reservoirs were defined in the Ford Lake SWAT model, the location of each reservoir is given in Figure 116. For evaluating the effect of reservoir on the sediment yield the existing reservoirs were removed from the model, and the SWAT model was rerun.

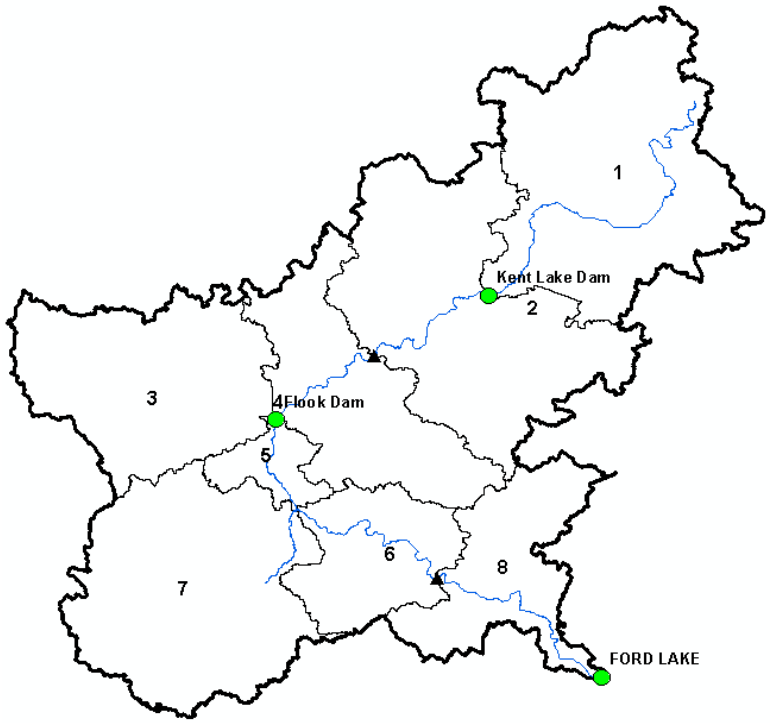

Figure 116- Dams Location Included in the SWAT Model of Ford Lake Dam

Table 86 displays the sediment yield at watershed outlet for two different scenarios; baseline and un-impoundment scenario. The average of sediment yield at watershed outlet is 33,041 (tn/yr) for baseline scenario, and increased to 271,226 (tn/yr) with removing the reservoirs from the model.

Table 86- Comparing Baseline, and Un-Impoundments Scenario for Ford Lake Dam Watershed

Year	Baseline			Un- Impoundment		
	SED_OUT_8 (tn/yr)			SED_OUT_8 (tn/yr)		
	L95PPU	M95PPU	U95PPU	L95PPU	M95PPU	U95PPU
1990	36,798	44,111	52,018	147,028	439,406	758,510
1991	20,559	21,617	22,737	48,168	155,851	258,748
1992	30,920	31,828	32,812	78,144	232,399	379,833
1993	30,283	31,811	33,530	71,709	209,506	359,357
1994	20,475	22,265	23,958	64,841	192,901	318,942
1995	26,873	28,955	31,032	83,460	246,441	406,160
1996	19,618	20,406	21,262	54,808	172,975	289,932
1997	27,693	31,401	35,052	80,501	237,849	388,814
1998	21,483	22,871	24,153	61,600	183,274	299,902
1999	20,387	22,805	24,905	78,696	242,149	385,071
2000	27,101	29,105	30,837	88,339	268,495	442,175
2001	44,891	49,327	54,114	156,817	417,092	715,288
2002	22,786	22,975	23,136	51,446	149,130	247,439
2003	15,888	16,174	16,500	49,736	166,207	275,882
2004	33,659	35,402	36,959	92,104	261,852	445,629
2005	28,835	31,414	34,564	91,480	257,675	426,576
2006	37,158	39,352	41,448	103,266	282,347	472,157
2007	37,037	39,426	41,766	114,011	304,842	500,611
2008	57,451	64,992	71,787	217,558	578,294	966,211
2009	50,275	54,586	58,542	162,107	425,829	711,397
Min	15,888	16,174	16,500	48,168	149,130	247,439
Ave	30,508	**33,041**	35,556	94,791	**271,226**	452,432
Max	57,451	64,992	71,787	217,558	578,294	966,211

Table 87 displays the sediment trapping efficiency of each reservoir within the Ford Lake watershed. The sediment trapping rate of each reservoirs is higher than 58%.

Table 87- Sediment Trapping Efficiency within the Reservoirs for the Ford Dam Watershed

Reservoir Number	Reservoir Name	Subbasin Number	Volume	Inflow	Retention	TE (Brune Curve)
			10^4 m^3	cms	yr	
1	Kent Lake	1	1480	3.71	0.13	94%
2	Flook	4	740	12.28	0.02	58%
3	Ford Lake	8	2220	19.31	0.04	78%

5.3.5. Mio and Alcona Dams

Seven reservoirs within the Mio and Alcona model are defined. Figure 117 display the location of each reservoir within this watershed. For evaluating the sediment yield within un-impoundment watershed, all seven reservoirs were removed from the SWAT model.

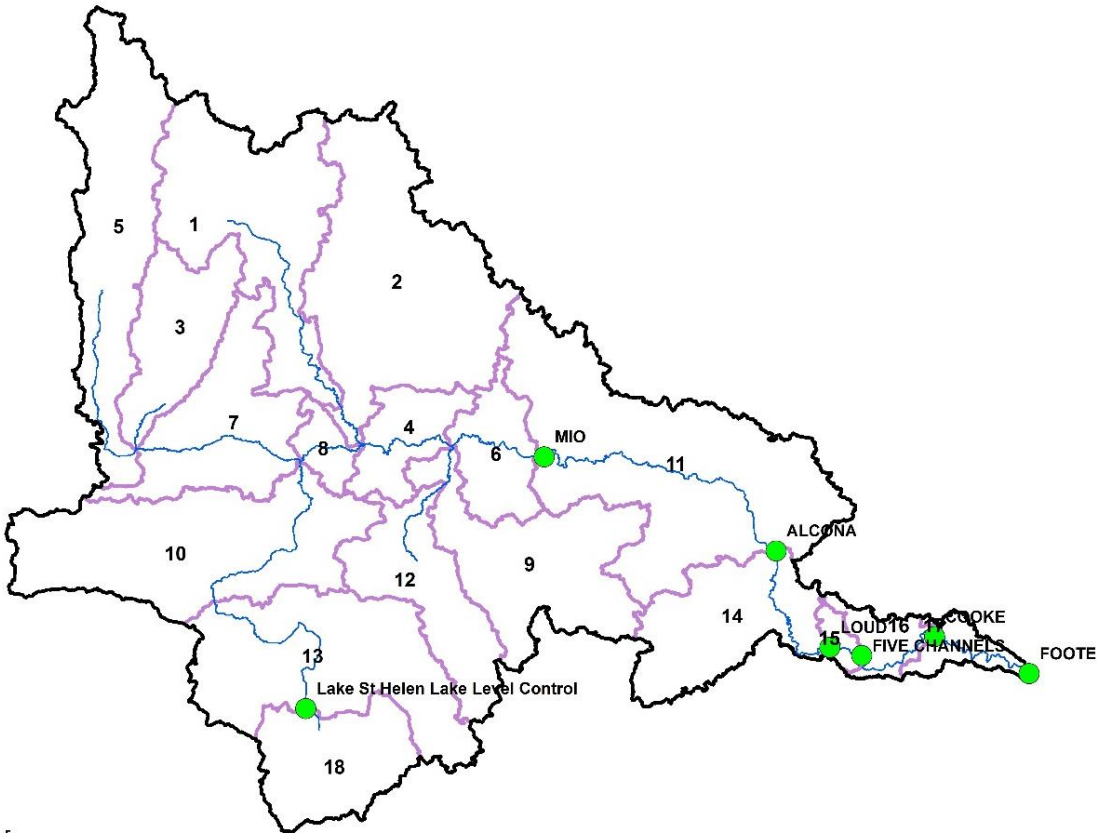

Figure 117- Dams Location Included in the Mio and Alcona SWAT Model

Table 88 displays the sediment yield at the Mio and Alcona watershed outlet for two scenarios; baseline scenario, and un- impoundment scenarios. The average of sediment yield leaving the watersheds is 15,776 (tn/yr), which increases to 94,807 (tn/yr) with removing dams from the models. On the words, the sediment yield increases by a factor of six, with removing dams.

Table 88- Comparing Baseline, and Un-Impoundments Scenario for Mio and Alcona Watershed

	Baseline			**Un- Impoundment**		
	SED_OUT_8 (tn/yr)			**SED_OUT_8 (tn/yr)**		
Year	**L95PPU**	**M95PPU**	**U95PPU**	**L95PPU**	**M95PPU**	**U95PPU**
1997	16,558	16,558	16,558	115,703	190,459	263,752
1998	14,897	14,897	14,897	37,528	61,673	85,234
1999	13,632	13,632	13,632	23,365	39,036	54,412
2000	11,953	11,953	11,953	14,912	24,788	34,476
2001	14,433	14,433	14,433	40,063	66,167	91,762
2002	15,278	15,279	15,280	60,442	99,030	136,692
2003	12,377	12,378	12,378	32,148	52,355	71,974
2004	16,990	16,991	16,991	50,798	83,817	116,120
2005	17,117	17,117	17,117	60,611	99,369	137,312
2006	19,025	19,025	19,025	58,270	96,569	134,128
2007	16,978	16,979	16,980	46,836	78,393	109,296
2008	17,246	17,248	17,248	99,664	166,206	231,395
2009	18,604	18,604	18,604	106,703	174,624	240,997
Min	11,953	11,953	11,953	14,912	24,788	34,476
Ave	15,711	**15,776**	15,712	52,612	**94,807**	120,316
Max	19,025	19,025	19,025	115,703	190,459	263,752

The sediment trapping efficiency of each reservoir is displayed in Table 89.

Table 89- Sediment Trapping Efficiency within the Reservoirs for Mio and Alcona Watershed

Reservoir Number	Reservoir Name	Subbasin Number	Volume	Inflow	Retention	TE (Brune Curve)
			10^4 m^3	cms	yr	
1	Lake St Helen	18	949.8	1.80	0.17	92%
2	Mio	6	1480.2	25.91	0.02	58%
3	Alcona	11	3083.7	30.11	0.032	72%
4	Loud	14	1554.2	31.77	0.02	58%
5	Five Channels	15	493.4	31.95	0.005	30%
6	Cooke	16	3700.4	32.36	0.036	15%
7	Foote	17	3700.4	32.75	0.036	15%

5.3.6. Discussion

The comparison results of two scenarios including un-impoundment and baseline scenarios are presented in Table 90. As expected, removing dams from those models with higher trapping efficiency, results in the higher sediment yield.

For those models that contain only one reservoir, the sediment accumulation rate within the reservoir is divided by the trapping efficiency to estimate sediment yield for un-impoundment scenario.

Table 90- Comparing the Sediment Yield Increases with Removing Dams for Study Reservoirs

Dams	Number of Dams	Weighted Average TE (%)	Sediment Yield ratio of Un-Impoundment/ Baseline Scenarios
Webber	10	20%	2
Riley	3	53%	2
Goshen	5	52%	2
Mio& Alcona	5	40%	6
Ford Lake	3	80%	8
Brown Bridge	1	20%	4
Upper Green	1	98%	50
Rockwell	1	83%	6
Potter's Falls	1	64%	3
Ballville	1	12%	1.2

5.4. Comparing different Methods for Estimating Sediment Accumulation Rate within the Study Reservoirs

The US Army Corps of Engineers (USACE) signed a contract with Civil Engineering Department, Wayne State University (Contract No. W911XK-14-C-2003) in 2010 To determine how the storage capacity of reservoirs in the Great Lakes Basin is changing over time. As a part of this project, both historic and new data were collected on the study reservoirs, which are the same with the study reservoirs of the present dissertation. Different methods were used to estimate the sediment yield including, USGS sediment gages, the application of trend lines, bathymetric subtraction, and radionuclide dating. Each method is explained in the following sentences briefly. In this section of this dissertation, the SWAT results are compared with the data collected as a part of Corp's project.

- **Sediment Gage Application 1**

  The average of suspended sediment load collected from the sediment gage located upstream of the reservoir, as well as sediment gage downstream of the reservoir, represent the sediment accumulation rate within the study watershed.

- **Sediment Gage Application 2**

  In this method, the sediment loading rate (tn/mi^2/yr) is estimated for each gage, and un- weighted average value is determined. This value is applied to the drainage area contributing to the impoundment, resulting in the loading rate (tn/yr) estimated for the impoundment.

- **Sediment Gage Application 3**

This approach is similar to (2) above, but a weighted average value is applied, resulting in a sediment loading rate for the watershed (tn/mi^2/yr). This value is applied to the drainage area contributing to the impoundment, resulting in the loading rate (tn/yr) estimated for the impoundment.

- **Sediment Gage Application 4**

Similar to (3) above, but the weighted average value is only applied to the un-gaged areas of the reservoir. The sediment load contributing from the other areas are calculated using the data reflected by the sediment gage. A summation is applied to incorporate all of these components.

- **Sediment Gage Application 5**

Similar to (1) above, but the interpolation makes use of the slope of the contributing watershed to the gages and the reservoir.

- **USACE Trend Line**

A regression equation has been developed by the United States Army Corps of Engineers Detroit District relating watershed drainage area with sediment yield in (tn/yr). This equation uses 13 data points from USACE 516(e) studies in the Great Lakes watersheds, and 48 Great Lake reservoirs from the Subcommittee on Reservoir Sedimentation database. Equation 19 shows the resulting equation as follows:

$$Y = 407.3A^{0.77}$$

Equation 19

Where,

Y= Sediment yield in (tn/yr)

A= Area of the watershed drainage area in (mi^2)

- **RESSED Trend Line**

RESSED is a database where sedimentation survey data is stored for selected reservoirs in the United States. Equation 20 shows the RESSED equation.

$$Y = 117.47A^{-0.269}$$

Equation 20

Where,

Y= Sediment yield in ($tn/yr/mi^2$)

A= Area of the watershed drainage area in (mi^2)

- **L-THIA**

The L-THIA model allows users estimate sediment loading at any point by clicking on the map on the L-THIA website. The annual sediment loading is calculated in (tn/yr). This is a very coarse estimation of sediment yield. Any dams or sediment sinks upstream are not considered in the calculations. The model was not able to compute a result for some of the study sites due to the size of the study site drainage area being too large.

- **Bathymetric**

Bathymetric subtraction is another approach which has been used for estimating the sediment accumulation rate within the study reservoirs. In this approach the post dam bathymetric map was subtracted from the historical map to estimate sediment accumulation rate for each study reservoir. Due to the lack of pre-dam construction bathymetric map availability, this method could not be applied to all reservoirs.

- **Dated Sediment**

A total of 112 sediment cores were taken from 11 of the study sites across the Great Lakes watershed, each having about 10-12 core samples. Each Core was analyzed for 137Cs and 210Pb to determine sedimentary records.

- **Sediment Core Length**

In this approach, it is assumed that the core samples ended at native soil. So each core sample represents the total number of sediment accumulate at each point since the dam was constructed. This alternative method was applied to every reservoir in this study, by assigning a contributing surface area and summing the results across the reservoir surface and dividing by the number of years since dam construction for each dam.

In this chapter of the dissertation, these methods are compared, and the best method which represents the reality condition are selected for the next steps of this research.

5.4.1. Lake Rockwell Dam

Table 91 presents the sediment accumulation rate estimates for Lake Rockwell using the methods of this research investigation.

Table 91- Sediment Accumulation Rate for Lake Rockwell

Method		Sediment Accumulation Rate (tn/yr)
Sediment Gage Application 1		19,000
Sediment Gage Application 2		30,000- 40,000
Sediment Gage Application 3		58,000- 60,000
Sediment Gage Application 4		18,000
Sediment Gage Application 5		21,000
USACE (R^2=0.78)		22,000- 25,000
RESSED (R^2=0.25)		5,000- 6,000
Bathymetric		18,000
Dated Sediment		7,000
Sediment Core Length		31,000
SWAT	Lower- 95 PPU	Min=11,000 Ave=25,000 Max=39,00
	Median - 95 PPU	Min=57,000 Ave=110,000 Max=167,000
	Upper- 95 PPU	Min=104,000 Ave=196,000 Max= 286,000

Based on the sediment gage methods, the sediment accumulation rate within Lake Rockwell varies between 14,000 and 60,000 (tn/yr). The large variation between the estimated accumulation rates for gage methods 1-5 is expected, given the range of assumptions used in the development of the five methods.

The estimated sediment accumulation rate for Lake Rockwell using the USACE trend line falls between 22,000 and 25,000 (tn/yr), while the RESSED trend line predicts a rate between 5,000 and 6,000 (tn/yr). The trend line methods provide a quick way to cross-check the results from the other methods. Drainage area is the only input parameter for use of the trend line methods. Therefore, it is expected that this approach would only provide rough guidance as to the sediment accumulation rate, as the empirical data that makes up the trend line includes reservoirs in many different settings with variable land use, weather data, soil structure, and topography.

The predicted sediment accumulation rate using radionuclide dating is 7,000 (tn/yr). An important consideration when applying this method is the number of times that the reservoir was drawdown or emptied. Drawdown impacts compaction and consolidation, an important factor in the inference of sediment accumulation rates on length basis from mass rate predictions. In the present application, drawdown fluctuations were not considered.

The bathymetric subtraction method was also used for estimating the sediment accumulation rates for Rockwell Lake. The method made use of historical bathymetry from 1911 and a much more recent bathymetric map created by the project team in the summer of 2011. The bathymetric subtraction resulted in an estimated sediment accumulation rate of 18,000 (tn/yr) for Rockwell Lake. This simple method can be used to provide an accurate estimate of the total sediment accumulated over time if the two base bathymetric surveys are accurate and aligned. However, this method is unable to provide any insight into changes in accumulation rates over time.

An alternative method used in the present dissertation relies on modeling the watershed hydrology and coupling that with a sediment model. The present study adopted the SWAT software for this purpose. SWAT can provide a variety of data regarding sediment yield and water yield in the entire watershed, and also can estimate sediment accumulation rate for each year of the simulation. However, there are some important and somewhat limiting assumptions associated with the SWAT tool, which may produce unrealistic results in some cases. For instance, SWAT estimates the sediment accumulation load within the reservoir by applying the mass balance equation without considering the sediment load which has already been accumulated behind dams.

However, it is expected the sediment accumulation rate is likely to decrease as the accumulated sediment volumes increases in the reservoir. Current version of SWAT also does not allow user input of variable sizing of particles from overland to stream to reservoir. The actual D50 of incoming sediment particles probably changes from year to year with the incoming flow. The assumption of a constant D50 for a reservoir is not very realistic. The Rockwell model overestimates sediment accumulation during low flow years and underestimates sediment accumulation during higher-flow years. The SWAT model predicted that the median (M95 PPU) of sediment accumulation rate within the Rockwell reservoir varies between 57,000 (tn/yr) to 167,000 (tn/yr), with the average of 110,000 (tn/yr). The lower boundary of sediment accumulation rate (L95 PPU) varies between 11,000 (tn/yr) and 39,000 (tn/yr), with the average of 25,000 (tn/yr). Bathymetric and nuclear dating estimates are similar to the lower boundary of SWAT results. It appears the SWAT simulation results overestimated the sediment accumulation rate for Rockwell Dam, although the sediment calibration was of high quality. Note that the measured average annual sediment load at Gage 04202000 (16 mi upstream of the dam) is about 2,000 (t/yr), and at Gage 04206000 (16 mi downstream of the dam) is about 36,000 (t/yr). With these observed values, an average annual sediment accumulation rate of 110,000 (tn/yr) within the reservoir is unexpected. The SWAT model of Rockwell Dam was successfully calibrated and validated to the sediment load at Gage 04208000 (outlet of watershed). The average of annual sediment load at Gage 04208000 is about 316 (tn/mi^2/yr) or 223,000 (tn/yr), while the sediment load is 16 (tn/mi^2/yr) or 2,000 (tn/yr) at Gage 04202000, and 93 (tn/mi^2/yr) or 36,000 (tn/yr) at Gage 04206000. It seems that the average of annual sediment yields at the outlet of watershed, where the model was

calibrated, is higher than two other gage locations. A potential explanation for relatively higher sediment yield at the outlet (or at Gage 04208000 location) is the greater relief (increased steepness) of the watershed towards the outlet. In conclusion, this analysis suggests that for Rockwell reservoir, the bathymetric and radionuclide dating estimates are more reliable than the SWAT simulation.

5.4.2. Ballville Dam

Table 92 presents the sediment accumulation rate estimates for the Ballville Dam reservoir using the various methods of this investigation.

Table 92- Sediment Accumulation Rate for Ballville Dam

Method		Sediment Accumulation Rate (tn/yr)
Sediment Gage Application 1		294,000
Sediment Gage Application 2		196,000- 206,000
Sediment Gage Application 3		258,000- 264,000
Sediment Gage Application 4		275,000
Sediment Gage Application 5		N/ A
USACE (R^2=0.78)		99,000
RESSED (R^2=0.25)		22,000
Bathymetric		N/ A
Dated Sediment		N/ A
Sediment Core Length		N/ A
SWAT	Lower- 95 PPU	Min= 5,000 Ave=13,000 Max=48,000
	Median - 95 PPU	Min= 10,000 Ave=37,000 Max=92,000
	Upper - 95 PPU	Min= 15,000 Ave=74,000 Max=235,000

Sediment gage and trend line methods were discussed in the previous section (associated with Rockwell reservoir). The SWAT model was also used to estimate the sediment accumulation rate, with a resulting average accumulation rate of 37,000 (tn/yr). This corresponds to a sediment trapping efficiency of 12%, the trapping efficiency

estimated using the Brune Curve is 7%. The SWAT model of Ballville Dam was successfully calibrated to the observed monthly average of sediment at Gage 04198000, which is just upstream of the dam. Therefore, the SWAT model appears, on several levels, to provide a realistic estimate of sediment accumulation for Ballville Dam. The maximum sediment accumulation rate of 92,000 (tn/yr) predicted for the M95PPU may be attributed to significant floods that occurred in the years 1981, 1984 and 1990.

5.4.3. Webber Dam

Table 93 presents the sediment accumulation rate estimates for the Webber Dam reservoir using the various methods of this investigation.

Table 93- Sediment Accumulation Rates for Webber Dam

Method		Sediment Accumulation Rate (tn/yr)
Sediment Gage Application 1		N/ A
Sediment Gage Application 2		N/ A
Sediment Gage Application 3		N/ A
Sediment Gage Application 4		N/ A
Sediment Gage Application 5		N/ A
USACE (R^2=0.78)		128,000
RESSED (R^2=0.25)		28,000
Bathymetric		N/ A
Dated Sediment		18,000
Sediment Core Length		27,000
SWAT	Lower- 95 PPU	Min= 4,000 Ave=21,000 Max=49,000
	Median- 95 PPU	Min= 13,000 Ave=39,000 Max=84,000
	Upper- 95 PPU	Min= 14,000 Ave=56,000 Max=126,000

As mentioned earlier, there are no active sediment gages in this study watershed, and therefore none of the sediment gage methods were available for analysis. There was also no historical bathymetry to compare current mapping against. SWAT was used to

simulate sediment accumulation rates with the results as shown above. The results of the other methods, including radionuclide dating and sediment core length corresponded well with the SWAT estimates. The SWAT- estimated trapping efficiency for this reservoir is 23%, which corresponds well to the prediction from the Brune Curve (28%). Therefore, the SWAT model is accepted as a useful tool for estimating the sediment accumulation rate for the Webber Dam.

5.4.4. Riley Dam

Table 94 presents the sediment accumulation rate estimates for the Riley Dam reservoir using the various methods of this investigation.

Table 94- Sediment Accumulation Rate for Riley Dam

Method		Sediment Accumulation Rate (tn/yr)
Sediment Gage Application 1		N/ A
Sediment Gage Application 2		8,000-12,000
Sediment Gage Application 3		6,000
Sediment Gage Application 4		5,000
Sediment Gage Application 5		600
USACE (R^2=0.78)		28,000- 50,000
RESSED (R^2=0.25)		6,000- 11,000
L- THIA		6,000
Bathymetric		N/ A
Dated Sediment		4,000
Sediment Core Length		21,000
SWAT	Lower- 95 PPU	Min= 300 Ave=5,000 Max=23,000
	Medium- 95 PPU	Min= 2,000 Ave=11,000 Max=43,000
	Upper- 95 PPU	Min= 5,000 Ave=17,000 Max=65,000

The predicted sediment accumulation rate based on the various sediment gage approaches ranges between 600 and 12,000 (tn/yr). It is important to note that these predictions are based on a very limited sediment gage record (1974-1977).

The trend line approaches (USACE, RESSED, and L- THIA) result in predicted sediment accumulation rates within the Riley Dam reservoir range between 6,000 and 50,000 (tn/yr), with the smaller estimates associated with the latter two approaches.

The two field methods (radionuclide dating and sediment core length) estimated the sediment accumulation rate, as 4,000 and 21,000 (tn/yr), respectively.

The SWAT model of Riley Dam predicted an average sediment accumulation rate which varies from the low estimate of 2,000 (tn/yr) to the maximum of 43,000 (tn/yr). Both these estimates have low probability of occurrence. The most likely average accumulation rate is estimated by SWAT to be 11,000 (tn/yr). The SWAT-estimated sediment trapping efficiency is 61%, while the Brune Curve suggests a value of 53%, well within a reasonable error bounds (deviation between the two approaches). The results of the radionuclide dating method and the sediment gage method were within the limits suggested by the SWAT simulations.

5.4.5. Upper Green Dam

Table 95 presents the sediment accumulation rate estimates for the Upper Green reservoir using the various methods of this investigation. Based on the sediment gage methodology, the sediment accumulation rate within Upper Green Dam is between 2,000 and 24,000 (tn/yr). Of the trend line methods, the USACE predicts the greatest rate, while L-THIA predicts the lowest accumulation rate. The range of values predicted by trend line approach is 600-14,000 (tn/yr). The bathymetric map and radionuclide dating approaches resulted in similar measured sediment accumulation rates, within the range of 36,000 to 89,000 (tn/yr).

Table 95- Sediment Accumulation Rate for Upper Green Dam

Method		Sediment Accumulation Rate (tn/yr)
Sediment Gage Application 1		N/ A
Sediment Gage Application 2		19,000- 24,000
Sediment Gage Application 3		4,000- 6,000
Sediment Gage Application 4		5,000- 6,000
Sediment Gage Application 5		2,000
USACE (R^2=0.78)		11,000- 14,000
RESSED (R^2=0.25)		2,000- 3,000
L- THIA		600
Bathymetric		89,000
Dated Sediment		35,000
Sediment Core Length		N/ A
SWAT	Lower- 95 PPU	Min= 5,000 Ave=11,000 Max= 21,000
	Medium- 95 PPU	Min= 9,000 Ave= 19,000 Max=38,000
	Upper- 95 PPU	Min= 14,000 Ave=29,000 Max=58,000

The SWAT-predicted average sediment trapping rate is calculated as between 9,000 and 38,000 (tn/yr), with a best estimate of 19,000 (tn/yr). The estimated sediment trapping efficiency for this reservoir is 93%, and 98%, using the SWAT analysis and Brune Curve approach, respectively. This similarity in values provides an additional level of confidence in the modeling results. Both the bathymetric and radionuclide dating approaches result in larger estimates of sediment accumulation than the SWAT simulation.

5.4.6. Goshen Dam

Table 96 displays the estimated sediment accumulation rate within the Goshen Pond using the various techniques of this investigation. The SWAT- predicted average sediment accumulation rate varies between 500 (tn/yr) and 6,000 (tn/yr), with the “best estimate” at 2,000 (tn/yr). The radionuclide method estimate is in-line with the SWAT

simulation, with a predicted accumulation rate of 4,000 (tn/yr). However, the trend line methods predicted a higher rate of sediment accumulation for this reservoir.

Table 96- Sediment Accumulation Rate for Goshen Pond

Method		Sediment Accumulation Rate (tn/yr)
Sediment Gage Application 1		N/ A
Sediment Gage Application 2		N/ A
Sediment Gage Application 3		N/ A
Sediment Gage Application 4		N/ A
Sediment Gage Application 5		N/ A
USACE (R^2=0.78)		36,000- 53,000
RESSED (R^2=0.25)		9,000- 12,000
L- THIA		N/ A
Bathymetric		N/ A
Dated Sediment		2,000
Sediment Core Length		5,000
SWAT	Lower- 95 PPU	Min= 100 Ave= 1,000 Max= 3,000
	Medium- 95 PPU	Min= 500 Ave= 2,000 Max= 6,000
	Upper- 95 PPU	Min= 913 Ave= 3,000 Max= 9,000

5.4.7. Ford Lake Dam

Table 97 displays the estimated sediment accumulation rate within Ford Lake reservoir using the various methods of this investigation.

Table 97- Sediment Accumulation Rate for Ford Lake Dam

Method		Sediment Accumulation Rate (tn/yr)
Sediment Gage Application 1		N/ A
Sediment Gage Application 2		N/ A
Sediment Gage Application 3		N/ A
Sediment Gage Application 4		N/ A
Sediment Gage Application 5		N/ A
USACE (R^2=0.78)		71,000
RESSED (R^2=0.25)		16,000
L- THIA		N/ A
Bathymetric		N/ A
Dated Sediment		13,000
Sediment Core Length		68,000
SWAT	Lower- 95 PPU	Min= 9,000 Ave=23,000 Max=52,000
	Medium- 95 PPU	Min= 62,000 Ave=115,000 Max=212,000
	Upper- 95 PPU	Min= 135,000 Ave=230,000 Max=406,000

The “best estimate” of SWAT-predicted average sediment accumulation rate is 115,000 (tn/yr). Radionuclide dating and sediment core length estimates are both less than this, with values of 36,000 (tn/yr), and 68,000 (tn/yr), respectively. However, these estimates are within the lower boundary of SWAT estimates, as shown in Table 9-8.

5.4.8. Potter’s Falls Dam

The estimated sediment accumulation rate within Potter’s Falls reservoir using the various techniques of this investigation is displayed in Table 98.

Table 98- Sediment Accumulation Rate for Potter's Falls Dam

Method		Sediment Accumulation Rate (tn/yr)
Sediment Gage Application 1		25,000
Sediment Gage Application 2		18,000- 19,000
Sediment Gage Application 3		18,000- 19,000 *
Sediment Gage Application 4		21,000
Sediment Gage Application 5		11,000
USACE (R^2=0.78)		7,000- 8,000
RESSED (R^2=0.25)		2,000
L- THIA		N/ A
Bathymetric		13,000
Dated Sediment		N/ A
Sediment Core Length		5,000
SWAT	Lower- 95 PPU	Min= 126 Ave=380 Max=840
	Medium- 95 PPU	Min= 8,000 Ave=11,000 Max=18,000
	Upper- 95 PPU	Min= 20,000 Ave= 28,000 Max=42,000

* It appears that SGA 2 and 3 yielded identical sediment accumulation estimates. However, this is simply an artifact of the reduction of significant digits.

The SWAT simulation "best-estimate" of median sediment accumulation rate within Potter's Falls reservoir includes the probabilistic band of 8,000 to 18,000 (tn/yr), with an average value of 11,000 (tn/yr). The bathymetric subtraction method applied to Potter's Falls reservoir results in an estimated sediment accumulation rate of 13,000 (tn/yr), which resides within the ranges of the SWAT "best estimate". The sediment gage also estimated sediment accumulation rates between 11,000 to 25,000 (tn/yr) which are within the SWAT-estimated ranges. As further support for the SWAT simulation results, both the Brune Curve and SWAT-predicted sediment trapping efficiency is 64% for this reservoir.

5.4.9. Brown Bridge Dam

Table 99 displays the estimated sediment accumulation rates for the Brown Bridge reservoir using the various techniques of this investigation.

Table 99- Sediment Accumulation Rate for Brown Bridge Dam

Methods		Sediment Accumulation Rate (tn/yr)
Sediment Gage Application 1		N/ A
Sediment Gage Application 2		N/ A
Sediment Gage Application 3		N/ A
Sediment Gage Application 4		N/ A
Sediment Gage Application 5		N/ A
USACE (R^2=0.78)		14,000- 20,000
RESSED (R^2=0.25)		3,000- 5,000
L- THIA		105
Bathymetric		N/ A
Dated Sediment		2,000
Sediment Core Length		7,000
SWAT	Lower- 95 PPU	Min= 100 Ave= 3,000 Max=6,000
	Median - 95 PPU	Min= 200 Ave= 3,000 Max= 8,000
	Upper- 95 PPU	Min= 300 Ave= 4,000 Max= 10,000

The “best-estimate” SWAT sediment trapping rate varies between 200 (tn/yr) to 8,000 (tn/yr), with an average value of 3,000 (tn/yr). The radionuclide dating and sediment core length methods resulted in estimated sediment accumulation rates of 2,000 (tn/yr), and 7,000 (tn/yr), respectively. This suggests relatively strong alignment with the SWAT-estimated values. The USACE trend line predicts the largest accumulation rates, beyond the bounds of the SWAT “best estimates”.

5.4.10. Mio and Alcona Dam

The predicted sediment accumulation rate within Mio Dam is provided in Table 100 for the various techniques adopted in this investigation. The SWAT “best estimate” of

sediment accumulation rate within this reservoir varies between 3,000 (tn/yr) and 87,000 (tn/yr), with an average value of 31,000 (tn/yr). The bathymetric subtraction and radionuclide dating approaches yielded sediment accumulation rates of 19,000 (tn/yr) and 20,000 (tn/yr), respectively. These estimates fall within the best-estimate SWAT boundaries. In further support of the SWAT simulation for this reservoir, both the SWAT and Brune Curve estimates of sediment trap efficiency resulted in a value of 66%.

Table 100- Sediment Accumulation Rate for Mio Dam

Method		Sediment Accumulation Rate (tn/yr)
Sediment Gage Application 1		N/ A
Sediment Gage Application 2		N/ A
Sediment Gage Application 3		N/ A
Sediment Gage Application 4		N/ A
Sediment Gage Application 5		N/ A
L- THIA		N/ A
USACE (R^2=0.78)		81,000-105,000
RESSED (R^2=0.25)		18,000-23,000
Bathymetric		19,000
Dated Sediment		20,000
Sediment Core Length		38,000
SWAT	Lower- 95 PPU	Min=1000 Ave=17,000 Max= 47,000
	Median - 95 PPU	Min= 3,000 Ave= 31,000 Max= 87,000
	Upper- 95 PPU	Min= 7,000 Ave= 51,000 Max= 122,000

The estimated sediment accumulation rate for the Alcona Dam reservoir is displayed in Table 101 for each of the methodologies adopted in this investigation. The “best estimate” result of using the SWAT model of Alcona Dam covers the range of 9,000 (tn/yr) to 98,000 (tn/yr), with an average value of 51,000 (tn/yr). The estimates from the radionuclide dating and sediment core length approaches are 11,000 (tn/yr) and 33,000 (tn/yr), respectively. These fall within the range of the best-estimate boundaries

suggested by the SWAT application. In further support of the applicability of SWAT simulation for the sediment accumulation at this site, it is noted that the sediment trap efficiency calculated by both the SWAT and Brune Curve approaches resulted in a value of 73%.

Table 101- Sediment Accumulation Rate for Alcona Dam

Method		Sediment Accumulation Rate (tn/yr)
Sediment Gage Application 1		N/ A
Sediment Gage Application 2		N/ A
Sediment Gage Application 3		N/ A
Sediment Gage Application 4		N/ A
Sediment Gage Application 5		N/ A
L- Thia		N/ A
USACE (R^2=0.78)		25,000- 119,000
RESSED (R^2=0.25)		6,000- 26,000
Bathymetric		N/ A
Dated Sediment		10,000
Sediment Core Length		33,000
SWAT	Lower- 95 PPU	Min= 4,000 Ave= 26,000 Max= 57,000
	Median- 95 PPU	Min= 9,000 Ave=51,000 Max=98,000
	Upper- 95 PPU	Min= 14,000 Ave= 71,000 Max= 136,000

5.5. Storage Capacity

With the knowledge of sediment accumulation rate within the reservoirs, the remaining storage capacity behind the study reservoirs can be estimated. The remaining storage capacity within the reservoir is quantified with regard to remaining volume and remaining time until the reservoirs are full. The result of the remaining storage capacity analysis is provided in this chapter of this dissertation.

As discussed in the previous chapters, the sediment accumulation rate within the study reservoirs is estimated by applying bathymetric, radionuclide dating, and modeling approaches. Section 5.5.1 describes the first two methods of estimating remaining storage capacity, while Section 5.5.25.5.1 describes the modeling approach.

5.5.1. Method One (Radionuclide Dating and Bathymetry)

To calculate accumulated sediment volume within the reservoir, Equation 21 was applied.

$$Vs = \frac{Q_s}{\rho_s . (1 - \varphi_s)} \times n$$

Equation 21

Where

V_s= Volume of accumulated sediment (m^3)

Q_s= Sediment accumulation rate (metric ton/yr)

ρ_s= Density of accumulated sediment particle (g/cm^3), (assumed to be 2.6 g/cm^3)

φ_s= Porosity of accumulated sediment

n= Reservoir age (yr)

The sediment accumulation rate used here is the average of sediment accumulation rate estimated by nuclear dating and bathymetric approaches. For those cases that only one of these methods (nuclear dating or bathymetric approaches) was available, the available estimate was applied.

The porosity of each sediment core was examined in the Geology Laboratory at Wayne State University. The average porosity of each sediment core in a specific reservoir is used as the porosity of that reservoir. Table 102 displays the volume and the percentage of accumulated sediment within the study reservoirs.

Table 102- Volume of Accumulated Sediment within the Reservoirs

Reservoir	NID Storage (m^3)	Accumulation Rate (t/yr)	Year Built	Age (yr)	Porosity (%)	Accumulated Sediment Volume (m^3)	Filled (%)
Ballville	2,962,819	NA	1911	105	NA	-	-
Webber	7,400,880	16,329	1907	109	0.74	2,672,227	36%
Riley	6,167,400	3,629	1923	93	0.84	794,570	13%
Upper Green	49,339,200	63,918	1869	147	0.71	12,384,402	25%
Goshen	3,823,788	2,722	1868	148	0.75	622,478	16%
Rockwell	22,511,010	11,794	1913	103	0.68	1,443,918	06%
Ford Lake	22,202,640	7,258	1932	84	0.56	534,659	02%
Potters Falls	1,591,189	11,689	1911	105	0.54	909,723	65%
Brown	3,453,744	1,814	1921	95	0.79	312,503	09%
Mio	14,801,760	10,680	1917	99	0.53	856,820	06%
Alcona	30,837,000	9,979	1924	92	0.76	1,489,969	05%

Table 103 displays the remaining dam capacity, and the time required to fill the study reservoirs. In developing this estimate, future sediment accumulation rate has been assumed the same with the current sediment accumulation rate in the reservoir.

Table 103- Remaining Reservoirs Capacity

Reservoir	NID Storage (m^3)	Remaining Capacity (m^3)	Time Required to Fill Reservoirs (yr)
Webber	7,400,880	4,728,653	193
Riley	6,167,400	5,372,830	629
Upper Green	49,339,200	36,954,798	439
Goshen Pond	3,823,788	3,201,310	761
Rockwell	22,511,010	21,067,092	1503
Ford Lake	22,202,640	21,667,981	3404
Potters Falls	1,591,189	564,683	58
Brown Bridge	3,453,744	3,141,241	955
Mio	14,801,760	13,944,940	1611
Alcona	30,837,000	29,347,031	1812

5.5.2. Method Two (SWAT Model)

An important element of this research is the use of SWAT to estimate remaining storage capacity of the reservoirs. Equation 22 was used to evaluate volume of accumulated sediment within the study reservoirs.

$$Vs = \frac{Q_s}{\gamma_s} \times n$$

Equation 22

Where

V_s= Volume of accumulated sediment (m^3)

Q_s= Sediment accumulation rate (metric ton/yr)

γ_s= Bulk density of accumulated sediment (g/cm^3)

n= Reservoir age (yr)

A SWAT model was developed for each study reservoir to estimate the sediment accumulation rate. Table 104 displays the sediment accumulation rate for each study reservoir estimated by SWAT. Within SWAT, the transported particle size is assumed to remain constant, and in all cases the grain size corresponds to silt sized (Neitsch, et al., 2011). In this project, it is assumed all study reservoir are continously submerge, and the initial bulk density for deposited silt assumed to be 1,120 (kg/m^3) (Morris et al., 2008). The sediment may compact, and consolidate for decades in a reservoir. Equation 23 estimates the sediment compaction over time (Lane and Koelzer, 1943):

$$W_t = W_1 + B \log t$$

Equation 23

W_t= Specific weight of deposited sediment at the age of t

W_1= Initial weight at the end of the first year of consolidation

B= Parameter value which is 91 (kg/m^3) for silt (Lane and Koelzer, 1943)

Table 104 provides the ultimate bulk density for each study reservoir, and accumulated sediment volume.

Table 104- Volume of Accumulated Sediment within the Reservoirs

Reservoir	NID Storage (m^3)	Accumulation Rate (t/yr)	Age (yr)	Ultimate Bulk Density (kg/m^3)	Accumulated Sediment Volume (m^3)	Filled (%)
Ballville	2,962,819	33,422	105	1,304	2,691,337	91%
Webber	7,400,880	35,498	109	1,305	2,964,061	40%
Riley	6,167,400	9,861	93	1,299	705,923	11%
Green	49,339,200	17,480	147	1,317	1,950,739	04%
Goshen	3,823,788	1,958	148	1,317	219,937	06%
Rockwell	22,511,010	100,214	103	1,303	7,920,737	35%
Ford Lake	22,202,640	104,022	84	1,295	6,746,833	30%
Potters	1,591,189	10,359	105	1,304	834,191	52%
Brown	3,453,744	3,051	95	1,300	222,971	06%
Mio	14,801,760	31,073	99	1,302	2,363,451	16%
Alcona	30,837,000	45,999	92	1,299	3,258,551	11%

91% of Ballville Dam reservoir is occupied by inflow sediment. Evans et al. in 2002 assessed the sediment accumulation rate in Ballville Dam reservoir; his bathymetry data showed that Ballville reservoir had lost 78% storage capacity due to sediment accumulation over the interval of 1911 to 1993. Therefore, based on Evan's estimation, the Ballville Dam reservoir should be full of sediment by 2016, which is consistent with the SWAT model results. Table 105 displays the remaining dam capacity, and the time required to fill the study reservoirs. The results suggest some reservoirs including Upper Green, Goshen Pond, and Brown Bridge have an extended life remaining to current accumulation rate in these calculations.

Table 105- Remaining Reservoirs Capacity

Reservoir	NID Storage (m^3)	Year Built	Age (yr)	Remaining Capacity (m^3)	Time Required to Fill Reservoirs (yr)
Ballville	2,962,819	1911	105	271,482	11
Webber	7,400,880	1907	109	4,436,819	163
Riley	6,167,400	1923	93	5,461,477	720
Upper Green	49,339,200	1869	147	47,388,461	3,571
Goshen Pond	3,823,788	1868	148	3,603,851	2,425
Rockwell	22,511,010	1913	103	14,590,273	190
Ford Lake	22,202,640	1932	84	15,455,807	192
Potters Falls	1,591,189	1911	105	756,998	95
Brown Bridge	3,453,744	1921	95	3,230,773	1,377
Mio	14,801,760	1917	99	12,438,309	521
Alcona	30,837,000	1924	92	27,578,449	779

5.5.3. Conclusion

As discussed in the previous section, with the knowledge of sediment accumulation rate, the remaining storage capacity of the reservoirs can be estimated. Table 106 shows the remaining time to fill each reservoir, and current fill percentage for each study reservoir based on methods one and two.

Table 106- Remaining Storage Capacity of each Study Reservoir based on Method 1 and 2

Reservoir	Percent of Occupied Storage		Time Required to Fill Reservoirs (yr)	
	Method 1	Method 2	Method 1	Method 2
Ballville	NA	91%	NA	11
Webber	36%	40%	193	163
Riley	13%	11%	629	720
Upper Green	25%	04%	439	3,571
Goshen Pond	16%	06%	761	2,425
Rockwell	06%	35%	1503	190
Ford Lake	02%	30%	3404	192
Potters Falls	65%	52%	58	95
Brown Bridge	09%	06%	955	1,377
Mio	06%	16%	1611	521
Alcona	05%	11%	1812	779

5.6. Developing Regression Model of Sediment Delivery

The simulation results of study watersheds have been applied to develop several statistical models for sediment delivery and accumulation prediction. There are many watersheds that do not have the gage data and for which there are no resources to model them. The developed regression models can help to predict the sediment delivery in these un-gaged watersheds. The regression analysis is discussed in this chapter.

5.6.1. Sediment Yield

A linear regression analysis has been done using the sediment yield output of the SWAT simulations. Sediment yield depends on many factors. In the present analysis, the following factors have been considered: percentage of agricultural area, soil erodibility factor, topographic relief, dam density and the drainage area of study watersheds. Table 107 displays the values of these factors for each of the study watersheds.

Table 107- Input Parameters for Analyzing Sediment Yield

Dam Name	Sediment Inflow (S)	Agricultural Area (AA)	Soil Erodibility Factor (K)	Relief (R)	Dam Density (D)	Drainage Area (A)
	t/yr	%		ft	dams/mi^2	mi^2
Potter's Falls	17,883	23	0.33	1,371	0.0085	46
Upper Green	20,642	62	0.18	325	0.0037	115
Brown Bridge	3,989	5	0.05	587	0.0025	151
Rockwell	21,929	18	0.38	843	0.0019	208
Riley	18,469	61	0.20	423	0.0022	523
Goshen Pond	4,134	70	0.28	302	0.0033	590
Ford Lake	147,682	25	0.20	554	0.0014	814
Mio	46,152	2	0.05	942	0.0004	1,100
Ballville	333,110	81	0.34	761	0.0003	1,254
Alcona	65,504	2	0.05	942	0.0005	1,469
Webber	168,748	60	0.23	614	0.0013	1,750
Independence*	2,064,498	78	0.31	715	0.0002	5,545

*This reservoir model has not been developed in this research, however for having enough data to complete regression analysis, the results of Independence SWAT model were used from Corps project (Contract No. W911XK-14-C-2003).

Table 108 displays the summary output of the regression analysis. In multiple regression, the *Multiple R* represents the coefficient of multiple correlation, and its square is the coefficient of determination. R-square (R^2) is a statistical measurement that represents how close the data are to the regression line. The R^2 is bounded by the range of zero to one. In general, a larger value of R^2 indicates the model fits the data very well, and smaller R^2 indicates little or no relationship between the dependent and independent variables. However, applying only the R^2 for evaluating the regression analysis, is insufficient, especially for multiple analysis. For multiple models, as independent variables are added to the model, the R^2 increases, even though the overall contribution of the added variable may be indeterminate. The *adjusted* R^2 is designed to address R^2 problem for multiple regression situations. The adjusted R^2 is a modified version of R^2 that has been adjusted for the number of variables in the model, and can be used if more than one independent variable exists. In the present analysis, the adjusted R^2 is adopted. Standard error represents the statistical accuracy of an estimate, and is equal to the standard deviation.

Table 108- Summary Output of Regression Statistic

Regression Statistics	Value
Multiple R	0.97
R Square	0.95
Adjusted R Square	0.91
Standard Error	178,643
Observations	12

In the present regression analysis, Multiple R, R^2, and Adjusted R^2 are more than 0.90, which suggests a strong correlation between the dependent and independent variables.

ANOVA stands for Analysis of Variance. The ANOVA is a statistical method used to test (compare) the differences between two or more variables. In other words, ANOVA

is useful for comparing variables for statistical significance. Table 109 displays the ANOVA factors.

Table 109- ANOVA Analysis

	df	SS	MS	F	Significance F
Regression	5	(SSR) 3.53×10^{12}	(MSR)7.06×10^{11}	22.14	0.0008 or 0.08%
Residual	6	(SSE) 1.91×10^{11}	(MSE)3.21×10^{10}		
Total	11	3.72×10^{12}			

Parameters in Table 109 are explained in the following bullet points.

5.6.1.1. Degree of Freedom (df)

Total df is the number of observation minus one. The *Regression df* is the number of independent variables in the model, which is 5 in this analysis. The *Residual df* is the difference between the total df and the regression df.

5.6.1.2. Sums of Squares (SS) and Mean Squares (MS)

These factors describe the variability in the dependent variable. Residual SS (SSE) represents sums of squared residuals. It is a measure of discrepancy between the actual data (in this case the estimated sediment yield by SWAT represents the actual value) and the estimation model. A small value of SSE indicates a tight fit of the model to the data. Sums of Squared Regression (SSR) is a factor that provides the sums of squared deviations.

$$\text{Residual SS (SSE)} = \sum_{i=1}^{n} (y_i - \hat{y}_i)^2$$

$$\text{Regression SS (SSR)} = \sum_{i=1}^{n} (\hat{y}_i - \bar{y})^2$$

$$\text{Total SS} = \text{Residual SS} + \text{Regression SS} = \sum_{i=1}^{n} (y_i - \bar{y})^2$$

Equation 24

$\bar{y}$=Mean value (mean of actual sediment yield)

y_i=Predicted value (estimated by SWAT)

$\hat{y}_i$=Predicted value (predicted sediment yield)

Mean Squares (MS) is calculated by dividing the sum of squared residuals by the degrees of freedom. For instance, the mean square of the residual is estimated by dividing the sum of squares of the residual error by the degrees of freedom. The mean square of the regression is calculated by dividing the sum of squared regression (RSS) by the degree of freedom.

5.6.1.3. F-stat

The F-stat is a statistical test which can assess the equality of variances. Equation 25 displays F- stat; this ratio evaluates how the means of two populations are significantly different from one another.

$$\mathrm{F-stat} = \frac{\text{Regression MS (MSR)}}{\text{Residual MS (MSE)}}$$

Equation 25

A larger F- stat suggests that the results (estimated sediment yield) did not happen by chance; in the other words, there is a relation between variables. For deciding if F ratio is significant, a critical F is defined in Equation 26. In this equation α=0.05 (0.05 is a common alpha level for tests). F distribution is a right -skewed distribution. Critical value depends on the number of observation data (the number of study reservoirs) and number of independent variables. In this study we assumed the percent of agricultural area, soil

erodibility factor, relief, dam density, and drainage area, as independent variables, therefore the number of independent variables is five.

$$\text{Critical F Value} = \text{F.INV.RT}(0.05, \text{K} - 1, \text{n} - \text{k}) = 4.39$$

Equation 26

In this equation, n represents the number of observation data, or the number of study dams which is 12. K represents the number of coefficients, or the number of independent variables, which is 5.

Because the critical F value of 4.39 is smaller than 22.14 (F ratio), we can conclude that there is a significant difference between the population means. In the other words, the probability of regression outputs is not random.

Table 110 displays the regression coefficients. Critical F value is only one measure of significance in an F- state, while other factors including T- state, and P- Value should be considered. T- stat and P- value are factors which indicate how random the regression is. In general, a small P- value (smaller than 0.05) indicates a strong probability that the outputs are not obtained by chance. However, an important feature of the present analysis is the very limited size of the observational data. This impacts the effect of an independent variable on the P-value.

Table 110- Regression Coefficient

	Coefficients	Standard Error	t- stat	P-value	Lower 95%	Upper 95%
Intercept	-203,212	216,259	-0.94	0.38	-732,378	325,955
AA	-2,682	3,571	-0.75	0.48	-11,420	6,056
K	888,713	707,038	1.26	0.26	-841,347	2,618,773
R	-292.55	295.41	-0.99	0.36	-1,015	430
D	43,976,144	32,054,905	1.37	0.22	-34,459,384	122,411,672
A	415.89	54.09	7.69	0.0003	283.54	548.24

Therefore, using the general threshold, such as 0.05 (α=0.05) for P- value, regardless of sample size, is not appropriate. The P- value associated with drainage area (A) is the least and equal to 0.0003. This means that the sediment yield is highly dependent on drainage area. Other parameters including AA, K, R, and D have a much larger P- value, greater than the 0.05 threshold. Because the sample size is very small, the large P- value does not help to check the regression model. In this work, because we do not have enough information (or sediment load data) it is not logical to conclude other independent variables such as AA, K, R, and D are not influential at estimating sediment load. Also because of lack of sediment data, doing non-linear regression may be impossible.

5.6.1.4. Comparing the Fitted Curve with the USACE Trend Line

As presented in Section 5.4, the USACE has developed a trend line based on a regression analysis which relates drainage area to sediment yield in the Great Lakes watershed. In order to mimic that approach with the present analysis, the regression of this investigation was reconsidered using only drainage area (A) as the independent variable (Table 111). The sediment yield value cannot be negative value, so in the Excel the intercept value set to zero value.

Table 111- Summary Output of Regression Statistic: Limiting the Analysis to Drainage Area

Regression Statistics	
Multiple R	0.95
R Square	0.91
Adjusted R Square	0.90
Standard Error	184,869
Observations	12

ANOVA

	df	SS	MS	F	Significance F
Regression	1	3.38×10^{12}	3.38×10^{12}	98.98	1.67×10^{-6}
Residual	10	3.42×10^{11}	3.42×10^{12}		
Total	11	3.72×10^{12}			

	Coefficients	Standard Error	t Stat	P-value	Lower 95%	Upper 95%
Intercept	-1.75×10^{5}	6.80×10^{4}	-2.57	0.05	-3.26×10^{5}	-2.36×10^{4}
A	369	37	9.95	1.67×10^{-6}	287	452

Figure 118 displays the relationship between sediment yield and drainage area. Both linear- and power-trend lines were applied to the data. The linear trend line with R^2 of 0.85 suggests a better fit than the power trend line, with R^2 of 0.55.

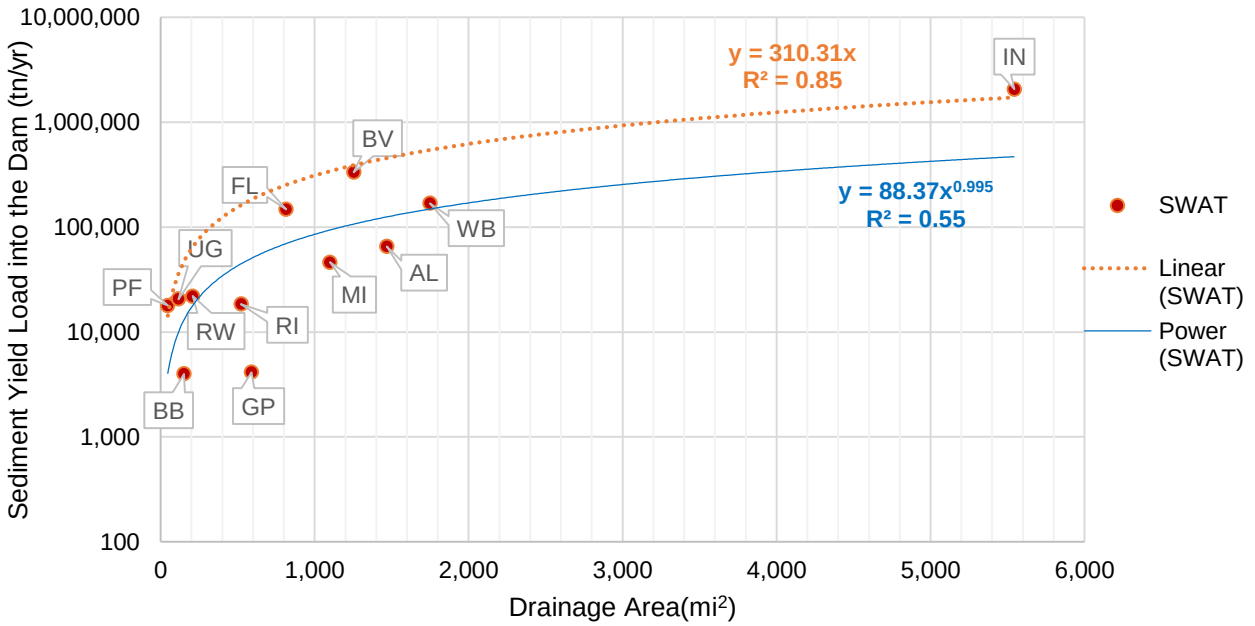

Figure 118- Sediment Yield in the Study Watersheds

The USACE 516 (e) studies trend line is compared against the trend line of the present analysis in Figure 119.

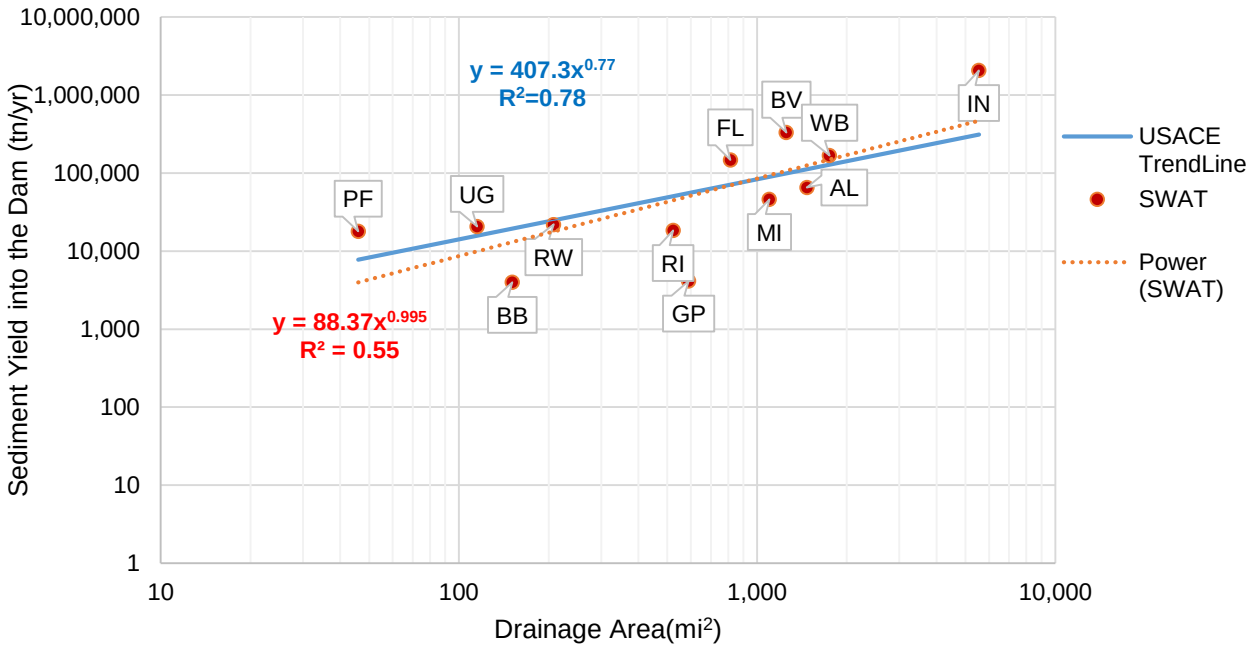

Figure 119- Sediment Load Inflow to the Dam versus Drainage Area

Table 112 provides a further comparison between these trend lines.

Table 112- Comparing the current trend line with USACE 516 (e) Studies

Dams		Drainage Area (mi^2)	Sediment Yield SWAT Regression (tn/yr)	Sediment Yield USACE (tn/yr)
Potters Falls	PF	46	17,883	7,767
Upper Green	UG	115	20,642	15,727
Brown Bridge	BB	151	3,989	19,397
Rockwell	RW	208	21,929	24,821
Riley	RI	523	18,469	50,485
Goshen Pond	GP	590	4,134	55,395
Ford Lake	FL	814	147,682	70,973
Mio	MI	1,100	46,152	89,493
Ballville	BV	1,254	333,110	98,993
Alcona	AL	1,469	65,504	111,820
Webber	WB	1,750	168,748	127,954
Independence	IN	5,545	2,064,498	310,970

While Figure 119 and the analysis of Table 10-6 include only drainage area as an independent variable, there are other factors that were further considered in the analysis including the percent agricultural land use, relief, dam density, and soil erodibility factor.

5.6.1.5. Developing Sediment Yield Curves with considering the effect of other Independent Variables

Brown Bridge, Potter Falls, Mio and Alcona dams are located within the forest-dominated watershed. In the forest-dominated watershed we expect less soil erosion in comparison to agriculture-dominated watersheds. For considering the effect of land use on the sediment yield, the study watersheds were classified in two groups including, forest-dominated and agriculture-dominated watersheds. Figure 120 shows the sediment yield curve for forest-dominated and agriculture-dominated watersheds. The R^2 of the graph in Figure 119 is 0.55, which increased to 0.62 for the agriculture-dominated group, and decreased to 0.47 for the forest group. Therefore, with separating the watershed study based on the land use, the trend line fitted better only for agriculture-dominated study watersheds. One of the reasons can be the number of observation data (study watersheds), which is only four in the forest group. The other reasons can be because of other influential factors, like soil erodibility factor (K), in the Potter's Falls watershed soil erodibility factor is 0.33 (tn.ac.hr/ac.ft.tn.in), while in Brown Bridge, Mio, and Alcona watersheds the soil erodibility factor is only 0.05 (tn.ac.hr/ac.ft.tn.in). Although Brown Bridge has larger drainage area, sediment yield in Potter's Falls watershed is higher than Brown Bridge, because of high soil erodibility factor in Potter's Falls. With removing Potter's Falls from forest group, the R^2 value increases to 1.

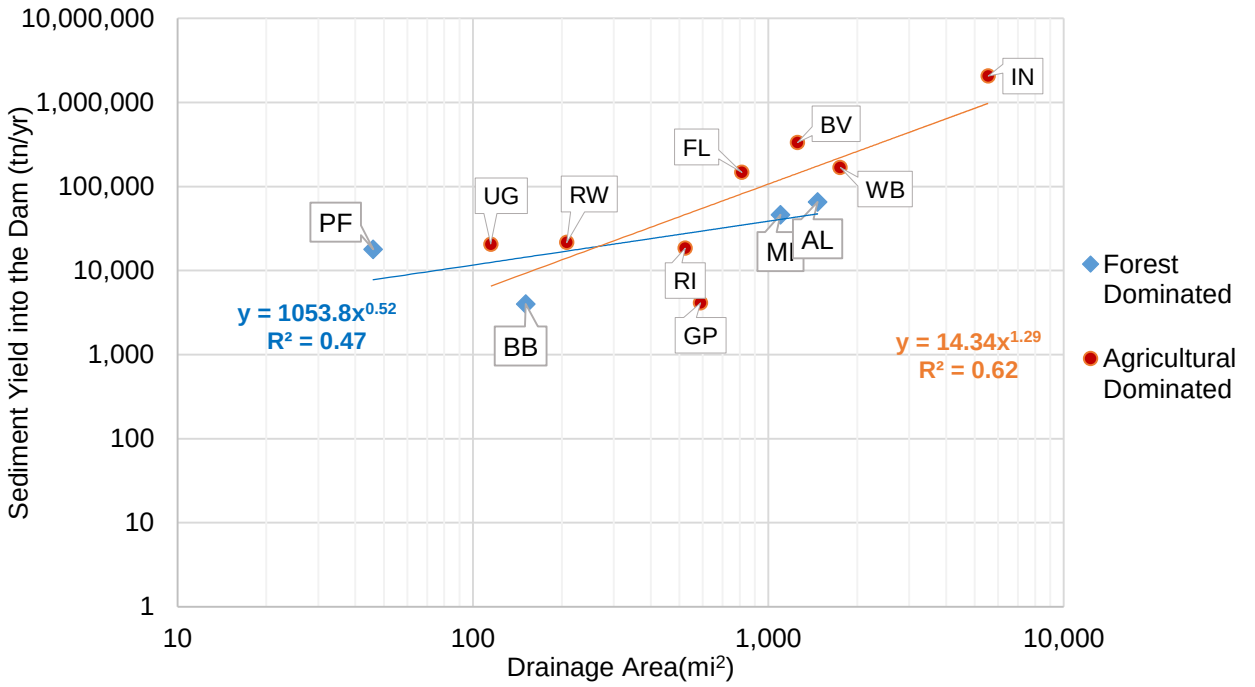

Figure 120- Sediment Load into the Dam versus Drainage Area with considering Land Use Effect

The observation data were also classified into two different groups based on their soil erodibility factor. Brown Bridge, Mio and Alcona, Upper Green, Riley, Ford Lake, and Webber dams with soil erodibility factor less than 0.25 are in one group. Goshen, Independence, Potter's Falls, Ballville, and Rockwell with soil erodibility higher than 0.25 are in another group. Figure 121 displays the sediment yield within the study watersheds with considering soil erodibility factor. The R^2 of the trend line for the reservoirs with K less than 0.25, is 0.64, and for the reservoirs, with k larger than 0.25 the R^2 is 0.55. As Figure 121 shows the sediment yield within the Goshen Pond watershed is far from the fitted trend line, with removing the Goshen Pond from the study watersheds, R^2 increases to 0.93. One potential reason for low sediment yield in the Goshen Pond watershed is the sediment trapping. There are five reservoirs within the Goshen Pond watershed, and their trapping efficiency is high enough to capture a considerable amount of sediment yield within this watershed.

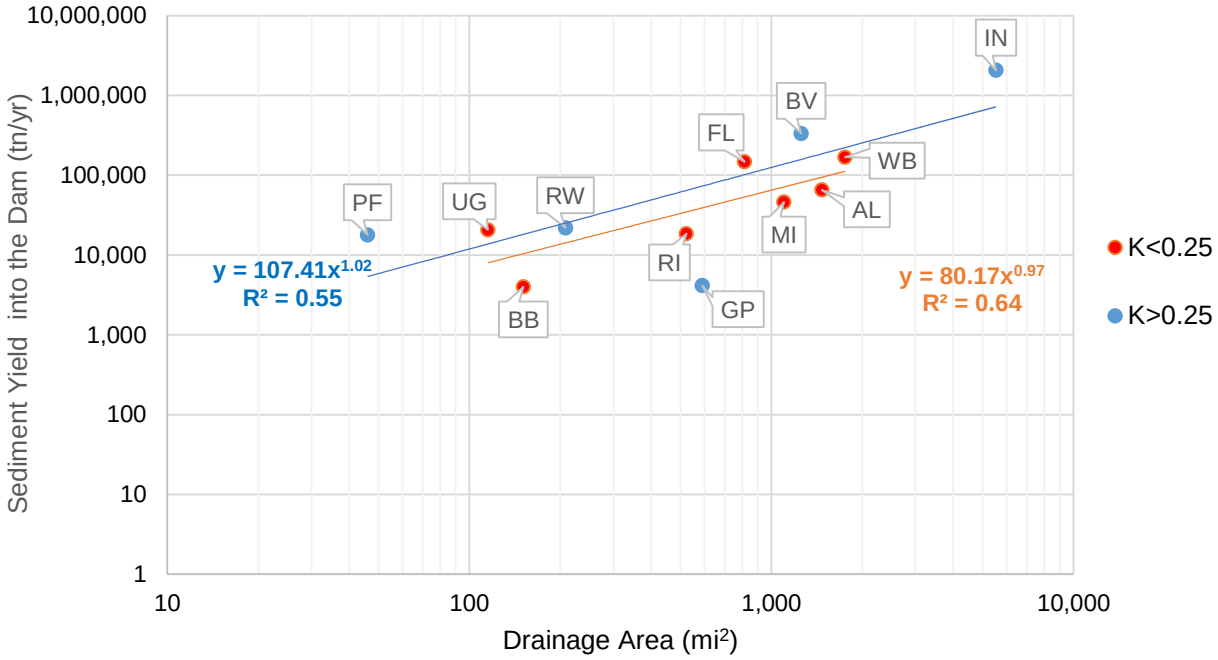

Figure 121- Sediment Load into the Dam versus Drainage Area with Considering Soil Erodibility

The study watersheds were divided into two groups to allow an evaluation of the impact of impoundments on sediment yield within a watershed. Potter's Falls, Upper Green, Brown Bridge, Rockwell, Mio, and Ballville Dams have been placed in the "single dam" group, as there are no impoundments upstream of the study dam. However, upstream of Alcona, Riley, Ford Lake, Independence, Goshen, and Webber dams, there is one or more than one impoundment. These dams are placed in the "multi-dam" group. Figure 122 displays the sediment yield for the two groups. The R^2 is 0.79 for multi-dam group, and 0.51 for single-dam group. In both groups the sediment yield has been estimated just upstream of the reservoirs. Therefore, no sediment accumulation load has been considered for estimating sediment yield in the "single-dam" group.

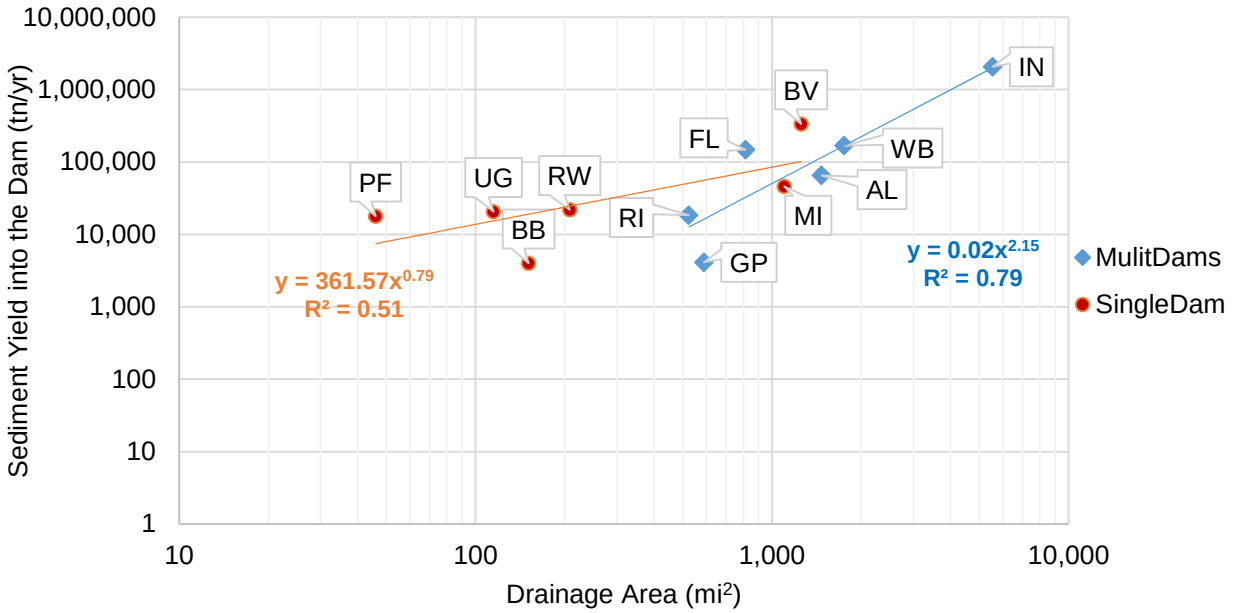

Figure 122- Sediment yield versus Drainage Area with considering Dams Number

The other variable which has been evaluated in this project is the relief. Relief is the difference between the highest and lowest elevation in a watershed, and can indicate the topography of a watershed. Figure 123 displays the sediment yield within the study watersheds when considering the relief factor.

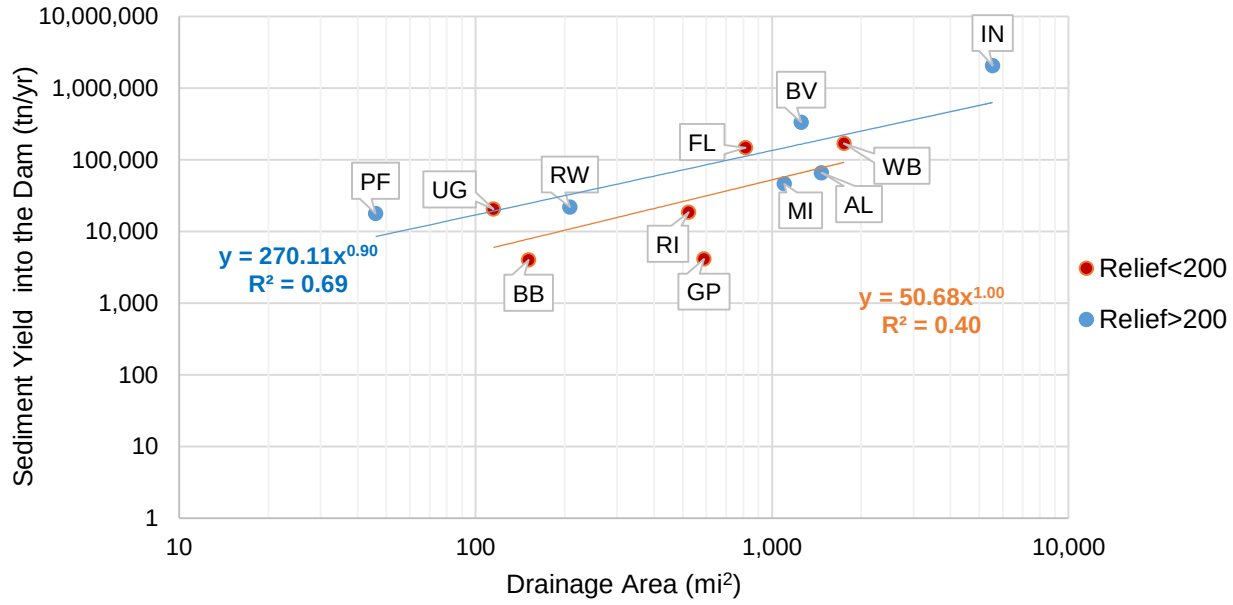

Figure 123- Sediment Yield versus Drainage Area, Considering Relief

Goshen Pond, Upper Green, Riley, Ford Lake, Brown Bridge, and Webber Dams have the relief lower than 200 (m), while Independence, Ballville, Rockwell, Mio, and Alcona, and Potter's Falls have a relief which exceeds 200 (m). Among these study watersheds, Potter's Falls with 418 (m), and Goshen Pond with 92 (m) have the highest and lowest relief, respectively. The R^2 for the watersheds with relief higher than 200 (m) is 0.69, and it is 0.40 for watersheds with relief lower than 200 (m). The both fitted trend lines show the sediment yield in the watersheds with relief >200 (m) is higher than the watershed with relief <200 (m). In removing Goshen Pond Reservoir from the analysis, R^2 increases to 0.68 for the group with relief >200 (m).

5.6.2. Sediment Accumulation

Figure 124 displays the sediment accumulation rate versus drainage area of each reservoir. Both linear and power trend lines are considered for the expression of the sediment accumulation rate data. The R^2 of the linear trend line is 0.82, while the R^2 of power trend line is 0.32. The linear trend line is clearly superior for this case.

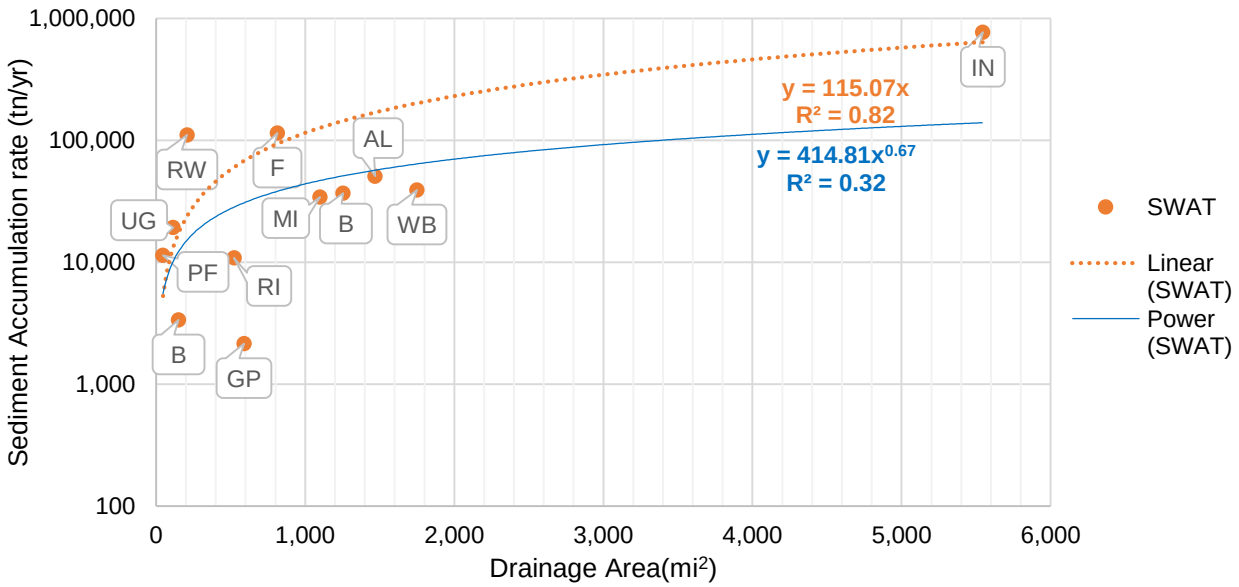

Figure 124- Sediment Accumulation versus Drainage Area

For comparing this sediment accumulation rate with the RESSED trend line which was described in Section 5.4, the sediment accumulation rate of each study reservoir was normalized by the watershed area. Figure 125 displays the comparison between the RESSED trend line and SWAT simulations trend line. The slope of SWAT trend line and RESSED trend line are very close. The R^2 associated with either trend line is low, with the R^2 of RESSED at 0.25, and SWAT simulation at 0.10.

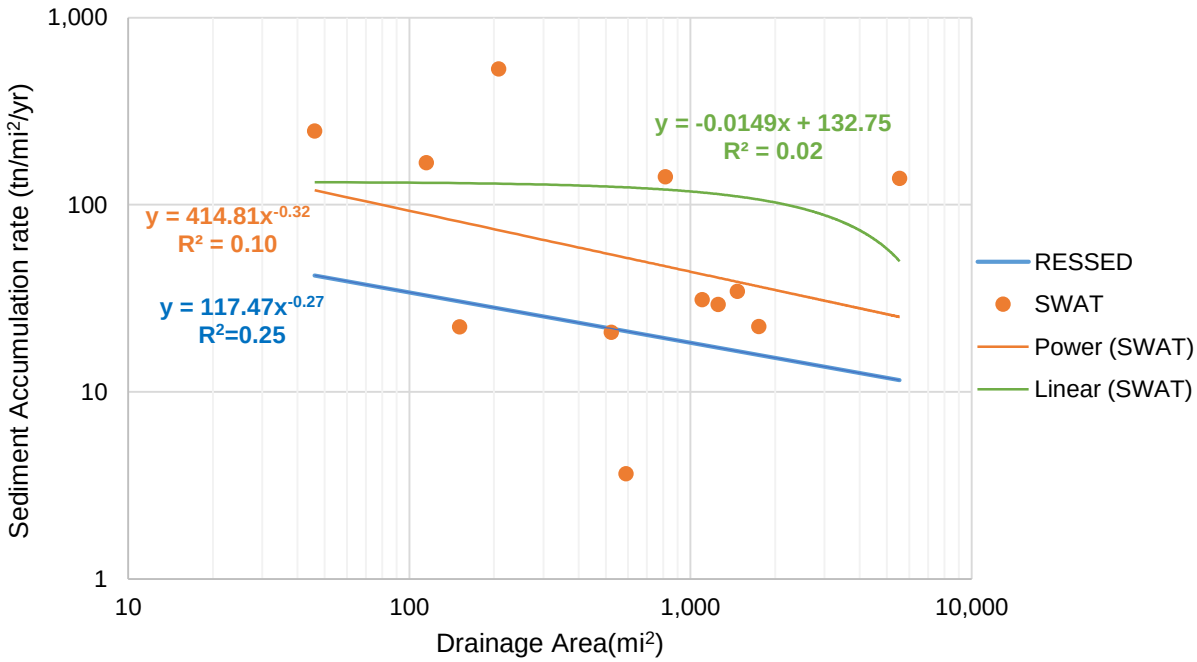

Figure 125 Sediment Accumulation Rate from SWAT and RESSED Trend Line

Sediment trapping efficiency depends on different factors including reservoir geometry, sediment inflow, sediment particle size, residence time, and drainage area. Brune Curve relates the sediment trapping efficiency with the residence time of water within the reservoir. Figure 126 displays the average of sediment trapping efficiency within the study reservoirs based on the SWAT models and Brune Curve. As shown in Figure 126, the logarithmic trend lines provided a good fit to sediment trapping efficiency from Brune Curve and SWAT.

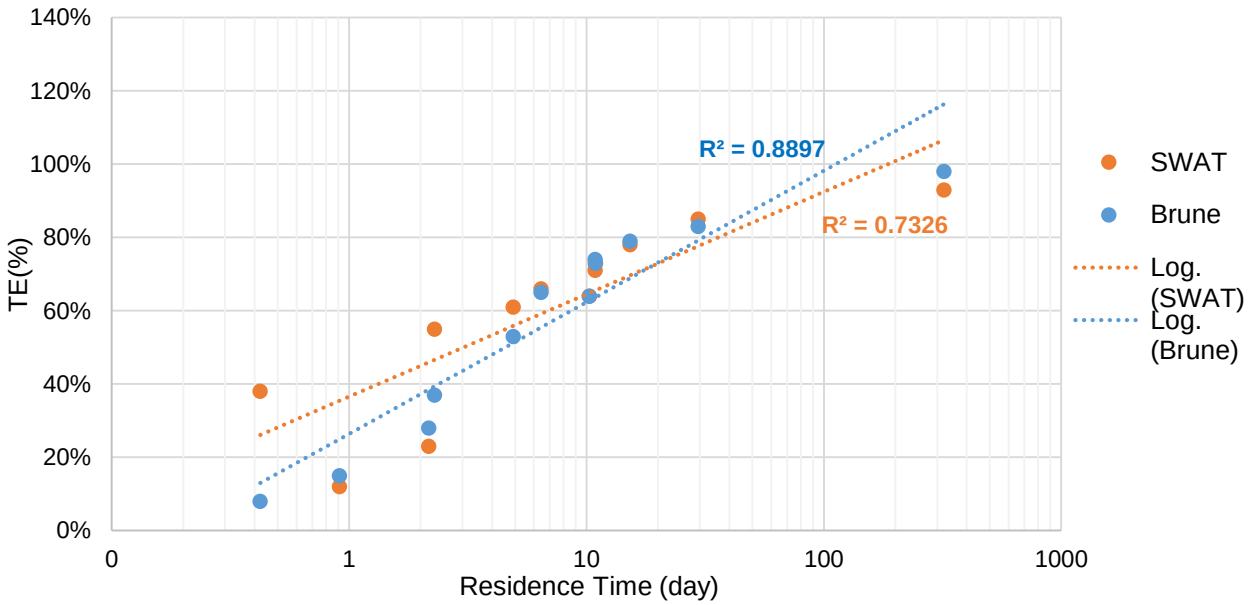

Figure 126- Trapping Efficiency from Brune Curve and SWAT

5.6.3. Natural Sediment Yield

Figure 127 displays the natural sediment yield within the study watersheds. A power trend line was fit through the sediment yield data, resulting in an R^2 value of 0.56.

The natural sediment yield in the Ford Lake watershed is far higher than other watersheds, and with removing the Ford Lake data from the curve, the R^2 of the added trend line increases from 0.56 to 0.68.

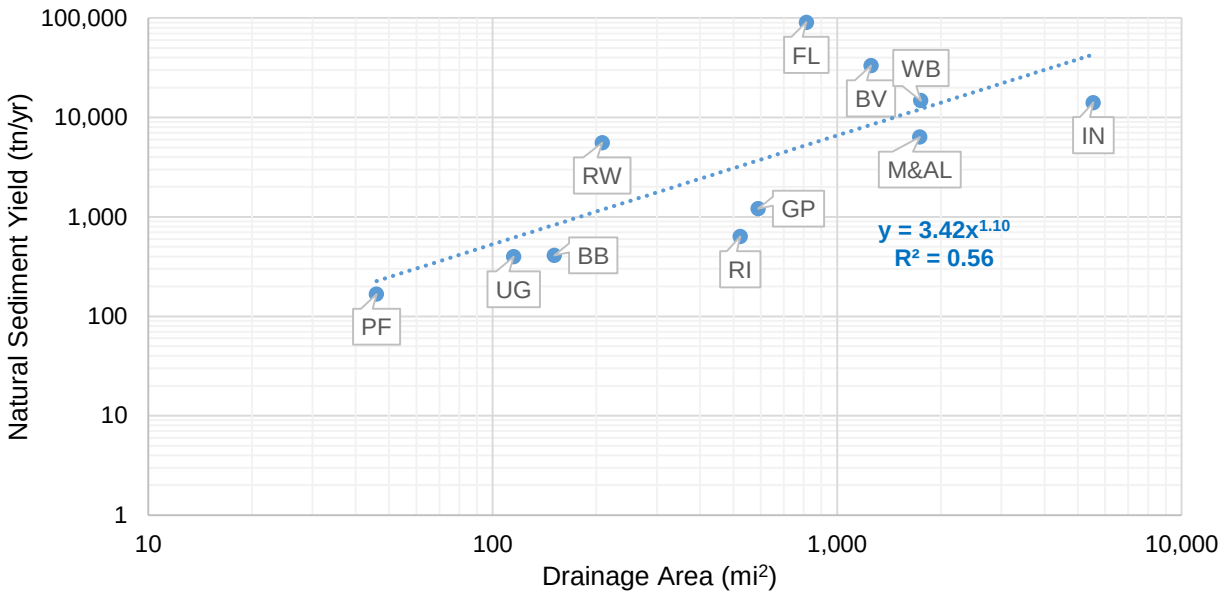

Figure 127- Natural Sediment Yield versus Drainage Area

Table 113 displays the pre-European land use percentages for the study watersheds. As the table displays, 12% of the Ford Lake, and 6% of Webber watershed are pasture, while there is negligible pasture in the rest of the watershed. More than 85% of the study watersheds are forest, while only 51% of the Ford Lake watershed is comprised of the forest land use type. This likely contributes to the higher natural sediment yield within the Ford Lake watershed.

Table 113- Pre- European Land Use in the Study Watersheds

Land Use	BV	IN	GP	UG	RI	WB	FL	RW	BB	PF	MI&AI
Water	0%	0%	0%	11%	2%	1%	5%	0%	0%	0%	2%
Forest	96%	100%	100%	57%	86%	85%	51%	96%	95%	100%	85%
Range	3%	0%	0%	28%	12%	8%	32%	3%	5%	0%	12%
Wetland	1%	0%	0%	3%	0%	0%	0%	0%	0%	0%	0%
Pasture	0%	0%	0%	0%	0%	6%	12%	0%	0%	0%	1%

5.7. Extrapolate Results across Great Lakes Basin

A mathematical regression model was developed for the results of the eleven SWAT models to predict the current and natural sediment yield in unmodeled watersheds. The regression analysis describes that there is a significant correlation between sediment yield and drainage area. The number of observation data (the number of reservoirs) was not large enough to capture the importance of other independent variables such as soil erodibility factor, relief, the percent of agricultural area, and reservoirs density on the sediment yield. The only independent variable of the mathematical regression models which has been considered in this study, is the drainage area. Each 8 digit HUC in Great Lakes Basin on the side of United States border is given in Figure 128.

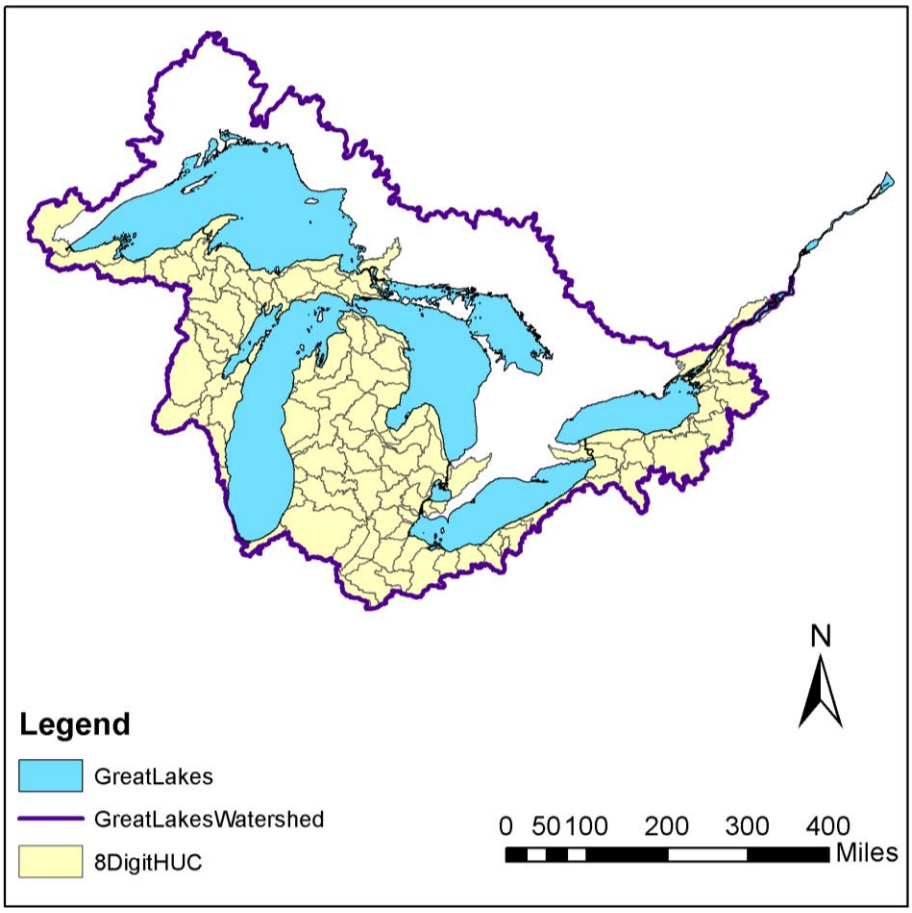

Figure 128- Eight Digit HUC Sub Watershed in the Great Lakes Region

The drainage area of each 8 digit HUC sub-watershed is plotted in the developed mathematical models to determine both current and pre- European sediment yield into each lake (Lake Superior, Huron, Michigan, Erie, and Ontario).Table 114 shows the drainage area, and the natural and current sediment yield into the Great Lakes.

Table 114- The Natural and Current Sediment Delivery into the Great Lakes

Lake Name	Area, A (mi^2)	Natural Sediment Yield, Qs (tn/yr)	Current Sediment Yield, Qs (tn/yr)		
		Power Trendline	Linear Trendline	Power Trendline	USACE Trendline
		$Qs=3.42A^{1.1}$ $R^2=0.56$	$Qs =310.31A$ $R^2=0.85$	$Qs =88.37A^{0.995}$ $R^2=0.55$	$Qs =407.3A^{0.77}$ $R^2=0.78$
Superior	19,180	175,857	5,951,746	1,613,389	808,552
Michigan	44,878	447,984	13,926,092	3,759,051	1,555,895
Huron	15,876	142,837	4,926,482	1,336,726	699,013
St. Clair	3,714	28,897	1,152,491	314,991	228,398
Erie	17,883	162,821	5,549,274	1,504,815	766,114
Ontario	29,026	277,391	9,007,058	2,436,566	1,112,399

The equation in the last column was developed through the USACE 516(e) studies in the Great Lakes watersheds. Other equations used the sediment yield data which were predicted by SWAT through the present study. The current and natural sediment yield for each 8 digit HUC are also listed in Table 115 to Table 120.

Table 115- The Sediment Yield for Each 8 Digit HUC in Lake Michigan Watershed

HUC 8	Name	Drainage Area (mi^2)	Natural Sediment Yield (tn/yr)	Current Sediment Yield (tn/yr)
4030101	Manitowoc-Sheboygan	1,630	11,680	138,813
4030102	Door-Kewaunee	766	5,090	65,481
4030103	Duck-Pensaukee	333	2,036	28,585
4030104	Oconto	961	6,532	82,057
4030105	Peshtigo	1,219	8,485	103,963
4030106	Brule	1,052	7,215	89,786
4030107	Michigamme	724	4,783	61,908
4030108	Menominee	2,293	17,001	194,943
4030109	Cedar-Ford	1,019	6,967	86,984
4030110	Escanaba	928	6,285	79,253
4030111	Tacoosh-Whitefish	642	4,191	54,929
4030112	Fishdam-Sturgeon	580	3,748	49,650
4030201	pperFox	1,620	11,601	137,966
4030202	Wolf	3,726	29,000	316,003
4030203	Lake Winnebago	572	3,691	48,968
4030204	owerFox	648	4,234	55,440
4040001	Little Calumet-Galien	690	4,537	59,015
4040002	Pike-Root	418	2,614	35,841
4040003	Milwaukee	879	5,921	75,089
4050001	St. Joseph	4,713	37,554	399,242
4050002	Black-Macatawa	608	3,947	52,034
4050003	Kalamazoo	2,032	14,885	172,858
4050004	Upper Grand	1,760	12,708	149,827
4050005	Maple	946	6,420	80,782
4050006	Lower Grand	2,022	14,804	172,011
4050007	Thornapple	849	5,699	72,538
4060101	Pere Marquette-White	2,083	15,296	177,174
4060102	Muskegon	2,727	20,572	231,639
4060103	Manistee	1,950	14,225	165,916
4060104	Betsie-Platte	796	5,309	68,032
4060105	Boardman-Charlevoix	1,668	11,980	142,033
4060106	Manistique	1,471	10,433	125,337
4060107	Brevoort-Millecoquins	553	3,557	47,350

Table 116- The Sediment Yield for Each 8 Digit HUC in Lake Superior Watershed

HUC 8	Name	Drainage Area (mi^2)	Natural Sediment Yield (tn/yr)	Current Sediment Yield (tn/yr)
4010101	Baptism-Brule	1,587	11,341	135,170
4010102	Beaver-Lester	624	4,062	53,397
4010201	St. Louis	2,941	22,355	249,722
4010202	Cloquet	794	5,295	67,862
4010301	Beartrap-Nemadji	1,928	14,049	164,054
4010302	Bad-Montreal	1,301	9,114	110,920
4020101	Black-Presque Isle	1,019	6,967	86,984
4020102	Ontonagon	1,388	9,787	118,299
4020103	Keweenaw Peninsula	1,112	7,669	94,881
4020104	turgeon	730	4,827	62,418
4020105	Dead-Kelsey	930	6,300	79,423
4020201	Betsy-Chocolay	1,167	8,087	99,550
4020202	ahquamenon	810	5,412	69,223
4020203	Waiska	295	1,782	25,338
4020300	Lake Superior	2,554	19,141	217,015

Table 117- The Sediment Yield for Each 8 Digit HUC in Lake Huron Watershed

HUC 8	Name	Drainage Area (mi^2)	Natural Sediment Yield (tn/yr)	Current Sediment Yield (tn/yr)
4070001	St. Marys	439	2,759	37,632
4070002	Carp-Pine	655	4,284	56,036
4070003	Lone Lake-Ocqueoc	824	5,515	70,413
4070004	Cheboygan	894	6,033	76,363
4070005	Black	600	3,890	51,353
4070006	Thunder Bay	1,250	8,722	106,593
4070007	Au Sable	2,049	15,022	174,297
4080101	Au Gres-Rifle	1,025	7,012	87,493
4080102	Kawkawlin-Pine	486	3,086	41,640
4080103	Pigeon-Wiscoggin	901	6,084	76,958
4080104	Birch-Willow	525	3,359	44,964
4080201	Tittabawassee	1,447	10,246	123,302
4080202	Pine	1,026	7,019	87,578
4080203	Shiawassee	1,266	8,845	107,951
4080204	Flint	1,330	9,338	113,380
4080205	Cass	908	6,136	77,553
4080206	Saginaw	251	1,492	21,576

Table 118- The Sediment Yield for Each 8 Digit HUC in Lake St. Clair Watershed

HUC 8	Name	Drainage Area (mi^2)	Natural Sediment Yield (tn/yr)	Current Sediment Yield (tn/yr)
4090001	St. Clair	1,157	8,011	98,701
4090002	Lake St. Clair	256	1,524	22,004
4090003	Clinton	797	5,317	68,117
4090004	Detroit	586	3,791	50,161
4090005	Huron	918	6,211	78,403

Table 119- The Sediment Yield for Each 8 Digit HUC in Lake Erie Watershed

HUC 8	Name	Drainage Area (mi^2)	Natural Sediment Yield (tn/yr)	Current Sediment Yield (tn/yr)
4100001	Ottawa- Stony	697	4,588	59,610
4100002	Raisin	1,063	7,298	90,721
4100003	St. Joseph	1,094	7,533	93,353
4100004	St. Marys	793	5,287	67,777
4100005	Upper Maumee	387	2,402	33,195
4100006	Tiffin	778	5,177	66,501
4100007	Auglaize	1,666	11,964	141,864
4100008	Blanchard	772	5,133	65,991
4100009	Lower Maumee	1,081	7,434	92,249
4100010	Cedar- Portage	969	6,591	82,736
4100011	Sandusky	1,827	13,242	155,502
4100012	Huron- Vermillion	764	5,075	65,310
4110001	Black Rocky	898	6,062	76,703
4110002	Cuyahoga	811	5,419	69,308
4110003	Ashtabula	634	4,134	54,248
4110004	Grand Chagrin	706	4,653	60,376
4120101	Chautauqua Conneaut	867	5,832	74,069
4120102	Cattaraugus	560	3,606	47,946
4120103	Buffalo	717	4,733	61,312
4120104	Niagara	799	5,331	68,287

Table 120- The Sediment Yield for Each 8 Digit HUC in Lake Ontario Watershed

HUC 8	Name	Drainage Area (mi^2)	Natural Sediment Yield (tn/yr)	Current Sediment Yield (tn/yr)
4130001	Oak Orchard-12mile	1,034	7,079	88,258
4130002	Upper Genesee	1,426	10,082	121,522
4130003	Lower Genesee	1,067	7,328	91,060
4140101	Irondequoit-Ninemile	702	4,624	60,036
4140102	Salmon-Sandy	973	6,621	83,076
4140201	Seneca	3,460	26,731	293,552
4140202	Oneida	1,498	10,644	127,626
4140203	Oswego	145	816	12,499
4150101	Black	1,907	13,881	162,276
4150102	Chaumont-Perch	355	2,184	30,464
4150301	Upper St. Lawrence	392	2,436	33,622
4150302	Oswegatchie	1,050	7,200	89,617
4150303	Indian	563	3,627	48,202
4150304	Grass	633	4,126	54,163
4150305	Raquette	1,260	8,799	107,442
4150306	St. Regis	869	5,847	74,239
4150307	Salmon	414	2,587	35,499
4150308	Chateaugay-English	1,262	8,814	107,612
4150401	Mettawee River	687	4,515	58,759
4150402	Otter Creek	943	6,397	80,527
4150403	Winooski River	1,063	7,298	90,721
4150404	Au sable River	515	3,289	44,112
4150405	Lamoille River	721	4,762	61,652
4150406	Saranac River	613	3,983	52,460
4150407	Miss quoi River	853	5,729	72,878
4150408	Lake Champlain	2,793	21,120	237,217
4150409	Richelieu River	1,087	7,480	92,758
4150500	St. Francois River	741	4,907	63,354

CHAPTER 6 CONCLUSION AND FUTURE STUDIES

6.1. Summary

In order to evaluate the remaining storage capacity within the Great Lakes Basin, a hydrology and sediment yield model of several subbasins throughout the Great Lakes basin were developed. The study reservoirs are Ballville and Lake Rockwell in Ohio, Webber, Riley, Ford Lake, Brown Bridge, Mio and Alcona in Michigan, Goshen Pond in Indiana, Upper Green Lake in Wisconsin, and Potter's Falls in New York.

The Soil and Water Assessment Tool (SWAT) was applied for the modeling purpose. SWAT is a powerful tool for simulating the effect of watershed management and process on water and soil resources at the Hydrological Response Unit (HRU) level. In this research, the SWAT models were calibrated to the flow and sediment gages within the study watersheds with using SWATCUP. SWATCUP was developed for doing sensitivity analysis, calibration, and validation of SWAT models. The hydrologically calibrated models of all study reservoirs were provided by the US Army Corps of Engineers (USACE). Calibrating and validating these models for sediment components and analyzing the model outputs are some parts of this dissertation.

Some study watersheds including Ballville, Lake Rockwell, Potter's Falls have one or more sediment gages, and the sediment models of these watersheds were calibrated to the recorded sediment data. While other approach was applied for calibrating the un-gaged watersheds including Webber, Riley, Goshen Pond, Upper Green, Ford Lake, Brown Bridge, Mio and Alcona. All study un-gaged watersheds were classified into one of three groups based on their characteristic (land use, climate data, soil characteristic,

and slope). The sediment calibrated parameters of the gaged watersheds in each group were used for calibrating the un-gaged watersheds which are in the same group.

After the SWAT models were calibrated, they were used to investigate three additional scenarios. These scenarios were defined to quantify the net effect that human has caused to the sediment delivery to the Great Lakes. The human interferes such as land use change and dam construction were considered in this study, and any impact associated with climate change due to the anthropogenic is outside the scope of this dissertation. The study scenarios are:

- Post- European Settlement Scenario,
- Pre- European Settlement Scenario, (Replacing the current land use with pre-European land use and removing existing reservoirs from the models.)
- Removing Impoundment Scenario, (Using the current land use and removing reservoirs from the models.)

The regression analyses were developed on the sediment load (output) of the SWAT models to predict current sediment yield, sediment accumulation rate, and natural sediment yield in un-modeled watersheds. The purpose of these calculations is to determine what the anthropogenic component of sediment delivery is to the Great Lakes.

Relying on the SWAT models, the remaining storage capacity behind the study dams were assessed. In this dissertation, the remaining storage capacity within the reservoirs were quantified in terms of remaining time and volume until the reservoirs are full. The remaining storage capacity determined by SWAT was also compared with the bathymetric and radionuclide dating approaches.

6.2. Conclusion

Reservoir sedimentation and the consequence loss of storage capacity have been a serious threat to the natural environment. As many dams are reaching their capacity for sediment storage, the current dissertation investigated the historical and current rates of sediment accumulation as well as the remaining storage capacity. This research helps to improve understanding of the mechanisms influencing sediment yield and storage in the watershed and will provide insight regarding potential control of this process. The following items are a list of conclusions made from this research:

- The SWAT can be used to analyze the hydrology and sediment components within the Great Lakes watershed. This tool can also provide the insights into the historical and present conditions of the Great Lakes watershed.
- The results of this research explains the possibility of calibrating the un-gaged watersheds with applying the calibrated parameters of gaged watersheds.
- It was shown that the SWAT can predict the sediment accumulation rate within the reservoirs, and with the knowledge of sediment accumulation rate, the remaining storage capacity can be forecasted. SWAT may help in the decision-making process of whether to remove a dam.
- The main changes to the study watersheds since the European settlement was converting the forest land to agricultural and urban land uses and the construction of dams. Building dams decreases sediment delivery to the downstream reaches, due to increased opportunity of sediment trapping within the reservoir, while expanding agricultural and urban area results in increasing sediment yield. All SWAT models except Ford Lake model predicted that the sediment yield

has increased since pre- European settlement. Ford Lake model suggested the sediment decreased by half since pre- European settlement. This is an expected result due to the construction of major dams upstream of the mouth, which has resulted in capturing of sediment. In this dissertation the impact of dam construction and land use change on the sediment yield have been assessed together not individually.

- Comparing the post- European and un-impoundment scenarios explains that with removing the reservoirs from the model the sediment delivery to the downstream reaches increased as expected. Among the watersheds with multiple reservoirs, Ford Lake watershed had the largest increases. The SWAT model predicted the construction reservoirs within the Ford Lake watershed had the biggest impact at sediment yield within the watershed.

- Sediment yield depends on many factors, in the current research the impact of some factors including percentage of agricultural area, soil erodibility factor, topographic relief, dam density and the drainage area of study watersheds were investigated. The linear regression analysis displays the strong correlation between the sediment yield and drainage area. Because of very limited size of the observational data, the regression analysis was not able to show the importance of other independent variables.

- The regression analysis shows that there is a strong correlation between the sediment yield and the drainage area. Both linear- and power-trend lines were applied to the sediment yield data. The linear trend line with R^2 of 0.85 proposed a better fit than the power trend line with R^2 of 0.55. The R^2 of USACE 516 (e) studies

trend line is 0.78. The power trend line of this study meet the power trend line of USACE 516 (e) study at the drainage area of 900 (mi^2). For the drainage area of less than 900 (mi^2) USACE 516 (e) studies suggested the bigger sediment yield than the SWAT models of this study, while for the drainage area of larger than 900 (mi^2), the SWAT models proposed the bigger value.

- For improving the R^2 of SWAT modeling results, the study reservoirs were classified into the smaller groups according to their land use, soil erodibility factor, number of dams, and relief. The results show that with classifying the study watersheds based on their soil erodibility factor, the R^2 will improve. The R^2 for the study watersheds with the soil erodibility factor of less than 0.25 is 0.64, and bigger than 0.25 the value of R^2 is 0.55.

- The regression analysis was also done on the sediment accumulation rate within the study reservoirs. Both linear and power trend lines are considered for the expression of the sediment accumulation rate data. The R^2 of the linear trend line is 0.82, while the R^2 of power trend line is 0.32.

- For comparing sediment accumulation rate results from SWAT modeling with the RESSED trend line, the sediment accumulation rate normalized by the watershed area. RESSED trend line proposed the R^2 of 0.25, while the R^2 SWAT trend line is 0.1. Both trend lines display with increasing the drainage area the sediment accumulation rate ($tn/mi^2/yr$) decreases, because the opportunity of sediment trapping increases as a function of drainage area.

- Natural sediment yields within each study watersheds were plotted versus the drainage area. The natural sediment yield trend line proposed the R^2 of 0.56.

The natural sediment yield in the Ford Lake watershed is higher than other watersheds, and with removing the Ford Lake data from the curve, the R^2 of the added trend line increases from 0.56 to 0.68. The reason of high natural sediment yields within the Ford Lake watershed is the natural vegetation in this watershed. More than 85% of each study watershed is forest, while only 51% of the Ford Lake watershed is comprised of the forest land use type. This likely contributes to the higher natural sediment yield within the Ford Lake watershed.

- The developed natural and current sediment delivery equations can be used to predict the natural and current sediment yield in un-modeled watersheds. In this study the sediment delivery into the Great Lakes were predicted by these regression equations.

- SWAT models can be used to predict the time and volume required to fill the reservoirs.

- The estimated sediment accumulation results by SWAT models were compared with other approaches including USGS gages, RESSED and USACE trend lines, bathymetric, and radionuclide dating methods. The trend line approach is not accurate, and it helps only for quick guess. The number of sediment gages are very limited, and there are only a few sediment gages within the Rockwell and Ballville watershed. Therefore, the sediment gage approach is not applicable for all study watersheds. Bathymetric and radionuclide methods also applied for estimating the sediment accumulation rate within some study reservoirs. The sediment accumulation rate predicted by radionuclide and bathymetric methods for most reservoirs fell within the sediment accumulation boundary (M 95 PPU) which was

predicted by SWAT models. However, for some reservoirs including Lake Rockwell Dam and Ford Lake Dam the average of sediment accumulation rate predicted by SWAT were higher than bathymetric and radionuclide approaches. In these reservoirs the bathymetric and radionuclide approaches were close to the lower boundary (L 95 PPU) predicted by SWAT. For Upper Green Lake reservoir, the sediment accumulation rate measured by bathymetric and radionuclide was higher than SWAT modeling results. The potential reason of these differences can be the assumptions associated with each approach.

6.3. Future Study

Based on the outcome of the current research the following suggestions for future study are recommended.

- It is recommended the bedload data are collected throughout the study watersheds to approve this assumption which Bed load is less than 5% of total sediment load. This can also help in validating the impoundments infilling rate.
- SWAT assumes that the transported particle size is assumed to remain constant, and in all cases the grain size corresponds to silt-sized. However, in the real condition the sediment size is changing with inflow rates. It is recommended to use the future version of SWAT that may keep track of sediment particle size.
- In this study for estimating the natural sediment delivery only the effect of land use change and dam construction on the sediment yield were considered, and the same climatic period of record were applied for the natural sediment delivery. It is recommended the impacts associated with climate change or climate variability due to anthropogenic sources to be evaluated in future studies.

- In this study because of limited number of observation data (or limited number of study watersheds) investigating different influential factors and considering these factors into the sediment equation were impossible. It is recommended to increase the number of study watershed to at least 30 watersheds. With increasing the number of study watersheds, the importance of other influential factors such as land use, dam density, soil erodibility factor and topography can be included in the sediment equation.
- In this study for forecasting remaining storage capacity, the sediment accumulation rate has been assumed to be constant over time. Because of the importance of climate change on the sediment yield, it is recommended to evaluate the effect of climate change and with applying the SWAT predict the future sediment accumulation rate.
- It is recommended to expand this research to other watersheds in other part of the country. This research spent some efforts to evaluate sediment yield only within the Great Lakes Basin.

For future study It is recommended to measure the actual erosion rates in each of the watersheds upstream of the study reservoirs, and compare the measured results with the bank erosion calculated by SWAT. In the current version of SWAT, the channel erosion is not partitioned between the stream bed and stream bank. And the deposition is assumed to happen only in the main channel.

REFERENCES

Abbaspour, K. C., (2015). "SWAT-CUP 2012/Calibration and Uncertainty Programs."

Abbaspour, K. C., Rouholahnejad, E., Vaghefi, S., Srinivasan, R., Yang, H., Kløve, B., (2015). "A continental-scale hydrology and water quality model for Europe: Calibration and uncertainty of a high-resolution large-scale SWAT model." Journal of Hydrology 524(0): 733-752.

Abbaspour, K. C., Yang. J., Maximov, I., Siber, R., Bogner, K., Mieleitner, J., Zobrist, J., Srinivasan, R., (2007). "Modelling hydrology and water quality in the pre-alpine/ alpine Thur watershed using SWAT." Journal of Hydrology 333(2–4): 413-430.

Adamowski, J., Adamoski, K., Bougadis, J., (2010). "Influence of Trend on Short Duration Design Storms." Water Resources Management 24(3): 401-413.

American River, (2014). “Why we remove dams.” Retrived form http://www.americanrivers.org/initiatives/dams/why-remove

Beasley, D. B., Huggins, L.F., and Monke, E.J. (1980). "ANSWERS: A model for watershed planning." Transactions of the ASAE 23(4): 6.

Bicknell, B. R., Imhoff, J.C., Kittle, J.L., Jr., Donigian, A.S., Jr., and Johanson, R.C. (1993). "Hydrologic Simulation Program – FORTRAN (HSPF): User’s manual for Release 10." U.S. EPA Environmental Research Lab, Athens, Georgia.

Bosch, N. S., Allan, J. David., Selegean, James P., Scavia, Donald., (2013). "Scenario-testing of agricultural best management practices in Lake Erie watersheds." Journal of Great Lakes Research 39(3): 429-436

Bosch, N.S., Evans, M.A., Scavia, D., Allan, J.D., (2014). "Interacting effects of climate change and agricultural BMPs on nutrient runoff entering Lake Erie." Journal of Great Lakes Research 40(3): 581-589.

Brune, G. M. (1953). "Trap Efficiency of Reservoirs." American Geophysical Union 34: 407-417.

Comer, P.J., Albert, D.A., (1998). “Vegetation of Michigan circa 1800. Lansing: Michigan Natural Features Inventory, 2 maps.”

Clar, M. L., Barfield, B. J. (2004). “Stormwater Best Management Practice Design Guide” EPA/600/R-04/121B

Creech, C., (2010). “Riley reservoir sedimentation study Union City, Michigan.” Unpublished report for Civil Engineering Department, Wayne State University.

Creech, C.T, Siqueira, R.B., Selegean, J.P., Miller, C.J., (2015). "Anthropogenic impacts to the sediment budget of São Francisco River navigation channel using SWAT " Int J Agric & Biol Eng 8: 140-157.

Czuba, J. A., Magirl, C.S, Czuba, C. R., Grossman, E. E., Curran, C. A., Gendaszek, A. S., Dinicola, R. S., (2011). “Sediment Load from Major Rivers into Puget Sound and its Adjacent Waters.” US. Department of the Interior, US. Geological Survey.

Downer, C. W., and Ogden, F.L., (2006). "Gridded Surface Subsurface Hydrology Analysis (GSSHA) User’s Manual." Watershed Modeling System 6.1, Sustem Wide Water Resources Program, Coastal and Hydraulics Laboratory, U.S. Army Corps of Engineers, Engineer Research and Development Center,: ERDC/CHL SR-06-01, 207 pp.

Ellison, G. (2013). “Federal judge orders brown bridge dam flooding case back to state court in Traverse City. Retrieved from http://www.mlive.com/news/index.ssf/2013/08/judge_orders_brown_bridge_dam.html

Ellis, E. C., Goldewijk, K. K., Siebert, S., Lightman, D., Ramankutty, N., (2010). “Anthropogenic transformation of the biomes, 1700 to 2000” Global Ecology and Biogeography, 19: 589- 606

Engstrom, D.R., Almendinger, J.E., Wolin, J.A., (2009). "Historical changes in sediment and phosphorus loading to the upper Mississippi River: mass-balance reconstructions from the sediments of Lake Pepin." Journal of Paleolimnology 41(4): 563-588.

Environmental Protection Agency, E., (2012). "Nonpoint Source Pollution: The Nation's Largest Water Quality Problem." from http://water.epa.gov/polwaste/nps/outreach/point1.cfm.

Evans, J.E., Levine, N.S., Roberts, S.J., (2002). "Assessment using GIS and sediment routing of the proposed removal of Ballville Dam,Sandusky River, Ohio." JAWRA Journal of the American Water Resources Association 38(6): 1549-1565.

Gill, M. A., (1979). "Sedimentation and useful life of reservoirs." Journal of Hydrology: 89-95.

Gray, J. R., Glyssom, G. D., Turcios, L. M., Schwarz, G. E., (2000). “Comparability of Suspended-Sediment Concentration and Total Suspended Solids Data” U.S. Department of the Interior, U.S. Geological Survey. 00-4191. USGS Water-Resources Investigations.

Griffin, M. L., Barfield, B. J., Warner, R. C. (1985). “Laboratory studies of dead storage in sediment ponds” Trans. Am. Soc. Agric, Eng. 28(3): 799-804

Heiple, R. W., Heiple, E. B., (1976). “A Heritage History of Beautiful Green Lake Wisconsin. Ripon, WI”: McMillian Printing, 1977. Print.

Hindall, S. M., (1991). "Temporal trends in fluvial-sediment discharge in Ohio, 1950-1987." Journal of Soil and Water Conservation 46: 3.

Homer, C., Dewitz, J., Fry, J., Coan, M., Hossain, N., Larson, C., Herold, N., McKerrow, A., VanDriel, J.N., and Wickham, J (2007). "Completion of the 2001 National Land Cover Database for the Conterminous United States, Photogrammetric Engineering and Remote Sensing." 73: 337-341.

Imeson, A. (2012). “Desertification, land degradation, and sustainability”, Wiley-Blackwell. 326:158-162

Jordan, Y.C., Ghulam, A., Hartling, S., (2014). "Traits of surface water pollution under climate and land use changes: A remote sensing and hydrological modeling approach." Earth-Science Reviews 128(0): 181-195.

Kelly, D., (2013). “Study maps Great Lakes Basin stream barriers; road crossings more abundant than dams”. Environmental Monitor. http://www.fondriest.com/news/study-maps-great-lakes-basin-stream-barriers-road-crossings-worse-than-dams.htm

Klein J. M., Koelmans, A. A., (2011). “ Quantifying seasonal export and retentioin of nutrients in West European lowland rivers at catchment scale” Journal of Hydrology 25: 2102-2111.

Leavesley, G. H., Lichty, R. W., Troutman, B. M., and Saindon, L. G., (1983). "Precipitation-runoff modeling system – User’s manual. ." USGS Water resources Investigative Report: 4155.

Leote, C., Epping, E. H. G., (2015). "Sediment–water exchange of nutrients in the Marsdiep basin, western Wadden Sea: Phosphorus limitation induced by a controlled release?" Continental Shelf Research 92(0): 44-58.

Maalim, F. K., Melesse, A. M., Belmont, P., Gran, K. B., (2013). "Modeling the impact of land use changes on runoff and sediment yield in the Le Sueur watershed, Minnesota using GeoWEPP." CATENA 107: 35-45.

Macdonald, O., (1942) “A History of Au Sable and Oscoda”. Master’s Thesis.: Wayne State University.

Macrae, M. L., English, M. C., Schiff, S. L., Stone, M., (2007). "Intra-annual variability in the contribution of tile drains to basin discharge and phosphorus export in a first-order agricultural catchment." Agricultural Water Management 92(3): 171-182.

McCully, P., (1996). A truly dazzling book. Silenced Rivers: The Ecology and Politics of Large Dams. London, Zed Books.

Michigan Department of Technology, Management, and Budget (DTMB) (2002). “Michigan Land Cover Circa 1800” *http://www.mcgi.state.mi.us/mgdl/?rel=ext&action=sext*

Molder, B., Cockburn, J., Berg, A., Lindsay, J., Woodrow, K., (2015). "Sediment-assisted nutrient transfer from a small, no-till, tile drained watershed in Southwestern Ontario, Canada." Agricultural Water Management 152(0): 31-40.

Moriasi, D.N., Arnold, J.G., Van Liew, M.W., Bingner R.L., Harmel, R.D., Veith T.L., (2007). "Model evaluation guidelines for systematic quantification of accuracy in watershed simulations." American Society of Agricultural and Biological Engineers 50(3): 885-900.

Mukundan, R., Pradhanang, S. M., Schneiderman, E. M., Pierson D. C., Anandhi, A., Zion, M. S., Matonse, A. H., Lounsbury, D. G., Steenhuis, T. S., (2013). "Suspended sediment source areas and future climate impact on soil erosion and sediment yield in a New York City water supply watershed, USA." Geomorphology 183(0): 110-119.

National Inventory of Dams “http://nid.usace.army.mil/cm_apex/f?p=838:12”

National Land Cover Database for the Conterminous United States,

Natural Resources Defense Council (2014). “Dam Shame, Five America’s worst” https://www.nrdc.org/onearth/dam-shame

Neitsch, S. L., Arnold, J.G., Kiniry, J.R.,Williams, J.R., (2011). SWAT Theoretical Documentation, version 2009., Texas A& M University System: 618.

Ohio Department of Natural Resources (2003). "Natural Vegetation of Ohio, at the Time of the Earliest Land Survey." from http://www2.ohiodnr.gov/geospatial/data-metadata/search-by-category

Oeurng, C., Sauvage, S., Sánchez-Pérez, J. M., (2010) “Dynamics of suspended sediment transport and yield in a large agricultural catchment, southwest France.” Earth Surface Processes and Landforms 35(11): 1289- 1301

Puit, G., Buksowski, A., Anderson, L. (2012). “Boardman flood: Heartbreak, relief, questions”. Traverse City Record Eagle.

Rajin, M.A., Merwade, V., Kim, I.L., Zhao, L., Song, C., Zhe, S., (2015). "SWATShare- A web platform for collaborative research and education through online sharing, simulation and visualization of SWAT models". Environmental Modelling & Software 536 (2015)1-15

Ramos, T. B., Gonçalves, M. C., Branco, M. A., Brito, D., Rodrigues, S., Sánchez-Pérez, J., Sauvage, S., Prazeres, Â., Martins, J. C., Fernandes, M. L., Pires, F. P., (2015). "Sediment and nutrient dynamics during storm events in the Enxoé temporary river, southern Portugal." CATENA 127(0): 177-190.

Randhir, T. O., Hawes, A. G., (2009). "Watershed land use and aquatic ecosystem response: Ecohydrologic approach to conservation policy." Journal of Hydrology 364(1–2): 182-199.

Rivers, I., (2016). "Dams and Migratory Fish." from https://www.internationalrivers.org/dams-and-migratory-fish.

Rovira, A., Batalla, R. J., (2006). “Temporal distribution of suspended sediment transport in a Mediterranean basin: The Lower Tordera (NESPAIN)” Journal of Gemorphology 79 (2): 58-71

Schiefer, E., Petticrew, E.L., Immell, R., Hasssan, M.A., Sonderegger, D.L., (2013). "Land use and climate change impacts on lake sedimentation rates in western Canada." Anthropocene 3(0): 61-71.

Stanley, E.H., Doyle, M.W., (2003). "Trading off: the ecological effects of dam removal." The Ecological Society of America 1(1): 15-22.

Stone, M., English, M. C., (1993). “Geochemical composition, phosphorus speciation and mass transport of fine-grained sediment in two Lake Erie tributaries.” Proceedings of the Third International Workshop on Phosphorus in Sediments. P. C. M. Boers, T. E. Cappenberg and W. van Raaphorst, Springer Netherlands. 84: 17-29.

Terrence, J. T., George, R. F., Renard, K. G., (2002). "Soil Erosion: Processes, Prediction,Measurement, and Control." John Wiley & Sons.: 338.

Tompkins Ready Emergency Preparation in Tompkins County, New York (2004). “http://www.tompkinsready.org/aboutsite.aspx”

U.S. Geological Survey, (2002). “Streamflow Data: Sandusky River at Station 04198000”. Available at waterdata.usgs.gov/oh/nwis/uv?04198000. Accessed on November 12, 2002.

USACE (U.S. Army Corps of Engineers), (1981). “Phase 1 Inspection Report: Ballville Dam, Sandusky County, Ohio”. U.S. Army Engineer District, Pittsburgh, Report OH-809, 78 pp.

USACE (2010). "Hydrologic Modeling System HEC-HMS User’s Manual. Version 3.5."

Warrick, J.A., Bountry, J.A., East, A.E., Magirl, C.S., Randle, T.J., Gelfenbaum, G., Ritchie, A.C., Pess, G.R., Leung, V., Duda, J.J., (2015). "Large-scale dam removal on the Elwha River, Washington, USA: Source-to-sink sediment budget and synthesis." Geomorphology(0).

Wisconsin Department of Natural Resources (2006). "Wisconsin- Original Vegetation"

Wallings, D. E., (1983). "The Sediment Delivery Problem." Journal of Hydrology 65: 28.

Wischmeier, W. H., Smith, D. D. (1965). “Predicting rainfall-erosion losses from cropland east of the Rocky Mountains.” Agr. Handbook No. 282, U.S. Dept. Agr., Washington, DC.

Wischmeier, W. H. (1975). “Estimating the soil loss equations cover and management factor for undisturbed lands. In Present and Prospective Technology for Predicting Sediment Yields and Sources, ARS-S-40.” Agr. Res. Scrv., U.S. Dept. of Agr., Wash ington, DC, pp. 118-125.

Wischmeier, W. H., Smith, D. D. (1978). “Predicting rainfall erosion losses.” Agr. handbook No. 537, U.S. Dept. of Agr., Science and Education Administration.

Yesuf, H.M., Assen, M., Alamirew, T., Melesse, A.M., (2015). "Modeling of sediment yield in Maybar gauged watershed using SWAT, northeast Ethiopia." CATENA 127(0): 191-205.

Yevenes, M. A., Mannaerts, C. M., (2011). "Seasonal and land use impacts on the nitrate budget and export of a mesoscale catchment in Southern Portugal." Agricultural Water Management 102(1): 54-65.

Young, R. A., Onstad, C.A., Bosch, D.D., and Anderson, W.P., (1987). "AGNPS: A nonpoint-source pollution model for evaluating agricultural watersheds." Journal of Soil and Water Conservation 44(2): 5.

ABSTRACT

EVALUATING SEDIMENT ACCUMULATION BEHIND DAMS IN THE GREAT LAKES WATERSHED FROM PAST TO PRESENT

by

FATEMEH ALIGHALEHBABAKHANI

May 2017

Advisor: Dr. Carol J. Miller

Major: Civil & Environmental Engineering

Degree: Doctor of Philosophy

Reservoir sedimentation and the consequence long term loss of storage capacity have been a serious threat to the natural environmental system. However, there is only few information and physical measurements regarding to the sediment accumulation rate within the reservoirs. The average age of dams in the country is more than 50 years old, and with aging dams, the number of high-hazard dams continues to increase. There are some serious risks associated with aging dams. Dam removal or dam failure can release considerable sediment load to downstream reaches, eventually deteriorate water quality and fish habitat. The present dissertation investigates the historical function of Great Lakes dams as sediment storage points and provides insight into the remaining capacity of dams in the Great Lakes watershed. to better understand the historical and current sediment yield, Soil and Water Assessment Tool (SWAT) has been used. The regression analysis has been done on SWAT output to predict the sediment yield in un-modeled watershed.

The overall objectives of this research are:

1- Determine the historical and current sediment yield within the Great Lakes watershed.

2- Estimate the sediment accumulation rate within the reservoirs and forecast the remaining capacity of reservoirs in the Great Lakes.

3- Evaluate the net effect that humans have caused to the sediment delivery to the Great Lakes. The difference between pre- European settlement and the present-day sediment delivery rate is anthropogenic effects.

The research of this investigation includes field studies and modeling for eleven reservoirs in the Great Lakes watershed.

Keywords*: forecasting reservoir capacity, sediment accumulation rate, Great Lakes basin, pre-European settlement, SWAT*

AUTOBIOGRAPHICAL STATEMENT

My overall goal is to help the quality and quantity of natural environment especially water resources to be improved sustainably and efficiently.

I was born and grown up in Tehran, Iran. When I was in high school, sever earthquake occurred in Bam, Iran. Many buildings were damaged, and many people lost their house. I went to Bam to help these people, in this trip I faced several challenges which completely changed the course of my life. I decided to purse my degree in Civil Engineering. I received my Bachelor of Science in Civil Engineering from Semnan University, in 2007, and my Master of Science in Water and Wastewater Engineering from Shahid Beheshti University, in 2009. After graduation I started to work in the field of water and wastewater treatment design at one consultant firm in Iran. Four years of work experience encourage me to pursue my study in other countries to earn more knowledge and get a PhD degree. I applied for a PhD position at Wayne State University, and Dr. Miller accepted me to be her student. I took some useful courses regarding to river restoration, open channel hydraulic, groundwater modeling, and hydrology design. I also earned some experience of working on one of the Michigan Sea Grant Projects associated with two- stage drain design. In the two last years of my PhD, I was working on a project funded by the US Army Corps of Engineers. This project had some field work and numerical modeling to better understand sediment transport in the Great Lakes watershed. With some knowledge and work experience that I earned in my life, I hope I can make positive impacts in the world.